ABSTRACT

FU, CEXIONG. Development of Micellar Selectivity Triangle for Classification of Pseudo-stationary Phase Selectivity in Electrokinetic Chromatography. (Under the direction of Morteza G. Khaledi.)

A novel Micellar selectivity triangle (MST) was developed to rationalize and classify the chemical selectivities for a wide variety of pseudo-phases in Electrokinetic Chromatography (EKC). The descriptors of polar selectivities for constructing the MST were derived from the linear solvation energy relationships (LSER). The effects of solvent modification of micelles, mixed-micellar systems along with surfactant type on the pseudo-phase selectivities were investigated using the MST.

To quantitatively describe the similarities and differences of the chemical selecitivities, a phase selectivity ranking system was constructed on the basis of the Euclidean distance between objects. Chemometric methods including the principal component analysis (PCA), hierarchical clustering and k-means clustering were used to elucidate the classification and characterization of the micellar phases in different perspectives. The results form the MST and the chemometric methods were in generally good agreement.

The micellar selectivity triangle was used as a guideline for optimizing the separation of 20 Phenylthiohydantoin (PTH) amino acids. The effects of the surfactant type and concentration, temperature and organic solvent additives on the PTH amino acids separation were evaluated. Additionally, the substituent constants of these PTH amino side chain obtained from the EKC methods were compared to those obtained from

octanol-water partitioning and free energy of transferring amino acid moieties from the globular proteins interior to surface.

Finally, the combined use of the unified selectivity triangle (UST), PCA and cluster analysis was explored for the comparison of the chemical selectivity between the two powerful chromatographic techniques, EKC and RPLC. The database consisted of 518 reversed-phase systems and 83 pseudo-phases. The primary factors to influence the phase selectivity of the two techniques were identified and compared. Suggestions for future works are also discussed.

Development of Micellar Selectivity Triangle for Classifications of Pseudo-stationary Phase Selectivity in Electrokinetic Chromatography.

By

CEXIONG FU

A dissertation submitted to the Graduate Faculty of North Carolina State University
in partial fulfillment of the requirement for the
Degree of Doctor of Philosophy

Chemistry

Raleigh, North Carolina

2005

APPROVED BY:

Charles B. Boss	Edmond F. Bowden
Tatyana I. Smirnova	Morteza G. Khaledi (Chair of Advisory Committee)

This work is dedicated to my parents for their lifelong love and support.

It's never enough for me to return for what I have been given.

谁言寸草心，报得三春晖

Biography

Cexiong Fu was born in Hainan, P. R. China, on November 9 1977. He received his Bachelor of Science degree in chemistry from Peking University, Beijing P. R. China in July 2000. In the summer of the same year, he enrolled in the North Carolina State University to pursue a Ph. D. in analytical chemistry under the direction of Professor Morteza G. Khaledi.

Acknowledgement

First and foremost I would like to thank my thesis advisor professor Morteza G. Khaledi for guiding me in the wonderful land of separation sciences. His constructive comments and challenges always spark new ideas for the improvement of this work.

I would also like to thank the current and former members of the Dr. Khaledi research group. As the words go, one would learn the most from the people around him. I certainly believe so. My special thanks shall go to Emnet Yitbarek for his company in the lab and those memorable moments at the state basketball and football games, win or lose. I shall also thank Sam Jenkins for proofreading my thesis, in spite of being born a Tar Heel fan.

I must also acknowledge to Yujie Lu, Jubo Zhang and other Chinese students in the chemistry department for the encouragement and support for each other’s success.

Last but not least, I am forever indebted to my family: my father Shiyun Fu, my mother Yufan Chen, my sister Chunyan Fu and my wife Jianyun Zhu for their understanding and support when it was most needed. My special thank to my little love, Christopher Fu, for giving me the responsibility for being a father.

TABLE OF CONTENTS

LIST OF TABLES

LIST OF FIGURES

Page

CHAPTER 2

CHAPTER 3

CHAPTER 1

INTRODUCTION

Micellar Electrokinetic Chromatography (MEKC) is a mode of capillary electrophoresis (CE) that is capable of separating neutral and charged solutes simultaneously. The mechanisms of separation are on the basis of differential partitioning of analytes between an aqueous phase and a micellar pseudo-phase. MEKC method has been shown to have at least equivalent precision, accuracy and sensitivity with Reversed Phase Liquid Chromatography (RPLC), but with improved resolution and efficiency, as well as fast analysis time. Regulatory authorities, such as the Food and Drug Administration (FDA) in the US, have accepted MEKC method as part of the validation and quantification regulations.

Since the chemical composition of the micellar phases plays an important role in the modulation of solute-micelle interaction, there are growing interests for the developments of novel micelle systems with distinct chemical selectivities in MEKC. A large number of synthetic surfactants above their CMC, ionic polymers [1-11], dendrimers [12,13], vesicles [14-18], and liposomes [19-21] can be used as pseudo-stationary phase in MEKC. The list can be dramatically enhanced by using mixed micelles, mixed surfactant-polymer systems as well as modified-micelles using a variety of organic co-solvents, cyclodextrins [22-25], or other organic components like urea [26-29] and glucose [30,31] in order to influence retention, selectivity, the size of the elution window, and ultimately resolution in MEKC. There is only few systematic study to characterize and classify the chemical selectivity of these pseudo-phases. Hence the selection of the right pseudo-phase for a given mixture and optimization strategy in MEKC can not fully take advantage of the broad variety of pseudo phases available.

In this project, various solvents from Snyder's solvent selectivity triangle (SST) are used to study the solvent modification effects on the interactive properties of micelles. Linear Solvation Energy Relationships (LSER) is the method of choice to qualitatively describe the solvation properties of solutes in MEKC. It was discovered that the fluorinated alcohols and aliphatic alcohols represent two groups of solvents imposing different selective patterns to the micelle systems. The perfluoro alcohols are able to enhance the hydrogen bond donating ability of the micelles, while the aliphatic alcohols improve the hydrogen bond basicity of the micelles. We also investigated the influence of solvent addition on the physicochemical properties of various micelles, such as critical micelle concentration (CMC), degree of ionization and others, as well as chromatographic parameters such as elution window, migration mobility of micelle, etc. The trends of the alterations of the physicochemical properties and the chromatographic parameters, in combination with other literature findings, all suggested possible micelle transitions from a spherical micelle to a worm-like and larger micelle.

A novel Micellar Selectivity Triangle (MST) was constructed to rationalize the polar selectivities of over 70 pseudo-stationary phases. The MST is a useful tool to classify pseudo-phases according to the relative strength of their polar selectivities in terms of hydrogen bond acidity, hydrogen bond basicity, dipolarity and polarizability. Sodium Dodecyl Sulfate (SDS), bile salts, Lithium Perfluorooctanate Sulfonate (LiPFOS) and siloxane-based polymers (allyl glycidyl ether-N-methyl taurine AGENT) represent four groups of pseudo-phases with significantly different chemical selectivities. Another significance of the application of the MST is it ability to recognize pseudo-phases with similar selectivity pattern. For example, we compare the pseudo-phases that are used in EKC to estimate the octanol-water partition coefficients. We found that the micelle-water partitioning coefficients of solutes in pseudo-phases (SC, DHP, Microemulsion, SDS/Brij 35) neighboring to the octanol-water system in the MST correlate best with the octanol-water partition coefficients.

Chemometric techniques [32-34], mainly factor analysis methods, were used to characterize the selectivity patterns of pseudo-phases in MEKC as well. Principal Component Analysis (PCA) specializes in decomposing multi-dimensional, complex data into new orthogonal vectors which are referred as principal components (PCs). Although PCA method is purely a mathematical approach, it effectively removes the redundant information in the original data and keeps only the essential information for characterization and classification of the selectivity of pseudo-phases. Hierarchical clustering is also employed for selectivity patterns recognition. Hierarchical clustering utilizes a series of stepwise procedures by merging the closest objects into cluster until all the objects are joined into one "ancestor" cluster. With this agglomerative clustering approach, the most similar pseudo-phases are to be found on the descendent side at the same end node of the hierarchical tree. While hierarchical clustering is a "bottom-up" clustering method, k-means clustering is a "top-down" clustering method. In k-means algorithm, objects are assigned randomly to N preset clusters. Then, rearrangement of cluster is made by iterative partition and diffusion of objects between the clusters until a stopping criterion is met. The classifications of pseudo-phase selectivity by chemometric methods are in good agreement with those in the MST.

With the guidance of MST, we optimized the separation of 20 Phenylthiohydantoin (PTH) amino acids with a multivariate approach including surfactant types, surfactant concentrations, temperature adjustments and organic additives. A parallel separation scheme was developed to resolve the complete set of the PTH amino acids with two micellar phases of significantly different selectivity patterns. Substituent constants of amino acid residues in MEKC are compared to those in the partitioning models and biological models.

In the last part of the study, a comparison between two analogous liquid-liquid partition chromatography methods: MEKC and RPLC, is made by characterization and classification the selectivity of phases of these two methods in the MST and chemometric techniques. The study is of great significance for two reasons: first, method development could be transferred between these two separation techniques by selecting phases with similar selectivity. Second, the combinatory database of the chromatographic phases of these two methods greatly expands the range of selectivity, which is beneficial for the separation of complex mixture. The suggestions for future work are also given.

REFERENCES

1. Palmer CP: **Micelle polymers, polymer surfactants and dendrimers as pseudo-stationary phases in micellar electrokinetic chromatography**. *Journal of Chromatography, A* 1997, **780**:75-92.

2. Palmer CP, Tanaka N: **Selectivity of polymeric and polymer-supported pseudo-stationary phases in micellar electrokinetic chromatography**. *Journal of Chromatography, A* 1997, **792**:105-124.

3. Chen T, Palmer CP: **Evaluation of polymers based on a silicone backbone as pseudostationary phases for electrokinetic chromatography**. *Electrophoresis* 1999, **20**:2412-2419.

4. Leonard MS, Khaledi MG: **A mixed ionic block copolymer-surfactant pseudostationary phase in micellar electrokinetic chromatography**. *Journal of Separation Science* 2002, **25**:1019-1026.

5. Ozaki H, Terabe S, Ichihara A: **Micellar electrokinetic chromatography using high-molecular surfactants. Use of butyl acrylate-butyl methacrylate-methacrylic acid copolymers sodium salts as pseudo-stationary phases**. *Journal of Chromatography, A* 1994, **680**:117-123.

6. Palmer CP: **Recent progress in the development, characterization and application of polymeric pseudophases for electrokinetic chromatography**. *Electrophoresis* 2002, **23**:3993-4004.

7. Palmer CP: **Polymeric and polymer-supported pseudostationary phases in micellar electrokinetic chromatography: performance and selectivity**. *Electrophoresis* 2000, **21**:4054-4072.

8. Peterson DS, Palmer CP: **Novel alkyl-modified anionic siloxanes as pseudostationary phases for electrokinetic chromatography: II. Selectivity studied by linear solvation energy relationships**. *Electrophoresis* 2001, **22**:3562-3566.

9. Shamsi SA, Palmer CP, Warner IM: **Molecular micelles: novel pseudostationary phases for CE**. *Analytical Chemistry* 2001, **73**:140A-149A.

10. Tanaka N, Fukutome T, Hosoya K, Kimata K, Araki T: **Polymer-supported pseudo-stationary phase for electrokinetic chromatography. Electrokinetic chromatography in a full range of methanol-water mixtures with alkylated starburst dendrimers**. *Journal of Chromatography, A* 1995, **716**:57-67.

11. Yang S, Bumgarner JG, Khaledi MG: **Separation of highly hydrophobic compounds in MEKC with an ionic polymer**. *Journal of High Resolution Chromatography* 1995, **18**:443-445.

12. Kuzdzal SA, Monnig CA, Newkome GR, Moorefield CN: **Dendrimer electrokinetic capillary chromatography: unimolecular micellar behavior of carboxylic acid terminated cascade macromolecules**. *Journal of the Chemical Society, Chemical Communications* 1994:2139-2140.

13. Castagnola M, Cassiano L, Lupi A, Messana I, Patamia M, Rabino R, Rossetti DV, Giardina B: **Ion-exchange electrokinetic capillary chromatography with Starburst (pamam) dendrimers: a route towards high-performance electrokinetic capillary chromatography**. *Journal of Chromatography, A* 1995, **694**:463-469.

14. Agbodjan AA, Bui H, Khaledi MG: **Study of solute partitioning in biomembrane-mimetic pseudophases by electrokinetic chromatography: Dihexadecyl phosphate small unilamellar vesicles**. *Langmuir* 2001, **17**:2893-2899.

15. Agbodjan AA, Khaledi MG: **Study of solute partitioning into cationic vesicles of dihexadecyldimethylammonium bromide using electrokinetic chromatography**. *Journal of Chromatography A* 2003, **1004**:145-153.

16. Bui HH, Khaledi MG: **Determination of vesicle-water partition coefficients by electrokinetic chromatography: Study of temperature effect**. *Journal of Colloid and Interface Science* 2002, **253**:397-401.

17. Pascoe R, Foley JP: **Effect of class I and II organic modifiers on retention and selectivity in vesicle electrokinetic chromatography**. *Electrophoresis* 2002, **23**:1618-1627.

18. Pascoe Robert J, Foley Joe P: **Characterization of surfactant and phospholipid vesicles for use as pseudostationary phases in electrokinetic chromatography**. *Electrophoresis* 2003, **24**:4227-4240.

19. Burns ST, Khaledi MG: **Rapid determination of liposome-water partition coefficients (K-lw) using liposome electrokinetic chromatography (LEKC)**. *Journal of Pharmaceutical Sciences* 2002, **91**:1601-1612.

20. Burns ST, Agbodjan AA, Khaledi MG: **Characterization of solvation properties of lipid bilayer membranes in liposome electrokinetic chromatography**. *Journal of Chromatography A* 2002, **973**:167-176.

21. Malek AH, Khaledi MG: **Monitoring liposome-mediated delivery and fate of an antisense drug in cell extracts and in single cells by capillary electrophoresis with laser-induced fluorescence**. *Electrophoresis* 2003, **24**:1054-1062.

22. Quang CY, Khaledi MG: **Improved Chiral Separation of Basic Compounds in Capillary Electrophoresis Using Beta-Cyclodextrin and Tetraalkylammonium Reagents**. *Analytical Chemistry* 1993, **65**:3354-3358.

23. Aumatell A, Wells RJ: **Enantiomeric differentiation of a wide range of pharmacologically active substances by cyclodextrin-modified micellar electrokinetic capillary chromatography using a bile salt**. *Journal of Chromatography, A* 1994, **688**:329-337.

24. Copper CL, Sepaniak MJ: **Cyclodextrin-modified micellar electrokinetic capillary chromatography separations of benzopyrene isomers: correlation with computationally derived host-guest energies**. *Analytical Chemistry* 1994, **66**:147-154.

25. Quang CY, Khaledi MG: **Direct Separation of the Enantiomers of Beta-Blockers by Cyclodextrin-Mediated Capillary Zone Electrophoresis**. *Hrc-Journal of High Resolution Chromatography* 1994, **17**:99-101.

26. Liu Z, Zou H, Ye M, Ni J, Zhang Y: **Effects of organic modifiers on solute retention and electrokinetic migrations in micellar electrokinetic capillary chromatography**. *Electrophoresis* 1999, **20**:2898-2908.

27. Muijselaar PGHM, Claessens HA, Cramers CA: **Parameters controlling the elution window and retention factors in micellar electrokinetic capillary chromatography**. *Journal of Chromatography, A* 1995, **696**:273-284.

28. Terabe S, Ishihama Y, Nishi H, Fukuyama T, Otsuka K: **Effect of urea addition in micellar electrokinetic chromatography**. *Journal of Chromatography* 1991, **545**:359-368.

29. Pyell U, Buetehorn U: **Optimization of resolution in micellar electrokinetic chromatography via computer-aided simultaneous variation of concentrations of sodium dodecyl sulfate and urea as modifier**. *Journal of Chromatography, A* 1995, **716**:81-95.

30. Kaneta T, Tanaka S, Taga M, Yoshida H: **Effect of addition of glucose on micellar electrokinetic capillary chromatography with sodium dodecyl sulfate**. *Journal of Chromatography* 1992, **609**:369-374.

31. Pyell U, Buetehorn U: **Optimization strategies in micellar electrokinetic capillary chromatography. One-parameter optimizations of the concentration of sodium dodecyl sulfate and the concentration of modifiers (urea and glucose)**. *Chromatographia* 1995, **40**:175-184.

32. Jolliffe IT: **Principal component analysis**. *New York : Springer-Verlag* 1986.

33. Malinowski ER: **Factor Analysis in Chemistry**. *Wiley New York* 1991.

34. Krzanowski WJ: **Principles of Multivariate Analysis**. *Oxford Statistical Science Series 3 Oxford Science Publications* 1988.

CHAPTER 2

Solvent Modification Effects on the Chemical Selectivity of Micelle Pseudo-Phases in Micellar Electrokinetic Chromatography (MEKC)

ABSTRACT

A systematic study of the solvent modification effects on the chemical selectivity of micellar phases in MEKC is carried out. The solvent modification effects on the interactive properties of the micellar phases are evaluated with the linear solvation energy relationships (LSER). Functional group selectivities (FGS) are determined to assess the additive effects on the specific functional moieties. The FGS study corroborates the classification of organic modifiers made by the LSER.

As revealed by the conductometric titration and fluorescence probing methods, organic modifiers have substantial effects on the physiochemical properties of the micelles. In our study, the critical micelle concentrations (CMC) of these surfactants (Sodium dodecyl sulfate SDS, Lithium Perfluorooctane sulfonate LiPFOS and Tetradecyltrimethylammonium bromide TTAB) were reduced with the addition of either hexafluoro isopropanol (HFIP) or pentanol, indicating that these types of solvents are favorable for micelle formation. At high concentrations of both pentanol and HFIP, significant increases in the degree of ionization of the micelles suggest the transitions of micelle structures. These structural transitions of the micelles are related to the alterations of the chromatographic parameters such as phase ratio, elution window, selectivity, resolution and efficiency. Finally, the impacts of solvent modification of micelles on MEKC separation were demonstrated with the separations of a series of test mixtures.

1. INTRODUCTION

Surfactants are a group of amphiphilic molecules with a non-polar moiety and a polar or ionic headgroup. Above a critical micelle concentration (CMC), surfactants molecules aggregate to form micelles spontaneously. This process of micellization is primarily driven by the hydrophobic effect. The co–existence of the aqueous and non-polar regions in a micelle solution is attractive to a wide range of applications, such as microreactors [1,2] two phases catalysis [3,4], cleaning agents [5], mimicking microenvironment of biological membranes [6,7] etc. The usefulness of surfactants in liquid and electrokinetic chromatographic techniques has also been demonstrated. Micellar liquid chromatography (MLC) [8,9] utilizes micellar solutions as mobile phases in HPLC. Similar applications are found in capillary electrophoresis (CE) [10-14], where charged micelles have been employed as carriers to enable the separation of uncharged solutes. The mechanism of the separation is based on the different partition coefficients between analytes and micelles. Thus, it is essential for one to know the physio-chemical properties of the micelle solution and the primary factors governing solute–micelle interactions. A significant amount of efforts has been devoted to this field. Variables including intrinsic characters of surfactants such as surfactant chain length [15,16], headgroup [17], surfactant counter ion [18], concentration and exterior factors such as temperature [19-23], salt concentration [18,24], pH of the buffers [13,14,25], organic additives [26-30] etc., contribute collaboratively to the outcomes of micelle properties; namely, size, degree of ionization, solubility, especially of our interest, the interactive properties with solutes. In spite of the diversity of surfactants that could be manufactured, only those with low absorbance in the UV range, ionic headgroup and kraft point below ambient temperature could be readily adopted as pseudo–stationary phases in micellar electrokinetic chromatography (MEKC).

Micellization and solubilization are both temperature dependent processes. Manipulation of temperature significantly influences the solute partitioning and critical micelle concentration by alteration of water structures. For instance, the dielectric constant of water is significantly reduced at elevated temperature (84.0 at 10^{o}C and 63.7 at 70^{o}C [31]), indicating a less polar aqueous media. There are some other secondary effects with the adjustment of temperature such as mobile phase viscosity [19,20], buffer pH [21,32] and the morphology of micelles [33,34]. It shall be noted that only modest modification of selectivity could be observed even in a wide span of temperature variants. Meanwhile high temperature could cause air bubble formation, column and buffer instability and loss of mobile phase due to evaporation; therefore, reproducibility remains as a serious problem [22,23].

The counter ion of surfactants is another interesting parameter that might influence the solute–micelle interaction. The counter ion effects on the CMC, shape and size, and the surface charge of micelles followed a lyotropic series as observed by Hofmeister [35]. The lyotropic series ranks cations and anions according to their charges and hydrated sizes. There are generally two sources of counter ions: the inherent counter ions of surfactants and the salt additives. Typical lyotropic series are as follows: anions, $SO_4^{2-} < C_2H_3O^{2-} < C1^- < Br^- < NO_3^-$, $C1_4O^- < I^- < CNS^-$; cations $(CH_3)_4N^+ < NH_4^+ < Rb^+$, K^+, Na^+, $Cs^+ < Li^+ < Mg^{2+} < Ca^{2+} < Ba^{2+}$. Several works [36-39] have found that the salt effects on surfactant solutions correlated with the lyotropic series where ions with higher order in the series are more effective in reducing the surface charge density of micelles and the free energy of micellizations. Other authors [18,24] investigated the counter ion effects on the chromatographic behaviors in MEKC. Trone and co–workers [18] observed that divalent ions such as Cu^{2+} and Mg^{2+} induced the dramatic changes of chromatographic behaviors such as shortened elution window, higher efficiency and different chemical selectivity when compared with monovalent counter ions Li^+ and Na^+ coupling to the same dodecyl sulfate surfactants. It should be noted that addition of divalent counter ions would increase the kraft point of the surfactants, which leads to an elevated temperature for the separation system to prevent potential precipitation of the surfactants. In the practice of capillary electrophoresis, salt provides sufficient ionic strength, which offers conductive medium. However, high salt concentration would cause Joule heating and subsequent loss of efficiency.

The amount of the deprotonated silanol groups on the capillary interior wall governs the magnitude of the elecotroosmotic flow (EOF) which is the primary driving force to pump the eluent toward the detector. Clearly at a higher pH, a larger fraction of silanol groups is ionized which results in a greater EOF. The pH of buffer is also an effective variable to manipulate the selectivity for the separations of acidic or basic solutes. However, our study focuses on the interactions of neutral solutes with the micelles where the pH of mobile phase plays a minor role. Therefore, the effects of pH on the solute–micelle interactions are beyond the scope of this study, and have been well–studied in other works [13,25].

There were significant amounts of studies [40-44] employing various types of surfactants as pseudo-stationary phases in MEKC. The diversity of the surfactants included anionic surfactants, cationic surfactants, fluorinated surfactants, bile salts, and polymeric micelles. It is not surprising that marked differences in the elution patterns were observed in these pseudo-stationary phases. Taking advantage of the flexibility of switching pseudo-stationary phases by simply flushing the capillary with a fresh surfactant solution, it is desirable to have micelles with the most distinguished chemical selectivities and availability. Our selections of three representative micellar phases are anionic surfactant SDS, cationic surfactant TTAB, and fluorinated surfactant LiPFOS.

Addition of organic modifiers is another important avenue to manipulate selectivity in MEKC. Several reports have investigated the use of polar organic solvents as mobile phase modifier, for instance, acetonitrile (ACN), tetrahydrofuran (THF), methanol (MeOH) or propanol (PrOH) [26-29,41] etc., which are classic mobile phase components in HPLC. These polar solvents induced only minor influence on the interactive properties of the micellar phases even at high content (40% v/v). In addition, the loss of volatile polar solvents and disruption of micelles could pose potential problems in the reproducibility of separation. In a recent study done by Trone and co-workers [30], a homologous series of 1-alcohols were employed as cosurfactant with SDS micelles to correlate micelle-water partition coefficients (K_{mw}) with octanol–water partition coefficients (P_{ow}). It was found that the addition of intermediate chain-length alcohols (butanol, pentanol) improved the correlation between the two systems by eliminating the congeneric behaviors in the solutes elution patterns with less than 10% (volume fraction) organic modifiers. These observations cast new light on the selection of organic modifiers in MEKC. Instead of using polar solvents as the modifiers, the modifiers with moderate hydrophobicity and a polar functional group are more promising to modulate the interactive properties of the micelles. In this study, organic modifiers with intermediate hydrophobic tail (either hydrocarbon chain or fluorocarbon moiety) and various functional groups were used to manipulate the hydrogen bond basicity, hydrogen bond acidity, and dipolarity of the micelles, respectively. The selection of the proper solvents are based on the Snyder's solvent selectivity triangle (SST) [45], where solvents are classified by their chemical selectivities of the hydrogen bond acidity, hydrogen bond basicity and dipolarity. To the best of our knowledge, this is the first systematic study of the modifier effects on these three representative micelles.

In order to elucidate the solute-micelle interaction of pseudo-stationary phases of MEKC, especially the micellar phases modified by various organic solvents, linear solvation energy relationships (LSER) method was adopted. The LSER methodology has been useful in describing the solvation-related physicochemical and biological processes [46-48] in a quantitative manners. The LSER models have also been successful for the interpretations of solute retentions in various chromatography methods [30,49-51]. According to the LSER model, retention factor k is associated with different molecular interactions as expressed in equation 2-1.

$$\log k = c + vV + bB + aA + sS + eE \qquad \text{Eq. 2-1}$$

Where V is the McGowan characteristic volume of solute, S represents the dipolarity of solute, E is the excess molar refraction, A describes solute hydrogen bond donating ability (HBD) and B is a measure of the hydrogen bond accepting strength of solutes (HBA). Each solute parameter has a corresponding system parameter to define the magnitude of the specific molecular interactions. System parameters, v, *b, a, s, e* describe the cohesiveness, HB acidity, HB basicity, dipolarity/polarizability and ability to interact with lone pair electrons of solute respectively. Regression constant c contains information about the phase ratio of pseudo-stationary phases.

The retention factor *k* is directly related to the solute partition coefficient between water and micellar phases (K_{mw}) and phase ratio (ϕ), as describe by equation 2-2. The phase ratio for a given micellar pseudo-phase can be calculated using equation 2-3,

$$k = K_{mw} \times \phi \qquad \text{Eq. 2-2}$$

$$\phi = \frac{Vmc}{Vaq} = \frac{v(C_{surf} - CMC)}{1 - v(C_{surf} - CMC)} \qquad \text{Eq. 2-3}$$

where *v* is the partial specific volume of surfactant molecule, C_{surf} represents surfactant concentration, and CMC is the critical micelle concentration of a given surfactant. In this study, conductometric titration and fluorescent probing methods were used to measure the CMCs of the three surfactants at various temperature, ionic strength, and organic modifiers composition. Conductometric titration method is a non–intrusive method to measure the CMC. Unlike the surfactant monomers which are fully ionized below CMC, upon the formation of micelles, the surfactant molecules in the micelles are only partially ionized to maintain the stability of the aggregates. Additionally, the bulky size of the micelles reduces the apparent mobilities of these weak "electrolytes". This also explains the fact that for a micelle aggregate with aggregation number N, the conductivity of micelle ion is estimated to be $N^{2/3}$ fold of the conductivity of a single long chain ion (N is the average aggregation number of micelle) [52] Therefore, a sharper increase of conductivity over surfactant concentration would be observed before reaching the break point (CMC). Fluorescent probing method is used as a comparison method to the conductivity titration. The use of the fluorescent probes for CMC measurements has been described elsewhere [52,53]. Pyrene is selected as the fluorescent probe, mostly due to its fine structure of the vibronic bands which are sensitive to the polarity of its solvated enivironment. The intensity (I_1) of the first vibronic band at 375 nm enhances with a polar environment, meanwhile the intensity (I_3) of the third vibronic band at 385 nm increases in non–polar surroundings. Thus the ratio of I_1/I_3 is an excellent indicator of the polarity of the microenvironment sensing by pyrene molecules. Dramatic decrease of I_1/I_3 is expected above the CMC, because pyrene has strong affinity with the non-polar interior of micelles, a region less exposed to the aqueous environment which leads to the decrease of I_1 and the increase of the intensity I_3 of the third peak.

2. EXPERIMENTAL

All of the micellar electrokinetic chromatographic experiments were performed on a laboratory-made CE system equipped with a 0-30 kV high-voltage power supply (Spellmann, Plainview, NY), a SSI 500 variable UV-Visible detector (SSI, State College, PA). Electropherograms were collected with the PC/chrom+ program version 4.0.9 (H&A Scientific, Greenville, NC). A 50-µm-i.d. × 375-µm-o.d. fused-silica capillary (Polymicro Technologies, Phoenix, AZ) was used. The total length of the capillary was 70 cm, with an effective length of 50 cm. Newly installed capillary was conditioned with a rinsing procedure as Mili-Q water for 20 min, 0.1 mM NaOH for 20min to ionize free silanol groups, and methanol for 20 min to clean organic impurity, finally buffer solution was running through capillary for 20 min and equilibrium at less 6 hours. The capillary was thermostated at 30.0 ^{o}C with a circulating oil bath (Lauda K-2/R, Brinkmann Instruments, Westbury, NY), and two 250-mL jacketed beakers were used to maintain the buffer reservoirs at 30.0 ^{o}C. A positive 20 kV was applied throughout the experiment, except in cationic surfactant TTAB, the polarity of power supply was reversed in order to acquire separation. The wavelength of the UV detector was set at 214 nm unless notify in the specific case.

All the test solutes for the training set and organic solvents were purchased from Aldrich (Milwaukee, WI), and were used as received without further purification. SDS (Sodium dodecyl sulfate) and TTAB (Tetradecyltrimethylammonium bromide) were obtained from Sigma (St. Louis, MO), LiPFOS (Lithium Perfluorooctane Sulfonate) was a gift from 3M. The fluorocarbon alcohols (Aldrich) were 2,2,2-trifluoroethanol (TFE), 2,2,3,3,3-pentafluoropropanol (FPrOH), 2,2,3,3,4,4,4-heptafluorobutanol (FBuOH), and 2,2,3,3,4,4,5,5–Octafluoropentanol (FPeOH), hexafluoro isopropanol (HFIP) were all purchased from Sigma (St. Louis, MO). SDS and TTAB solutions were made in 20 mM potassium phosphate buffer (pH 7.0) and LiPFOS solution was made in 20 mM lithium buffer (pH 7.0). Required amount of organic modifiers were then added to the surfactant solutions. All the surfactant solutions were filtered with a 0.45-μm polypropylene filter and sonicated for ~10 min. Water used in the study was all doubly distilled.

Solutes were dissolved in methanol with concentrations around 40 μM, which were introduced to the capillary by a 2-s hydrodynamic injection at the anodic end of the capillary. The retention time of each solute was averaged from three measurements. The retention factor was calculated using eq 2-4:

$$k = \frac{t_r - t_{eo}}{t_{eo}(1 - t_r / t_{mc})} \qquad \text{Eq. 2-4}$$

where t_{eo} is the migration time of an unretained solute, t_r is the retention time of a solute, and t_{mc} is the migration time of the micelle. Methanol was used as the electroosmotic flow (EOF) marker, dodecanophenone as the t_{mc} marker.

Conductivity experiments were performed on a Fisher Model 4079 digital conductivity meter. Temperature of titration system was regulated with a Fisher Scientific Isotemp Refrigerated Circulator (Model 90). Triplicate measurements for each titration point were collected. The CMC value was determined by the crosspoint of the two linear segments of the plot of the conductivity vs. surfactant concentration as shown in figure 2-1, 2-2, 2-3 and 2-4. Note that non-linear regression was used for the second segment (above CMC) in the cases of high content of pentanol or ionic strength.

Fluorescence measurements were performed on a Perkin-Elmer luminescence spectrometer (LS 50B). Excitation wavelength was set at 336 nm; the slit widths for excitation and emission were adjusted to 5 nm and 1.5 nm respectively. Pyrene concentration at 2×10^{-7} mole/L is diluted enough to avoid the quenching effects by the formation of pyrene excimer. The break point in the plot of I_1/I_3 vs. surfactant concentration indicates the CMC as shown in figure 2-5.

3. RESULT AND DISCUSSION

3.1 Conductometric titration and fluorescent probing measurements.

Table 2-1 summarizes the CMC data for the three representative surfactants under various temperatures, ionic strengths and organic additives. Our CMC values by conductometric titration and fluorescent probing method agree fairly well with the published results. Some variances exist because of the differences in the measuring techniques, buffer solutions and temperature etc. It shall be noted that the break point for determining CMC becomes ambiguous in the presence of high percentage of pentanol. This explains the fact that the CMC values in the pentanol-modified micelle systems have considerably larger variance with the literature values. As the data shows, TTAB obtains the lowest CMC in the pure aqueous solution without buffering, due to its longer C14 hydrophobic tail. LiPFOS with a shorter chain length (i.e. C8) has a CMC value close to that of SDS (C12), because fluorocarbon chains are more hydrophobic than their hydrocarbon counterparts. Also, comparisons between conductometric titration and fluorescent probing methods were made. The CMC values between these two methods are in good agreement, considering that pyrene as a probe has different affinities with these three micelles. As a result, subtle difference from conductivity method is expected in fluorescent probing. It is worth noting that the I_1/I_3 values for pyrene in these three surfactant solutions above CMC are SDS (1.07), TTAB (1.15) and LiPFOS (1.29) respectively. As discussed in the introduction, I_1/I_3 value is a good measure of the polarity of pyrene sensoring. Thus, Pyrene senses a slightly more non–polar environment in SDS than TTAB. This could be explained by the strong interactions between the π electrons of the aromatic rings of pyrene molecules and the positively charged ternary amines in the TTAB headgroups which make the pyrene molecules favorably 'adsorb' on the TTAB headgroup region. In the case of fluorosurfactant (LiPFOS), Pyrene senses a more polar and water accessible surroundings, probably due to the hydrocarbon–fluorocarbon phobicity repelling the bulky pyrene molecules from accessing the fluorocarbon-rich LiPFOS micelle interior. The CMC values of the three surfactants all show consistent reduction with the addition of salt. It is mostly due to electrolytes effectively shielding the electrostatic repulsions between charged headgroups of surfactant, consequently lowering the free energy for micellization.

The addition of organic solvents to the surfactant solutions has significant effects on micellization, ionization of micelle and interactive properties with solutes. The use of aliphatic alcohols as organic modifiers in MEKC has been extensively investigated. [27,29,54-56]. It is widely known that the short chain alcohols (up to three carbons) dissolve mainly in the polar aqueous phase and medium chain alcohols (e. g., butanol and pentanol) solubilize in the palisade layer of the micelles (including the polar headgroups and the first two or three carbons of the surfactants in the perimeter). As shown in table 2-2, the CMCs remain rather constant or only exhibit subtle change in the presence of small concentrations of pentanol. As the pentanol concentration continues to increase, the CMCs tend to decrease gradually until reaching a point, where CMC values decrease dramatically. The CMC depression at moderate modifier concentration is because the solubilized pentanol molecules function as spacers between the charged headgroup of surfactant, alleviating the electrostatic repulsion of the charged headgroups. Meanwhile, the sudden drop of the CMC with high pentanol concentration indicates a transition of the shape and size of the micelles. Some authors [57,58] reported similar observations. They found that at high pentanol concentration, the pentanol molecules saturated the palisade layer and further penetrated into the non-polar core of the micelles. Hence, the pentanol-swollen effects promote the transition of micelles from a spherical to a larger wormlike micelle. Schemic description of the transition could be found in figure 2-6. The applications of the fluorinated alcohols as micellar phase modifiers, especially hexafluoro isopropanol (HFIP), do not gain much attention as those with hydrocarbon alcohols. In our study, the addition of HFIP can also significantly decrease the CMCs of three surfactants but in a different fashion as compared with pentanol. Both modifiers reduce the CMC of SDS micelles in a similar way. However, pentanol is more effective in reducing the CMC of LiPFOS micelles. This shall be explained by the special structure of HFIP molecules. On one hand, the branching -CF_3 groups of HFIP could provide extra spacing to reduce the electrostatic repulsion between the surfactant headgroups. On the other hand, the steric hindrance becomes pronounced in the presence of high HFIP concentration. Obviously, the bulky fluorocarbon side chains of LiPFOS micelles is less likely to favor the solubilization of the branching HFIP over pentanol, although one might argue that the hydrocarbon-fluorocarbon phobicity will hamper the solubilization of pentanol as well. Further evidences of the retention factors of these two solvents in LiPFOS micelles support that pentanol (k=0.345) has stronger binding affinity to LiPFOS micelles than HFIP (k=0.119). In the case of TTAB micelles, HFIP is more capable of reducing the CMC of TTAB micelles than pentanol. This is explained by the fact that highly electronegative fluorine groups on the side chain of HFIP could form intermolecular hydrogen bonds with the ammonium headgroups of the TTAB micelles and stabilize the charges on the headgroups. Therefore, much less free energy was required for the micellization.

The degree of ionization (α) of these micelles is calculated using the method described by Evans [52]. The degree of ionization is found to relate to the ratio of the slopes of two linear segments of the conductivity titration curve after and before CMC as equation 2-5, where S_1, S_2 are the slopes of two linear segments of the titration curve before and after the CMC break point respectively.

$$\alpha = \frac{S_2}{S_1} \qquad \text{Eq. 2-5}$$

The degree of ionization of micelle is associated with the hydration of the hydrophilic headgroups and the counter ions binding. Inferring from the slopes of the conductivity titration curve, the order of ionization for three micelles are as following from highest to lowest, LiPFOS (0.64) > SDS (0.47) > TTAB (0.26). Addition of organic modifiers also has substantial effects on the ionization of micelles. As shown in table 2-2, the degree of ionization do not show noticeable change at modifiers concentration smaller than 1.1% (v/v), and increase gradually with the addition of more modifiers, finally a sudden increase of ionization appears in the presence of the highest modifier concentration applied. The solubilization of organic additives greatly impacts the ionization of micelles for two reasons: first, modifier molecules intercalate between the surfactant headgroups, reducing the electrostatic repulsion. Second, as the less polar solvents replace water at palisade layer it creates a less polar medium between surfactant headgroups which strengthened the headgroup repulsions. In our case the relative dielectric constant of 17.8 for HFIP [59] and 15.1 for pentanol [31] are much lower than that of water which is 78. The repulsion force between two objects with the same type of charge is governed by the Columbic Law (Eq. 2-6), where F is the strength of repulsion force, q_1, q_2 are the charges of the two particles, ε_o represents electric constant of the vacuum, ε is the relative electric constant of the media and r is the distance between the two particles.

$$F = \frac{q_1 q_2}{4\pi\varepsilon_o \varepsilon r^2} \qquad \text{Eq. 2-6}$$

At organic solvent concentration lower than 1.1% (v/v), the distance between two neighboring headgroups increase as solvent molecules solubilize in the palisade layer well counteracting the effect of decreasing polarity of the media in the palisade layer. However at very high organic solvent (4.34% pentanol), the ionization of SDS micelles almost double (1.7) and the polarity at palisade layer is close to one half of the polarity of water ($\varepsilon \approx 40$) [60]. The sudden increase of the repulsion force (~6 folds) could not be balanced merely by the increase in distance (~2.4 fold increase in r to balance) while maintain the overall size of the micelle. A possible explanation would be a solvent–swollen mechanism, where the solubilized organic solvents penetrate into the hydrocarbon core of the micelles after saturating the palisade layers, swelling the size of micelles. The overall appearance would be a larger micelle and a lower surface charge density. The conclusion is in agreement with our CMC measurement, and other results from the viscosity, light scattering and calorimetric experiments [58,61,62]

3.2 Phase Ratio Calculation

Phase ratio is an important parameter in chromatographic methods that has pronounced effects on separation time and efficiency. In LC methods, phase ratio cannot be determined accurately and varies between columns. By contrast, phase ratio in MEKC could be accurately determined from the known intrinsic volumes of surfactants, the CMC and the operating surfactant concentration. Since phase ratio is only related to the intrinsic properties of surfactant molecules and other mobile phase components, consistent value of phase ratio is expected under the same experimental conditions (e. g., buffer, ionic strength, temperature, additives). Unfortunately, investigations on the phase ratio in MEKC are scarce, especially for micelle systems in the presence of organic solvents. Hereby, we will calculate the phase ratio for the three representative micelles together with the organic modifiers. Phase ratio for micelles in the presence of organic additive is calculated with equation 2-7.

$$\phi \approx \frac{k}{1+k} \cdot C_{org} \cdot v_{org} + (C_{surf} - CMC) \cdot v_{surf} \qquad \text{Eq. 2-7}$$

In the equation, ϕ represents the phase ratio of the micellar system, C_{org} is the total concentration of organic solvent added, ν_{org} is the partial molar volume of organic solvent, C_{surf} represents the total concentration of surfactant, CMC is the critical micelle concentration in the presence of organic solvent, ν_{surf} is the partial molar volume of surfactant molecule and k is the retention factor of organic solvent in a given micelle phase. The phase ratio data are summarized in table 2-3. For the single surfactant systems, LiPFOS and SDS have almost identical phase ratios owing to the similar sizes (v_{LiPFOS}= 256 ml/mol, v_{SDS}= 250 ml/mol) of the surfactant monomers and the identical concentrations. The TTAB micelles have much lower phase ratios because of a smaller concentration applied. The application of small concentration of TTAB is due to the strong absorbance of bromide ion at lower UV wavelength and the oxidation of bromide ion on the cathode end at high concentration. For the micelle phase with organic additives, phase ratio generally increases with all the additives in the study. We also examined the relationships between the phase ratio ϕ (table 2-3) and the regression constant *c* of the LSER models (table 2-5). SDS micelle has the lowest phase ratio and the most negative *c* among the systems. SDS / TFE, SDS / Hexanone and SDS / Butyronitrile possess values of phase ratios that are very similar to the SDS micelle. As expected, the LSER regression constants for these phases are almost equivalent and not significantly different from SDS (-1.75). The fluorinated alcohol series (FPrOH, FBuOH, FPeOH and HFIP) have the highest phase ratios among all the systems, however only FPeOH and HFIP are significantly larger (less negative) in their LSER regression constant c. It is surprising to observe that pentanol with an intermediate phase ratio has the least negative regression constant *c*. The reason for this anomaly is still unclear.

Since all the phase ratios are measured with the same buffering condition as the MEKC running buffer in the study, (e. g. , 20 mM Phosphate buffer at pH 7.00 and temperature at 30.0^{o}C) the phase ratio data could be used to calculate partition coefficients of solutes from the known retention factor data in MEKC.

3.3 Solvent Effect on Solute Retention in MEKC

Polar organic solvents such as MeOH, ACN, and THF are effective in adjusting selectivity in RPLC, mainly by modulating the polarity of mobile phase. In MEKC, however, the instability of micelles under high organic solvent contents restrains the use of polar solvents to a narrow range of modifier concentration. Alternatively, we utilize a series of moderately hydrophobic solvents with polar functional headgroups and non-polar moieties. The surfactant-like organic solvents take part in the micellization as co-surfactants. The selection of hydrophobic organic modifiers was based on their selectivity classifications according to the Solvent Selectivity Triangle (SST). In Snyder's scheme [45], aliphatic alcohols represent a group of solvents with stronger hydrogen bond basicity, weaker dipolarity and hydrogen bond acidity; fluorinated alcohols feature a group of solvents with stronger HB acidity but much weaker HB basicity; while ketones, nitriles and esters are considered as dipolar solvents but weak HB acidity and basicity (in comparison with water). Note that the length of the hydrophobic tail does not have any significant effect on the solvent polarity in terms of hydrogen bonding and dipolarity.

In this part of the study, we will focus on the solvent modification effects on various chromatographic parameters such as, selectivity, resolution, efficiency and elution window. The LSER methodology is adopted to elucidate the solvent modification effects on the solute–micelle interactions. Contributions of the individual functional group to the solute retention are also rationalized and compared with different solvent modification effect.

3. 3. a. LSER Analysis of Solvent Modification Effect.

LSER regression data are summarized in table 2-5. We have discussed the relationship between regression constant *c* and the phase ratio. It is important to note that phase ratio only affects the retention strength of solutes without the alteration of selectivity. In other words, relative band spacing remains unchanged.

Figure 2-7 shows the variations of the LSER system parameters for the selected pseudo-phases. It is clear that the hydrophobic effect (*v*V) and type A hydrogen bond acidity term (*b*B) are the two primary forces that govern the solute retentions in all the systems under study. The large positive value of hydrophobic parameter (*v*) indicates that micellar phases are less cohesive than the aqueous mobile phase and more favorable for cavity formation. The hydrophobic parameter *v* is statistically constant for the solvent–modified SDS pseudo-phases. As can be seen that the addition of organic modifiers has little or no effect on cohesiveness of micellar phases at concentrations below 5% (v/v). Thus, hydrophobic effect is the driving force for solute partitioning into micelle; however, it does not play a significant role on influencing selectivity or relative band spacing in MEKC for the solvent-modified SDS micelles.

Type A hydrogen bonding interaction (*b*B) where solute acts as hydrogen bond acceptor and micellar system as hydrogen bond donor, is another important type of interaction governing the solute–micelle interactions. A large negative hydrogen bond acidity parameter (*b*) for the micellar phases is observed, implying that the aqueous phase is a better hydrogen bond donor than the micellar phases. Addition of a weaker hydrogen bond donor such as aliphatic alcohols or non hydrogen bond solvents likes, nitriles, ketones and esters, result in the SDS micelles that are weaker hydrogen bond donors as evident by the large negative *b* coefficients. In contrast, fluorinated alcohols are classified as strong hydrogen bond donating solvents in the Snyder's selectivity triangle. As expected, the incorporation of these strong hydrogen bond donor solvents into SDS micelles enhances the hydrogen bond donating ability of the micelles. The observation is in accordance with the Snyder's classification of organic solvents.

Type B hydrogen bonding interaction (*a*A), in which solute acts as hydrogen bond donor and micelle phase as hydrogen bond acceptor, is also influenced by the organic solvent modifications of the SDS micelles. For the SDS micelle in a purely aqueous solution, the system hydrogen basicity parameter (*a*) is slightly negative. However, with the incorporation of moderate HB basic solvents such as aliphatic alcohols, the hydrogen bond acceptor strengths of the micellar phases increase as evident from the less negative system parameters (*a*). Also, addition of poor hydrogen bond acceptor solvents, such as fluorinated alcohols, dramatically reduces the hydrogen bond basicity of the SDS micelles, appearing as a larger negative *a* value. Other solvents such as nitriles, esters and ketones, do not have significant influences on the hydrogen bond basicity of the micellar phase probably because of similar hydrogen bond accepting ability between these solvents and water. The scale of type B hydrogen bonding interaction is relatively small in comparison with the two primary factors: hydrophobic effect and type A hydrogen bonding. However, with the addition of organic solvents, flexible control of the hydrogen bond basicity of micellar phases could be achieved. This is especially useful for a complex mixture involving hydrogen bond donating solutes.

The system parameter (*s*) measures the capability of micelle to induce dipole-type interactions with solutes. Negative values of coefficient *s* for all the solvent–modified micelle systems suggest that the aqueous phase is more dipolar than the micellar phase and dipolar type interactions are not favorable for solute partitioning into micelle. It shall be noted that small *s* parameter (more negative) is observed with the incorporation of the less dipolar solvent pentanol. By contrast, addition of fluorinated alcohols moderately enhances the dipolar interactions strength of the micellar phase. Surprisingly, we did not observe any noticeable change of dipolar type interactions induced by nitriles, sulfone, ketones and esters, solvents that are more dipolar than water according to Snyder's classification of solvents. The reason for this unexpected behavior is not known at current stage, and requires more investigation.

Micelle interaction strength with n or π electron pairs is described by the system parameter *e* which is a positive value for the SDS micelles, indicating an exoergic process for solute-micelle interaction. Moreover, addition of aliphatic alcohols, nitriles, ketones, sulfone and ester results in an increase of *e* that suggests an increase in the polarizability of the micelles. An opposite trend is observed when fluorinated alcohols are added. In fact the coefficient *e* is smaller for the fluorinated alcohols with longer chain length (from 0.32 for TFE to a value close to zero for HFIP, FBuOH, and FPrOH).

This unique observation is also found in the fluorinated stationary phases in RPLC [63]. The different extents of interaction energy between fluorocarbon–π electrons interaction and hydrocarbon–π electrons interaction were demonstrated by Kawahara *et. al.* [64]. In their findings, hydrocarbon-π electrons interaction had a negative (attractive) interaction energy (–1.47kcal/mol), in comparison to the positive (repulsive) interaction energy (+0.12 kcal/mol) for fluorocarbon - π electrons interaction.

The LSER results clearly indicate that moderately hydrophobic organic modifiers with various polarities and hydrogen bonding properties could be used to modify the selectivity of micellar phases in a controllable fashion. Among them, Pentanol is capable of tuning the micelles into a better hydrogen bond acceptor but less dipolar micelle. In contrast, fluorinated alcohols series enhance the hydrogen bond acidity and dipolarity of the micelles. This tendency is more remarkable with the increase in the fluorocarbon chain length. A third group of solvents consist of nitriles, ketones, ester and sulfone did not modify the micelle dipolarity as expected. The LSER analysis also included modifying the SDS micelles with two nonionic surfactants Brij 35 (Polyoxyethylene Lauryl Ether) and FC 4430 (Perfluorobutane sulfonate based polymer) which have similar structure as to the aliphatic alcohols and fluorinated alcohols respectively. These nonionic surfactants have a nonpolar backbone and an uncharged bulky polar headgroup with abundance of electron–rich oxygen atoms. The aliphatic alcohols are likely to be the mimics of Brij 35, both have an aliphatic non-polar moiety and an oxygen-containing headgroup. The solvation properties of SDS-Brij 35 mixed micelles are similar to those of SDS micelles modified with aliphatic alcohols, for example both exhibit strong HB acceptor strength but less HB acidic and dipolar than SDS micelles without modifiers.

Surprisingly, Brij 35 and FC 4430, in spite of having significant differences in chemical compositions, exert very similar selectivity patterns on the micelle polarity and hydrogen bonding capability.

3.3. b Functional Groups Selectivity (τ)

While the LSER study gives systematic information on the interactive properties of micelle phases, functional groups selectivity (τ) provides complementary information on the extent of the interactions between the individual functional groups and the micelles. Functional groups selectivity (τ) for a group *R*, is defined as the ratio of the retention factors (or partition coefficient) between mono substituted benzene (C_6H_5-*R*) and benzene (C_6H_5-*H*), shown in Eq. 2-8.

$$\tau = \frac{k(C_6H_5 - R)}{k(C_6H_5 - H)} = \frac{K(C_6H_5 - R)}{K(C_6H_5 - H)} \qquad \text{Eq. 2-8}$$

Also, the free energy for transferring a functional group from the aqueous phase to micellar phase could be derived from equation 2-8 and expressed as Eq. 2-9:

$$\Delta\Delta G_R = -RT \ln \frac{K(C_6H_5 - R)}{K(C_6H_5 - H)} = -RT \ln \tau \qquad \text{Eq. 2-9}$$

Where, $\Delta\Delta G_R$ is the transfer free energy of functional group R from the aqueous phase into the micellar phase and τ is the functional group selectivity of R.

Functional group selectivity for a variety of functional groups is summarized in table 2-6. Positive value of transfer free energy suggests that the addition of the functional group to benzene is not favorable for solute–micelle interactions. In contrast, a negative transferring energy indicates a favorable substituent for solute–micelle interaction. Thus, Functional group selectivity could be a useful tool to monitor the modification effect of organic solvents on different type of micelles.

Solute groups #1-3 are typical hydrophobic solutes with aliphatic side chains and the partition process is predominantly determined by the hydrophobic effect. It could be seen that the addition of short chain halogenated alcohols (i.e. TFE, TCE) has only minor impact on the selectivity of the aliphatic groups at low concentration, however as the solvent content approaches to a higher value, these alkyl functionalities interact less strongly with the modified micellar phases. The enhanced interactions between the alkyl groups and the aqueous phase suggest that the aqueous phase becomes less polar with the incorporation of high concentration of the short-chain halogenated alcohols. For longer fluorinated alcohols such as FPeOH and HFIP-modified SDS micelles, the alkyl groups selectivities are significantly reduced (less negative) indicating weaker interactions with these fluorinated alcohols modified SDS micelles. A probable explanation is that these long fluorinated alcohols refine the SDS micelles with a fluorocarbon-like interface hampering the solvation of the alkyl functionalities (hydrocarbon-fluorocarbon phobicity). The addition of pentanol, butyl formate and hexanone do not have noticeable effects on the selectivities of the aliphatic groups. However the addition of tetramethylene sulfone induces a less favorable solvation environment for the hydrophobic functionalities. Incorporation of non-ionic surfactants is also found less favorable for the solvation of alkyl groups. It is noteworthy that all the additives that make the SDS micelles less favorable for hydrophobic alkyl groups have rather bulky polar headgroups. Thus, steric hindrance of these bulky headgroups could be responsible to block the access of hydrophobic alkyl groups, resulting in free energies less favorable for transferring alkyl groups from the aqueous phase to the micellar phases. In the case of fluorinated alcohols, the hydrocarbon-fluorocarbon phobicity is the primary cause for the less favorable interaction between the alkyl groups and the modified SDS micelles. We also investigated the free energy of transferring hydrophobic solutes in fluorinated surfactant (LiPFOS) and cationic surfactant (TTAB). It can be seen that LiPFOS micelle is the most unfavorable surfactant system for transferring of hydrocarbon solutes, mostly due to hydrocarbon–fluorocarbon phobicity. As expected, addition of fluorinated alcohol (HFIP) to LiPFOS would increase the 'fluorocarbon richness' in the micelle; therefore the solvation of alkyl groups is even less favorable in LiPFOS/HFIP system. The addition of pentanol to fluorosurfactant (LiPFOS) has an opposite effect to that of HFIP, which alleviates the hydrocarbon-fluorocarbon phobia effect in the LiPFOS micelles. TTAB with a longer hydrophobic tail provides a more hydrophobic environment in the micelles, which enhances the affinities of alkyl groups with the micellar phases. Again, the addition of fluorinated alcohol (HFIP) dramatically reduces micelle ability to accommodate alkyl groups. Free energy of transfer of a methylene group ($\Delta\Delta G_{CH_2}$) is –2.40 kJ/mol in SDS micelles and –1.99 kJ/mol in LiPFOS micelles in our study. And these values are in good agreement with the published values such as –2.50 kJ/mol [65] and -2.30 kJ/mol [66] for SDS micelles, -1.84 kJ/mol [66] and –1.73 kJ/mol [67] in sodium perfluoro ocatanoate (SPFO). Even with different headgroups and counter ions, the methylene selectivity in the fluorosurfactants obtain a similar value, indicating that the methylene selectivity is less dependent on the surfactant headgroups and counter ions [17].

Solutes 4 to 7 are halogen moieties which are strongly polarizable, with large sizes (except for F) and weak hydrogen bonding capabilities according to their LSER descriptors. As expected, large negative free energies of transfer of these moieties are observed which is attributed to the size and polarizability of these halogen moieties. Halogen selectivities show similar values in most solvent–modified SDS micelle systems, with the exception of SDS micelles modified with fluorinated alcohols where the fluorine groups obtained stronger affinity with fluorinated alcohol modified SDS micelle. However, other halogen moieties receive less negative energies of transfer mostly due to the weakened hydrophobic effect with the addition of fluoroalcohols. Likewise, halogen moieties (except F) interact more weakly with fluorinated surfactant LiPFOS, which is the most cohesive surfactant among all in this work. An opposite trend is observed for the halogen selectivity in the cationic surfactant TTAB system. Halogen moieties have the strongest affinities with TTAB micelles. These results can be attributed to the cooperative effects from enhanced hydrophobic effect and strong polarizability of TTAB micelles. The addition of HFIP weakens the interaction of halogen moieties with TTAB micelles which is consistent with the observation in SDS and LiPFOS micelle systems.

Solutes 8-12 are dipolar and hydrogen bond acceptor functional groups that are readily involved in dipolar–type interaction and type B hydrogen bond interaction. These solutes have a positive or slightly negative selectivity with the exception of solute 12 in SDS micelle, implying that SDS micelle is a moderately polar and weak hydrogen bond donating micelle. However, functional selectivity of these solutes could be regulated by the addition of different types of solvent additives. For example, the addition of fluorinated alcohol series into SDS micelle greatly enhances the interactions between these solutes and micelle. Fluoroalcohols make the SDS micelles stronger HB donors that interact strongly with these hydrogen bond acceptor functionalities. By contrast, pentanol, butyl formate, hexanone and TMS modified SDS micelles have weaker interactions with these polar solutes, probably because these solvents are good hydrogen bond acceptors. As for the LiPFOS micelle, these polar solutes have intense interactions with the strong HB acidic LiPFOS micelle. By comparison, these polar solutes only have weak affinity with much weaker HB donating TTAB micelles (strong HB accepting micelles). Again, the strength of the interactions of these polar with the TTAB micelles could be easily controlled by the addition of HB acidic solvent (fluorinated alcohols) or HB basic solvents (pentanol, Butyronitrile, Hexanone etc.) respectively.

The selectivity of hydrogen bonding solute 13,14 is somewhat difficult to interpret, partly because these hydroxyl moieties play dual roles in hydrogen bonding type interactions as they behave both as HB donors and acceptors. However the relative value of the selectivity between these two solutes is extremely sensitive to the hydrogen bonding capability. For example, LiPFOS is a strong HB acidic micelle and interacts more favorably with a better HB acceptor solute benzyl alcohol (B = 0.56) than with phenol (B = 0.3). Likewise, TTAB as a strong HB basic micelle binds strongly with the better HB donating solute Phenol (A = 0.6) in comparison with benzyl alcohol (A = 0.33).

3. 3. c. Elution profiles in various pseudo-phases.

In order to illustrate the effects of solvent modifications on the MEKC selectivity, the elution profiles of a test mixture of five carefully selected substituted benzenes with known LSER descriptors in various pseudo-phases were examined (figure 2-8). The LSER descriptor values for the five compounds are listed in table 2-7. As can be seen from the chromatograms, different elution patterns are observed for various solvent-modified SDS and LiPFOS micelles. The chromatograms clearly indicate that significant differences in elution patterns among various solvent-modified SDS and LiPFOS micelles. More importantly, the selectivity control is accomplished through the judicious selections of organic modifiers with defined selectivity.

Chromatogram A shows that two pairs of solutes (2, 3) and (4, 5) coelute when using SDS micelle alone. However, with the addition of a hydrogen bond acidic solvent (HFIP) or a hydrogen bond basic solvent (PeOH), one can easily resolve these two coeluted solute pairs. Obviously, different elution patterns exist for these resolved separations, implying different types of underlying interactions. Based on the LSER results, pentanol modified SDS micelle is a more hydrogen bond basic and less dipolar micelle system. On the other hand, HFIP modified SDS micelle appears to be a stronger hydrogen bond acidic and more dipolar micelle. As a result, hydrogen bond donor solute 4-ethyl phenol (A = 0.55) will favor the retention in the SDS/PeOH system over hydrogen bond accepting solute Methyl benzoate (A = 0). Meanwhile, polar solute 1-chloro-4-nitrobenzene (S = 1.17) tends to have less retention in SDS/PeOH micelle as compared to the non–polar solute toluene. The trend is reversed in the SDS/HFIP pseudo-phase, where better HB accepting solute Methyl benzoate (B = 0.46) resides longer in the HB acidic pseudo phase than weak HB donor 4-ethyl phenol. Meanwhile, more polar 1-chloro-4-nitrobenzene interacts much stronger with HFIP/SDS than non–polar solute toluene.

Studies of other solvent-modified micelles provide interesting information on the solvent modification effects, although this test mixture is not completely resolved in these micelle systems. For instance, in chromatogram D, TFE could only slightly alter the selectivity of the test mixture as compared to SDS alone (chromatogram A). This is partly because TFE mainly modifies the aqueous phase and has little impact on the solute-micelle interactions. The TCE modified SDS micelle (Chromatogram E) have very similar LSER parameter as the TFE modified SDS micelle, except for being a weaker HB acceptor. Thus, the HB acidic solute 2 has smaller affinity to the SDS/TCE system, which is due to the deceased HB basicity (more negative *a*) of the micelle system. It is also observed that the critical pair solute 4 and 5 still remains unresolved in the SDS/TCE system. Another set of solvents includes butyl formate, hexanone and tetramethylene sulfone. As indicated by the LSER model, these solvent–modified micelles share a variety of common characters such as very weak HB basicity, HB acidity close to the aqueous phase (*a* is not significantly different from zero) and similar strengths for the cavity formation. They differ only by the capability for dipolar–type interaction following the order Butyl formate < Hexanone < Tetramethylene sulfone. As a result, there is only a minor difference in the elution patterns of the three micellar systems as shown in chromatogram F, G, H. We also examine the impact of urea as an additive to the SDS micelles. Urea is widely used to increase the solubility of very hydrophobic solute in aqueous solution. In our study, 3 M urea was applied along with 400 mM pentanol to modify the SDS micelles. As seen in chromatogram I and B, the elution order of solutes 3 and 4 is reversed with the addition of urea. Furthermore, higher efficiency is obtained in presence of urea. It shall be noted that the increase of separation time in Fig 2-8 I was due to a relative high SDS concentration (80 mM).

Interestingly, elution patterns of the test solutes are almost identical for non-ionic surfactants modified SDS micelles (chromatogram J and K), despite that these two non-ionic surfactants have significant different nonpolar backbone compositions and polar headgroups. However, these observations are consistent with the LSER characterizations of these two micelle systems. Furthermore, it should be noted that the elution order of solutes in chromatogram (J, K) are in great similarity with that of the pentanol modified SDS systems. The only difference is that solute 2 binds less strongly in these non-ionic surfactants modified SDS micelles. In previous LSER discussion, pentanol can be seen as a ‘miniature’ non-ionic surfactant with only slightly stronger HB acidity and less dipolarity. Therefore, it is not surprising that solute 2, as a good hydrogen bond acceptor, would have decreased affinity with a much weaker hydrogen bond acidic micellar phases (SDS with Brij 35 or FC 4430).

LiPFOS is known as a very cohesive, weak HB basic and strong HB acidic micelle. In chromatogram L, non–polar solute toluene interacts weakly with LiPFOS because the relative difficulty to create cavity in a rather cohesive micellar microenvironment. HB donating solute 2 (4-ethyl phenol) also tends to have less retention with the weak HB basic micelle. In the meantime, HB acceptor solute 3 (methyl benzoate) has longer retention in a more HB acidic LiPFOS micelle. One interesting finding is that with the addition of hydrocarbon solvent pentanol to the LiPFOS micelle, one would observe a similar elution order of the test mixture to that in the SDS/PeOH. On the other hand, one can resolve the critical pair solutes 2 and 5 with the addition of fluorinated alcohol HFIP to the fluorosurfactant while maintaining the relative spacing of other solutes. The observations are evident that organic solvents (especially PeOH and HFIP) are capable of refining the chemical selectivity of the micellar phases.

3.4 Chromatographic parameters of solvent-modified micelles

The quality of separation is generally evaluated by three chromatographic criteria: speed, efficiency and selectivity. In a previous section, we have demonstrated the usefulness of organic solvents in manipulating chemical selectivity of pseudo stationary phases. The other two important elements of the chromatographic performance will be discussed in this section.

In MEKC, electroosmotic flow (EOF) carries the eluent to the downstream. In the meantime, negatively charged micelles migrate in the opposite direction of EOF at its own electrophoretic mobility μ_{ep}. Generally, μ_{EOF} is greater than micelle mobility μ_{ep}. Consequently, all eluents migrate toward the cathode where the detector is installed. According to the mechanism of separation, it could be seen that there is a window between the μ_{EOF} eluent and micelle migration, as a consequence, solutes are separated within the window and the relative elution sequence is determined by their affinities to the micelles. It is worth noting that when μ_{EOF} equals to the electrophoretic mobility of micelle, micelle phases become stagnant in the capillary because of the offset between μ_{EOF} and $\mu_{ep.}$ In this special case, one can have an infinite window of separation similar to the typical HPLC. The magnitude of the μ_{EOF} depends on factors such as ionization of silanol groups on the capillary wall, ionic strength and buffer composition etc. While the magnitude of the EOF governs the duration of separation time, the change of the EOF does not necessarily alter the selectivity of separation since it uniformly affects all the solutes without selective effects.

Mobility calculation is performed following equations 2.10–12, where L_t is the total length of the capillary, L_d is the effective capillary length from the injection end to the detector, V is the applied voltage in volts, while t_{eo} and t_{mc} are the retention times of the EOF and the micelle respectively. Peak capacity is evaluated with according to equation 2-13, where t_{mc}/t_{eo} represents the elution window and the typical average efficiency (N) using here is 350,000 theoretical plates.

$$\mu_{EOF} = \frac{L_t \cdot L_d}{V \cdot t_{eo}} \qquad \text{Eq. 2-10}$$

$$\mu_{APP} = \frac{L_t \cdot L_d}{V \cdot t_{mc}} \qquad \text{Eq. 2-11}$$

$$\mu_{EP} = \mu_{APP} - \mu_{EOF} \qquad \text{Eq. 2-12}$$

$$\text{Peak Capacity} = 1 + \frac{\sqrt{N}}{4} \ln(\frac{t_{mc}}{t_{eo}}) \qquad \text{Eq. 2-13}$$

$$N = 5.54 \cdot (\frac{t_R}{W_{1/2}})^2 \qquad \text{Eq. 2-14}$$

Figure 2-9 shows that the size of elution window increases linearly with the SDS concentrations in the range of our study while the EOF remains rather constant with the SDS concentrations ranging from 20 mM to 60 mM (the variations of t_{eo} are within ±3.0%), indicating that the eletrophoretic mobility of SDS micelles increases as the surfactant concentration increases. With this information, we can optimize the separation window by adjusting the SDS concentrations. However, as stated earlier, changing SDS concentration alone has little or no effect on the separation selectivity. Addition of organic solvent is an advisable solution combining both manipulation of chemical selectivity of pseudo-stationary phases and adjustment of the elution window. Interestingly, significantly different trends are observed as pentanol addition to three different SDS concentrations (figure 2-10). At 20 mM SDS, addition of pentanol results in a gradually narrower elution window. At 30 mM SDS, however, an abrupt reduction of elution window is initially seen upon addition of small amount of pentanol, which levels off at higher pentanol concentration. The trend at 40 mM SDS is different from the first two. The elution window first shows an increase with the addition of pentanol. After reaching a highest value, the elution window becomes narrower at higher pentanol concentration. Within the range of SDS concentrations we studied, the elution windows show consistent reduction with high concentration of pentanol which is explained by the reduced micelle mobility of the pentanol-swollen micelles with larger sizes and lower surface charge densities.

Table 2-8 summarizes the solvent effects on various chromatographic parameters such as, elution window, EOF and efficiency etc. The SDS / TMS system has the highest elution window (5.02) and FC4430-modified SDS, TTAB/HFIP, TTAB/PeOH, and LiPFOS/PeOH are among the systems with the smallest elution window. The differences in elution windows, which are directly related to the relative magnitudes of the EOF and the micelle electrophoretic mobility, are governed by the zeta potential of capillary walls, zeta potential of the pseudo phases, ionic strength and the viscosity of the eluent. For example, the addition of a small amount of TFE to SDS micelles results in only a small reduction of μ_{EOF} and μ_{EP} to a similar degree, leading to a slightly widened elution window as compared to the unmodified SDS system. However, at a higher TFE concentration (2M), the μ_{EOF} is decreased to a larger extent than the μ_{EP}, implying that water properties (viscosity, dielectric constant etc.) undergo dramatic changes under high TFE content. A different trend is observed with the non–ionic surfactants modified SDS systems. In these micelle systems, the bulky neutral headgroups of non–ionic surfactants effectively shield the charges of the SDS headgroups attributing to a decrease of the surface charge density. Additionally, the sizes of the micelles increase substantially with the incorporation of these bulky non–ionic surfactants. These modification effects lead to a sudden drop of μ_{EP}, with only a slightly decreases in μ_{EOF}. As a result, a narrower elution window is observed in these non-ionic surfactants modified micelles. For the fluorinated alcohols, the modification only increases the elution window slightly. We also interested in comparing the modification effects of the hydrocarbon solvent (PeOH) and the fluorocarbon solvent (HFIP) on the other two surfactants (TTAB and LiPFOS). TTAB has a lower value of elution window. It shall be noted that TTAB monomer has strong electrostatic interactions with the ionized silanol groups on the capillary wall, resulting in adsorption of TTAB monomers on the capillary walls and reversal of the EOF. Addition of pentanol and HFIP both decrease the elution window of modified TTAB systems. LiPFOS has a wider elution window than the SDS micelle. Addition of HFIP does not have a noticeable effect on the size of elution window of the LiPFOS micelles. By contrast, pentanol greatly reduces the elution window of the LiPFOS micelles. The peak capacity is one of the chromatographic parameters closely related to the size of elution window. As shown in table 2-8, the peak capacities in all solvent-modified micelle system are rather large owing to the high efficiency in MEKC. Given the large number of solutes could be accommodated into one separation theoretically and the substantial alterations of chemical selectivity in solvent-modified micellar phases, these systems are powerful to resolve very complicated mixture.

We also successfully separated a group of eleven Methylthiohydantoin (MTH) amino acids with diverse polarities and more complicated structures. Detail structures information of these eleven MTH amino acids are summarized in table 2-9. Figures 2-11 A to H show excellent separations of these 11 MTH amino acids in various micellar phases. The elution patterns show generally three groups of compounds that tend to cluster together, specifically peaks 1 and 2, 3 to 6, and 7 to 11. Note that peaks1 and 2 are very polar compounds, 7 and 8 could be slightly negatively charged, solutes 9 to 11 are highly hydrophobic and 3 to 6 represent compounds with nonpolar and polar moiety at the same time.

In the SDS micelles without any additive (Fig. 2-11 A), solute pairs 1 and 2, 5 and 6, 8 and 9 are considered as critical solute pairs. Addition of hexanone and hexanitrile (Fig. 2-11 D and E) could enhance the resolution of solute pair 8 and 9. However the other two critical solute pairs still remain incompletely resolved. In the case of the pentanol modified SDS micelles (Fig. 2-11 B), although 5 and 6 are baseline resolved, unfortunately solute 6 co-elutes with solutes 4 and 3. Similarly, addition of HFIP (Fig. 2-11 C) could easily resolve the 8 and 9 solute pair, but could only partially resolve the other two solute pairs. It seems that the SDS based micelle systems are not sensitive enough to differentiate the slight variance of the polarities of the more polar solutes. LiPFOS micelle shows better ability to resolve the polar solute in this case, probably due to the strong hydrogen bond acidity of the micelle that could specifically bind with the HB donor functionality of polar solutes. Therefore, it is not surprising to observe that these three critical pairs of solute are baseline resolved in LiPFOS micelle (Fig. 2-11 F). Even the most 'notorious' critical pair polar solutes 1 and 2 has a resolution of 1.48 in this LiPFOS system. We also notice a decrease of retention for hydrophobic compounds such as MTH Phenylalanine and MTH Tryptophan. It is due to the cohesive nature of LiPFOS that suppress the accommodation of these bulky hydrophobic solutes. Addition of pentanol (Fig. 2-11 G) and HFIP (Fig. 2-11 H) has significant impact on the alteration of elution pattern, however complete resolution of all 11 solutes is only seen in LiPFOS micelle (figure 2-11 F).

4. CONCLUSIONS

The systematic study of the solvent modification effects on micelle systems suggests that organic solvents are capable of modulating the chemical natures of micelles. Among the solvents, those with hydrophobic moieties can incorporate into micelle as co-surfactants and most effectively modify the solute-micelle interactive properties.

LSER study points out that the chemical selectivity of micellar phases could be tailored in a predictable manner with the judicious selection of a specific solvent. For instance, fluorinated alcohols, represented by HFIP, are strong HB acidity, weak HB basicity solvents. The addition of these fluoroalcohols can enhance the hydrogen bond acidity of micelles while reduce the hydrogen bond acceptor strength of micelles. By contrast, aliphatic alcohols, such as pentanol, are weak HB donor and dipolar, but strong HB acceptor solvents. As expected, the addition of pentanol enhances the HB basicity of the micelles while weakens the HB donating strength and dipolarity of micelles. Functional group selectivity study provided further evidences to support these solvent modification effects.

We also investigated the origins of the solvent modification effects by monitoring the changes in physicochemical properties of the micelles such as the degree of ionization and critical micelle concentration. Solvent addition also has an impact on the chromatographic behaviors such as phase ratio, elution window, resolution and efficiency. Generally, enhanced separations could be seen by the addition of organic solvents in terms of efficiency, resolution and selectivity.

REFERENCES

1. Pileni MP: **Water in oil colloidal droplets used as microreactors**. *Advances in Colloid and Interface Science* 1993, **46**:139-163.

2. Pileni MP: **Reverse micelles as microreactors**. *Journal of Physical Chemistry* 1993, **97**:6961-6973.

3. Tascioglu S: **Micellar solutions as reaction media**. *Tetrahedron* 1996, **52**:11113-11152.

4. Piszkiewicz D: **Positive cooperativity in micelle-catalyzed reactions**. *Journal of the American Chemical Society* 1977, **99**:1550-1557.

5. Smulders E, Krings P, Verbeek H: **Recent developments in the field of laundry detergents and cleaning agents**. *Tenside, Surfactants, Detergents* 1997, **34**:386-392.

6. Fendler JH: **Membrane Mimetic Chemistry**. *Wiley New York* 1982.

7. Garavito RM, Ferguson-Miller S: **Detergents as tools in membrane biochemistry**. *Journal of Biological Chemistry* 2001, **276**:32403-32406.

8. Khaledi MG: **Hydrophobic Selectivity in Micellar and Hydro Organic Reversed-Phase Liquid-Chromatography**. *Analytical Chemistry* 1988, **60**:876-887.

9. Berthod A, Garcia-Alvarez-Coque C: **Chromatographic Science Series. Volume 83. Micellar Liquid Chromatography**. *Marcel Dekker: New York and Basel* 2000.

10. Khaledi MG: **Micelles as separation media in high-performance liquid chromatography and high-performance capillary electrophoresis: overview and perspective**. *Journal of Chromatography, A* 1997, **780**:3-40.

11. Terabe S: **Micellar electrokinetic chromatography**. *Analytical Chemistry* 2004, **76**:240A-246A.

12. Terabe S, Otsuka K, Ando T: **Electrokinetic chromatography with micellar solution and open-tubular capillary**. *Analytical Chemistry* 1985, **57**:834-841.

13. Khaledi MG: **High-Performance Capillary Electrophoresis: Theory, Techniques, and Applications**. *Wiley, New York* 1998.

14. Khaledi MG, Smith SC, Strasters JK: **Micellar electrokinetic capillary chromatography of acidic solutes: migration behavior and optimization strategies**. *Analytical chemistry* 1991, **63**:1820-1830.

15. Trone MD, Khaledi MG: **Characterization of chemical selectivity in micellar electrokinetic chromatography: V. The effect of the surfactant hydrophobic chain**. *Journal of Microcolumn Separations* 2000, **12**:433-441.

16. Vitha MF, Carr PW: **A linear solvation energy relationship study of the effects of surfactant chain length on the chemical interactions governing retention and selectivity in micellar electrokinetic capillary chromatography using sodium alkyl sulfate buffers**. *Separation Science and Technology* 1998, **33**:2075-2100.

17. Trone MD, Khaledi MG: **Characterization of chemical selectivity in micellar electrokinetic chromatography. 4. Effect of surfactant headgroup**. *Analytical Chemistry* 1999, **71**:1270-1277.

18. Trone MD, Mack JP, Goodell HP, Khaledi MG: **Characterization of chemical selectivity in micellar electrokinetic chromatography VI. Effects of surfactant counter-ion**. *Journal of Chromatography A* 2000, **888**:229-240.

19. Reid RC, Prausnitz JM, Poling BE: **The Properties of Gases and Liquids, 4th ed,**. *McGraw-Hill, New York,* 1987.

20. Pyell U, Buetehorn U: **Optimization strategies in micellar electrokinetic capillary chromatography. Optimization of the temperature of the separation capillary**. *Chromatographia* 1995, **40**:69-77.

21. Cross RF, Cao J: **Salt effects in capillary zone electrophoresis. II. Mechanisms of electrophoretic mobility modification due to Joule heating at high buffer concentrations**. *Journal of Chromatography, A* 1998, **809**:159-171.

22. Djordjevic NM, Houdiere F, Lerch G, Fitzpatrick F: **Application of temperature and applied voltage programming in micellar electrokinetic capillary chromatography**. *Journal of High Resolution Chromatography* 1999, **22**:443-448.

23. Djordjevic NM, Fitzpatrick F, Houdiere F: **Separation of peptides utilizing ultrahigh-temperature micellar electrokinetic chromatography**. *Electrophoresis* 2001, **22**:2398-2402.

24. Peterson AG, Foley JP: **Influence of the inorganic counterion on the chiral micellar electrokinetic separation of basic drugs using the surfactant N-dodecoxycarbonylvaline**. *Journal of Chromatography, B: Biomedical Sciences and Applications* 1997, **695**:131-145.

25. Quang CY, Strasters JK, Khaledi MG: **Computer-Assisted Modeling, Prediction, and Multifactor Optimization in Micellar Electrokinetic Chromatography of Ionizable Compounds**. *Analytical Chemistry* 1994, **66**:1646-1653.

26. Ozaki H, Ichihara A, Terabe S: **Micellar electrokinetic chromatography using high-molecular-mass surfactants: comparison between anionic and cationic surfactants and effects of modifiers**. *Journal of Chromatography, A* 1995, **709**:3-10.

27. Chen N, Terabe S: **A quantitative study on the effect of organic modifiers in micellar electrokinetic chromatography**. *Electrophoresis* 1995, **16**:2100-2103.

28. Liu Z, Zou H, Ye M, Ni J, Zhang Y: **Effects of organic modifiers on solute retention and electrokinetic migrations in micellar electrokinetic capillary chromatography**. *Electrophoresis* 1999, **20**:2898-2908.

29. Pascoe R, Foley JP: **Effect of class I and II organic modifiers on retention and selectivity in vesicle electrokinetic chromatography**. *Electrophoresis* 2002, **23**:1618-1627.

30. Trone MD, Leonard MS, Khaledi MG: **Congeneric behavior in estimations of octanol-water partition coefficients by micellar electrokinetic chromatography**. *Analytical Chemistry* 2000, **72**:1228-1235.

31. **CRC Handbook 85th**.

32. Vindevogel J, Sandra P: **Micellar electrokinetic chromatography of ionic compounds: the analysis of hop bitter acids**. *Journal of High Resolution Chromatography* 1991, **14**:795-801.

33. Hoiland H, Blokhus AM: **Solubilization in aqueous surfactant systems**. *Handbook of Surface and Colloid Chemistry (2nd Edition)* 2003:345-385.

34. Ljosland E, Blokhus AM, Veggeland K, Backlund S, Hoeiland H: **Shape transitions in aqueous micellar systems as a function of pressure and temperature**. *Progress in Colloid & Polymer Science* 1985, **70**:34-37.

35. F. Hofmeister: *Arch. Exp. Pathol. Pharmacol.* 1888, **24**:247 - 260.

36. Cohen I, Vassiliades T: **Critical phenomena in aqueous solutions of long-chain quaternary ammonium salts. II. Specificity and lightscattering properties**. *Journal of Physical Chemistry* 1961, **65**:1774-1781.

37. Mukerjee P, Mysels KJ, Kapauan P: **Counterion specificity in the formation of ionic micelles: size, hydration, and hydrophobic bonding effects**. *Journal of Physical Chemistry* 1967, **71**:4166-4175.

38. Anacker EW, Ghose HM: **Counterions and micelle size. I. Light scattering by solutions of dodecyltrimethylammonium salts**. *Journal of Physical Chemistry* 1963, **67**:1713-1716.

39. Lindenbaum S, Boyd GE: **Osmotic and activity coefficients for the symmetrical tetraalkyl ammonium halides in aqueous solution at 25.degree**. *Journal of Physical Chemistry* 1964, **68**:911-917.

40. Yang S, Bumgarner JG, Khaledi MG: **Chemical selectivity in micellar electrokinetic chromatography. II. Rationalization of elution patterns in different surfactant systems**. *Journal of Chromatography, A* 1996, **738**:265-274.

41. Poole SK, Poole CF: **Characterization of surfactant selectivity in micellar electrokinetic chromatography**. *Analyst (Cambridge, United Kingdom)* 1997, **122**:267-274.

42. Yang S, Khaledi MG: **Chemical selectivity in micellar electrokinetic chromatography: characterization of solute-micelle interactions for classification of surfactants**. *Analytical chemistry* 1995, **67**:499-510.

43. Palmer CP, Terabe S: **Micelle Polymers as Pseudostationary Phases in MEKC: Chromatographic Performance and Chemical Selectivity**. *Analytical Chemistry* 1997, **69**:1852-1860.

44. Palmer CP: **Polymeric and polymer-supported pseudostationary phases in micellar electrokinetic chromatography: performance and selectivity**. *Electrophoresis* 2000, **21**:4054-4072.

45. Snyder LR, Carr PW, Rutan SC: **Solvatochromically based solvent-selectivity triangle**. *Journal of Chromatography* 1993, **656**:537-547.

46. Platts JA, Abraham MH, Butina D, Hersey A: **Estimation of Molecular Linear Free Energy Relationship Descriptors by a Group Contribution Approach. 2. Prediction of Partition Coefficients**. *Journal of Chemical Information and Computer Sciences* 2000, **40**:71-80.

47. Zhao YH, Le J, Abraham MH, Hersey A, Eddershaw PJ, Luscombe CN, Boutina D, Beck G, Sherborne B, Cooper I, et al.: **Evaluation of human intestinal absorption data and subsequent derivation of a quantitative structure-activity relationship (QSAR) with the Abraham descriptors**. *Journal of Pharmaceutical Sciences* 2001, **90**:749-784.

48. Abraham MH: **Scales of solute hydrogen bonding: their construction and application to physicochemical and biochemical processes**. *Atual. Fis.-Quim. Org., [Conf. Latinoam. Fis.-Quim. Org.], 1st* 1991:89-109.

49. Tan LC, Carr PW: **Study of retention in reversed-phase liquid chromatography using linear solvation energy relationships. II. The mobile phase**. *Journal of Chromatography, A* 1998, **799**:1-19.

50. Tan LC, Carr PW, Abraham MH: **Study of retention in reversed-phase liquid chromatography using linear solvation energy relationships. I. The stationary phase**. *Journal of Chromatography, A* 1996, **752**:1-18.

51. Muijselaar PG, Claessens HA, Cramers CA: **Characterization of Pseudostationary Phases in Micellar Electrokinetic Chromatography by Applying Linear Solvation Energy Relationships and Retention Indexes**. *Analytical Chemistry* 1997, **69**:1184-1191.

52. Evans HC: **Alkyl sulfates. I. Critical micelle concentrations of the sodium salts**. *Journal of the Chemical Society, Abstracts* 1956:579-586.

53. Kalyanasundaram K, Thomas JK: **Environmental effects on vibronic band intensities in pyrene monomer fluorescence and their application in studies of micellar systems**. *Journal of the American Chemical Society* 1977, **99**:2039-2044.

54. Katsuta S, Tsumura T, Saitoh K, Teramae N: **Control of selectivity in micellar electrokinetic chromatography by modification of sodium dodecyl sulfate micelles with organic hydroxyl compounds**. *Journal of Chromatography, A* 1995, **705**:319-324.

55. Adlard M, Okafo G, Meenan E, Camilleri P: **Rapid estimation of octanol-water partition coefficients using deoxycholate micelles in capillary electrophoresis**. *Journal of the Chemical Society, Chemical Communications* 1995:2241-2243.

56. Aiken JH, Huie CW: **Effects of 1-alkanols on separation performance in micellar electrokinetic capillary chromatography**. *Journal of Microcolumn Separations* 1993, **5**:95-99.

57. Forland GM, Samseth J, Gjerde MI, Hoiland H, Jensen AO, Mortensen K: **Influence of alcohol on the behavior of sodium dodecylsulfate micelles**. *Journal of Colloid and Interface Science* 1998, **203**:328-334.

58. Zana R: **Aqueous Surfactant-Alcohol Systems - a Review**. *Advances in Colloid and Interface Science* 1995, **57**:1-64.

59. Hong D-P, Hoshino M, Kuboi R, Goto Y: **Clustering of Fluorine-Substituted Alcohols as a Factor Responsible for Their Marked Effects on Proteins and Peptides**. *Journal of the American Chemical Society* 1999, **121**:8427-8433.

60. Mukerjee P, Cardinal JR: **Benzene derivatives and naphthalene solubilized in micelles. Polarity of microenvironments, location and distribution in micelles, and correlation with surface activity in hydrocarbon-water systems**. *Journal of Physical Chemistry* 1978, **82**:1620-1627.

61. Lindemuth PM, Bertrand GL: **Calorimetric observations of the transition of spherical to rodlike micelles with solubilized organic additives**. *Journal of Physical Chemistry* 1993, **97**:7769-7773.

62. Grieser F: **Nitrite quenching of terbium luminescence in sodium dodecyl sulfate solutions**. *Journal of Physical Chemistry* 1981, **85**:928-932.

63. Reta M, Carr PW, Sadek PC, Rutan SC: **Comparative study of hydrocarbon, fluorocarbon, and aromatic bonded RP-HPLC stationary phases by linear solvation energy relationships**. *Analytical Chemistry* 1999, **71**:3484-3496.

64. Kawahara S-I, Tsuzuki S, Uchimaru T: **Theoretical Study of the C-F/p Interaction: Attractive Interaction between Fluorinated Alkane and an Electron-Deficient p-System**. *Journal of Physical Chemistry A* 2004, **108**:6744-6749.

65. Russell JC, Whitten DG: **Photochemical reactivity in organized assemblies. 24. Solute partitioning in aqueous surfactant assemblies: comparison of hydrophobic-hydrophilic interactions in micelles, alcohol-swollen micelles, microemulsions, and synthetic vesicles**. *Journal of the American Chemical Society* 1982, **104**:5937-5942.

66. Fisicaro E, Pelizzetti E, Bongiovanni R, Borgarello E: **Perfluorinated surfactants: properties and applications. I. Thermodynamic properties**. *Colloids and Surfaces* 1990, **48**:259-275.

67. Carlfors J, Stilbs P: **Solubilization in sodium perfluorooctanoate micelles: a multicomponent self-diffusion study**. *Journal of Colloid and Interface Science* 1985, **103**:332-336.

68. Benito I, Garcia MA, Monge C, Saz JM, Marina ML: **Spectrophotometric and conductimetric determination of the critical micellar concentration of sodium dodecyl sulfate and cetyltrimethylammonium bromide micellar systems modified by alcohols and salts**. *Colloids and Surfaces, A: Physicochemical and Engineering Aspects* 1997, **125**:221-224.

69. Mukerjee P, Mysels KJ: *Critical Micelle Concentrations of Aqueous Surfactant Systems (NSRDS-NBS 36)*; 1971.

70. Shinoda K, Hato M, Hayashi T: **Physicochemical properties of aqueous solutions of fluorinated surfactants**. *Journal of Physical Chemistry* 1972, **76**:909-914.

71. Kissa E: **Fluorinated Surfactants: Synthesis, Properties, Applications Surfactant Science Series; V. 50**. *New York Marcel Dekker, Inc.* 1994:220-243.

72. Yoda K, Tamori K, Esumi K, Meguro K: **Critical micelle concentrations of fluorocarbon surfactant mixtures in aqueous solution**. *Journal of Colloid and Interface Science* 1989, **131**:282-283.

73. Shinoda K, Soda T: **Partial molal volumes of surface-active agents in micellar, singly dispersed, and hydrated solid states**. *Journal of Physical Chemistry* 1963, **67**:2072-2074.

74. Tamori K, Esumi K, Meguro K: **Phase behavior in the mixed surfactant system: lithium dodecyl sulfate/lithium perfluorooctanesulfonate/water**. *Journal of Colloid and Interface Science* 1991, **142**:236-243.

75. De Lisi R, Milioto S, Verrall RE: **Partial molar volumes and compressibilities of alkyltrimethylammonium bromides**. *Journal of Solution Chemistry* 1990, **19**:665-692.

76. Vikingstad E: **Partial molal volumes and compressibilities of n-alcohols in micellar solutions of sodium alkylcarboxylates**. *Journal of Colloid and Interface Science* 1979, **72**:75-80.

77. Mehta SK, Sharma AK, Bhasin KK, Parkash R: **Physicochemical properties in mixtures of hexamethylphosphortriamide with 2,2,2-trichloroethanol or 2,2,2-trifluoroethanol or 1,1,1,3,3,3-hexafluoropropan-2-ol**. *Fluid Phase Equilibria* 2002, **201**:203-216.

78. Muto Y, Yoda K, Yoshida N, Esumi K, Meguro K, Binana-Limbele W, Zana R: **The effect of alcohols on the properties of aqueous solutions of hydrocarbon and fluorocarbon surfactants**. *Journal of Colloid and Interface Science* 1989, **130**:165-175.

79. Abboud JLM, Notario R: **Critical compilation of scales of solvent parameters. Part I. Pure, non-hydrogen bond donor solvents**. *Pure and Applied Chemistry* 1999, **71**:645-718.

Table 2-1 Comparison of the CMC data (in mM) from different methods and literature values.

Temperature (303.0 K) Surfactant	Conductivity titration	Fluorescent pyrene probing	Literature values
SDS			
water	7.80 (0.09)	8.80(0.12)	8.00[a], 8.44[b], 8.33[b]
20 mM phosphate buffer	5.97 (0.06)		
400 mM PeOH	4.96 (0.05)	5.21 (0.08)	4.17[c]
400 mM HFIP	5.22 (0.08)		
LiPFOS			
Water	7.36 (0.08)	8.00 (0.11)	6.3[d], 7.5[e], 6.72[f]
20 mM phosphate buffer	6.02 (0.07)		
400 mM PeOH	5.25 (0.06)		
400 mM HFIP	5.21 (0.07)		
TTAB			
Water	3.76 (0.05)	2.96 (0.07)	3.51[b], 3.60[b]
20 mM phosphate buffer	2.83 (0.04)		
200 mM PeOH	3.33 (0.04		1.00[c]
200 mM HFIP	2.79 (0.05)		

a: Ref. [68]

b: Ref. [69]

c: Ref. [58]

d: Ref. [70]at temperature 25.0 ^{o}C

e: Ref. [71]

f: Ref. [72]

For abbreviation, see text in the experimental section.

Table 2-2 Selected organic additives effect on surfactant CMC and degree of ionization (α). (T=303.15 K)

(PeOH) v/v%	0.11	0.26	0.43	1.10	2.20	3.20	4.34
SDS (CMC)	7.56	7.42	7.28	6.38	6.11	5.95	5.21
α	0.47	0.46	0.49	0.52	0.54	0.63	0.79
LiPFOS (CMC)	7.02	6.71	6.71	6.14	5.50	5.22	4.55
α	0.64	0.62	0.61	0.67	0.73	0.72	0.74
TTAB	4.03	4.47	4.02	3.77	3.54	3.29	3.11
α	0.27	0.28	0.27	0.25	0.26	0.29	0.34
(HFIP) v/v %	0.104	0.208	0.416	1.04	2.08	3.12	4.16
SDS (CMC)	7.60	7.42	7.16	6.73	6.29	5.95	5.21
α	0.48	0.49	0.45	0.47	0.48	0.60	0.55
LiPFOS (CMC)	6.67	7.34	7.56	6.58	6.37	6.08	5.20
α	0.62	0.64	0.65	0.65	0.73	0.80	0.82
TTAB(CMC)	3.70	3.70	3.80	3.22	3.00	2.61	2.34
α	0.25	0.23	0.28	0.21	0.21	0.23	0.33

Table 2-3 Phase ratios of micelle systems

Pseudo phases	$\nu_{Solvent}$ ml/mol	40 mM SDS ν_{SDS} = 250 ml/mol [a]		40 mM LiPFOS ν_{LiPFOS} = 256 ml/mol [b]		10 mM TTAB ν_{TTAB} = 325 ml/mol [c]	
		k	ϕ	k	ϕ	k	ϕ
No additive			0.0085		0.0087		0.0023
PeOH	102.4[d]	0.208	0.0157	0.345	0.0194	0.398	0.008
TFE	72.3[e]	0.047	0.0100	0.063	0.0106	0.111	0.0036
HFIP	105.7[e]	0.726	0.0264	0.119	0.0134	2.268	0.008
FPrOH	99.7[f]	0.550	0.0228	0.091	0.0122	0.837	0.0067
FBuOH	125.6[f]	0.896	0.0205	0.147	0.0121	6.152	0.0130
FPeOH	140.1[f]	1.066	0.0231	0.175	0.0131	16.686	0.0154
Butyl formate	115.1[g]	0.168	0.0111	0.960	0.0174	0.239	0.00439
Hexan-2-one	124.1[g]	0.134	0.0101	1.360	0.0161	0.204	0.00428
Butyronitrile	87.8[g]	0.034	0.0098	0.391	0.0188	0.058	0.00314

ν: Partial molar volume of molecules, k: retention factor, ϕ: phase ratio

a: Ref. [73]

b: Ref. [74]

c: Ref. [75]

d: Ref. [76]

e: Ref. [77]

f: Ref. [78]

g: Ref. [79]

Table 2-4 LSER descriptors for training solutes.

	Solutes	V	B	A	S	E
1	Benzene	0.72	0.14	0.00	0.52	0.61
2	Toluene	0.86	0.14	0.00	0.52	0.60
3	Ethylbenzene	1.00	0.15	0.00	0.51	0.61
4	Propylbenzene	1.14	0.15	0.00	0.50	0.60
5	Butylbenzene	1.28	0.15	0.00	0.51	0.60
6	o-xylene	1.00	0.16	0.00	0.56	0.66
7	naphthalene	1.09	0.20	0.00	0.92	1.34
8	1-methylnaphthalene	1.23	0.20	0.00	0.90	1.34
9	Chlorobenzene	0.84	0.07	0.00	0.65	0.72
10	Bromobenzene	0.89	0.09	0.00	0.73	0.88
11	Iodobenzene	0.98	0.12	0.00	0.82	1.19
12	4-chlorotoluene	0.98	0.07	0.00	0.67	0.71
13	4-bromotoluene	1.03	0.09	0.00	0.74	0.88
14	Acetophenone	1.01	0.48	0.00	1.01	0.82
15	Propyrophenone	1.15	0.51	0.00	0.95	0.80
16	Butyrophenone	1.30	0.51	0.00	0.95	0.80
17	valerophenone	1.44	0.50	0.00	0.95	0.80
18	Benzonitrile	0.87	0.33	0.00	1.11	0.74
19	nitrobenzene	0.89	0.28	0.00	1.11	0.87
20	benzyl chloride	0.98	0.33	0.00	0.82	0.82
21	1-chloro-4-nitrobenzene	1.01	0.25	0.00	1.17	0.98
22	Phenyl acetate	1.07	0.54	0.00	1.13	0.66
23	Methylbenzoate	1.07	0.46	0.00	0.85	0.73
24	ethyl benzoate	1.21	0.46	0.00	0.85	0.69
25	Propyl benzoate	1.35	0.46	0.00	0.80	0.68
26	methyl-2methylbenzoate	1.21	0.43	0.00	0.87	0.77
27	3-chloro acetophenone	1.14	0.40	0.00	1.07	0.92
28	4-chloroacetophenone	1.14	0.44	0.00	1.09	0.96
29	Resorcinol	0.83	0.58	1.10	1.00	0.98
30	Phenol	0.78	0.30	0.60	0.89	0.81
31	Phenethyl alcohol	1.06	0.66	0.30	0.83	0.78
32	3-methyl phenol	0.92	0.34	0.57	0.88	0.82
33	4-ethyl phenol	1.06	0.36	0.55	0.90	0.80
34	3,5-dimethyl phenol	1.06	0.36	0.57	0.84	0.82
35	3-nitrophenol	0.95	0.23	0.79	1.57	1.05

36	Benzyl alcohol	0.92	0.56	0.33	0.87	0.80
37	4-methyl benzyl alcohol	1.06	0.60	0.33	0.88	0.81
38	4-fluorophenol	0.79	0.23	0.63	0.97	0.67
39	3-chlorophenol	0.90	0.15	0.69	1.06	0.91
40	3-bromo phenol	0.95	0.16	0.70	1.15	1.06
41	4-iodophenol	1.03	0.20	0.68	1.22	1.38

Table 2-5 Solvent effects on the interactive properties of SDS micelles.

Pseudo-phases	C	v	b	a	s	e	R^2
1) 40 mM SDS	-1.75	2.91	-1.76	-0.15	-0.49	0.36	0.982
	(0.10)	(0.10)	(0.08)	(0.06)	(0.09)	(0.09)	
2) 40 mM SDS + 400 mM PeOH	-1.27	2.93	-2.44	-0.02	-0.81	0.40	0.983
	(0.09)	(0.08)	(0.09)	(0.05)	(0.07)	(0.07)	
3) 40 mM SDS + 1% Brij 35	-1.76	2.83	-2.24	0.08	-0.55	0.53	0.981
	(0.08)	(0.08)	(0.07)	(0.04)	(0.05)	(0.05)	
4) 40 mM SDS + 1% FC4430	-1.96	2.95	-2.32	0.04	-0.55	0.54	0.982
	(0.08)	(0.08)	(0.07)	(0.04)	(0.05)	(0.05)	
5) 40 mM SDS + 400 mM TFE	-1.69	2.81	-1.68	-0.29	-0.47	0.32	0.983
	(0.07)	(0.08)	(0.07)	(0.04)	(0.06)	(0.06)	
6) 40 mM SDS + 400 mM TCE	-1.40	2.74	-1.71	-0.57	-0.51	0.23	0.982
	(0.08)	(0.09)	(0.08)	(0.05)	(0.07)	(0.06)	
7) 40 mM SDS + 400 mM FPrOH	-1.65	2.89	-1.67	-0.54	-0.31	0.04	0.975
	(0.09)	(0.09)	(0.09)	(0.06)	(0.08)	(0.07)	
8) 40 mM SDS + 200 mM FBuOH	-1.62	3.05	-1.98	-0.51	-0.30	-0.08	0.986
	(0.09)	(0.09)	(0.09)	(0.06)	(0.08)	(0.07)	
9) 40 mM SDS + 200 mM FPeOH	-1.46	2.85	-1.60	-0.59	-0.51	0.15	0.975
	(0.10)	(0.10)	(0.09)	(0.05)	(0.08)	(0.08)	
10) 40 mM SDS + 400 mM HFIP	-1.56	2.81	-1.49	-0.62	-0.36	0.10	0.984
	(0.08)	(0.08)	(0.07)	(0.04)	(0.06)	(0.06)	
11) 40 mM SDS + 400 mM BuCN	-1.66	2.85	-1.98	-0.12	-0.50	0.38	0.982
	(0.08)	(0.08)	(0.07)	(0.04)	(0.06)	(0.06)	
12) 40 mM SDS + 100 mM HexCN	-1.77	2.96	-1.92	-0.11	-0.61	0.50	0.979
	(0.11)	(0.11)	(0.08)	(0.06)	(0.10)	(0.10)	
13) 40 mM SDS + 100 mM Hexanone	-1.66	2.93	-2.25	-0.06	-0.67	0.59	0.973
	(0.13)	(0.14)	(0.10)	(0.07)	(0.12)	(0.12)	
14) 40 mM SDS + 100 mM Butyl Formate	-1.53	2.97	-2.26	-0.04	-0.81	0.51	0.979
	(0.11)	(0.09)	(0.10)	(0.06)	(0.09)	(0.09)	
15) 40 mM SDS + 100 mM Tetramethlene Sulfone (TMS)	-1.80	2.81	-2.14	-0.03	-0.54	0.47	0.978
	(0.10)	(0.09)	(0.10)	(0.05)	(0.09)	(0.09)	

Table 2-6 Functional Group Selectivity (FGS) in various pseudo-phases.

Functional group	$\Delta\Delta G_R$ (kJ/mol)					
	40 mM SDS	40 mM SDS 200 mM TFE	40 mM SDS 400 mM TFE	40 mM SDS 2M TFE	40 mM SDS 200 mM TCE	40 mM SDS 400 mM TCE
1) CH_3	-2.40	-2.56	-2.50	-2.31	-2.51	-2.45
2) CH_2CH_3	-4.80	-5.13	-5.00	-4.62	-5.03	-4.90
3) $CH_2CH_2CH_3$	-7.21	-7.70	-7.50	-6.93	-7.54	-7.35
4) F	-0.19	-0.63	-0.60	-0.47	-0.62	-0.73
5) Cl	-2.75	-3.10	-2.95	-2.66	-2.95	-2.90
6) Br	-3.61	-3.89	-3.67	-3.35	-3.62	-3.47
7) I	-5.30	-5.28	-4.97	-4.62	-4.85	-4.49
8) NO_2	-0.11	-1.06	-0.80	-0.65	-0.54	-0.47
9) CN	1.17	0.07	0.28	0.36	0.56	0.55
10) $COCH_3$	-0.20	-0.91	-0.72	-0.70	-0.40	-0.19
11) O_2CCH_3	0.34	-0.94	-0.73	-0.65	-0.36	-0.25
12) CO_2CH_3	-1.74	-2.36	-2.21	-2.10	-1.97	-1.75
13) OH	1.93	1.77	1.97	3.23	2.89	3.55
14) CH_2OH	2.14	2.09	2.19	2.66	2.91	3.48

Table 2-6 (continued)

Functional group	$\Delta\Delta G_R$ (kJ/mol)					
	40 mM SDS 400 mM FPrOH	40 mM SDS 200 mM FBuOH	40 mM SDS 200 mM FPeOH	40 mM SDS 400 mM HFIP	40 mM SDS 200 mM BuCN	40 mM SDS 400 mM PeOH
1) CH_3	-2.49	-2.47	-2.26	-2.27	-2.44	-2.35
2) CH_2CH_3	-4.97	-4.93	-4.53	-4.54	-4.87	-4.71
3) $CH_2CH_2CH_3$	-7.46	-7.40	-6.79	-6.82	-7.31	-7.07
4) F	-0.73	-0.76	-0.57	-0.46	-0.48	-0.32
5) Cl	-2.82	-2.70	-2.42	-2.40	-3.00	-2.72
6) Br	-3.37	-3.17	-2.92	-3.01	-3.80	-3.33
7) I	-4.35	-4.00	-3.82	-4.12	-5.28	-4.62
8) NO_2	-0.46	-0.32	-0.22	-0.60	-0.55	1.15
9) CN	0.50	0.54	0.62	0.23	0.68	2.50
10) $COCH_3$	-0.40	-0.40	-0.43	-1.04	-0.24	1.56
11) O_2CCH_3	-0.54	-0.62	-0.51	-1.15	0.04	2.33
12) CO_2CH_3	-2.01	-2.06	-1.96	-2.48	-1.69	-0.29
13) OH	3.00	3.32	3.48	3.24	1.73	2.64
14) CH_2OH	2.92	2.98	2.80	2.17	2.43	3.79

Table 2-6 (continued)

Functional group	$\Delta\Delta G_R$ (kJ/mol)				
	40 mM SDS 150 mM Butyl Formate	40 mM SDS 100 mM TMS	40 mM SDS 100 mM Hexanone	40 mM SDS 1% Brij 35	40 mM SDS 1% FC 4430
1) CH_3	-2.40	-2.26	-2.39	-2.28	-2.37
2) CH_2CH_3	-4.81	-4.53	-4.78	-4.56	-4.75
3) $CH_2CH_2CH_3$	-7.21	-6.79	-7.18	-6.84	-7.13
4) F	-0.21	-0.27	-0.21	-0.25	-0.27
5) Cl	-2.75	-2.76	-2.95	-2.85	-2.97
6) Br	-3.49	-3.55	-3.84	-3.70	-3.84
7) I	-5.03	-5.10	-5.59	-5.34	-5.54
8) NO_2	0.80	0.02	0.19	0.01	-0.05
9) CN	2.18	1.32	1.65	1.39	1.36
10) $COCH_3$	1.00	0.33	0.59	0.45	0.38
11) O_2CCH_3	1.79	0.92	1.38	1.12	1.04
12) CO_2CH_3	-0.78	-1.13	-0.97	-1.00	-1.12
13) OH	2.39	1.75	1.93	1.39	1.56
14) CH_2OH	3.21	2.57	2.93	2.54	2.65

Table 2-6 (continued)

Functional group	$\Delta\Delta G_R$ (kJ/mol)					
	40 mM LiPFOS	40 mM LiPFOS 400 mM PeOH	40 mM LiPFOS 400 mM HFIP	10 mM TTAB	10 mM TTAB 100 mM PeOH	10 mM TTAB 50 mM HFIP
1) CH_3	-2.00	-2.08	-1.74	-2.54	-2.34	-2.26
2) CH_2CH_3	-3.99	-4.15	-3.48	-5.09	-4.68	-4.52
3) $CH_2CH_2CH_3$	-5.98	-6.23	-5.21	-7.63	-7.02	-6.78
4) F	-0.71	-0.48	-0.82	-0.34	-0.28	-0.43
5) Cl	-2.13	-2.12	-1.67	-3.47	-2.85	-2.78
6) Br	-2.70	-2.47	-1.95	-4.50	-3.55	-3.46
7) I	-3.50	-3.19	-2.21	-6.47	-5.02	-4.78
8) NO_2	-2.62	0.57	-2.24	-0.22	1.02	0.10
9) CN	-2.31	1.38	-2.23	1.47	2.48	1.33
10) $COCH_3$	-3.43	0.40	-3.16	0.75	1.64	0.58
11) O_2CCH_3	-4.47	0.51	-4.43	1.61	2.54	1.04
12) CO_2CH_3	-4.22	-1.22	-3.94	-0.75	-0.12	-0.92
13) OH	1.51	2.74	2.73	-1.30	1.02	0.40
14) CH_2OH	-0.32	2.72	0.29	1.80	3.09	2.12

Table 2-7 Test solutes and their solvation properties.

	Solutes	V	B	A	S	E	Log Pow
1	Phenethyl alcohol	1.06	0.66	0.30	0.83	0.78	1.36
2	4-ethyl phenol	1.06	0.36	0.55	0.90	0.80	2.47
3	Methyl benzoate	1.07	0.46	0	0.85	0.73	2.20
4	1-chloro-4-nitrobenzene	1.01	0.25	0	1.17	0.98	2.60
5	Toluene	0.86	0.14	0	0.52	0.60	2.68

Table 2-8 Solvent effects on chromatographic parameters.

	tmc/teo	μ_{EOF}[a]	μ_{EP}[a]	μ_{app}[a]	PC[b]	N
40 mM SDS	3.42	6.94	-4.91	2.03	183	290000
40 mM SDS 400 mM PeOH	3.28	5.97	-4.15	1.82	191	365000
40 mM SDS 200 mM TFE	3.61	6.11	-4.42	1.69	191	300000
40 mM SDS 400 mM TFE	3.49	6.10	-4.36	1.75	186	300000
40 mM SDS 2 M TFE	4.38	4.97	-3.84	1.13	219	320000
40 mM SDS 200 mM TCE	3.78	6.29	-4.62	1.66	198	280000
40 mM SDS 400 mM TCE	3.85	5.62	-4.16	1.46	200	310000
40 mM SDS 400 mM FPrOH	3.83	6.03	-4.46	1.58	199	320000
40 mM SDS 200 mM FBuOH	3.69	7.17	-5.23	1.94	194	305000
40 mM SDS 200 mM FPeOH	3.83	6.67	-4.93	1.74	199	320000
40 mM SDS 400 mM HFIP	3.70	6.50	-4.74	1.76	195	355000
40 mM SDS 100 mM Hexanone	3.49	6.51	-4.65	1.86	186	410000
40 mM SDS 400 mM BuCN	3.83	6.73	-4.97	1.76	200	322000
40 mM SDS 100 mM TMS	5.02	5.36	-4.29	1.07	240	260000
40 mM SDS 150 mM Butyl Formate	3.65	6.50	-4.72	1.78	192	280000
40 mM SDS 1% Brij 35	3.25	6.40	-4.43	1.97	175	300000
40 mM SDS 1% FC4430	2.79	6.85	-4.39	2.46	153	290000
10 mM TTAB 200 mM PeOH	2.10	6.62	-3.46	3.16	110	270000
10 mM TTAB	3.16	5.23	-3.58	1.65	171	260000
10 mM TTAB 50 mM HFIP	2.24	8.29	-4.59	3.70	120	270000
40 mM LiPFOS	3.82	6.30	-4.65	1.65	199	360000
40 mM LiPFOS 400 mM HFIP	3.93	5.51	-4.11	1.40	203	410000
40 mM LiPFOS 400 mM PeOH	2.27	5.70	-3.19	2.51	122	290000

a: μ_{EOF} Electroosmotic mobility, μ_{EP}: Effective electrophoretic mobility of micelle phase, μ_{app} Apparent electrophoretic mobility (10^{-4} cm^2 V^{-1}s^{-1})

b: PC stands for Peak Capacity.

Table 2-9 Structures of MTH amino acids.

Methylthiohydantoin (MTH) Amino acids	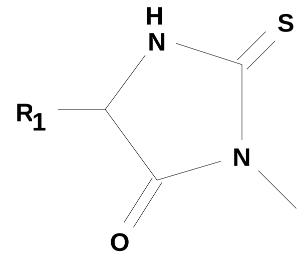
1. MTH Glycine	R1= H
2. MTH Glutamine	R1= 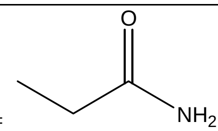
3. MTH Valine	R1= *i*-propane
4. MTH Methionine	R1= 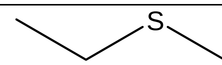
5. MTH-Norvaline	R1= *n*- propane
6. MTH-Tyrosine	R1 = 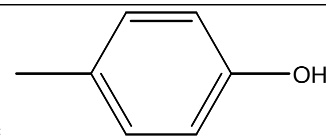
7. MTH-Asparatic acid	R1= 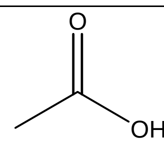
8. MTH Glutamic acid	R1 = 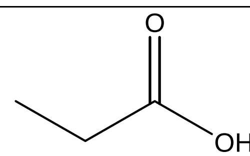
9. MTH-Leucine	R1= 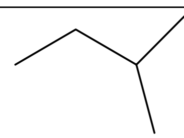
10. MTH-Phenylalanine	R1= 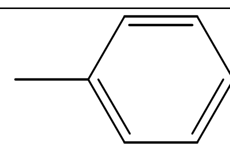
11. MTH-Tryptophan	R1= 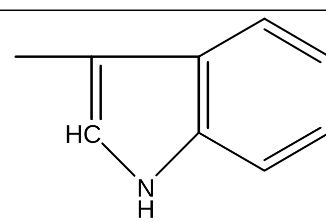

Figure Captions.

Figure 2-1 Conductivity as a function of surfactant concentration at 30^oC (In pure water).

Figure 2-2 Conductivity as a function of surfactant concentration at 30^oC (with 20 mM Phosphate buffer)

Figure 2-3 Effects of solubilized pentanol on the CMC of the three representative surfactants.

Figure 2-4 Effects of solubilized hexafluoro isopropanol (HFIP) on the CMC of the three representative surfactants.

Figure 2-5 CMC measurements by fluorescence probing.

Figure 2-6 Schematic description of the transition of micelle structure induced by solvent addition.

Figure 2-7 Histogram of solvent modification effects on LSER system parameter for selected micellar systems.

Figure 2-8 Chromatograms of selected mixture in various solvent-modified micellar phases.

Figure 2-9 Effect of SDS concentrations on elution window.

Figure 2-10 Effect of pentanol concentration on elution window.

Figure 2-11 Chromatograms of MTH amino acids separation

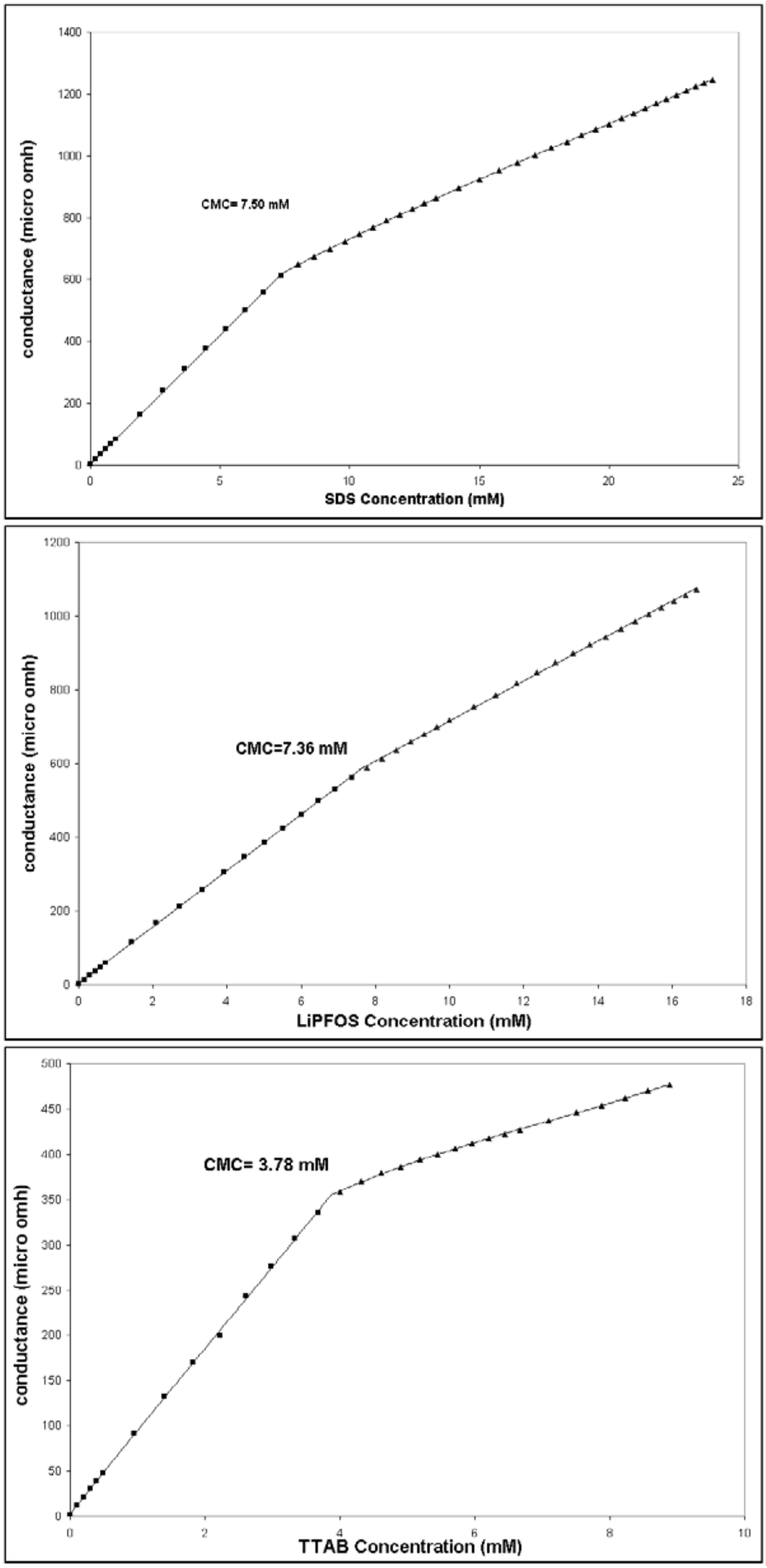

Figure 2-1 Conductivity as a function of surfactant concentration at 30^{o}C (In pure water). From top to bottom: SDS, LiPFOS and TTAB.

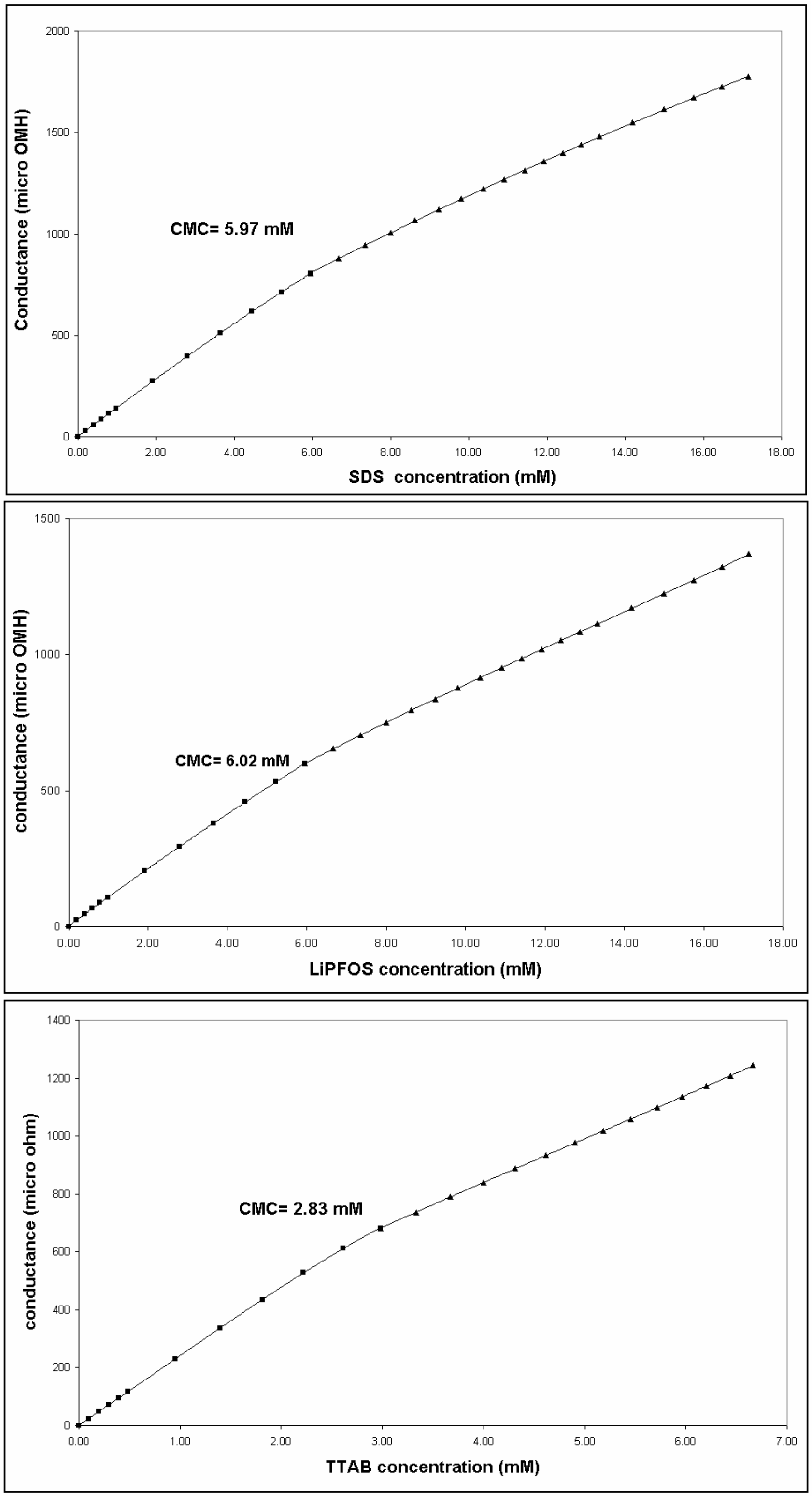

Figure 2-2 Conductivity as a function of surfactant concentration at 30^{o}C (with 20 mM Phosphate buffer). From top to bottom: SDS, LiPFOS and TTAB

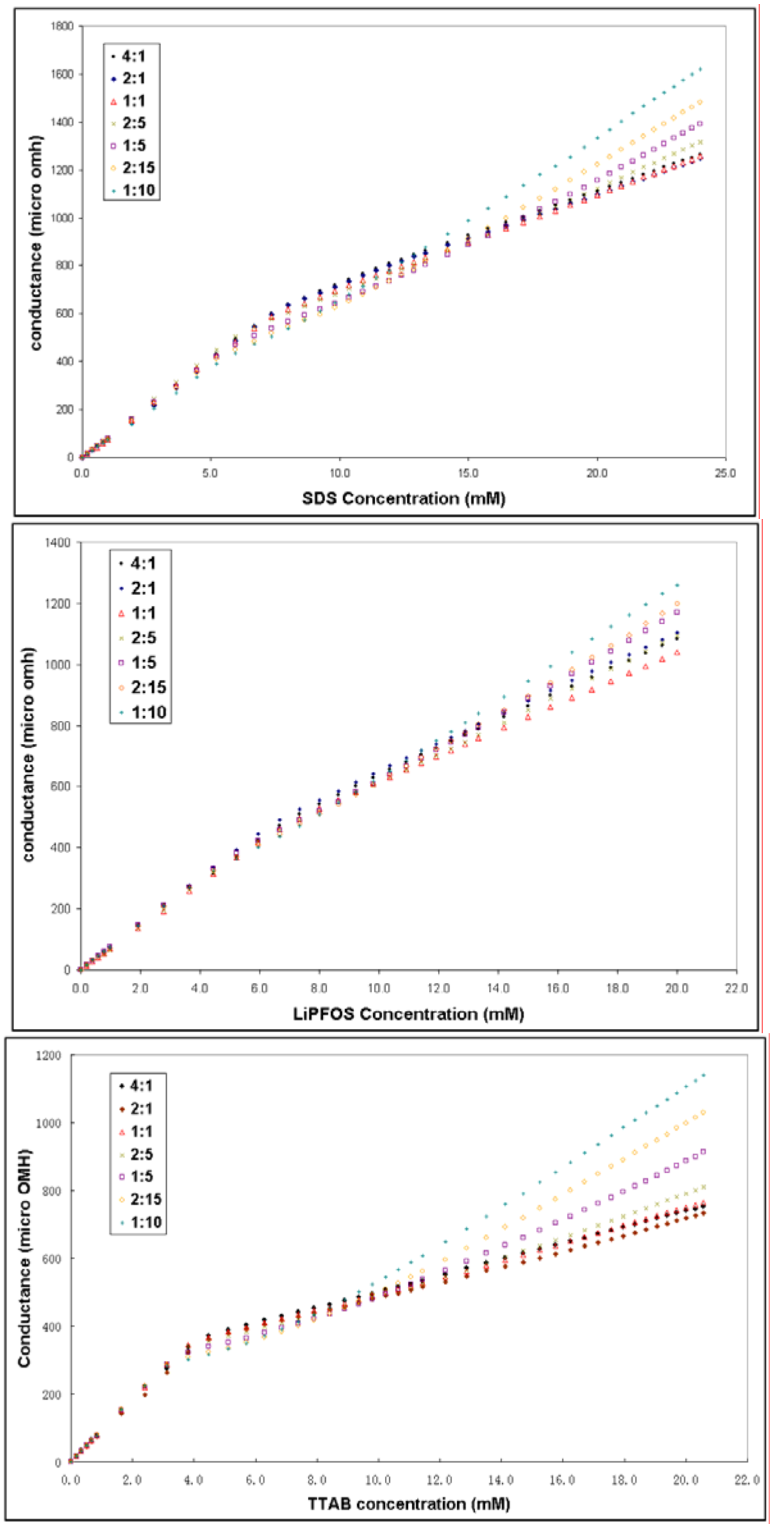

Figure 2-3 Effects of solubilized pentanol on the CMC of the three representative surfactants. From top to bottom as SDS, LiPFOS and TTAB respectively(30^{o}C)

Note: Numbers in the legend are the molar ratio of surfactant over Pentanol.

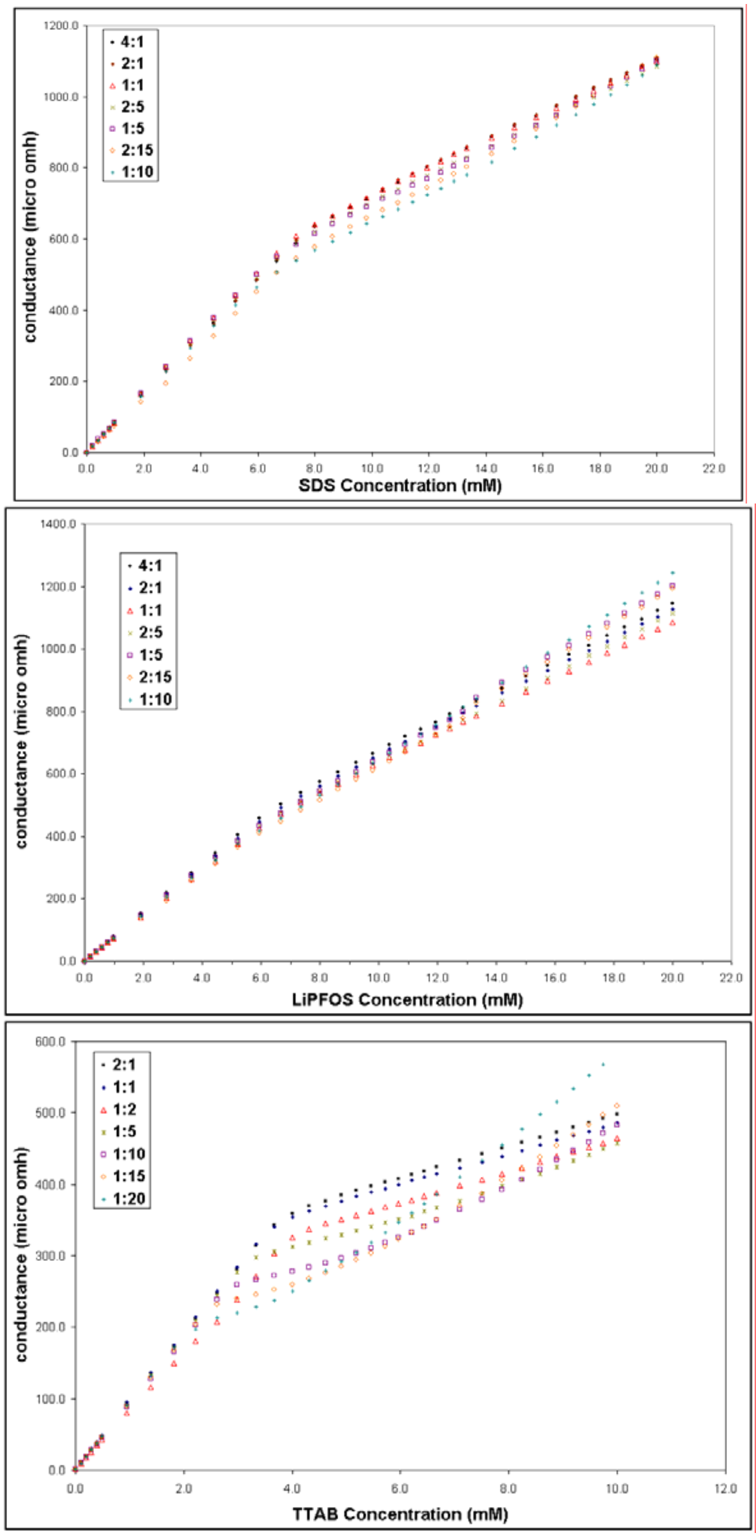

Figure 2-4 Effects of solubilized hexafluoro isopropanol (HFIP) on the CMC of the three representative surfactants. From top to bottom as SDS, LiPFOS and TTAB (30^{o}C)

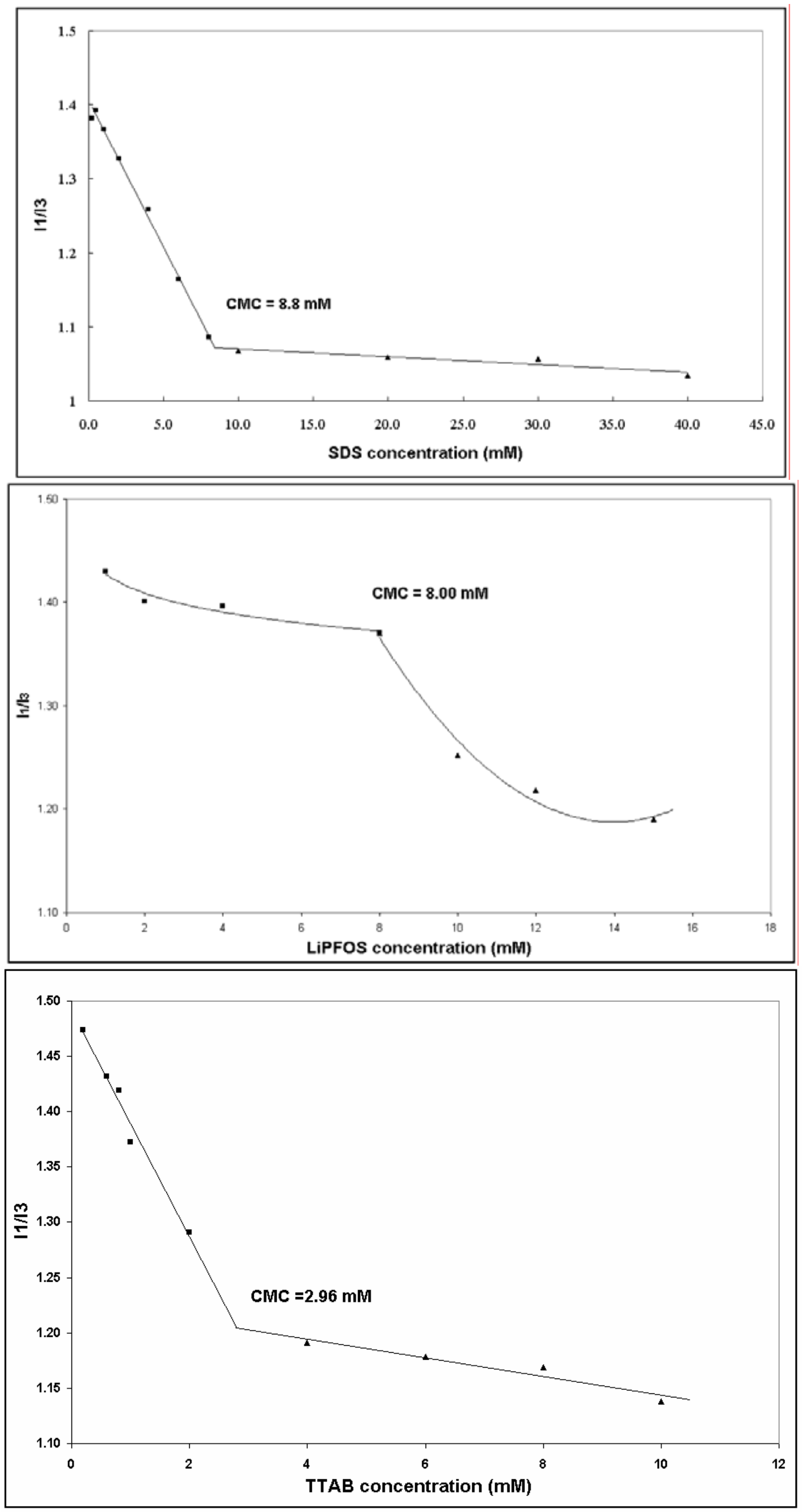

Figure 2-5 CMC measurements by fluorescence probing. From top to bottom: SDS, LiPFOS and TTAB (30^{o}C)

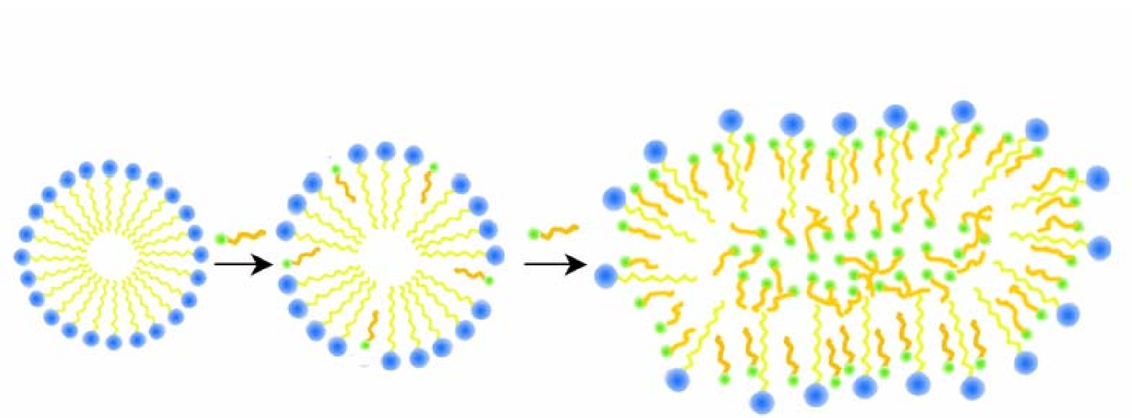

Figure 2-6 Schematic description of the transition of micelle structure induced by solvent addition.

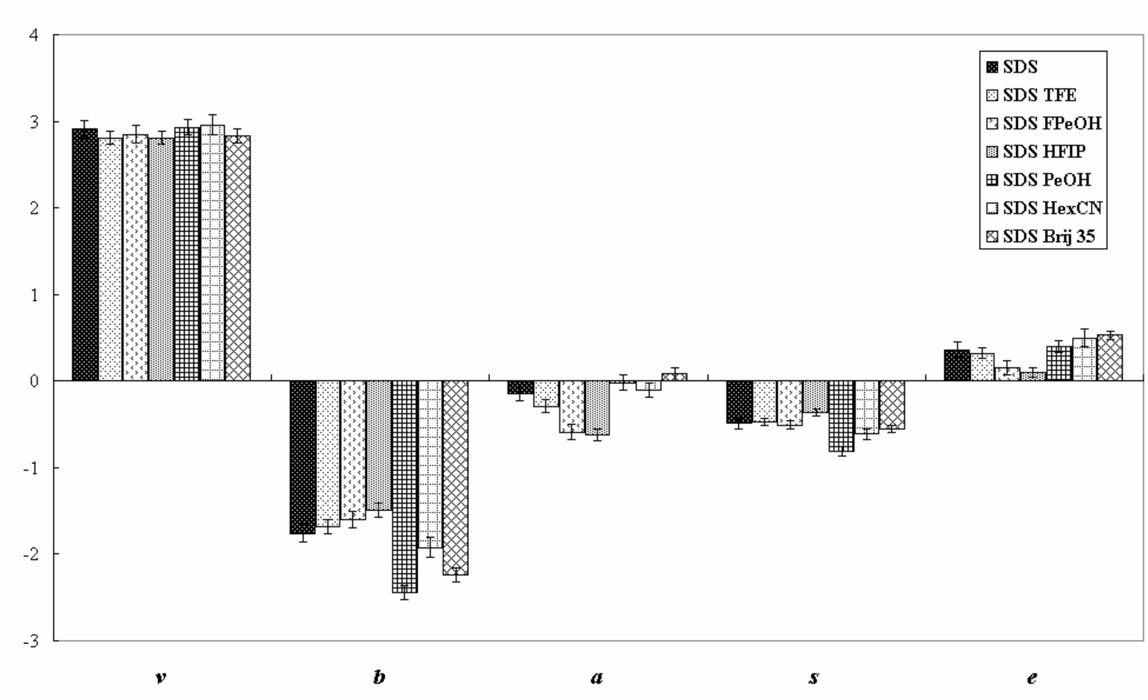

Figure 2-7 Histogram of solvent modification effects on LSER system parameter for selected micellar systems.

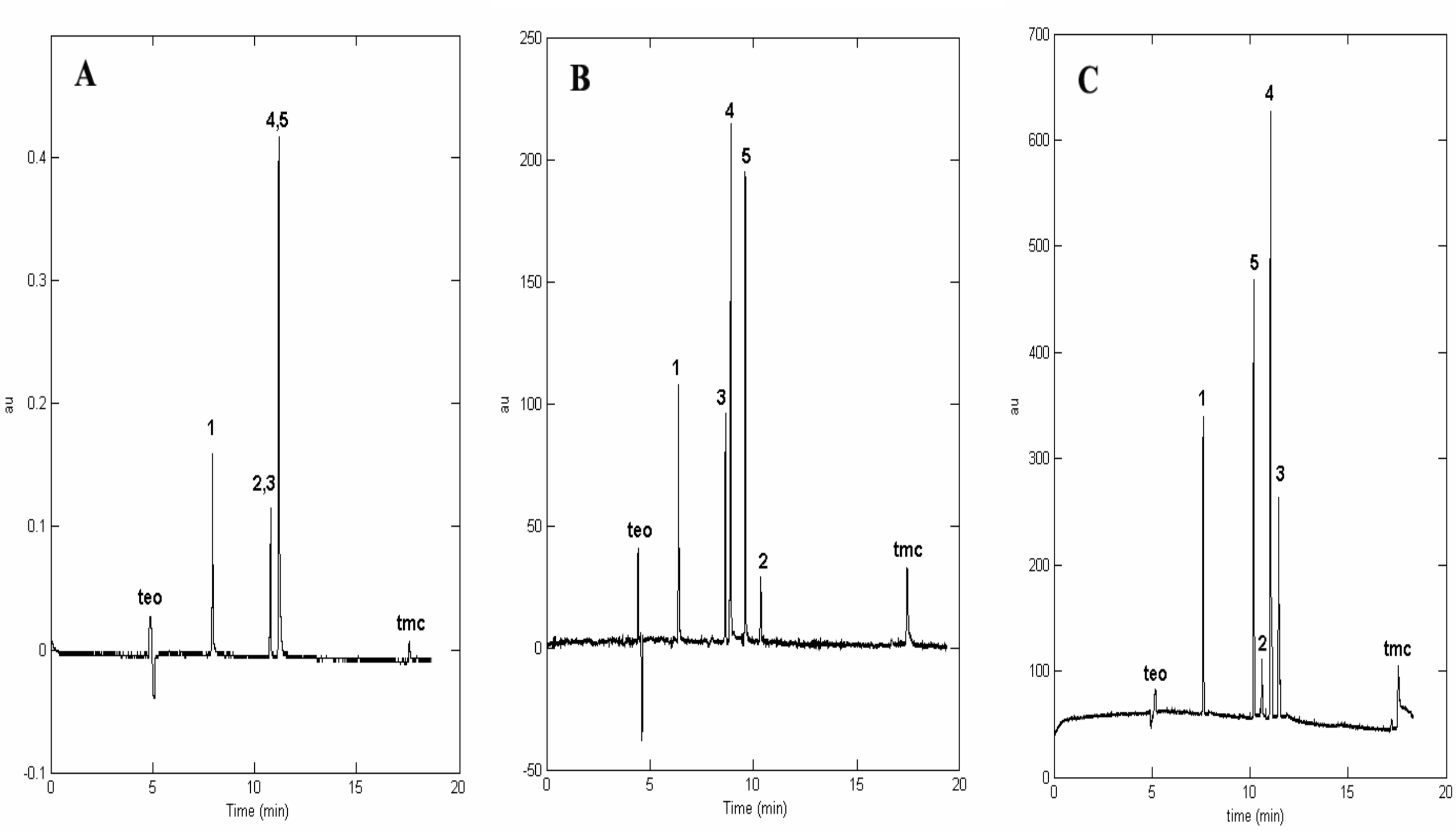

Figure 2-8 Chromatograms of selected mixture in various solvent-modified micellar phases. Solutes identity: 1.) Phenethyl alcohol, 2.) 4–ethyl phenol, 3.) Methyl benzoate, 4.) 1–chloro–4–nitrobenzene, 5.) Toluene. Pseudo-phases A.) 40 mM SDS, B.) 40 mM SDS with 400 mM PeOH, C.) 40 mM SDS with 400 mM HFIP

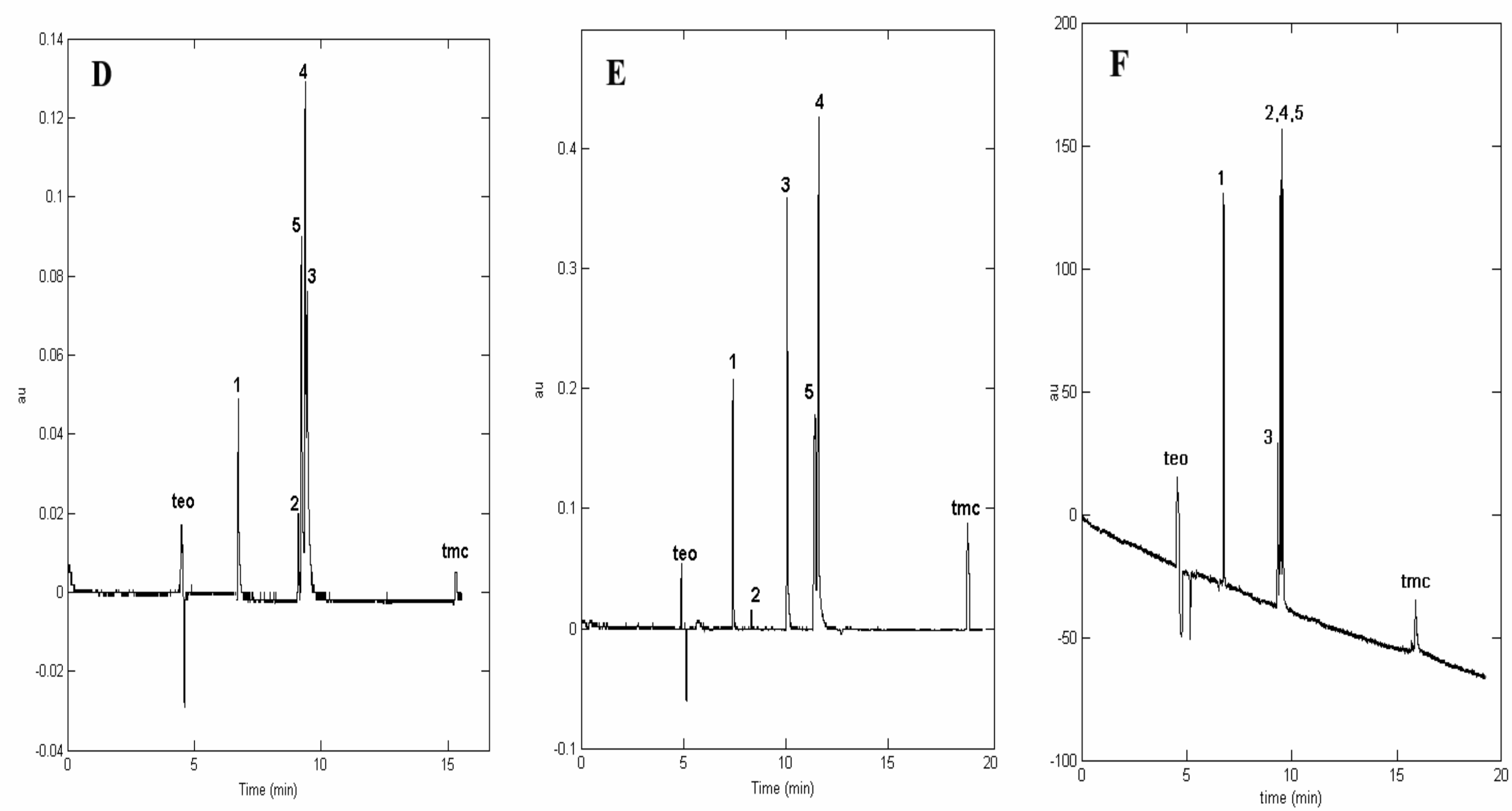

Figure 2-8 continued. Pseudo-phases D) 40 mM SDS with 400 mM TFE, E) 40 mM SDS with 400 mM TCE, F.) 40 mM SDS with 150 mM Butyl formate.

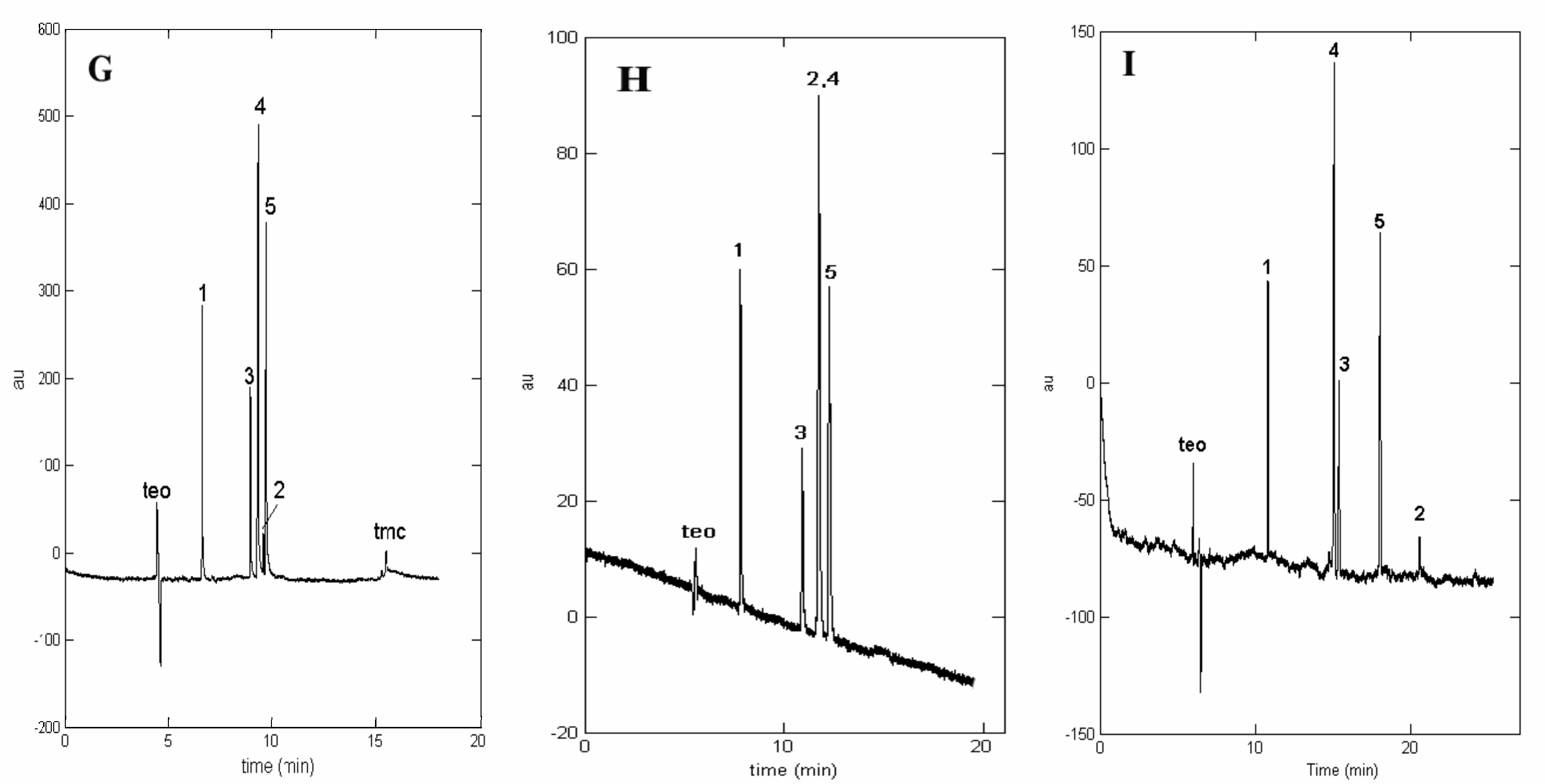

Figure 2-8 continued. Pseudo-phases G) 40 mM SDS with 100 mM Hexanone, H) 40 mM SDS with 100 mM Tetramethylene Sulfone, I.) 80 mM SDS with 400 mM PeOH and 3 M Urea.

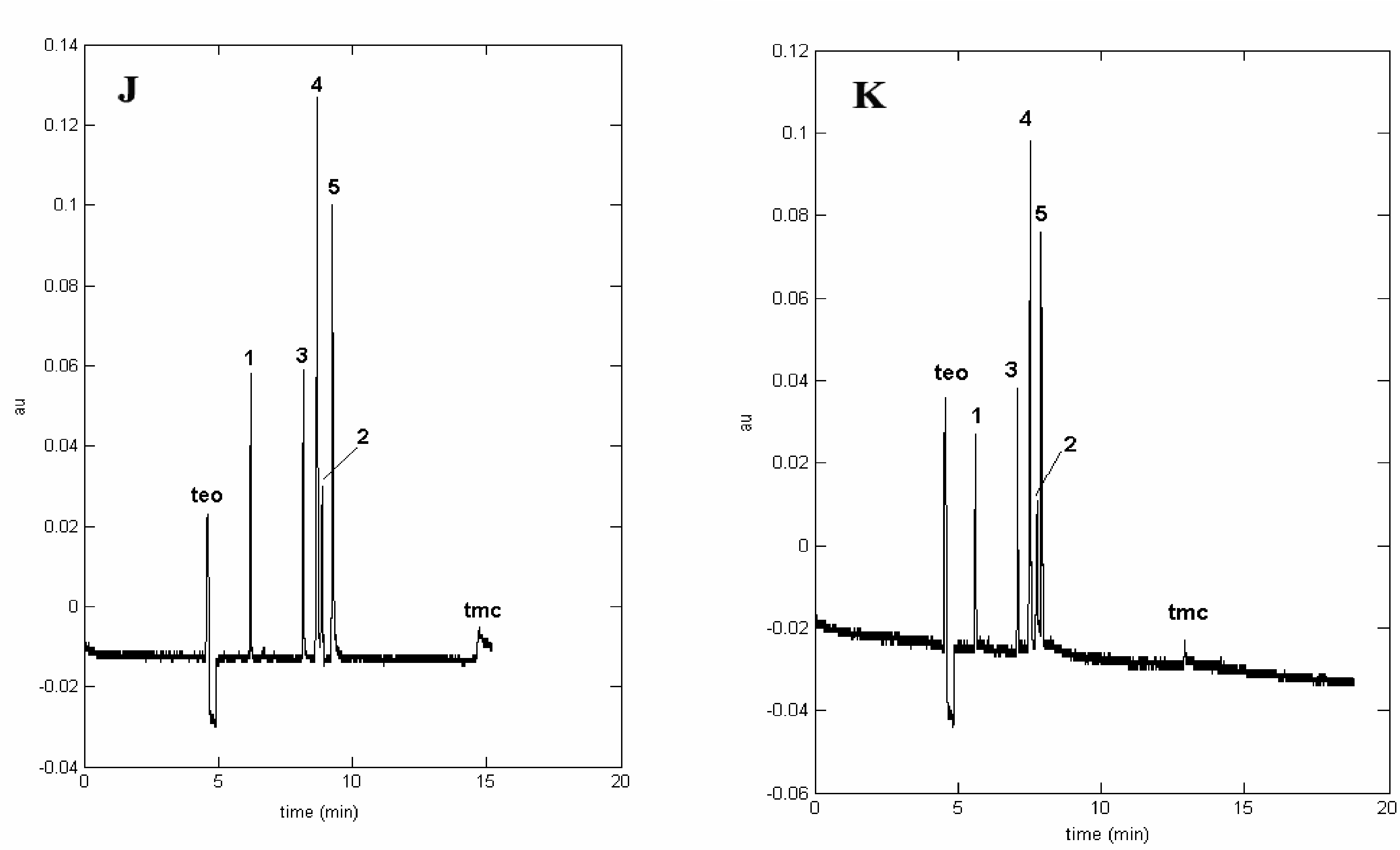

Figure 2-8 continued. Pseudo-phases J.) 40 mM SDS with 1% Brij 35, K.) 40 mM SDS with 1% FC 4430.

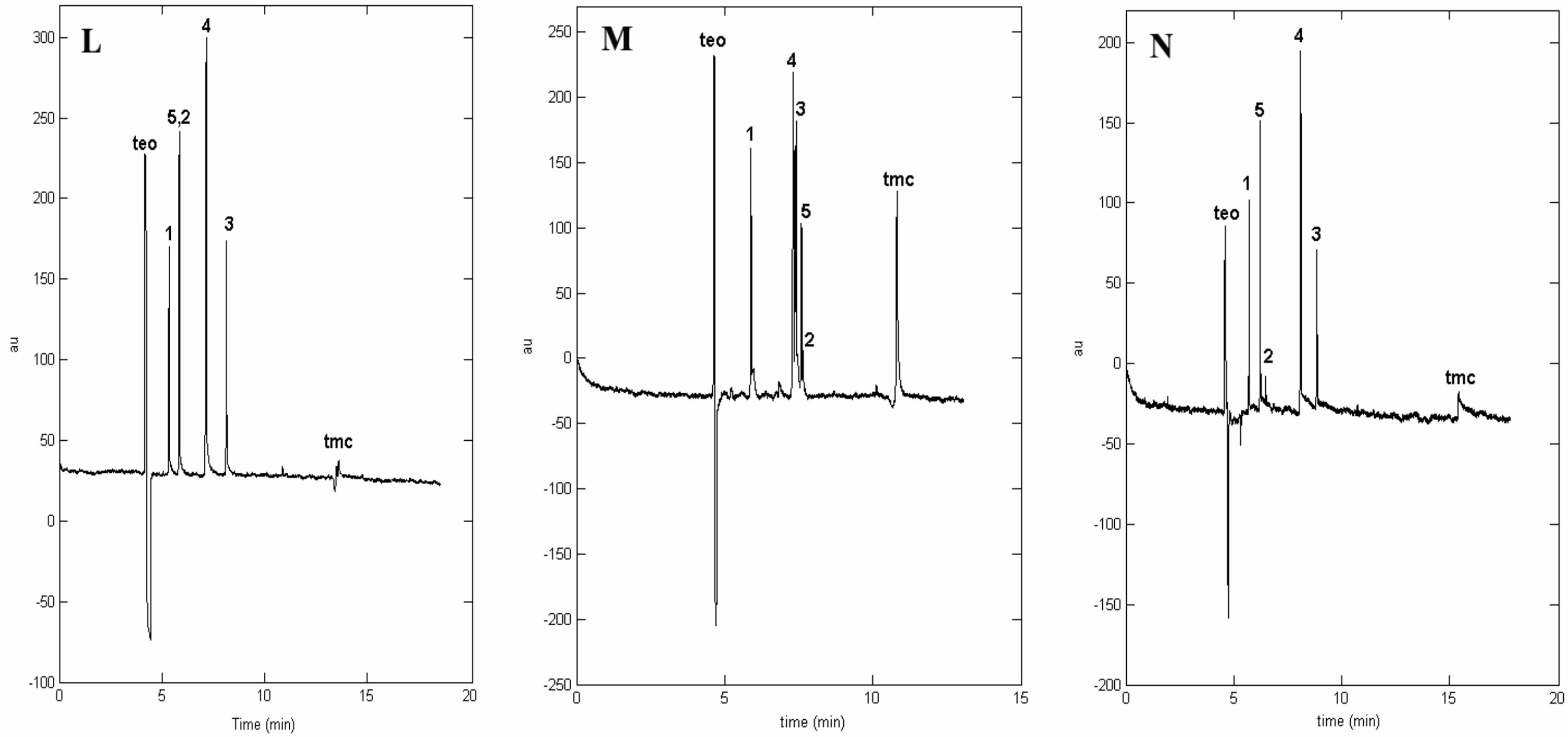

Figure 2-8 continued. Pseudo-phases L.) 40 mM LiPFOS, M.) 40 mM LiPFOS with 400 mM PeOH, N.) 40 mM LiPFOS with 400 mM HFIP.

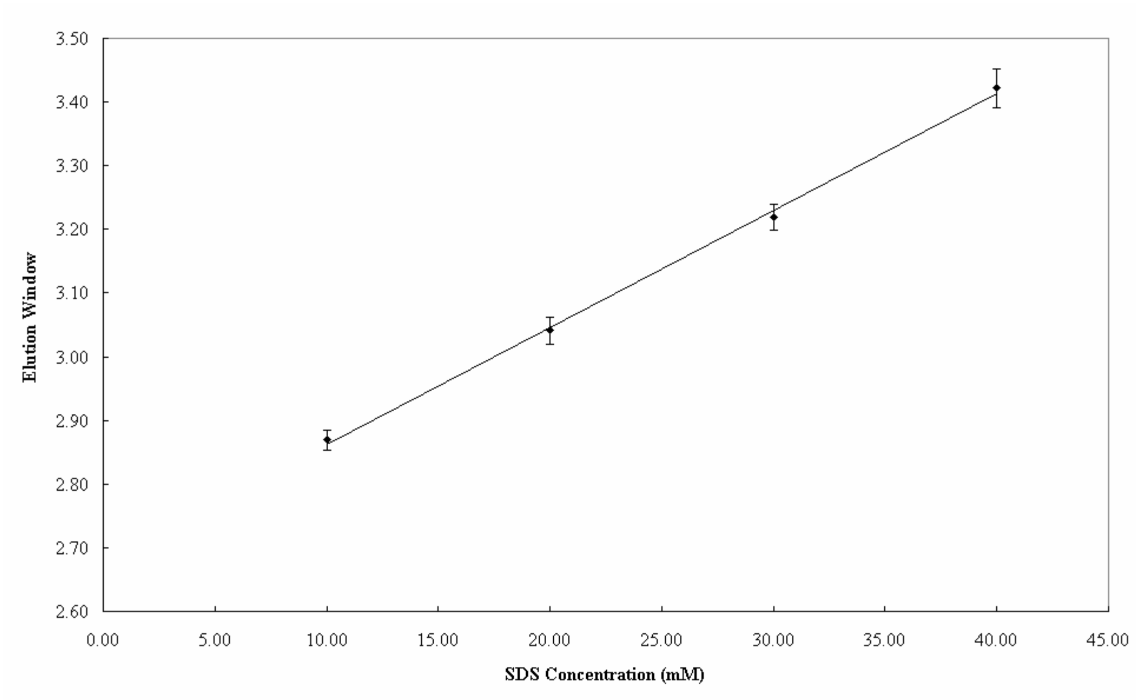

Figure 2-9 Effect of SDS concentrations on elution window.

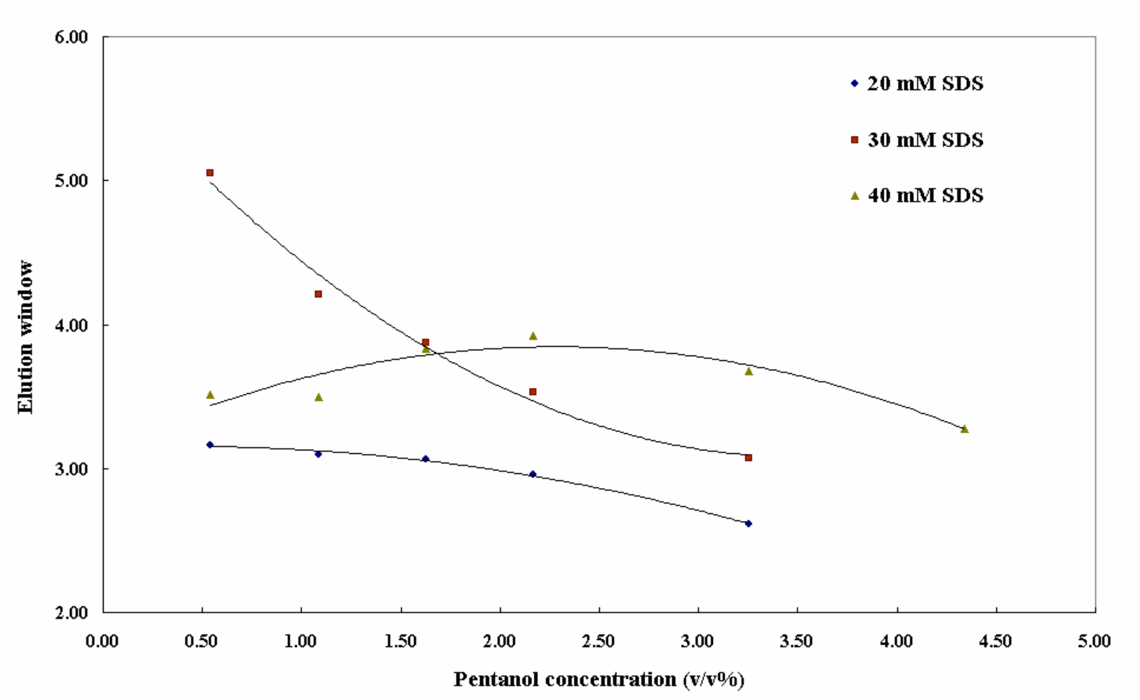

Figure 2-10 Effect of pentanol concentration on elution window.

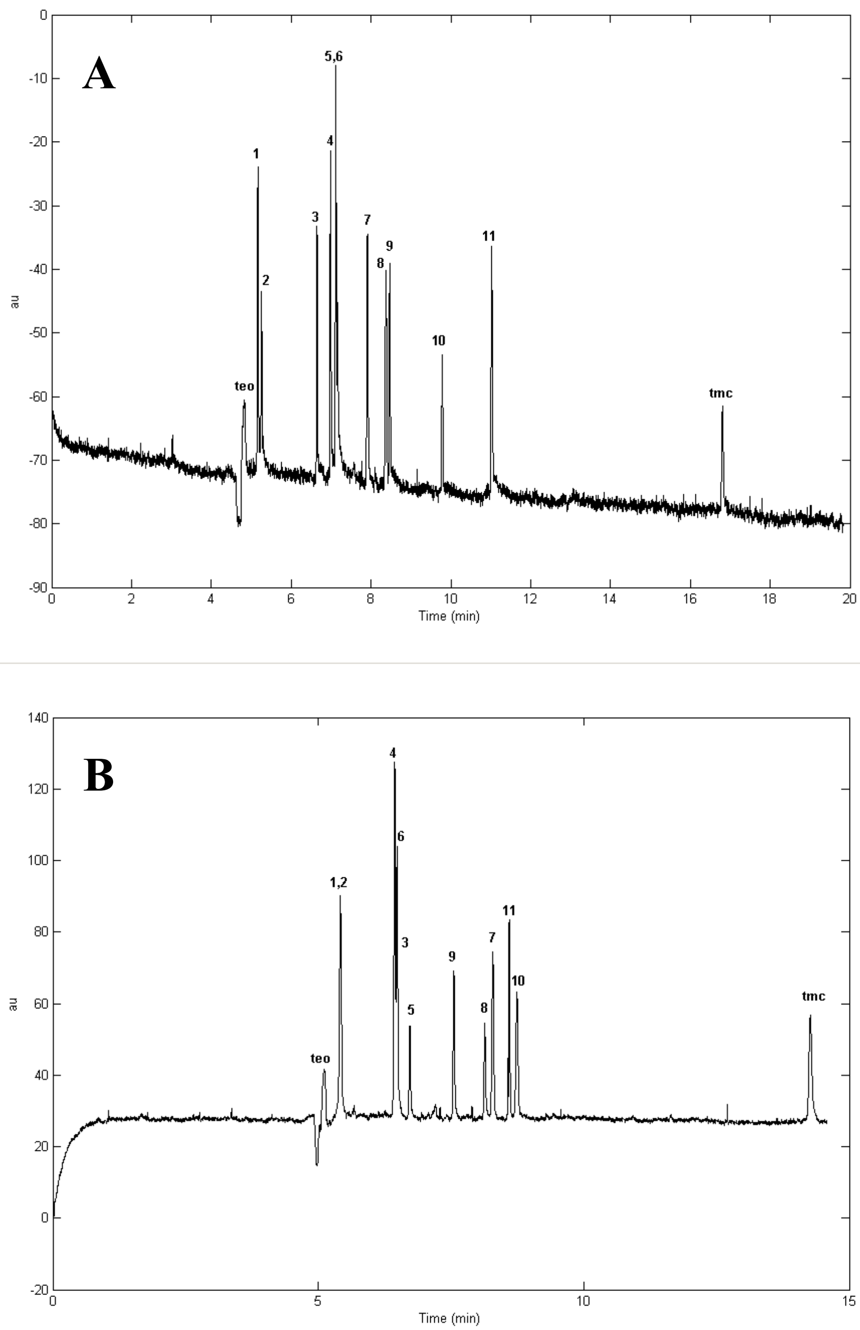

Figure 2-11 Chromatograms of MTH amino acids separation in A) 40 mM SDS and B) 40 mM SDS and 400 mM PeOH (Peak IDs are the same as table 2-9)

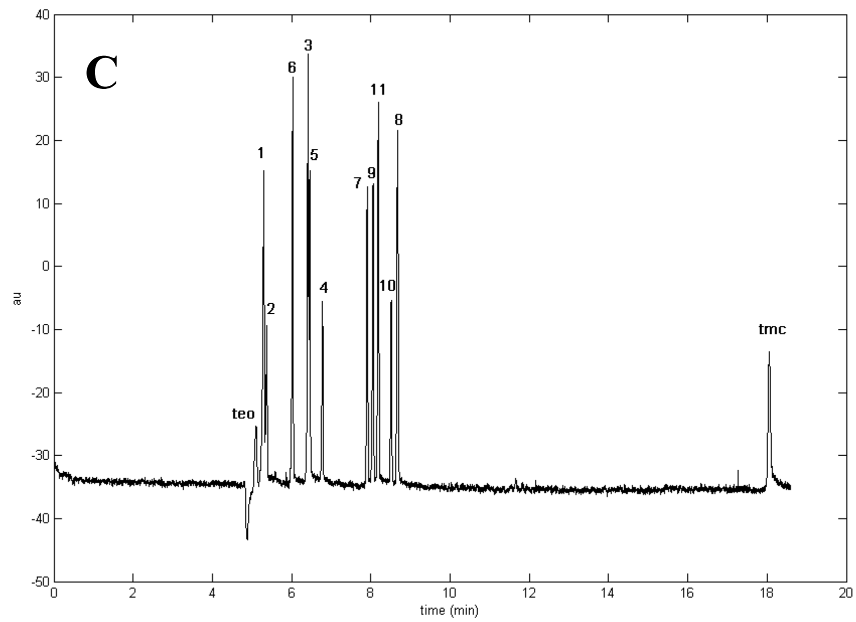

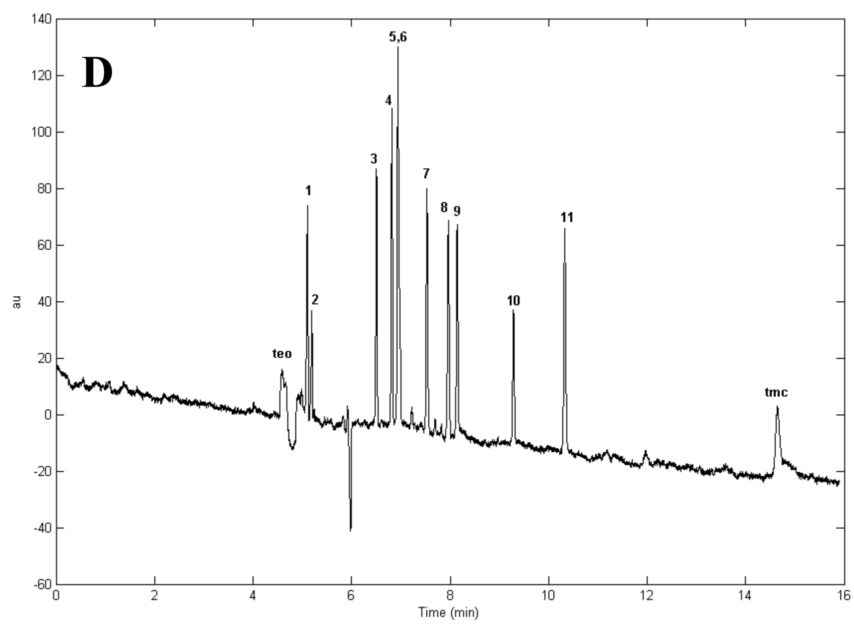

Figure 2-11 continued, Chromatograms of MTH amino acids separation in C) 40 mM SDS and 400 mM HFIP, D) 40 mM SDS and 100 mM HexCN.

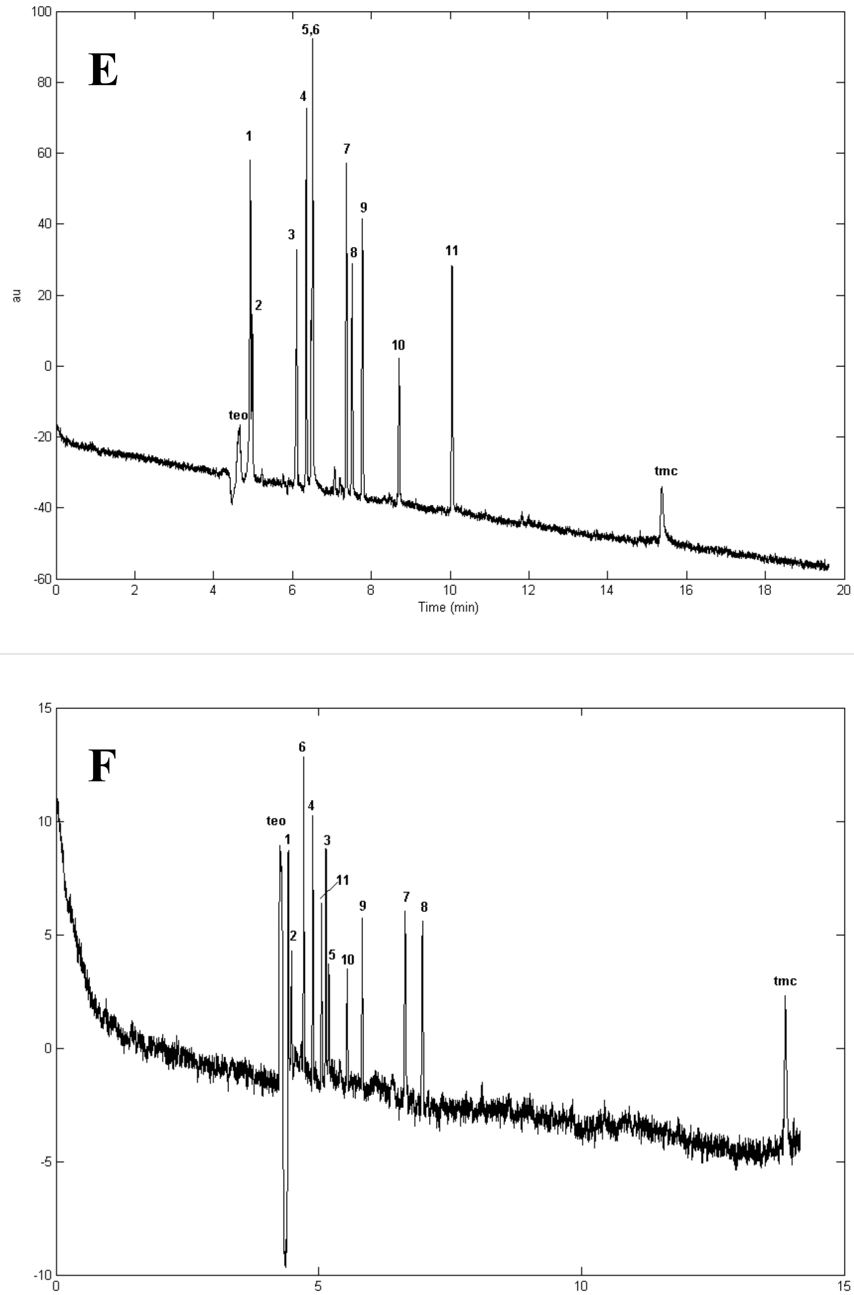

Figure 2-11 continued, Chromatograms of MTH amino acids separation in E) 40 mM SDS and 100 mM Hexanone and F) 40 mM LiPFOS.

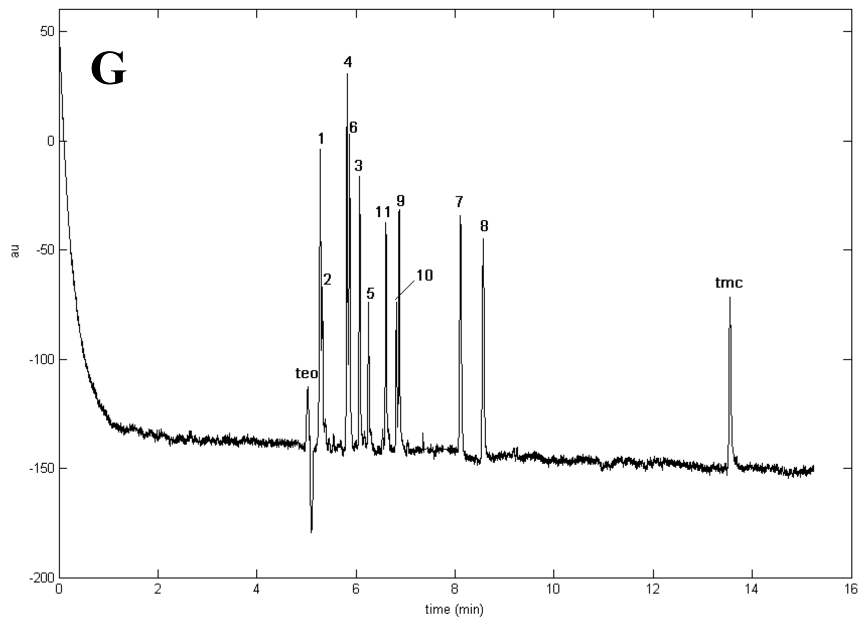

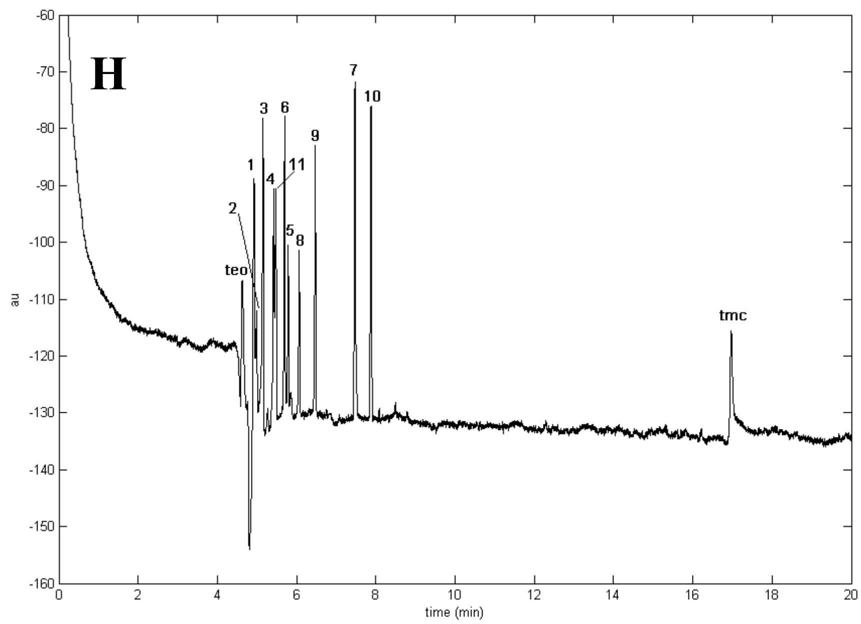

Figure 2-11 continued, Chromatograms of MTH amino acids separation in G) 40 mM LiPFOS and 400 mM PeOH and H) 40 mM LiPFOS and 400 mM PeOH

CHAPTER 3

Micellar Selectivity Triangle (MST) for Classification of Chemical Selectivity in Micellar Electrokinetic Chromatography (MEKC)

Cexiong Fu and Morteza G. Khaledi
Department of Chemistry, North Carolina State University
Raleigh, NC 27695-8204

For submission to *Analytical Chemistry*

ABSTRACT

A novel micellar selectivity triangle (MST) is developed and used to characterize and classify the chemical selectivities of 74 pseudo-phases of MEKC. The similarities and differences of these pseudo-phases are determined by the relative scales of hydrogen bond donating ability (X_b), hydrogen bond accepting ability (X_a) and dipolarity (X_s). The MST scheme classifies these micelle systems into four clusters. The MST also shows that hydrogen bonding ability of micellar phases including hydrogen bond acidity and hydrogen bond basicity, are the primary variables to influence the selectivity pattern in MEKC. The only exception is the siloxane based polymeric micelles (allyl glycidyl ether-N-methyl taurine AGENTs), which could span a wide range of dipolarity with the adjustment of the length and percentage of the hydrophobic side chain. The MST demonstrates its usefulness for the evaluation of the solvent modification effects, mixed-micelle effects on the polar selectivities of the micelles. Other popular pseudo-phases such as microemulsion, liposome, vesicle and bicelle were also investigated by the MST.

1. INTRODUCTION.

Chemical compositions of pseudo-stationary phases in Micellar Electrokinetic Chromatography (MEKC) play a great role in the separation process. A large number of synthetic surfactants above their critical micelle concentration (CMC), ionic polymers[1-11], dendrimers[12,13], vesicles [14-18], and liposomes [19-21] can be used as pseudo-stationary phase in MEKC. The list can be dramatically enhanced by using mixed micelles, mixed surfactant-polymer systems as well as modified micelles using a variety of organic co-solvents, cyclodextrins [22-25], or other organic components like urea [26-29] and glucose [30,31] in order to influence retention, selectivity, the size of the elution window, and ultimately resolution in MEKC. The combination of various types of organized assemblies and modifiers has provided an unprecedented wide range of choices for manipulation of selectivity that could be easily incorporated in the separation process. In order to fully take advantage of this great flexibility, however, a better characterization of the pseudo-stationary phases and roles of various modifiers is necessary.

In spite of a phenomenal growth and many reported applications of the technique, there exists a lack of understanding of the effects of pseudo-stationary phase compositions on retention and selectivity in MEKC separations. Thus, the selection of pseudo-stationary phase has been primarily based on trial–and–error and has been limited to a handful number of pseudo-phases, mainly involving sodium dodecyl sulfate (SDS) micelles. Due to the inherent high efficiency of MEKC, the need for optimum selectivity might not seem as urgent as in conventional chromatography for certain routine applications. However, in order to effectively utilize the high resolving power of the technique for the separation of complex mixtures, and to further broaden the range of applications, it is essential to combine the inherent high efficiency of the technique with optimized retention and selectivity. This is especially important considering the existence of a limited elution window in MEKC as all uncharged solutes would have to be separated between the elution of an unretained solute (teo) and the migration time of micelles (tmc).

Since the first introduction of the technique, it has been generally assumed that retention in MEKC occurs according to the solute hydrophobicity. This assumption, however, does not explain the fact that manipulation of micelle composition (especially the surfactant type) can lead to significant changes in retention patterns, selectivity, and consequently the overall MEKC separations. Variation in retention behavior with surfactant type is indicative of the selective nature of solute interactions with micelles. Hydrophobic interaction is not the source of selectivity differences between pseudo - stationary phases in many cases, however, it does play a major role in partitioning of solutes into micelles and consequently on their retention. In MEKC, selectivity stems from specific interactions between solute molecules and pseudo-stationary phase. The type and extent of these interactions vary with the chemical nature of the medium.

The first attempt for characterization and classification of the chemical selectivity of pseudo-stationary phases in MEKC was reported nearly a decade ago using Linear Solvation Energy Relationships (LSER). Since then, the LSER methodology has been extensively used for achieving a better understanding of the underlying interactions that control retention and selectivity of various surfactants with different hydrophobic chains, head-groups, and counter-ions. Numerous types of pseudo-phase systems composed of various types of micelles [32], block copolymers [4,6], polymerized micelles [6], mixed micelles [33,34], organically modified micelles [35], as well as vesicular [16] and liposomes [20] have been characterized. The retention factor, *k*, in MEKC can be described by the general LSER model as:

$$\log \boldsymbol{k} = \boldsymbol{c} + \boldsymbol{vV} + \boldsymbol{bB} + \boldsymbol{aA} + \boldsymbol{sS} + \boldsymbol{eE} \qquad \text{Eq. 3-1}$$

The LSER models quantitatively describe the contributions of hydrophobic / dispersion (*v*V term), type A hydrogen bonding (*b*B term), type B hydrogen bonding (*a*A term), dipolarity (*s*S term), and polarizability (*e*E term). Solute properties are described by the *McGowan* volume (V), hydrogen bond acceptor strength (B), hydrogen bond donor strength (A), dipolarity (S), and polarizability (E). The interactive properties of the micellar pseudo-phase are described by coefficient *v,* a measure of cohesiveness and dispersion interactions; coefficient *b* which is a measure of the hydrogen bond donor strength, coefficient *a* which is proportional to the hydrogen bond acceptor strength of the micelles, *s* which describes dipolarity, and *e* that is a measure of the affinity of micelles for *n* and π electrons of solutes, and c is the regression constant and has no chemical significance.

The LSER analysis clearly indicates that the while hydrophobic interaction (as quantified by the *v*V term) is the main driving force for retention in MEKC, the main source of selectivity variations between pseudo-phases is their hydrogen bonding donor strength (the *b* coefficient) followed by hydrogen bonding acceptor strength and dipolarity / polarizability interactions.

In this paper, a Micellar Selectivity Triangle (MST) is developed to rationalize and classify chemical selectivities for a wide variety of pseudo-stationary phases. Snyder first reported the use of a Solvent Selectivity Triangle (SST) [36,37] for the characterization and classification of LC solvents. The Selectivity Triangle scheme has shown its usefulness in classifying mobile phases and stationary phases in chromatographic techniques [36-40]. Specifically, Snyder's selectivity triangle, a scheme to classify HPLC solvents into several groups according to their similarities in the strength of dipolarity, hydrogen bond acidity and hydrogen bond basicity, greatly benefits the method development of mobile phase design in RPLC. The solvation properties of organic solvents could be conveniently obtained by using solvatochromic indicators. Other authors [38,40] extended the selectivity triangle scheme to characterize the selectivity of liquid stationary phases in gas chromatography, where the inert gaseous mobile phases are considered to have negligible hydrogen bonding and dipolar capabilities and only involve with dispersive interaction. Zhang and Carr [40] proposed a novel selectivity triangle based on the system parameters from LSER regression to describe the selectivity strength of liquid stationary phases in gas chromatography. In their scale, three system parameters, dispersive interaction (l), hydrogen bond basicity (a) and dipolarity (s) derived from LSER were used to classify the selectivity of the liquid stationary phases. The exclusion of the hydrogen bond acidity of the liquid phase as a descriptor in their triangle scheme was mainly due to the fact that the majority of the liquid stationary phases were non-hydrogen bonding acids. Unlike the homogenous solvents in previous cases, micellar phases are intrinsically heterogeneous and the physiochemical properties differ greatly from the non-polar core to the aqueous-micelle interface. In fact, part of the solvation characteristics of micellar phases originates from the hydrated water. Several attempts [41-44] have been made to determine the micelle polarity by direct solvatochromic probing. Limited and sometimes conflicting results have been reported, perhaps partially due to the microscopically heterogeneous nature of the micellar phases and different localizations of the probe molecules. Alternatively, the LSER method provides an indirect measure of the polarity of micellar phases, where the selective strengths of micelles are encoded in those free–energy related LSER system parameters.

The MST is conceptually similar to the SST in concept and the same selectivity descriptors are used. However, the MST is based on the LSER models that have been determined in this laboratory as well as those reported by other groups. In addition to the previously reported pseudo-phases, the selectivities of several organically modified micelles were characterized using a combination of the information from the MST and the SST.

2. EXPERIMENTAL

All chromatographic experiments were performed on a laboratory-built CE system equipped with a 0-30 kV high-voltage power supply (Spellmann, Plainview, NY) and a SSI 500 variable UV-Visible detector (SSI, State College, PA). Data were acquired and processed with PC/Chrom^{+} version 4.0.9 (H&A Scientific, Greenville, NC). A 50-µm i.d. × 375-µm-o.d. fused-silica capillary (Polymicro Technologies, Phoenix, AZ) was used. The total length of the capillary was 70 cm, with an effective length of 50 cm to detector. Newly installed capillary was conditioned with a rinse procedure using Mili-Q water for 10 minutes, 0.1 mM NaOH (0.1 M LiOH was used when LiPFOS was the pseudo-stationary phase) for 20 minutes to ionize free silanol groups, methanol for 20 minutes to clean organic impurities, (5 minutes Mili–Q water rinses were carried out between all washing steps). Finally buffer solution was running through capillary for 20 min before letting it sit and equilibrate in the capillary for no less than 3 hours to ensure a constant micelle elution time. The capillary was thermostated at 30.0 ^{o}C with a circulating oil bath (Lauda K-2/R, Brinkmann Instruments, Westbury, NY) and two 250-mL jacketed beakers were used to maintain the buffer reservoirs at 30.0 ^{o}C. A positive 20 kV was applied throughout the experiment, except in cationic surfactant TTAB, where the polarity was reversed.

All solutes for the training set and organic solvents were purchased from Aldrich (Milwaukee, WI) and used as received without any further purification. SDS (Sodium dodecyl sulfate) and TTAB (Tetradecyltrimethylammonium bromide) were obtained from Sigma (St. Louis, MO). LiPFOS (Lithium Perfluorooctane Sulfonate) was a gift from 3M. SDS and TTAB solutions were made in 20 mM sodium phosphate buffer (pH 7.0) and LiPFOS solution was made in 20 mM lithium buffer (pH 7.0). The required amount of organic modifiers was then added to the surfactant solutions. All the surfactant solution were filtered with a 0.45-μm polypropylene filter and sonicated for ~5 min.

The solutes were dissolved in methanol with concentrations around 80 μM, which were introduced to the capillary by a 2s hydrodynamic injection at the anodic end of the capillary. The retention time of each solute was averaged from three measurements. The retention factor was calculated using eq 3-2:

$$k = \frac{t_r - t_{eo}}{t_{eo}(1 - t_r / t_{mc})} \qquad \text{Eq. 3-2}$$

Where t_{eo} is the migration time of an unretained solute, t_r is the retention time of a solute, and t_{mc} is the migration time of the micelle. Methanol was used as the electroosmotic flow (EOF) marker and decanophenone as the t_{mc} marker.

3. RESULT AND DISCUSSIONS

3.1 Constructing the Micellar selectivity Triangle (MST)

3.1.1 Characterization of micellar pseudo-stationary phases. Linear solvation energy relationships (LSER) have been successfully used to qualitatively describe solutes partitioning behavior into a wide variety of micellar stationary phases. The micellar phases of interest include cationic, anionic and polymeric surfactants; in addition, organic modifiers were employed as co–surfactants to modulate the interactive properties of micellar phases in predictable patterns. A training set of 35 test solutes with various sizes, polarities and hydrogen bonding capabilities were carefully selected as listed in table 3-1. The cross–correlation test (shown in table 3-2) indicates that there is no significant correlation between the solute descriptors. Most of the LSER regressions resulted in reasonably high correlations (R^2 > 0.98), thus reliable comparisons between multiple pseudo stationary phases could be achieved. According to the LSER models, hydrophobic interaction (*v*V) and A type hydrogen bond interaction (*b*B) are the primary forces for solute partitioning into micelles, while other interactions play minor roles. A positive system parameter indicates an energy-favorable interaction for solute partitioning, while a negative term accounts for an endoergic process. The LSER methods are quite useful in describing individual micellar systems. However, given the increasing numbers of pseudo-stationary phases in MEKC, using merely the LSER model to rationalize them could be laborious and redundant. Additionally, the LSER regression coefficients for a given micelle system exhibit some dependency on the nature of the training set. Therefore inconsistency of inter-laboratory LSER results for a given micelle system is not completely unexpected. For example, we compared the LSER characterizations of SDS micelles from various laboratories in table 3-3. The *v* parameter varies from 2.56 to 3.11, *b* ranges from – 1.95 to – 1.56, *a* has a value anywhere between – 0.44 and – 0.05, *s* spans a range from – 0.67 to – 0.24 and *e* varies from 0.25 to 0.57. One shall also note that, other than the different training sets used by different laboratories, the variation of the LSER results may also originate from the different experimental conditions such as ionic strength, counter ion, temperature, pH etc. These variations in the inter-laboratory LSER results increase the uncertainty in the micellar phase characterizations. These issues have not been addressed previously. There exists a need for a systematic approach for the comparison and classification of pseudo-stationary phases in MEKC. Here we propose a Micellar Selectivity Triangle (MST) for recognizing similarities and differences in the selectivity patterns of various micellar phases and for classifying them accordingly.

3.1.2 Constructing the MST. A LSER database for 74 micelle systems as well as liposome, vesicle and bicelle, is collected and listed in table 3-4. As stated above, the hydrophobic interaction term is one of the two primary factors affecting solute retention in MEKC. We note that most of the micelle systems have very similar values for *v* parameter with the exception of LiPFOS, liposomes and some polymeric micelles. In other words, the hydrophobic interaction does not significantly influence the selectivity patterns of solute retention in MEKC for the majority of the micelle systems. Thus, classification of pseudo-phases in the MST was based on the relative strengths of polar interactions including hydrogen bonding (*b*B, *a*A), dipolarity (*s*S) and polarizability (*e*E). By taking the ratios of these parameters with respect to *v*, these four polar system parameters are normalized by the hydrophobic parameter (Table 3-4). Figure 3-1 shows the distribution of these normalized polar parameters for the 74 pseudo-phases. We note that hydrogen bond acidity parameter of the micelle systems (*b*) spans a wide range from –0.20 to –1.40, while the other three polar parameters have relatively smaller scales in terms of the range and magnitudes. Thus, it is not advisable to use these normalized LSER parameters directly for the comparison of the micelle systems, because the hydrogen bond acidity of the micelle systems with a larger magnitude would dominate the outcomes. Therefore, a scaling procedure is necessary to standardize the individual parameter into the range between 0 and 1. This is accomplished using equation 3-3, where I_i represents the normalized system parameters (*s/v, a/v, b/v, e/v*), I_{low} and I_{high} define the lowest and highest values of the polar system parameters in the LSER database. The preset values of the I_{low} and I_{high} values for the current database are listed in table 3-5. U_i stands for the corresponding system parameter after scaling. With such a treatment, the magnitudes of these four polar interactions would be comparable.

$$U_i = \frac{I_i - I_{low}}{I_{high} - I_{low}} \qquad i = s, a, b \text{ or } e \qquad \text{Eq. 3-3}$$

Finally, the scaled value of each polar interaction is calculated according to equation 3-4. Such that the sum of X_i for any micelle systems will be unity.

$$X_i = \frac{U_i}{U_a + U_b + U_s} \qquad i = s, a, b \text{ or } e \qquad \text{Eq. 3-4}$$

The pre-treated system parameters (X_i) are inputted into a ternary plot program, JMP release 5. 1. 1 (SAS Institute Inc., Cary NC), for graphic processing.

3.2. Analysis of pseudo-phases with MST

3.2.1 Micelle systems classification in the MST. First of all, we address the problem of the robustness of the LSER method in the MST. As demonstrated for the SDS micelles, inter-laboratory variations of LSER results can occasionally be seen for a given micelle system. In order to evaluate the influences of these variations of the LSER parameters on the MST characterizations, we examined the normalized LSER scales of 14 SDS systems acquired from various laboratories into one selectivity triangle (figure 3-2). It is clear that the majority of the SDS micelle systems converge to a narrow area, with the exception of SDS phases 8, 9, and 12. Further investigations of these "outliers" reveal that the buffer compositions are very different from those in the cluster. Unlike the clustering micelle systems using mainly sodium phosphate for buffering, system 9 employed a mixture of 60 mM/100 mM sodium phosphate and sodium borate buffer. In the case of system 12, a Tris (hydroxymethyl) aminomethane buffer at pH 7.0 was used. In system 8, sodium phosphate buffer was used, but the separation was carried out at a lower temperature (25 ^{o}C) than others. One shall also note that significantly different training sets have been used in all these studies. The observations suggest that the MST has excellent tolerance toward the variances in the LSER results. For an accurate description of SDS polar selectivities, the averaged LSER parameters are used to represent these 14 SDS micelles in the MST.

Since there are four polar molecular interactions contributing to the solute partitioning into micelles, selection of the primary three polar selectivities that are crucial for the classification of micellar phases in the triangle scheme is not straightforward. We compared three selectivity triangles composed of three combinations of system parameters as the followings: 1) X_b, X_a, and X_s, 2) X_b, X_a, and X_e, 3) X_b, X_s and X_e. The hydrogen bond acidity (X_b) is the most important polar interactions, which justifies its presence in all three MST combinations.

The successful representation of all 74 micelle systems and liposomes in a triangular coordinate with polar selectivity parameters X_b, X_a, and X_s, is shown in figure 3-3. The overall trends show that the micellar phases could be modulated with a larger range of hydrogen bonding acidity and basicity than dipolarity with the only exception being a group of siloxane based polymeric micelles (AGENTs) [8] in cluster D. Several groups of micelle systems distinguish themselves from others in the plot. Group B is mainly comprised of fluorinated surfactants and could be considered as the strongest hydrogen bond donor and weakest hydrogen bond acceptor among all the micelle systems. Group A consists of SDS and its analogs (surfactants with the same headgroup but different length of non-polar chains or the same non-polar chainlength but with different headgroups). Group C includes bile salts, microemulsion, alkyl methacrylate based polymeric micelles (pLMAt-type polymeric micelles) [45], liposomes and octanol-water systems. We can see that group C partially overlaps with its neighboring group A, due to similar polarities of these components. In general, the components of group C are marginally stronger hydrogen bond acceptors and slightly weaker hydrogen bond donor than those in group A. The dipolarities for these three groups (A, B, C) do not show significant differences. Group D mainly comprises of AGENT-type polymeric micelles and the cationic surfactant TTAB. The components of group D possess the strongest hydrogen bond accepting ability as compared to the other micellar phases. In addition, these siloxane-based polymers (AGENTs) of group D exhibit unique flexibility to adjust the dipolarity over a wide range.

A second micellar selectivity triangle is constructed with system coefficients X_b, X_a and X_e and illustrated in figure 3-4. It can be seen that upon replacing the dipolarity parameter (X_s) with the polarizability (X_e) of micellar systems, the distribution pattern undergoes significant changes. This is not surprising because a handful number of these 74 phases have different, sometimes opposing, values between the dipolarity and polarizability parameters. For instance, fluorosurfactant LiPFOS and its analogues have large dipolar coefficients (X_s ~0.49), but weak interaction with n or π lone pair electrons (X_e ~0.11). A different trend is found with AGENT-type polymeric micelles, where they have poor affinities to dipolar-type interaction (X_s ~0.15), but large polarizability scales (X_e ~0.44). As shown in figure 3-4, those fluorinated micelles (group B) are closer to the HB acidic vertex of the triangle. This indicates that the strong HB donating ability of fluorinated micelles overshadows the contributions from the small X_e parameter and weak HB basicity of these fluorosurfactants. In comparison, the selectivity triangle (X_b, X_a, X_e) identifies AGENT-type polymeric micelles as more polarizable, medium strength of hydrogen bond basicity but the weakest hydrogen bond acidity micelles. Groups A and C congregate in the center of the triangle implying a medium strength for the three polar selectivities X_b, X_a, and X_e. Slight differences can be observed between these two groups. Group A containing SDS and its analogs is marginally stronger in hydrogen bond acidity but weaker in polarizability and hydrogen bond basicity as compared to the micelle systems from group C.

The third selectivity triangle in figure 3-5, utilizes X_b, X_s and X_e as the three coordinates for the selectivity triangle. The classification of the 74 micelle systems in the (X_b, X_s, X_e) triangle schemes is similar to the previous micellar selectivity triangles. Of all the groups, the fluorinated micelles of group B are considered the strongest hydrogen bond donors but weakest polarizable micelles. Micelle systems centering in the selectivity triangle are mainly comprised of the components from groups A and C. These two partially overlapping groups only differ by the fact that the components of group A are slightly better hydrogen bond donors and weaker polarizable micelles than those of group B. Note that all of the above micelle systems in group A, B and C demonstrate very similar dipolarity strength. By contrast, AGENT-type polymeric micelles of group D exhibit flexible control over the dipolarity of the micelles.

The classifications of the 74 micelle systems in our three selectivity triangle schemes are in good agreement with each other. Although these classifications are subjective, we can see that four groups of micelle systems could be consistently separated in our three triangle schemes. The detailed rationalizations of micellar selectivity of each group have been discussed and summarized in table 3-6. These triangles convey similar classification information and the selectivity triangle with (X_b, X_a, X_s) results in a better separation of the four micelle groups. Moreover, direct comparison with the Snyder's solvent selectivity triangle (SST) is possible because the same molecular interaction scales (b, a, s) are used. Thus we will use the selectivity triangle (X_b, X_a, X_s) for analyzing micelle systems of interest hereafter.

3.2.2 Representative pseudo-phases. Figure 3-6 highlights the representative phases of interest in a (X_b, X_a, X_s) selectivity triangle. We also included an octanol-water system to compare with those representative phases in the EKC method. The octanol-water partition coefficients (P_{ow}) have been widely used to evaluate the lipophilicity of compounds. Numerous efforts have been made to use the partition coefficient of EKC as an alternative measure of the solute lipophilicity. EKC is preferred because as a chromatographic method, it has the advantages of rapid and high throughput analysis compatibility, small sample size, lack of sample purity requirement, and flexibility in adjustment of the composition of the pseudo-stationary phases. However, finding an appropriate pseudo-stationary phase to simulate the octanol-water environment is not a simple task. Fortunately, with the assistance of the MST we could easily identify suitable pseudo-stationary phases with similar partitioning behaviors to the octanol-water system, because one of the merits of the MST is that the similarity and differences in selectivities between two phases are readily determined by their distance in the triangle. In other words, the closer two phases are located on the triangle, the more similar they are in terms of selectivities. LiPFOS micelles are found to be significantly more hydrogen bond acidic but less hydrogen bond basic than the octanol-water system in the MST, which is the reason behind the poor correlation (r=0.559) between the octanol-water and micelle-water partition coefficients as reported by Yang and co-workers [46], despite that hydrophobic interaction plays a predominant role in both partition systems. In the cases of SDS and TTAB, SDS micelles are stronger HB donors but weaker hydrogen bond acceptors than the octanol-water system, while TTAB micelles have higher HB basicity and similar HB acidity to the octanol-water system. Congeneric behaviors of solutes retention were found when comparing these two phases with the octanol-water system. Specifically, hydrogen bond acceptor solutes (phenones, anilines etc.) tend to have selectively stronger affinities with the HB acidic SDS micelles, while hydrogen bond donor solutes (phenols, etc.) interact strongly with the HB basic TTAB micelles when compared to the octanol-water system. The overall correlation coefficients of the logarithm of the solute retention factors with log P_{ow} were higher than that for the LiPFOS micelles, 0.888 for TTAB and 0.931 for SDS. Liposomes and vesicles belong to another interesting class of pseudo-phases. Their bilayer structures and fluidic natures exhibit great similarity to biomembranes. The MST describes them as very hydrogen bond basic but weak hydrogen bond donor phases. Burns and Khaledi [19] reported the addition of cholesterol into the composition of liposomes improved the correlation of retention factors in LEKC with log P_{ow} to a R^2 of 0.95 for uncharged aromatic solutes. A thermodynamically stable SDS/DTAB vesicle was investigated by Hong and colleagues [47] and they obtained a correlation coefficient of 0.98 for 20 compounds. However, their set of compounds did not include hydrogen bond donor solutes (phenols, etc.), which typically deviate from the linear correlation and show congeneric retention behaviors interacting strongly with this basic vesicle. In our MST plot, Sodium Cholate (SC) micelles and dihexadecyl phosphate (DHP) vesicle are the two closest pseudo-phases to the octanol-water system, thus we expect great likeness in the selectivity patterns for these systems. Yang and Khaledi [46] reported nice fit between the retention factors of 60 aromatic compounds in SC micelles with the log P_{ow} with a correlation coefficient r equal to 0.983. Other bile salt micelles also demonstrated reasonable estimations of octanol water partition coefficients. Adlard and co-workers [48] used deoxycholic acid salts as pseudo-phases in MEKC to investigate a variety of more complicated drugs with log P_{ow} values ranging from 0.51 to 4.05. The estimated octanol-water partition coefficients of the drug compounds from their MEKC measurements were well correlated with the experimental values (r=0.973). The DHP vesicle is another pseudo-phase locating closely to the octanol-water system. Agbodjan and co-workers [14] initially reported the use of the DHP vesicles in MEKC and examined the correlations with log P_{ow}. The retention factors of 41 aromatic compounds were well correlated with their octanol-water partition coefficients (R^2=0.98). Here we will rationalize the selectivity characteristics of various representative pseudo-phases in MEKC in comparison to the octanol-water system. Among them, LiPFOS micelles are the pseudo-phase with least resemblance to the octanol-water system due to their opposing hydrogen bonding strengths. SDS, TTAB, SDS/DTAB type vesicles and liposomes represent a group of pseudo-phases that have one or more polar selectivities resembling the corresponding interactive strength in the octanol-water, but also possess one or more polar selectivities that significantly differ from the octanol-water system. Consequently, congeneric migration behaviors are often observed and result in a moderately good fit. All three polar interactive properties of the SC and DHP systems match those of the octanol-water system. Thus, SC and DHP systems obtain the best correlations with the octanol-water and are the preferred pseudo-phases for the estimation of P_{ow} in EKC method. Organic modifiers and mixed micelles are also intensely studied in MEKC for estimation of octanol-water partition coefficients and will be discussed in combination with the MST in a later section.

3.2.3 Analysis of polymeric micelles by the MST. Polymeric micelles have been of great interest along with the development of MEKC. The covalent linkage of the polymer ensures the micelle stability in harsh solvent conditions, which otherwise would cause the collapse of conventional surfactant micelles. The usefulness of polymeric micelles in the separation of highly hydrophobic solutes such as PAHs, fullerene and others at high levels of organic solvent have been demonstrated by several groups [4,49]. Terabe and co-workers reported that several ionic copolymers with different headgroups exhibited unique selectivities when compared to SDS [50]. The authors attributed the selectivity effects to the collective influence of structural rigidity and headgroups variety of the polymers. Recently, many studies focused on synthesizing unique building blocks for the sidechain of polymeric micelles to fine-tune the selectivity of the micelles. In the polymeric micellar selectivity triangle (figure 3-7), poly(sodium undecylenate) (pSUA) represents one class of *polymerized surfactants*. We can see that the polar selectivities of pSUA do not differ significantly from SDS. It is only marginally more dipolar and less HB basic than SDS micelles. This observation suggests that although the inner ends of the hydrophobic chain of these micelles are covalently anchored to each other, pSUA have very similar micelle-aqueous interface environments to the self-aggregates of its monomer-analogous surfactant SDS. The triblock copolymer of methylacrylate–ethylacrylate-methyacrylic acid (Elvacite 2669) and 2-acrylamido-2-methyl-1-propanesulfonic acid (AMPS) copolymers can be considered as another class of polymeric pseudo-phases. These multi-block copolymers, as shown in the MST, are significantly more dipolar but less HB acidic than SDS micelles. Meanwhile, the HB basicity of these copolymers only shows a slight increase in comparison to SDS micelles. Palmer and co-workers introduced a novel family of siloxane based polymeric micelles (allyl glycidyl ether-N-methyl taurine AGENT) [8,51], which consisted of a hydrophobic alkyl side chain and a polar side chain with the abundance of electronegative atoms such as O and N. The control of micellar selectivity is achieved through controlling the lengths of the hydrophobic alkyl chains or by varying the ratio of hydrophobic side chain to the polar sidechain. Since these micelle polymers demonstrate unique and flexible control of selectivity, it is interesting to incorporate them into the micellar selectivity triangle and compare them with the conventional micelles. As shown in figure 3-7, the siloxane polymeric micelle family possesses strong HB basicity and weak HB acidity. Palmer and coworkers pointed out that the strong HB basicity of AGENT-type micelles might originate from the tertiary amine group on the polar side chain. This is analogous to the cationic TTAB micelles where the quaternary amine headgroup is believed to be the source of strong hydrogen bond acceptors. The dipolarity of AGENT polymeric micelle depends greatly on the ratio of the alkyl chain to the polar sidechain as well as the length of the alkyl chain present in the micelle. The unique selectivity modulations are best described in the micellar selectivity triangle in figure 3-7. As the octyl side chain composition increases from 10% to 25% percent (phases 2 to 5 in figure 3-7), the dipolarity of the polymeric micelles is reduced accordingly. The hydrogen bond basicity of micelles shows minor changes. The reason for the increase of hydrogen bond acidity of micelles with the increase of alkyl chain percentage is not clear. We shall note that some of the AGENT-type polymeric micelles had LSER regression correlation coefficients lower than 0.95 and were omitted from the comparison in our MST. Synthesis of polymeric micelles with high purity and uniform size still remains a challenge.

3.2.4 Analysis of solvent-modified micelles and mixed micelles by the MST.

Organic solvents are introduced to micellar phase as co–surfactants to expand the selectivity range of individual micellar phases and more importantly to manipulate micellar selectivity in a predictable fashion. Several traditional RPLC polar solvent modifiers (methanol, acetonitrile, tetrahydro furan, dioxane, 2-propanol, etc.) [35,52,53] have been shown to have only modest modulations of the solute-micelle interaction in terms of the solavtion parameters. This could be attributed to the narrow range of organic solvent concentrations applied in these studies to prevent the collapse of micelles under high organic solvent concentration. Instead of using polar solvents, we employed solvents with hydrophobic tails to enhance their solubilization in micelles; meanwhile, the polar functional groups of these solvents would effectively modulate the solute–micelle interactions. Pentanol (PeOH) and hexafluoro isopropanol (HFIP) are two solvents shown to effectively modify the micellar selectivity in different fashions. Pentanol with the solvent solvatochromic parameters [54] ($\alpha = 0.84, \beta = 0.86, \pi = 0.40$), appears to be a stronger hydrogen bond acceptor and a weaker hydrogen bond donor than water ($\alpha = 1.17, \beta = 0.47, \pi = 1.09$). So as pentanol molecules are incorporated into the micelles, they replace the water molecules in the interface region and consequently create a more hydrogen bond basic and less hydrogen bond acidic micellar environment. Addition of HFIP ($\alpha =1.96, \beta = 0.00, \pi = 0.65$) would make the micellar phases more hydrogen bond acidic, and at the same time less hydrogen bond basic reflecting similar solvent properties to HFIP. The effects of solvent modification on selected micelle are illustrated in the MST in figure 3-8 along with mixed micelles. The addition of HFIP to micelle systems SDS and LiPFOS enhances their hydrogen bond acidity markedly, and reduces their hydrogen bond basicity while their dipolarity is slightly increased. When pentanol is used as the solvent additive, an increase in hydrogen bond basicity and decrease in both hydrogen bond acidity and polarity are observed for these two micelle systems. The order of the hydrogen bond basicity strength of these selected micelle systems are as follows: TTAB ~ TTAB/PeOH > SDS/PeOH > SDS > LiPFOS/PeOH > SDS/HFIP > LiPFOS > LiPFOS/HFIP. One notable exception is for the pentanol-modified TTAB system. The addition of hydrogen basic pentanol, instead of enhancing the hydrogen bond basicity of TTAB micelles, slightly reduces it. To further elucidate the solvent modification effects, elution patterns of 20 aromatic compounds with various sizes and polarities were investigated with these representative micelle systems and are shown in the chromatograms in figure 3-9.

The test mixture consists of three major groups of solutes: non-hydrogen bonding solutes (NHB), hydrogen bond donating solutes (HBD), and hydrogen bond accepting solutes (HBA). Since the organic modifiers in this study are specialized in manipulating the hydrogen bonding capacity of pseudo-stationary phases, it is interesting to monitor the migration behaviors of HBA and HBD solutes in selected micellar phases. Solutes 5 (Nitrobenzene), 6 (Acetophenone), 8 (Methylbenzoate), 14 (4-chloroacetophenone) and 16 (Methyl-2-methyl benzoate) are considered to be good HBA solutes, while 1 (Resorcinol), 2 (Phenol), 7 (3-chlorophenol), 10 (4-ethylphenol), 12 (3,5–dimethyl phenol) and 15 (4-Iodophenol) are referred to as HBD solutes. The remaining solutes in the 20 test compounds are considered to be non-hydrogen bonding solutes. The LSER solvation parameters for these 20 solutes could be found in table 3-1. In chromatograms B and C of figure 3-9, we compared the modification effects of pentanol and HFIP on SDS micelles respectively. Significant alterations of elution patterns for the test solutes among the modified and unmodified micelles were observed. To quantify the solvent modification effects, we designed a retention scale $\Delta \log k_{X-Y}$ to measure the solvent modification effects on the solute retention in comparison to the unmodified micellar phases, which is basically the difference of retention factors between the modified micelle system and the unmodified micelle.

$$\Delta \log k_{X-Y} = \log k_{X} - \log k_{Y} \qquad \text{Eq. 3-5}$$

X represents pentanol or HFIP modified micelles and Y represents the unmodified micelles (SDS or LiPFOS). The differences in the retention factors largely depend on the solvent modification effects and would be a good indicator for understanding the solvent modification effects.

Figure 3-10 illustrates Δ log $k_{X\text{-}Y}$ for 20 test solutes in the pentanol and HFIP modified SDS. When SDS was mixed with the HB basic solvent PeOH, the HBD solutes 2, 7, 10, 12 and 15 preferred to retain longer in these HB basic micelles, while the HBA solutes 5, 6, 8, 14 and 16 had weaker interactions with the SDS/PeOH micelles. However the trend was reversed as a HB acidic solvent (HFIP) was employed as the micelle modifier. It was found that the HBD solutes had less retention, while the HBA solutes resided longer in the HB acidic SDS/HFIP micelles. Therefore the hydrogen bonding acidity of these micelle systems can be ranked as: SDS/HFIP > SDS > SDS/PeOH.

The elution patterns of the test solutes in the fluorinated surfactant LiPFOS and the solvent-modified LiPFOS micelles are compared in the chromatograms D, E and F in figure 3-9. The HBA solutes interacted strongly with the fluorinated surfactant (LiPFOS), which is a strong HB acidic micelle, while the HBD solutes had a weaker interaction with the LiPFOS micelles. Moreover, the hydrophobic characters of the LiPFOS micelles differed greatly from those hydrocarbonaceous micelles, mostly due to the fluorocarbon-hydrocarbon phobicity. Therefore, it is not surprising to observe dramatic alterations of elution orders between chromatogram A (SDS) and D (LiPFOS). The solvent modification effects on the LiPFOS micelles are also examined with Δ log $k_{X\text{-}Y}$ scales. As shown in figure 3-11, the addition of the HB acidic solvent (HFIP) strengthened the HB acidity of the LiPFOS micelles. As a result, the HBD solutes had weaker affinity for the

HFIP-modified LiPFOS micelles and the HBA solutes tended to retain longer in the micelles. In contrast, the addition of HB basic solvent (PeOH) weakened the affinity of the HBA solutes with the LiPFOS/PeOH micelles and caused stronger binding with the HBD solutes as compared to the unmodified LiPFOS micelles. The strength of the HB acidity of the micelle systems follows the order LiPFOS/HFIP > LiPFOS > LiPFOS/PeOH, which are in accordance with the observations in the MST. Another interesting finding is that according to the MST, the interactive properties of pentanol modified LiPFOS resemble those of SDS micelles as indicate their small interpoint distance in the MST. This could be verified through a correlation analysis of the retention factors in these three systems: SDS, LiPFOS and LiPFOS/PeOH. For example, figure 3-12 shows a relatively poor correlation (R^2=0.618) of retention factors of those 35 LSER training solutes between the SDS and LiPFOS micelles. The solutes exhibit congeneric partitioning behaviors, which means the HB donor solutes bind more strongly with the HB basic SDS micelles, the HB acceptor solutes have stronger interaction with the HB acidic LiPFOS selectively and the NHB solutes have greater affinity toward the hydrocarbonaceous SDS micelles. However, these divergent migration behaviors of solutes could be attenuated with the addition of pentanol to the LiPFOS micelles. As shown in figure 3-13, the correlation improves significantly to R^2=0.948 due to the addition of pentanol to LiPFOS micelles. This could be explained by the fact that pentanol is capable of enhancing the hydrogen bond basicity of the LiPFOS micelles and impose a more hydrocarbon-like micelle environment. This observation is readily predicted from the MST, because the SDS and LiPFOS/PeOH micelles are located closely in the MST.

Mixed-micelle is another interesting group of pseudo-phases to explore in EKC, especially when single micelles could not provide adequate resolving ability in MEKC. A mixture of micelles with complementary solavtion properties could be an alternative to solve a given problem. There are generally two categories of mixed micellar phases that have been most popularly studied: the first one consists of ionic micelles and nonionic micelles; another group is a mixture of surfactants with same type of charges. It is noteworthy that anionic-cationic mixed "micelles" is another possible kind of mixed micelles, but the stability of these anionic-cationic mixed-micelles is a concern and often vesicles are formed from mixtures of oppositely charged surfactants as reported by Pascoe and Foley [17,18]. We have rationalized these vesicle systems along with other representative pseudo-phases in an earlier section.

Previous works in our group have revealed the usefulness of mixed anionic micelles to manipulate the selectivity in various binary systems including SC/SDS, SDC/SDS and LiPFOS/LiDS [33,34,46,55] It is also worthy to note as Pyell observed that the addition of a cationic surfactant (OTAB) with a shorter hydrocarbon chain but same type of headgroup to its analogues (TTAB), did not affect the selectivity of neutral solutes, whereas the elution window was widened greatly. [56] Mixed-micelles extend the range of selectivity in MEKC. The use of MST would shed light on the nature of their selectivity as compared to individual micelles and organically modified micellar pseudo-phases.

In the MST scheme for mixed micelles (figure 3-8), the SDS surfactant is used as one component in all the binary micelles systems mainly because of the commercial availability and well-studied physical-chemical properties of SDS. As shown in the selectivity triangle, the mixed micelles of the equimolar hydrocarbon micelle LiDS and fluorocarbon micelle LiPFOS, resulted in an intermediate selectivity between the two individual micelles systems. Matsuki *et al*. and Mukerjee *et al.* independently reported [57,58] that the hydrocarbon surfactant LiDS and fluorosurfactant LiPFOS were only partially miscible in a mixed micellar form owing to the repulsion of the fluorocarbon and hydrocarbon moieties. Thus, the mixed LiDS/LiPFOS system would possibly contain two types of micelles, one rich in fluorocarbon surfactants, the other mostly made of hydrocarbon surfactants. Subsequently, the mixed LiDS/LiPFOS micelles in MEKC exhibit selectivity pattern that is a hybrid of the two micelles and is according to the mole fraction of surfactants in the mixed micelle. A recent report by Fuguet and coworkers [59] suggested that the optimization of separation could be achieved by adjusting the composition of mixed micelles of LiDS and LiPFOS. Further support that the selectivity in MEKC could be readily manipulated by the adjustments of the composition of mixed micelles and can be observed from the MST (figure 3-9). However, the selectivity of most mixed micelles would not necessarily depend on the mole fractions of constituent surfactants in a linear manner. For example, in the case of the mixed bile salt (e. g. Sodium Cholate) and SDS micelles, the selectivity characters of mixed micelles appears to be determined primarily by the SC micelles, even at equimolar ratio. This is probably due to the modification of the SDS micelles by the bulky apolar backbones of the SC monomers which in effect shield the contributions of SDS.

Nonionic surfactants have been widely used as co–surfactants with ionic surfactants in all ratios. These neutral surfactants act as spacers between the charged headgroups of ionic surfactants to reduce the electrostatic repulsions of neighboring ionic surfactant headgroups. Additionally, the abundance of polar functional groups in nonionic surfactants such as polyoxyethylene moieties modifies the interactive properties of the mixed micelles. For the mixed micelles of the nonionic micelle Brij 35 and anionic micelle SDS, the MST in figure 3-8 shows that the Brij 35 surfactants enhance the HB basicity of the SDS micelles but reduces the HB acidity of the SDS micelles. We also note that another type of nonionic surfactant FC4430, a fluoroaliphatic polymeric ester, exhibits similar modification effects to Brij 35 on the polarities of the SDS micelles. Brij35/SDS [60-62], pentanol/SDS [63] and butanol-SDS-heptane based microemulsions [64-66] are three interesting phases that have been intensely applied to estimate the octanol-water partition coefficients. Butanol-SDS-heptane microemulsion shows very similar polar selectivities to the pentanol-modified SDS micelles because both phases feature an alcohol-rich interface. The main difference between these two phases is that the microemulsion has a hydrophobic heptane-rich core, swelling the oil-in-water droplet (beneficial for cavity formation) and slightly enhancing the microemulsion ability for the hydrophobic-type interactions. However these heptane enriched hydrocarbon core has little or no effect on the polar selectivity in MEKC as recently reported by Mack and Khaledi [67]. As a micelle modifier, pentanol has very similar 'polarity' characteristics as Brij 35 due to their same polar hydroxyl end groups, however in Brij 35 the polar groups are bulkier in size due to the multiple oxyethylene moieties. As revealed by the MST, microemulsion is the phase most resembling the octanol-water system, and the Brij 35 modified SDS ranks the next. Pentanol-modified SDS micelles are slightly more hydrogen bond acidic than the octanol-water system. This observation suggests that these three analogous micelle systems shall be classified into the same group with similar polar selectivities.

4. CONCLUSIONS

Four clusters of micelle systems with different polar selectivities were recognized in the MST. LiPFOS and its modified analogs are considered to be strong hydrogen bond donors and weak hydrogen bond acceptors. AGENT-type micelles represent a special group with strong hydrogen bond basicity and very weak hydrogen bond acidity. It is noteworthy that these AGENT polymeric micelles allow for flexible control of dipolarity, which also distinguish them from other micelles. SDS micelle and its hydrocarbon analogs comprise a group with intermediate values of all three interactive properties. Organic solvents and mixed micelles have significant effects on the micellar selectivity and these changes could be monitored and manipulated in a controllable fashion with the assistance of the MST

The micellar selectivity triangle is a useful tool for micelle system characterization and classification. It is quite useful for method development in MEKC through identification of levels of similarities and differences in selectivities between different pseudo-phases. This could be beneficial for the rational selection of optimum pseudo-phase composition in MEKC separations.

The MST demonstrates its usefulness for identifying pseudo-phases for estimation of the octanol-water partition coefficients by EKC. Sodium Cholate (SC), DHP vesicles, SDS/Brij 35, Pentanol-modified SDS micelles and butanol-SDS-heptane microemulsion are pseudo-phases with nearly identical solvation properties as octanol and provide excellent correlation between micelle-water and octanol-water partition coefficients.

REFERENCES

1. Palmer CP: **Micelle polymers, polymer surfactants and dendrimers as pseudo-stationary phases in micellar electrokinetic chromatography**. *Journal of Chromatography, A* 1997, **780**:75-92.

2. Palmer CP, Tanaka N: **Selectivity of polymeric and polymer-supported pseudo-stationary phases in micellar electrokinetic chromatography**. *Journal of Chromatography, A* 1997, **792**:105-124.

3. Chen T, Palmer CP: **Evaluation of polymers based on a silicone backbone as pseudostationary phases for electrokinetic chromatography**. *Electrophoresis* 1999, **20**:2412-2419.

4. Leonard MS, Khaledi MG: **A mixed ionic block copolymer-surfactant pseudostationary phase in micellar electrokinetic chromatography**. *Journal of Separation Science* 2002, **25**:1019-1026.

5. Ozaki H, Terabe S, Ichihara A: **Micellar electrokinetic chromatography using high-molecular surfactants. Use of butyl acrylate-butyl methacrylate-methacrylic acid copolymers sodium salts as pseudo-stationary phases**. *Journal of Chromatography, A* 1994, **680**:117-123.

6. Palmer CP: **Recent progress in the development, characterization and application of polymeric pseudophases for electrokinetic chromatography**. *Electrophoresis* 2002, **23**:3993-4004.

7. Palmer CP: **Polymeric and polymer-supported pseudostationary phases in micellar electrokinetic chromatography: performance and selectivity**. *Electrophoresis* 2000, **21**:4054-4072.

8. Peterson DS, Palmer CP: **Novel alkyl-modified anionic siloxanes as pseudostationary phases for electrokinetic chromatography: II. Selectivity studied by linear solvation energy relationships**. *Electrophoresis* 2001, **22**:3562-3566.

9. Shamsi SA, Palmer CP, Warner IM: **Molecular micelles: novel pseudostationary phases for CE**. *Analytical Chemistry* 2001, **73**:140A-149A.

10. Tanaka N, Fukutome T, Hosoya K, Kimata K, Araki T: **Polymer-supported pseudo-stationary phase for electrokinetic chromatography. Electrokinetic chromatography in a full range of methanol-water mixtures with alkylated starburst dendrimers**. *Journal of Chromatography, A* 1995, **716**:57-67.

11. Yang S, Bumgarner JG, Khaledi MG: **Separation of highly hydrophobic compounds in MEKC with an ionic polymer**. *Journal of High Resolution Chromatography* 1995, **18**:443-445.

12. Kuzdzal SA, Monnig CA, Newkome GR, Moorefield CN: **Dendrimer electrokinetic capillary chromatography: unimolecular micellar behavior of carboxylic acid terminated cascade macromolecules**. *Journal of the Chemical Society, Chemical Communications* 1994:2139-2140.

13. Castagnola M, Cassiano L, Lupi A, Messana I, Patamia M, Rabino R, Rossetti DV, Giardina B: **Ion-exchange electrokinetic capillary chromatography with Starburst (pamam) dendrimers: a route towards high-performance electrokinetic capillary chromatography**. *Journal of Chromatography, A* 1995, **694**:463-469.

14. Agbodjan AA, Bui H, Khaledi MG: **Study of solute partitioning in biomembrane-mimetic pseudophases by electrokinetic chromatography: Dihexadecyl phosphate small unilamellar vesicles**. *Langmuir* 2001, **17**:2893-2899.

15. Agbodjan AA, Khaledi MG: **Study of solute partitioning into cationic vesicles of dihexadecyldimethylammonium bromide using electrokinetic chromatography**. *Journal of Chromatography A* 2003, **1004**:145-153.

16. Bui HH, Khaledi MG: **Determination of vesicle-water partition coefficients by electrokinetic chromatography: Study of temperature effect**. *Journal of Colloid and Interface Science* 2002, **253**:397-401.

17. Pascoe R, Foley JP: **Effect of class I and II organic modifiers on retention and selectivity in vesicle electrokinetic chromatography**. *Electrophoresis* 2002, **23**:1618-1627.

18. Pascoe RJ, Foley JP: **Characterization of surfactant and phospholipid vesicles for use as pseudostationary phases in electrokinetic chromatography**. *Electrophoresis* 2003, **24**:4227-4240.

19. Burns ST, Khaledi MG: **Rapid determination of liposome-water partition coefficients (K-lw) using liposome electrokinetic chromatography (LEKC)**. *Journal of Pharmaceutical Sciences* 2002, **91**:1601-1612.

20. Burns ST, Agbodjan AA, Khaledi MG: **Characterization of solvation properties of lipid bilayer membranes in liposome electrokinetic chromatography**. *Journal of Chromatography A* 2002, **973**:167-176.

21. Malek AH, Khaledi MG: **Monitoring liposome-mediated delivery and fate of an antisense drug in cell extracts and in single cells by capillary electrophoresis with laser-induced fluorescence**. *Electrophoresis* 2003, **24**:1054-1062.

22. Quang CY, Khaledi MG: **Improved Chiral Separation of Basic Compounds in Capillary Electrophoresis Using Beta-Cyclodextrin and Tetraalkylammonium Reagents**. *Analytical Chemistry* 1993, **65**:3354-3358.

23. Aumatell A, Wells RJ: **Enantiomeric differentiation of a wide range of pharmacologically active substances by cyclodextrin-modified micellar electrokinetic capillary chromatography using a bile salt**. *Journal of Chromatography, A* 1994, **688**:329-337.

24. Copper CL, Sepaniak MJ: **Cyclodextrin-modified micellar electrokinetic capillary chromatography separations of benzopyrene isomers: correlation with computationally derived host-guest energies**. *Analytical Chemistry* 1994, **66**:147-154.

25. Quang CY, Khaledi MG: **Direct Separation of the Enantiomers of Beta-Blockers by Cyclodextrin-Mediated Capillary Zone Electrophoresis**. *Hrc-Journal of High Resolution Chromatography* 1994, **17**:99-101.

26. Liu Z, Zou H, Ye M, Ni J, Zhang Y: **Effects of organic modifiers on solute retention and electrokinetic migrations in micellar electrokinetic capillary chromatography**. *Electrophoresis* 1999, **20**:2898-2908.

27. Muijselaar PG, Claessens HA, Cramers CA: **Parameters controlling the elution window and retention factors in micellar electrokinetic capillary chromatography**. *Journal of Chromatography, A* 1995, **696**:273-284.

28. Terabe S, Ishihama Y, Nishi H, Fukuyama T, Otsuka K: **Effect of urea addition in micellar electrokinetic chromatography**. *Journal of Chromatography* 1991, **545**:359-368.

29. Pyell U, Buetehorn U: **Optimization of resolution in micellar electrokinetic chromatography via computer-aided simultaneous variation of concentrations of sodium dodecyl sulfate and urea as modifier**. *Journal of Chromatography, A* 1995, **716**:81-95.

30. Kaneta T, Tanaka S, Taga M, Yoshida H: **Effect of addition of glucose on micellar electrokinetic capillary chromatography with sodium dodecyl sulfate**. *Journal of Chromatography* 1992, **609**:369-374.

31. Pyell U, Buetehorn U: **Optimization strategies in micellar electrokinetic capillary chromatography. One-parameter optimizations of the concentration of sodium dodecyl sulfate and the concentration of modifiers (urea and glucose)**. *Chromatographia* 1995, **40**:175-184.

32. Yang SY, Bumgarner JG, Khaledi MG: **Chemical selectivity in micellar electrokinetic chromatography .2. Rationalization of elution patterns in different surfactant systems**. *Journal of Chromatography A* 1996, **738**:265-274.

33. Bumgarner JG, Khaledi MG: **Mixed micelles of short chain alkyl surfactants and bile salts in electrokinetic chromatography: enhanced separation of corticosteroids**. *Journal of chromatography. A* 1996, **738**:275-283.

34. Khaledi MG, Bumgarner JG, Hadjmohammadi M: **Characterization of mixed micellar pseudostationary phases in electrokinetic chromatography using linear solvation energy relationships**. *Journal of Chromatography A* 1998, **802**:35-47.

35. Liu Z, Zou H, Ye M, Ni J, Zhang Y: **Effects of organic modifiers on retention mechanism and selectivity in micellar electrokinetic capillary chromatography studied by linear solvation energy relationships**. *Journal of Chromatography A* 1999, **863**:69-79.

36. Snyder LR: **Classification of the solvent properties of common liquids**. *Journal of Chromatography A* 1974, **92**: 223-230.

37. Snyder LR, Carr PW, Rutan SC: **Solvatochromically based solvent-selectivity triangle**. *Journal of Chromatography* 1993, **656**:537-547.

38. Kersten BR, Poole CF: **Considerations for Using the Solvent Selectivity Triangle Approach for Stationary Phase Characterization**. *Journal of Chromatography* 1988, **452**:191-208.

39. Poole CF, Poole SK: **Characterization of solvent properties of gas chromatographic liquid phases**. *Chemical Reviews (Washington, DC, United States)* 1989, **89**:377-395.

40. Li J, Zhang Y, Carr PW: **Novel triangle scheme for classification of gas chromatographic phases based on solvatochromic linear solvation energy relationships**. *Analytical Chemistry* 1992, **64**:210-218.

41. Fuguet E, Rafols C, Roses M: **Characterization of the Solvation Properties of Surfactants by Solvatochromic Indicators**. *Langmuir* 2003, **19**:6685-6692.

42. Fuguet E, Rafols C, Bosch E, Roses M: **Characterization of the Solvation Properties of Sodium n-Dodecyl Sulfate Micelles in Buffered and Unbuffered Aqueous Phases by Solvatochromic Indicators**. *Langmuir* 2003, **19**:55-62.

43. Vitha MF, Carr PW: **Study of the Polarity and Hydrogen-Bond Ability of Dodecyltrimethylammonium Bromide Micelles by the Kamlet-Taft Solvatochromic Comparison Method**. *Journal of Physical Chemistry B* 1998, **102**:1888-1895.

44. Vitha MF, Weckwerth JD, Odland K, Dema V, Carr PW: **Study of the Polarity and Hydrogen Bond Ability of Sodium Dodecyl Sulfate Micelles by the Kamlet-Taft Solvatochromic Comparison Method**. *Journal of Physical Chemistry* 1996, **100**:18823-18828.

45. Shi W, Palmer CP: **Effect of pendent group structures on the chemical selectivity and performance of sulfonated copolymers as novel pseudophases in electrokinetic chromatography**. *Electrophoresis* 2002, **23**:1285-1295.

46. Yang S, Bumgarner JG, Kruk LFR, Khaledi MG: **Quantitative structure-activity relationship studies with micellar electrokinetic chromatography. Influence of surfactant type and mixed micelles on estimation of hydrophobicity and bioavailability**. *Journal of Chromatography, A* 1996, **721**:323-335.

47. Hong M, Weekley B, Grieb SJ, Foley JP: **Electrokinetic chromatography using thermodynamically stable vesicles and mixed micelles formed from oppositely charged surfactants**. *Analytical Chemistry* 1998, **70**:1394-1403.

48. Adlard M, Okafo G, Meenan E, Camilleri P: **Rapid estimation of octanol-water partition coefficients using deoxycholate micelles in capillary electrophoresis**. *Journal of the Chemical Society, Chemical Communications* 1995:2241-2243.

49. Yang SY, Bumgarner JG, Khaledi MG: **Separation of Highly Hydrophobic Compounds in Mekc with an Ionic Polymer**. *Hrc-Journal of High Resolution Chromatography* 1995, **18**:443-445.

50. Ozaki H, Ichihara A, Terabe S: **Micellar electrokinetic chromatography using high-molecular-mass surfactants: comparison between anionic and cationic surfactants and effects of modifiers**. *Journal of Chromatography, A* 1995, **709**:3-10.

51. Peterson DS, Palmer CP: **Alkyl modified anionic siloxanes as pseudostationary phases for electrokinetic chromatography I. Synthesis and characterization**. *Journal of Chromatography, A* 2001, **924**:103-110.

52. Poole SK, Poole CF: **Characterization of surfactant selectivity in micellar electrokinetic chromatography**. *Analyst (Cambridge, United Kingdom)* 1997, **122**:267-274.

53. S.K. Poole CFP: *Anal. Commun.* 1997, **34**:57.

54. Marcus Y: **The Properties of Organic Liquids that are Relevant to their Use as Solvating Solvents**. *Chemical Society Reviews* 1993, **22**:409 - 416.

55. Bumgarner JG, Khaledi MG: **Mixed micellar electrokinetic chromatography of corticosteroids**. *Electrophoresis* 1994, **15**:1260-1266.

56. Dworschak A, Pyell U: **Widening of the elution window in micellar electrokinetic chromatography with cationic surfactants. II. Cationic additives and modifiers of the electroosmotic flow**. *Journal of Chromatography, A* 1999, **855**:669-679.

57. Matsuki H, Ikeda N, Aratono M, Kaneshina S, Motomura K: **Study on the miscibility of lithium tetradecyl sulfate and lithium perfluorooctane sulfonate in the adsorbed film and micelle**. *Journal of Colloid and Interface Science* 1992, **154**:454-460.

58. Mukerjee P, Yang AYS: **Nonideality of mixing of micelles of fluorocarbon and hydrocarbon surfactants and evidence of partial miscibility from differential conductance data**. *J. Phys. Chem* 1976, **80**:1388-1390.

59. Fuguet E, Rafols C, Torres-Lapasio JR, Garcia-Alvarez-Coque MC, Bosch E, Roses M: **Solute-Solvent Interactions in Micellar Electrokinetic Chromatography. 6. Optimization of the Selectivity of Lithium Dodecyl Sulfate-Lithium Perfluorooctanesulfonate Mixed Micellar Buffers**. *Analytical Chemistry* 2002, **74**:4447-4455.

60. Poole SK, Poole CF: **Separation methods for estimating octanol-water partition coefficients**. *Journal of Chromatography, B: Analytical Technologies in the Biomedical and Life Sciences* 2003, **797**:3-19.

61. Muijselaar PG, Claessens HA, Cramers CA: **Characterization of Pseudostationary Phases in Micellar Electrokinetic Chromatography by Applying Linear Solvation Energy Relationships and Retention Indexes**. *Analytical Chemistry* 1997, **69**:1184-1191.

62. Ishihama Y, Oda Y, Uchikawa K, Asakawa N: **Correlation of octanol-water partition coefficients with capacity factors measured by micellar**

electrokinetic chromatography. *Chemical & Pharmaceutical Bulletin* 1994, **42**:1525-1527.

63. Trone MD, Leonard MS, Khaledi MG: **Congeneric behavior in estimations of octanol-water partition coefficients by micellar electrokinetic chromatography**. *Analytical Chemistry* 2000, **72**:1228-1235.

64. Poole SK, Durham D, Kibbey C: **Rapid method for estimating the octanol-water partition coefficient (log Pow) by microemulsion electrokinetic chromatography**. *Journal of Chromatography, B: Biomedical Sciences and Applications* 2000, **745**:117-126.

65. Abraham MH, Treiner C, Roses M, Rafols C, Ishihama Y: **Linear free energy relationship analysis of microemulsion electrokinetic chromatographic determination of lipophilicity**. *Journal of Chromatography, A* 1996, **752**:243-249.

66. Ishihama Y, Oda Y, Uchikawa K, Asakawa N: **Evaluation of Solute Hydrophobicity by Microemulsion Electrokinetic Chromatography**. *Analytical Chemistry* 1995, **67**:1588-1595.

67. Mack JP, Khaledi MG: **Unpublished results**.

68. Abraham MH, Chadha HS: **Applications of a solvation equation to drug transport properties**. *Methods and Principles in Medicinal Chemistry* 1996, **4**:311-337.

69. Abraham MH: **Hydrogen bonding. 31. Construction of a scale of solute effective or summation hydrogen-bond basicity**. *Journal of Physical Organic Chemistry* 1993, **6**:660-684.

70. Herbert BJ, Dorsey JG: **n-Octanol-Water Partition Coefficient Estimation by Micellar Electrokinetic Capillary Chromatography**. *Analytical Chemistry* 1995, **67**:744-749.

71. Yang SY, Khaledi MG: **Chemical Selectivity in Micellar Electrokinetic Chromatography - Characterization of Solute Micelle Interactions for Classification of Surfactants**. *Analytical Chemistry* 1995, **67**:499-510.

72. Chen N, Zhang Y, Terabe S, Nakagawa T: **Effect of physico-chemical properties and molecular structure on the micelle-water partition coefficient in micellar electrokinetic chromatography**. *Journal of Chromatography, A* 1994, **678**:327-332.

73. Trone MD, Khaledi MG: **Characterization of chemical selectivity in micellar electrokinetic chromatography: V. The effect of the surfactant hydrophobic chain**. *Journal of Microcolumn Separations* 2000, **12**:433-441.

74. Vitha MF, Carr PW: **A linear solvation energy relationship study of the effects of surfactant chain length on the chemical interactions governing retention and selectivity in micellar electrokinetic capillary chromatography using sodium alkyl sulfate buffers**. *Separation Science and Technology* 1998, **33**:2075-2100.

75. Poole CF, Poole SK, Abraham MH: **Recommendations for the determination of selectivity in micellar electrokinetic chromatography**. *Journal of Chromatography, A* 1998, **798**:207-222.

76. Trone MD, Khaledi MG: **Characterization of chemical selectivity in micellar electrokinetic chromatography. 4. Effect of surfactant headgroup**. *Analytical Chemistry* 1999, **71**:1270-1277.

77. Trone MD, Khaledi MG: **Influence of ester and amide-containing surfactant headgroups on selectivity in micellar electrokinetic chromatography**. *Electrophoresis* 2000, **21**:2390-2396.

78. Barker J: *Thesis (Ph.D.)--North Carolina State University* 2004.

Table 3-1 LSER training solutes and their solvation descriptors [a]

	Solutes	V	B	A	S	E
1	Benzene	0.716	0.14	0	0.52	0.61
2	Toluene	0.857	0.14	0	0.52	0.6
3	Ethylbenzene	0.998	0.15	0	0.51	0.61
4	Propylbenzene	1.139	0.15	0	0.5	0.6
5	Butylbenzene	1.28	0.15	0	0.51	0.6
6	o-xylene	0.998	0.16	0	0.56	0.66
7	Chlorobenzene	0.839	0.07	0	0.65	0.72
8	Bromobenzene	0.891	0.09	0	0.73	0.88
9	Iodobenzene	0.975	0.12	0	0.82	1.19
10	4-chlorotoluene	0.98	0.07	0	0.67	0.71
11	4-bromotoluene	1.032	0.09	0	0.74	0.88
12	Naphthalene	1.085	0.2	0	0.92	1.34
13	Resorcinol	0.834	0.58	1.1	1	0.98
14	Phenol	0.775	0.3	0.6	0.89	0.81
15	4-ethyl phenol	1.057	0.36	0.55	0.9	0.8
16	3,5-dimethyl phenol	1.057	0.36	0.57	0.84	0.82
17	3-nitrophenol	0.949	0.23	0.79	1.57	1.05
18	4-fluorophenol	0.793	0.23	0.63	0.97	0.67
19	3-chlorophenol	0.898	0.15	0.69	1.06	0.91
20	3-bromo phenol	0.95	0.16	0.7	1.15	1.06
21	4-iodophenol	1.033	0.2	0.68	1.22	1.38
22	3-methyl phenol	0.916	0.34	0.57	0.88	0.82
23	Phenethyl alcohol	1.057	0.66	0.3	0.83	0.78
24	Benzyl alcohol	0.916	0.56	0.33	0.87	0.8
25	4-methylbenzyl alcohol	1.057	0.6	0.33	0.88	0.81
26	Acetophenone	1.014	0.48	0	1.01	0.82
27	3-chloroacetophenone	1.137	0.4	0	1.07	0.92
28	Benzonitrile	0.871	0.33	0	1.11	0.74
29	Nitrobenzene	0.891	0.28	0	1.11	0.87
30	1-chloro-4-nitrobenzene	1.013	0.25	0	1.17	0.98
31	Benzyl chloride	0.98	0.33	0	0.82	0.82
32	Phenyl acetate	1.073	0.54	0	1.13	0.66
33	Methylbenzoate	1.073	0.46	0	0.85	0.73
34	Ethyl benzoate	1.214	0.46	0	0.85	0.69
35	Methyl-2-methylbenzoate	1.214	0.43	0	0.87	0.77

a: Ref. [68]

Table 3-2 Variance–covariance matrix of LSER solute descriptors.

	V	B	A	S	E
V	1				
B	0.23	1			
A	-0.32	0.21	1		
S	-0.06	0.31	0.49	1	
E	0.01	-0.07	0.35	0.60	1

Table 3-3 Characterization of SDS micellar phases in MEKC

	SDS Micelles	v	b	a	s	e
1	0.01 M SDS	2.95	-1.77	-0.12	-0.59	0.43
2	0.015 M SDS	3.11	-1.95	-0.05	-0.58	0.52
3	0.02 M SDS	2.95	-1.92	-0.08	-0.64	0.52
4	0.025 M SDS	2.89	-1.88	-0.11	-0.63	0.54
5	0.04 M SDS	3.01	-1.88	-0.20	-0.46	0.33
6	0.06 M SDS	2.95	-1.76	-0.17	-0.54	0.41
7	SDS [a]	2.99	-1.88	-0.30	-0.44	0.46
8	SDS [b]	2.62	-1.57	-0.31	-0.67	0.56
9	SDS [c]	2.91	-1.87	-0.44	-0.24	0.31
10	SDS [d]	2.83	-1.71	-0.15	-0.44	0.47
11	SDS [d]	2.81	-1.71	-0.16	-0.48	0.46
12	SDS [e]	2.56	-1.56	-0.33	-0.66	0.57
13	SDS [f]	2.86	-1.70	-0.15	-0.31	0.25
14	SDS [g]	2.98	-1.91	-0.24	-0.42	0.36
	Average	2.86	-1.77	-0.20	-0.52	0.45
	Std	0.17	0.14	0.11	0.14	0.10

a: Ref. [52],
b: Ref. [69],
c: Ref. [70],
d: Ref. [71],
e: Ref. [72],
f: Ref. [73],
g: Ref. [74]

Table 3-4 Characterization of pseudo-phases in EKC

IDs	Pseudo-phases	Abbreviations	*b/v*	*a/v*	*s/v*	*e/v*
1	40 mM Sodium dodecyl sulfate (averaged)	SDS	-0.62	-0.07	-0.18	0.16
2	Sodium tetradecyl sulfate [a]	STS	-0.60	-0.06	-0.11	0.09
3	Sodium octyl sulfate [b]	SOS	-0.66	-0.04	-0.11	0.16
4	Sodium decyl sulfate [b]	SDecS	-0.59	0.00	-0.09	0.12
5	Sodium dodecyl sulfate + Pentanol	SDS/PeOH	-0.84	-0.01	-0.31	0.18
6	Sodium dodecyl sulfate +Trifluoro Ethanol	SDS/TFE	-0.59	-0.11	-0.17	0.14
7	Sodium dodecyl sulfate +Trichloro Ethanol	SDS/TCE	-0.61	-0.23	-0.22	0.15
8	Sodium dodecyl sulfate +Hexafluoro Isopropanol	SDS/HFIP	-0.51	-0.23	-0.14	0.07
9	Sodium dodecyl sulfate + Octafluoro Pentanol	SDS/ FPeOH	-0.57	-0.24	-0.18	0.09
10	Sodium dodecyl sulfate + Butyronitrile	SDS/BuCN	-0.70	-0.06	-0.19	0.15
11	Sodium dodecyl sulfate + 1% Brij 35	SDS/Brij 35	-0.79	0.02	-0.21	0.22
12	Sodium dodecyl sulfate +1% FC 4300	SDS/FC 4300	-0.80	0.01	-0.23	0.20
13	Microemulsion (1.4% wt SDS 6.49% butanol 0.82% heptane) [c]	Microemulsion	-0.92	-0.02	-0.23	0.09
14	Hexadecyltrimethylammonium bromide [c]	HTAB	-0.91	0.17	-0.16	0.18
15	Tetradecyltrimethylammonium bromide	TTAB	-0.78	0.28	-0.22	0.27
16	Cetyltrimethylammonium bromide [d]	CTAB	-0.93	0.29	-0.09	0.16
17	10 mM TTAB + 300 mM Pentanol	TTAB/PeOH	-0.87	0.10	-0.33	0.25
18	40 mM Lithium perfluorooctanesulfonate	LiPFOS	-0.29	-0.24	0.13	-0.10

19	40 mM Lithium perfluorooctanesulfonate [c]	LiPFOS	-0.23	-0.30	0.13	-0.19
20	40mM Lithium perfluorooctanesulfonate [e]	LiPFOS	-0.26	-0.34	0.19	-0.29
21	0.04 M Lithium perfluorooctanesulfonate + 0.4 M PeOH	LiPFOS/PeOH	-0.64	-0.12	-0.20	0.01
22	0.04 M Lithium perfluorooctanesulfonate + 0.4 M HFIP	LiPFOS/HFIP	-0.22	-0.43	0.17	-0.23
23	60mM Sodium Cholate [e]	SC	-0.91	0.03	-0.24	0.20
24	40 mM Sodium (S)-N-dodecoxycarbonyl valine [e]	SDCV	-0.82	0.05	-0.19	0.14
25	40mM Sodium laurylsulfoacetate [e]	LSA	-0.84	0.05	-0.13	0.19
26	2% Elvacite 2669 [e]	Elvacite 2669	-0.92	0.03	-0.09	0.18
27	20/20mM Lithium dodecyl sulfate/ LiPFOS [e]	LiDS/LiPFOS	-0.46	-0.18	-0.02	-0.04
28	30/30mM Sodium dodecyl sulfate / Sodium Cholate [e]	SDS/SC	-0.84	0.03	-0.19	0.17
29	30/30mM Sodium dodecyl sulfate / Sodium deoxycholate [e]	SDS/SDC	-0.75	0.01	-0.22	0.18
30	40 mM Sodium dodecyl sulfate + 400mM PeOH	SDS/PeOH	-0.86	0.00	-0.22	0.11
31	poly(sodium undecylenate) [f]	PSUA	-0.56	-0.13	-0.08	0.12
32	Allyl glycidyl ether N-methyl taurine siloxane [g]	AGENT	-0.93	0.22	-0.04	0.37
33	OAGENT 10% C8 [g]	OAGENT 10%	-1.38	0.14	-0.13	0.32
34	OAGENT 15% C8 [g]	OAGENT 15%	-1.08	0.11	-0.21	0.26
35	OAGENT 20% C8 [g]	OAGENT 20%	-1.14	0.05	-0.41	0.22
36	OAGENT 25% C8 [g]	OAGENT 25%	-1.11	0.05	-0.52	0.34
37	DAGENT 20% C 12 [g]	DAGENT 20%	-1.00	0.09	-0.36	0.13
38	SAGENT 10% C 18 [g]	SAGENT 10%	-1.34	-0.06	-0.38	0.11
39	Polymeric octyl methacrylate –21 [f]	pOMAt-21	-1.05	-0.11	-0.17	0.13

40	Polymeric lauryl methacrylate 15 [f]	pLMAt-15	-1.01	-0.08	-0.18	0.12
41	Polymeric stearyl methacrylate -16 [f]	pSMAt-16	-1.01	-0.13	-0.22	0.17
42	Polymeric lauryl acrylate –13 [f]	pLAt-13	-0.98	-0.01	-0.11	0.11
43	Polymeric lauryl methacrylamide -19 [f]	pLMAm-19	-0.85	0.09	-0.11	0.13
44	Polymeric dihydrocholesteryl acrylate -33 [f]	pDHCHAT-33	-0.94	0.07	-0.14	0.19
45	Polymeric t-octyl acrylamide -49 [f]	ptOAm-49	-0.96	0.13	-0.13	0.10
46	40 mM Sodium dodecyl sulfonate [h]	SDSu	-0.63	-0.01	-0.15	0.12
47	40 mM Sodium dodecyl carboxylate [h]	SDC	-0.60	0.08	-0.13	0.05
48	40 mM Sodium dodecyl phosphate [h]	SDP	-0.66	0.05	-0.18	0.08
49	40 mM Sodium (S)-N-dodecoxycarbonyl valine [h]	SDCV	-0.81	0.04	-0.21	0.14
50	40 mM Sodium larurylsulfoacetate [h]	SLSA	-0.81	0.03	-0.13	0.14
51	40 mM N-lauroyl-N-methyltaurate [i]	LMT	-0.82	0.14	-0.12	0.18
52	40 mM N-lauroyl-N-methyl-β-alaninate [i]	ALE	-0.83	0.17	-0.13	0.15
53	40 mM Sodium N-lauroyl sarcosinate [i]	SLN	-0.79	0.15	-0.13	0.15
54	40 mM Sodium N-lauroyl sarcosinate [a]	SLN	-0.77	0.16	-0.11	0.13
55	40 mM Sodium N-myristoyl sarcosinate [a]	SMN	-0.82	0.15	-0.14	0.16
56	40 mM Sodium N-parmitoyl sarcosinate [a]	SPN	-0.83	0.15	-0.15	0.14
57	15mM DPPG 20 DPPC 80 [j]	DPPG 20 DPPC 80	-1.03	0.19	-0.15	0.13
58	15mM DPPG 20 DPPC 80 3 mM cholesterol [j]	DPPG 20 DPPC 80 Chol 3mM	-1.04	0.13	-0.14	0.14
59	15mM DPPG 20 DPPC 80 6 mM cholesterol [j]	DPPG 20 DPPC 80 Chol 6mM	-1.09	0.08	-0.17	0.17
60	15mM DPPG 20 DPPC 80 9.7 mM cholesterol [j]	DPPG 20 DPPC 80 Chol 9.75mM	-1.17	0.00	-0.22	0.22

61	15mM PI 10 DPPC 30 DPPE30 SPM 20 9.7 mM cholesterol [j]	PI 10 DPPC 30 DPPE30 SPM 20 Chol	-1.14	0.00	-0.27	0.25
62	15 mM DPPG 20 DHPC 30 DPPC 50 [j]	DPPG 20 DHPC 30 DPPC 50	-1.04	0.19	-0.16	0.15
63	15 mM DPPG 20 DHPC 40 DPPC 40 [j]	DPPG 20 DHPC 40 DPPC 40	-1.06	0.16	-0.15	0.15
64	15 mM DPPG 20 DHPC 50 DPPC 30 [j]	DPPG 20 DHPC 50 DPPC 30	-1.04	0.15	-0.22	0.18
65	15 mM DPPG 20 DHPC 60 DPPC 20 [j]	DPPG 20 DHPC 60 DPPC 20	-1.04	0.14	-0.19	0.17
66	15 mM DPPG 20 DHPC 70 DPPC 10 [j]	DPPG 20 DHPC 70 DPPC 10	-1.04	0.13	-0.20	0.18
67	Dihexadecyl phosphate [k]	DHP	-0.91	0.13	-0.18	0.12
68	10 mM DHP/4.4 mM cholesterol (70%/30%) [k]	DHP 4.4 mM Chol	-0.97	0.10	-0.24	0.16
69	10 mM DHP/7.0 mM cholesterol (51%/49%) [k]	DHP 7.0 mM Chol	-0.98	0.13	-0.23	0.16
70	Cetyltrimethylammonium bromide (1.8% w/v, 3:7) [l]	CTAB/SOS	-1.09	0.22	-0.17	0.14
71	Octyltrimethylammonium bromide (1.0% w/v, 7:3) [l]	OTAB/SDS	-0.99	0.22	-0.28	0.18
72	Bis(2-ethylhexyl)sodium sulfosuccinate (40 mM 10% v/v MeOH) [l]	AOT	-1.06	-0.05	-0.15	0.24
73	POPC/PS (3 mM, 8:2) [l]	POPC/PS	-1.08	0.01	-0.20	0.26
74	Octanol/Water	O-W	-0.96	0.02	-0.23	0.10

DPPG: Dipalmitoyl-L-α-phosphotidylglycerol (sodium salt), **DPPC**: Dipalmitoyl-L-α-phosphotidylcholine, **Chol**: Cholesterol,

DHPC: 1,2-Diheptanoyl-*sn*-Glycero-3-Phosphocholine, **POPC**: 1-palmitoyl-2-oleyl-*sn*-glycero-3-phosphocholine, **PS**: Phosphatidyl serine, **DPPE**: 1,2-Dipalmitoyl-sn-Glycero-3-Phosphoethanolamine, **SPM**: *N*-Palmitoyl-D-sphingomyelin.

a: REF. [73], b: REF. [74], c: REF. [75], e: REF. [63], f: REF. [6], g: REF. [8], h: REF. [76], i: REF. [77], j: REF.[78] k: REF. [14], l: REF [18]

Table 3-5 Preset range for LSER system parameter normalization in MST

	b/v	a/v	s/v	e/v
I_{low}	-1.50	-0.50	-0.60	-0.50
I_{high}	0.00	1.00	0.90	1.00

Table 3-6 Classifications of EKC stationary phases selectivity.

Groups	Phases	HB Acidity	HB Basicity	Dipolarity	Polarizability
A	SDS, SOS, STS, SDeS, SDSu, SDC, SDP, SDS/BuCN, SDS/TFE, SDS/PeOH, SDS/Brij 35, SDS/FC4430	medium^{+}	medium^{-}	low ~ medium	medium
B	SDS/HFIP, SDS/TCE, SDS/FBuOH, LiPFOS, LiPFOS/HFIP, LiDS/LiPFOS	high	low	medium	low
C	Microemulsion, Liposomes, Elvacite 2669, pLMAt-type polymeric micelles, Octanol-water, Bile Salts, Sarcosinate surfactants.	low ~ medium	medium^{+}	medium^{+}	medium^{+}
D	AGENT-type polymeric micelles, TTAB, TTAB/PeOH	low ~ medium	high	medium ~ high	high

Figure Captions

Figure 3-1 Distribution of normalized LSER coefficients representing polar selectivities for 76 pseudo-phases.

Figure 3-2 Micellar selectivity triangle for characterization of 15 SDS micellar phases.

Figure 3-3 Micellar selectivity triangle (*b, a, s*) for characterization of polar selectivities of pseudo-phases.

Figure 3-4 Micellar selectivity triangle (*b, a, e*) for characterization of polar selectivities of pseudo-phases.

Figure 3-5 Micellar selectivity triangle (*b, s, e*) for characterization of polar selectivities of pseudo-phases.

Figure 3-6 Micellar selectivity triangle for characterization of the representative pseudo-phases.

Figure 3-7 Micellar selectivity triangle for characterization of the polar selectivity of polymeric micelles.

Figure 3-8 Micellar selectivity triangle for characterization of the solvent modification effects and mixed micelles effects.

Figure 3-9 Chromatograms of the separation of 20 aromatic solutes

Figure 3-10 Comparisons of the solvent modification effects on SDS.

Figure 3-11 Comparisons of the solvent modification effects on LiPFOS.

Figure 3-12 Correlation of the retention factors of test solutes between 40 mM SDS and 40 mM LiPFOS.

Figure 3-13 Correlation of the retention factors of test solutes between 40 mM SDS and pentanol modified LiPFOS.

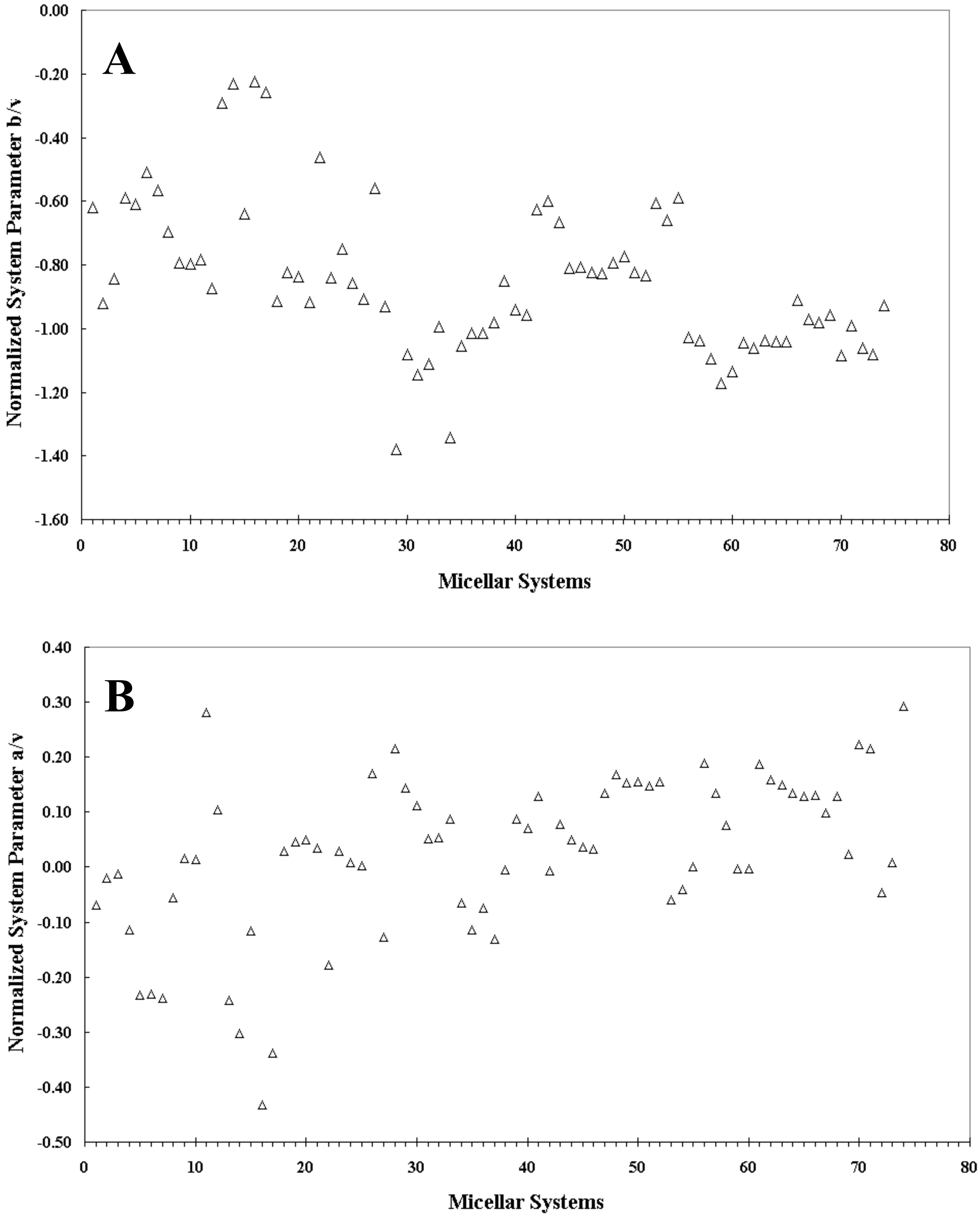
A
Normalized System Parameter b/v
Micellar Systems
B
Normalized System Parameter a/v
Micellar Systems

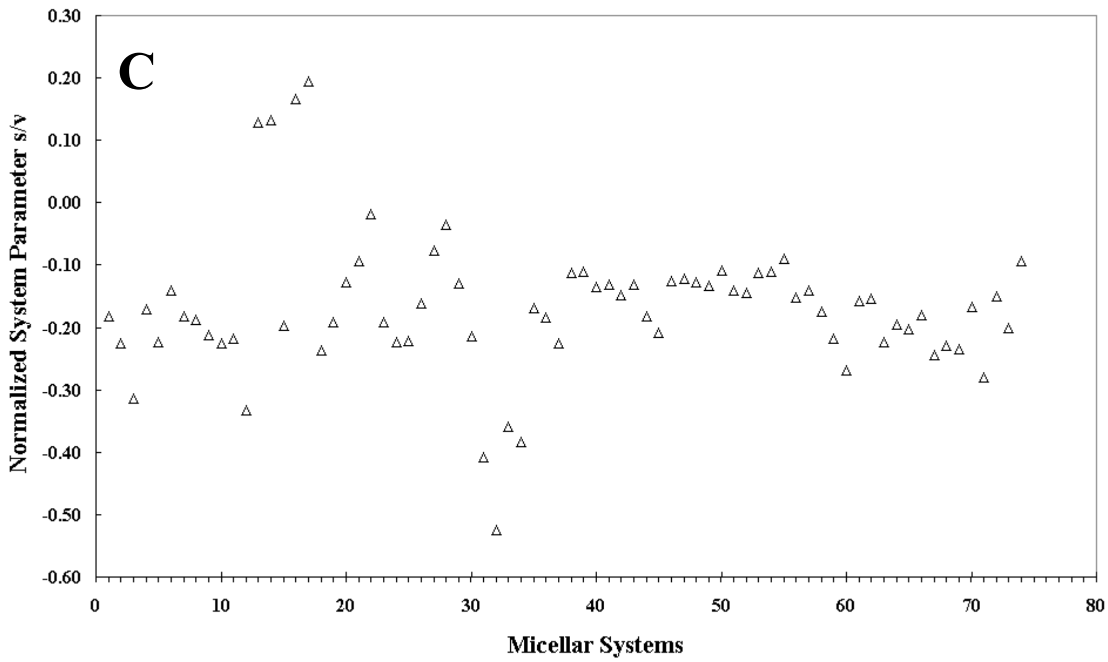
C
Normalized System Parameter s/v
0.30
0.20
0.10
0.00
-0.10
-0.20
-0.30
-0.40
-0.50
-0.60
0
10
20
30
40
50
60
70
80
Micellar Systems

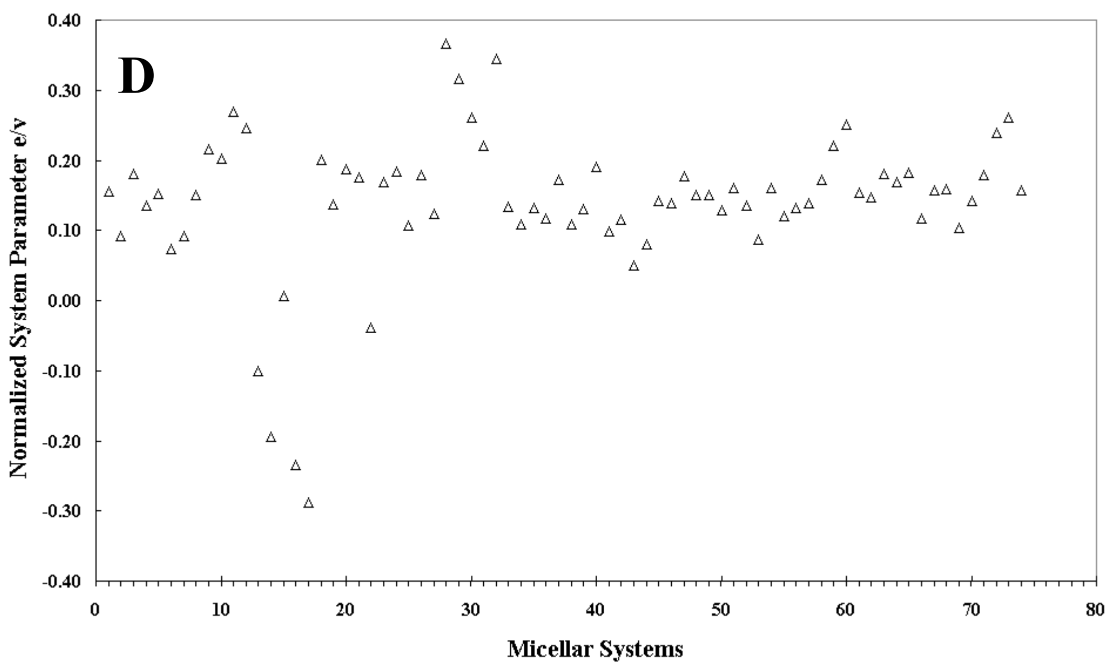
D
Normalized System Parameter e/v
0.40
0.30
0.20
0.10
0.00
-0.10
-0.20
-0.30
-0.40
0
10
20
30
40
50
60
70
80
Micellar Systems

Figure 3-1 Distribution of normalized LSER coefficients representing polar selectivities for 76 pseudo-phases. A) Normalized HB acidity of pseudo-phases. B) Normalized HB basicity of pseudo-phases. C) Normalized dipolarity of pseudo-phases. D) Normalized polarizability of pseudo-phases.

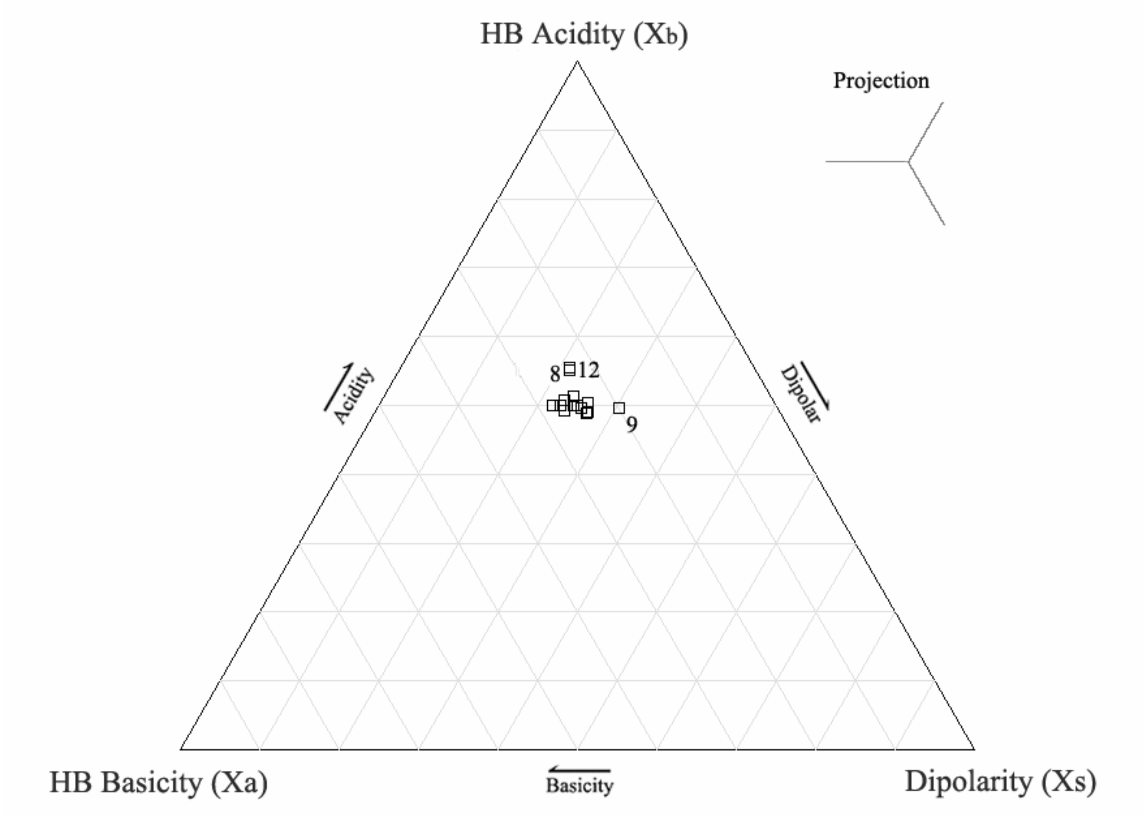

Figure 3-2 Micellar selectivity triangle for characterization of 14 SDS micellar phases from the LSER models reported by various laboratories. (The numbers of the micelle systems are identical with table 3-3)

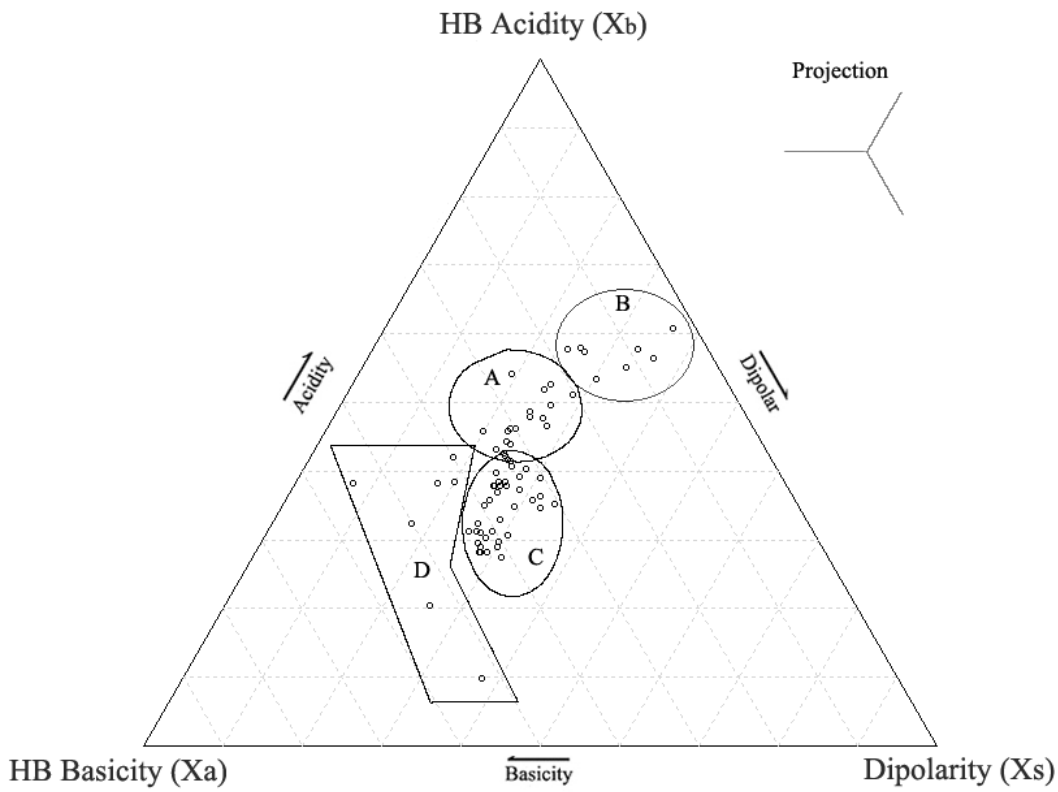

Figure 3-3 Micellar selectivity triangle (X_b, X_a, X_s) for characterization of polar selectivities of pseudo-phases.

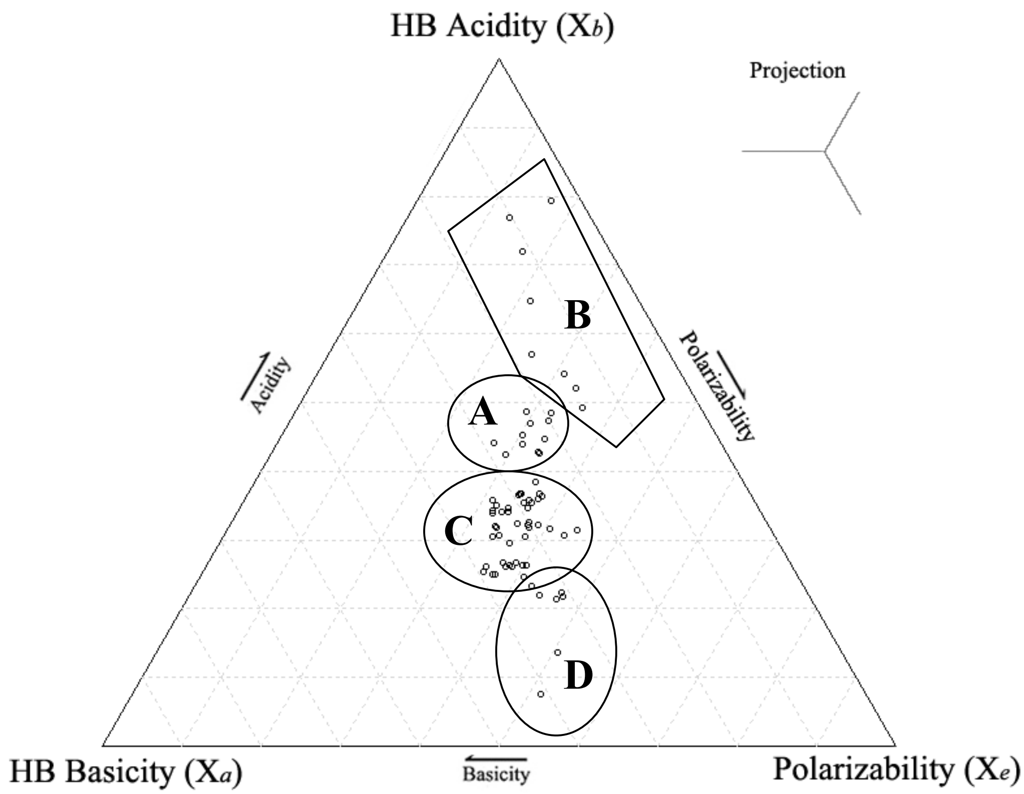

Figure 3-4 Micellar selectivity triangle (X_b, X_a, X_e) for characterization of polar selectivities of pseudo-phases.

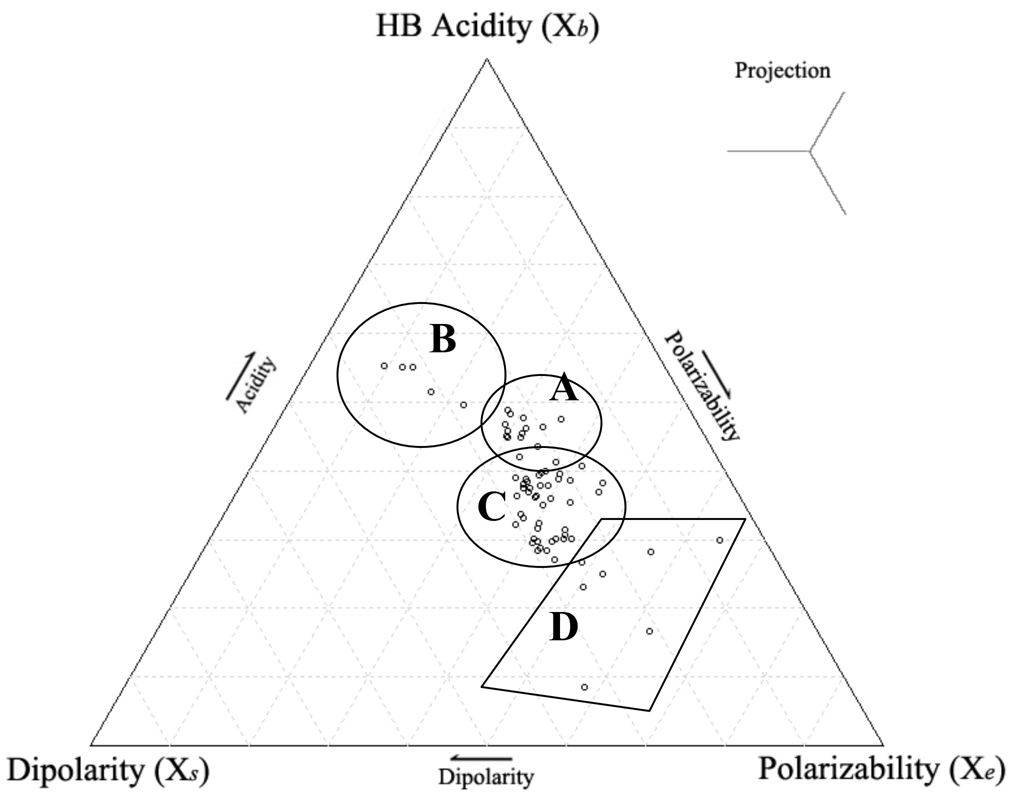

Figure 3-5 Micellar selectivity triangle (X_b, X_s, X_e) for characterization of polar selectivities of pseudo-phases.

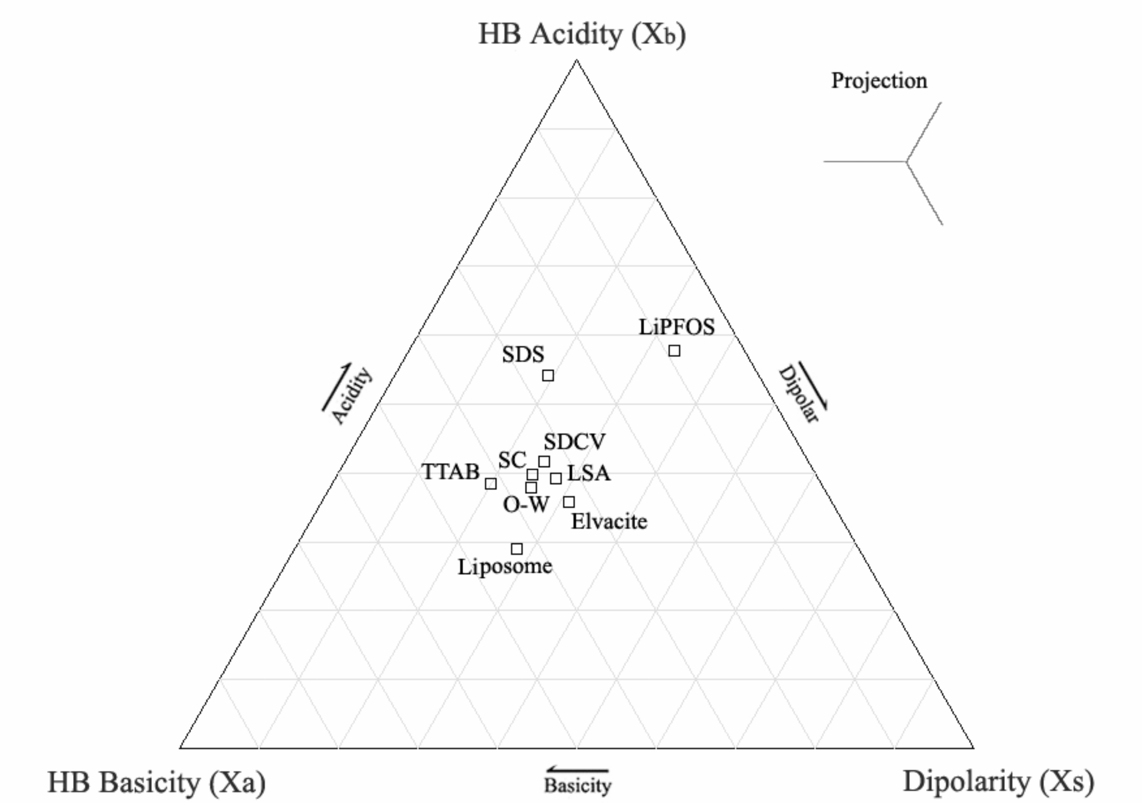

Figure 3-6 Micellar selectivity triangle for characterization of the representative pseudo-phases

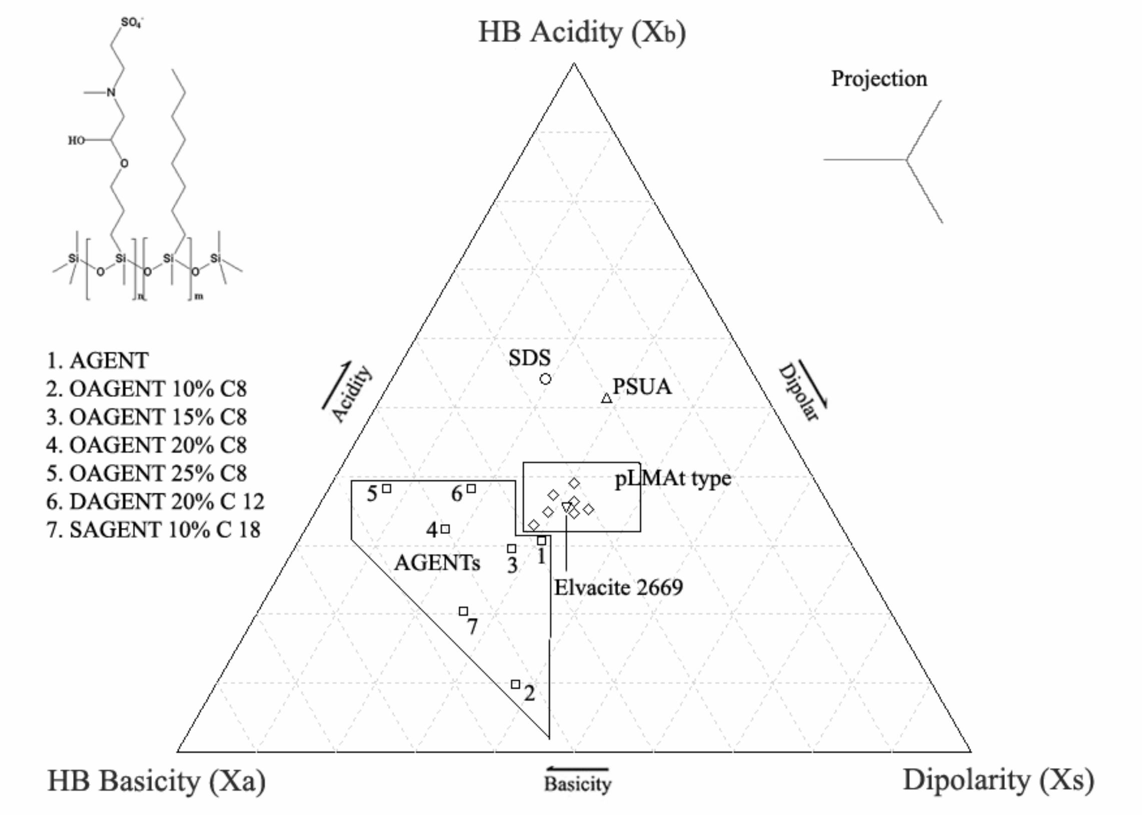

Figure 3-7 Micellar selectivity triangle for characterization of the polar selectivity of polymeric micelles

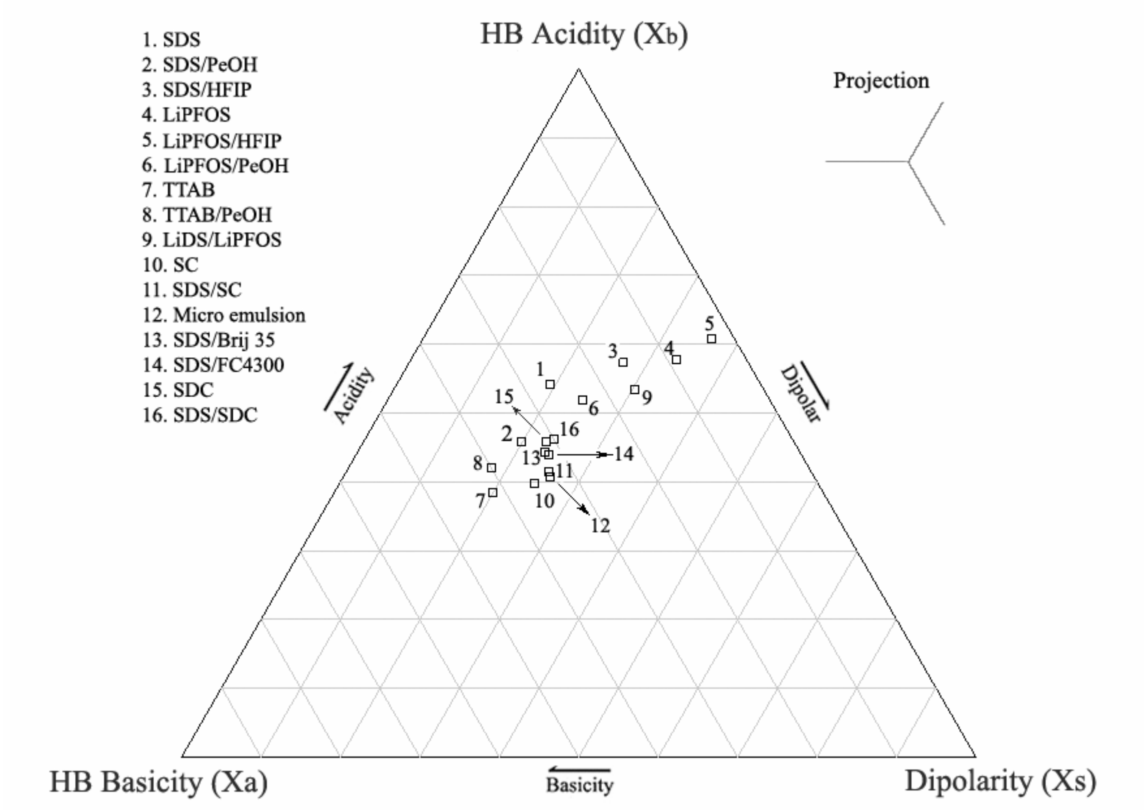

Figure 3-8 Micellar selectivity triangle for characterization of the solvent modification effects and mixed micelles effects.

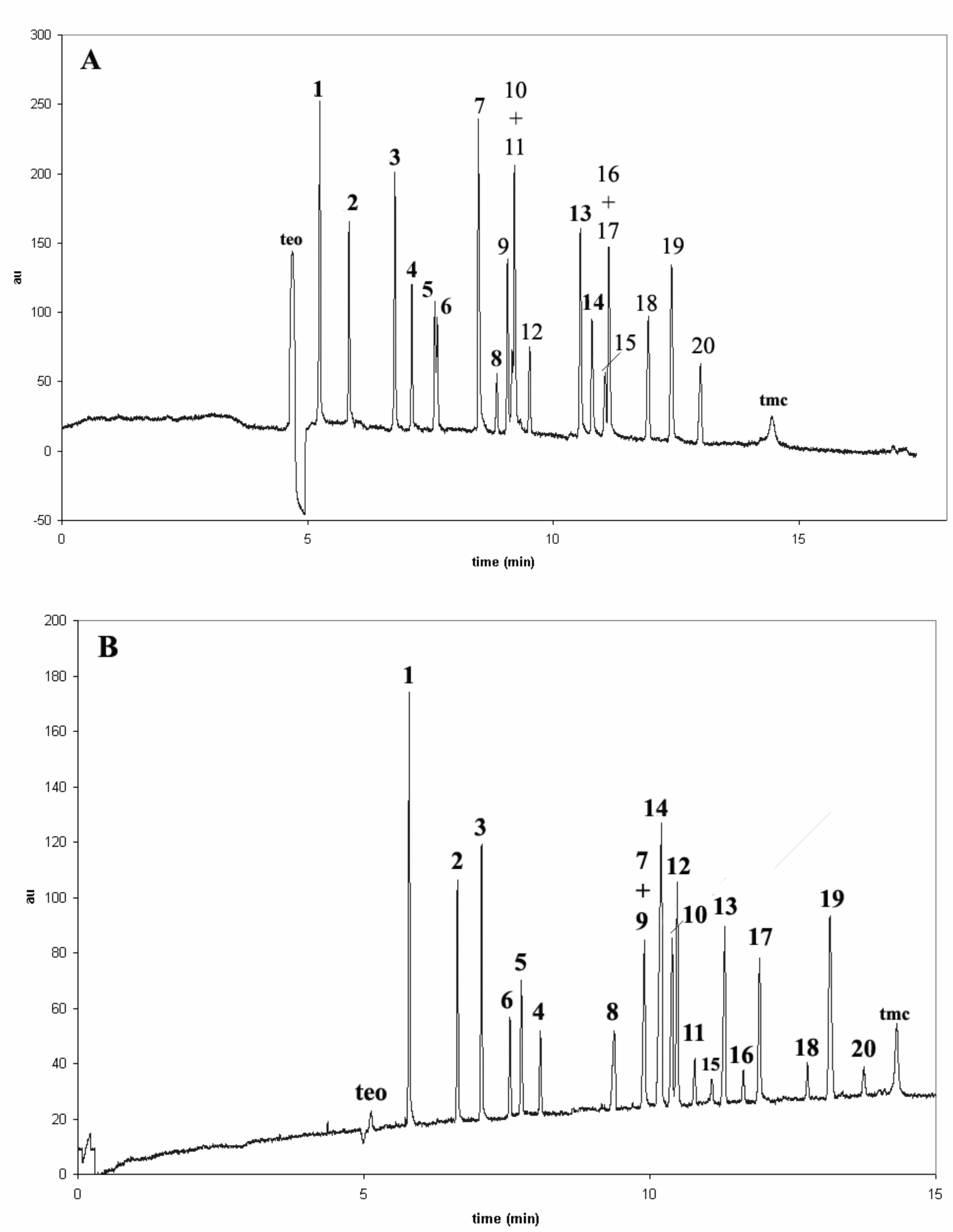
A
B
au
time (min)
teo
tmc
1
2
3
4
5
6
7
8
9
10
+
11
12
13
14
15
16
+
17
18
19
20
7
+
9

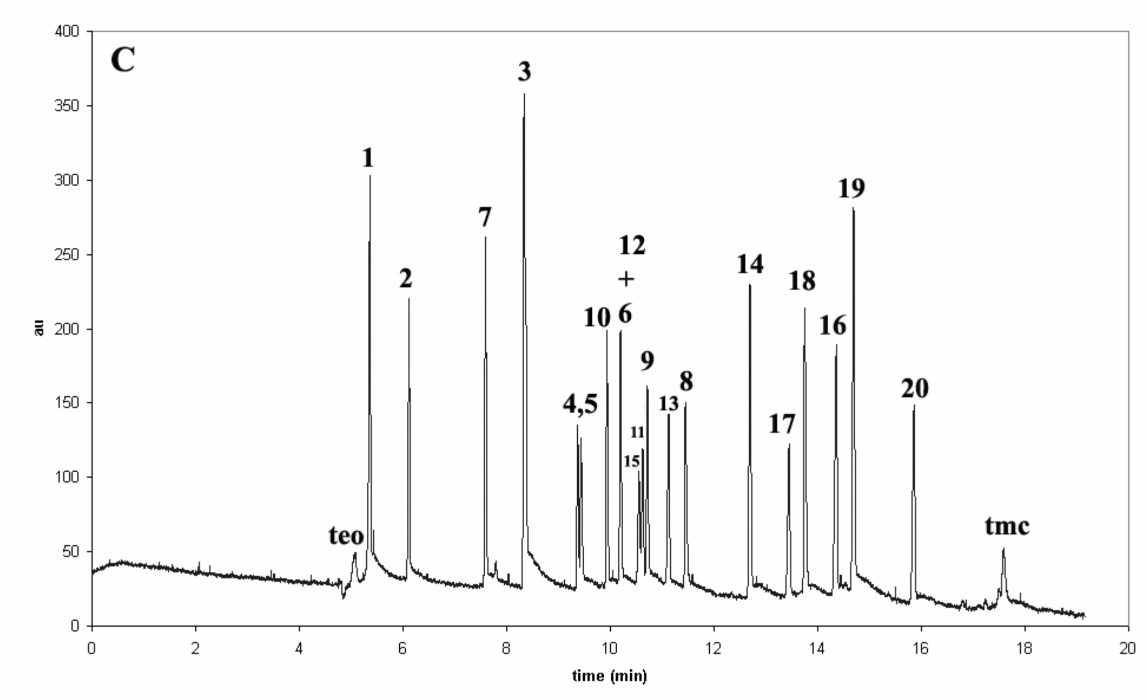
C
au
time (min)
teo
1
2
7
3
4,5
10
12
+
6
15
11
9
13
8
14
17
18
16
19
20
tmc

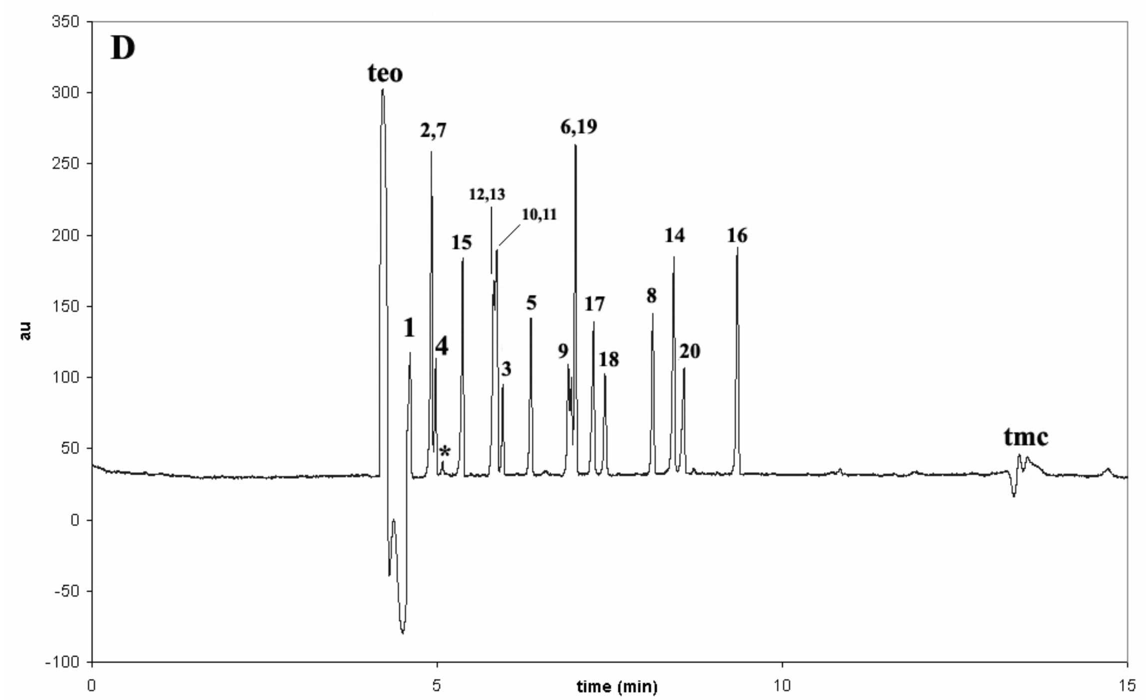
D
au
time (min)
teo
1
2,7
4
*
15
12,13
10,11
3
5
9
6,19
17
18
8
14
20
16
tmc

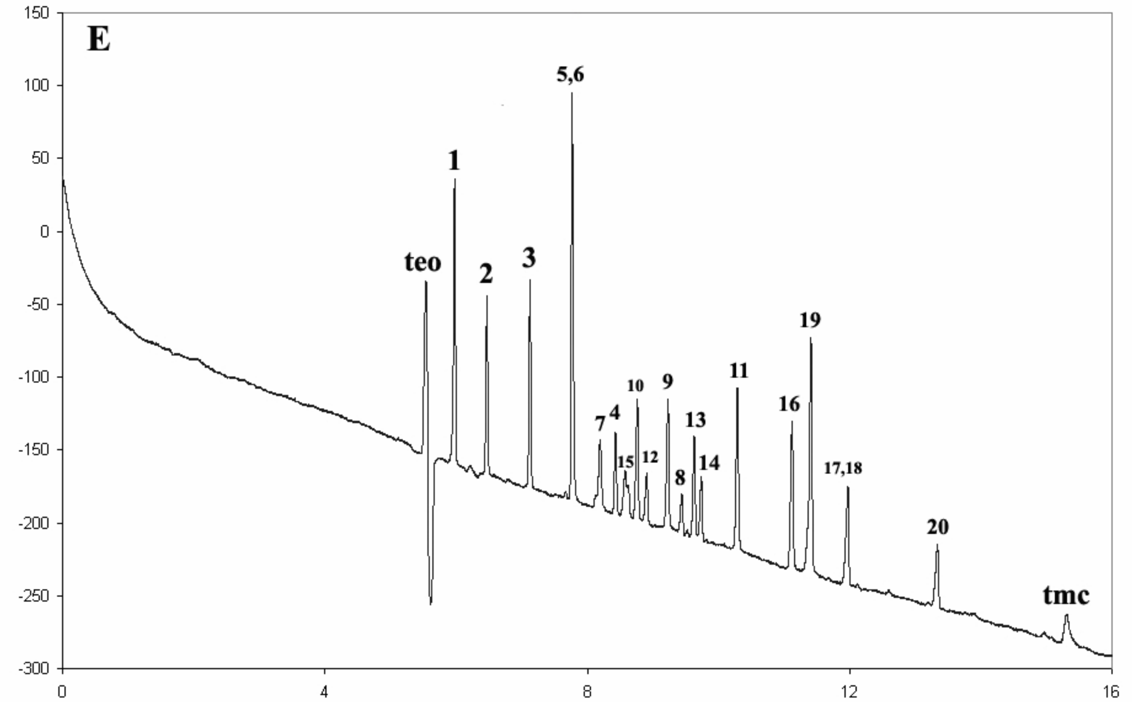
E
teo
1
2
3
5,6
7
4
10
15
12
9
8
13
14
11
16
19
17,18
20
tmc

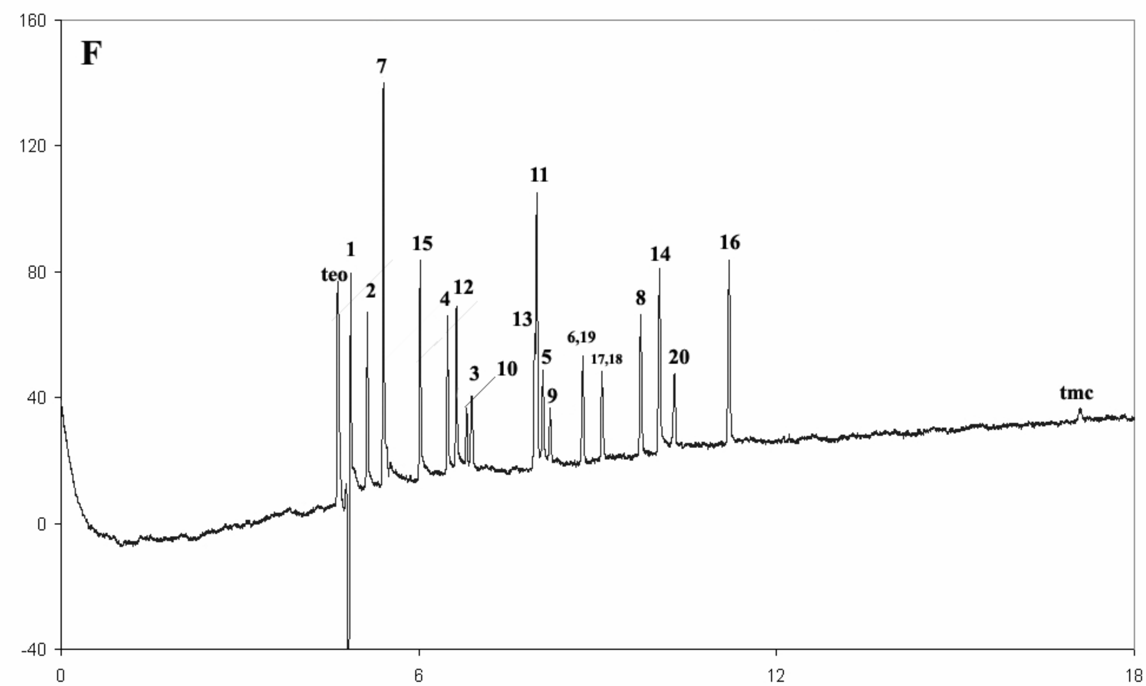
F
teo
1
2
7
15
4
12
3
10
13
11
5
9
6,19
17,18
8
14
20
16
tmc

Figure 3-9. Chromatograms of the separation of 20 aromatic solutes, peak IDs: **1**. Resorcinol, **2**. Phenol, **3**. Phenethyl alcohol, **4**. Benzene, **5**. Nitrobenzene, **6**. Acetophenone, **7**. 3-chlorophenol, **8**. Methylbenzoate, **9**. Benzyl chloride, **10**. 4-Ethylphenol, **11**. Toluene, **12**. 3,5-dimethyl phenol, **13**. Chlorobenzene, **14**. 4-chloroacetophenone, **15**. 4-Iodophenol, **16**. Methyl-2-methyl benzoate, **17**. Ethylbenzene, **18**. 4-chlorotoluene, **19**. Naphthalene, **20**. Propylbenzene; micellar phases IDs: A) 40 mM SDS, B) 40 mM SDS/400 mM PeOH (4.34 v/v%), C) 40 mM SDS/400 mM HFIP (4.16 v/v%), D) 40 mM LiPFOS, E) 40 mM LiPFOS/400 mM PeOH (4.34 v/v%), F) 40 mM LiPFOS/400 mM HFIP (4.16 v/v%); a 20 mM sodium phosphate buffer pH 7.0 was used in all SDS micelle systems, running buffer for LiPFOS micelles was 20 mM lithium phosphate buffer at pH 7.0; 20 kv applied on a 70 cm length capillary (effective length 50 cm).

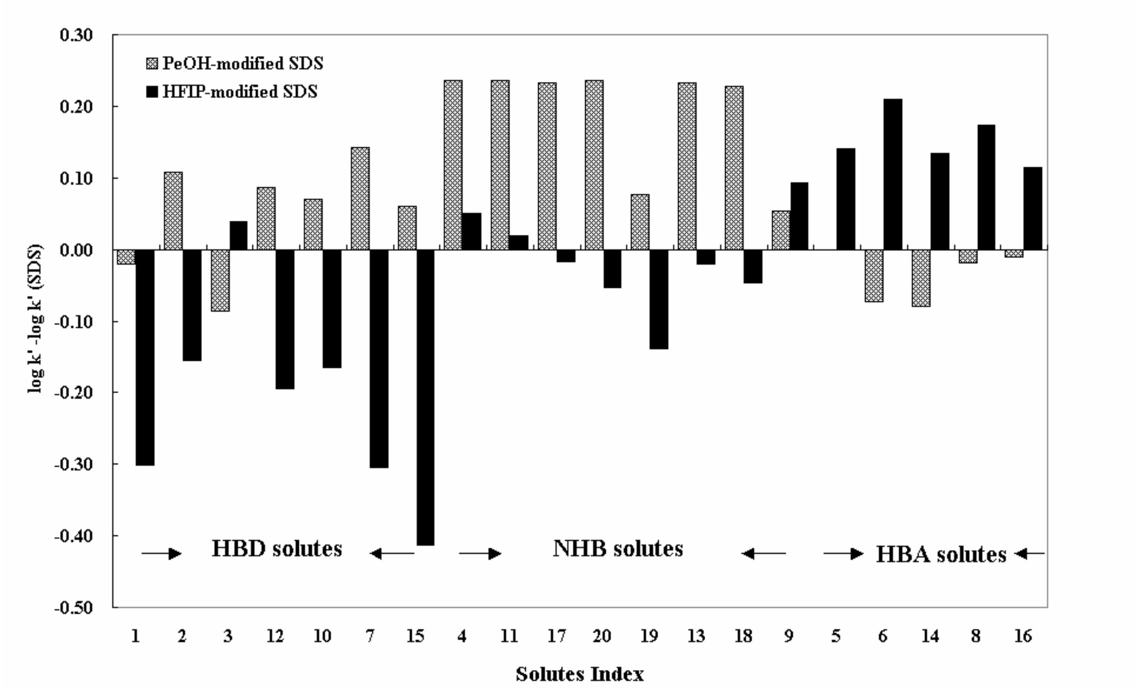

Figure 3-10 Comparisons of the solvent modification effects on SDS.

(Solutes IDs are the same with figure 3-9)

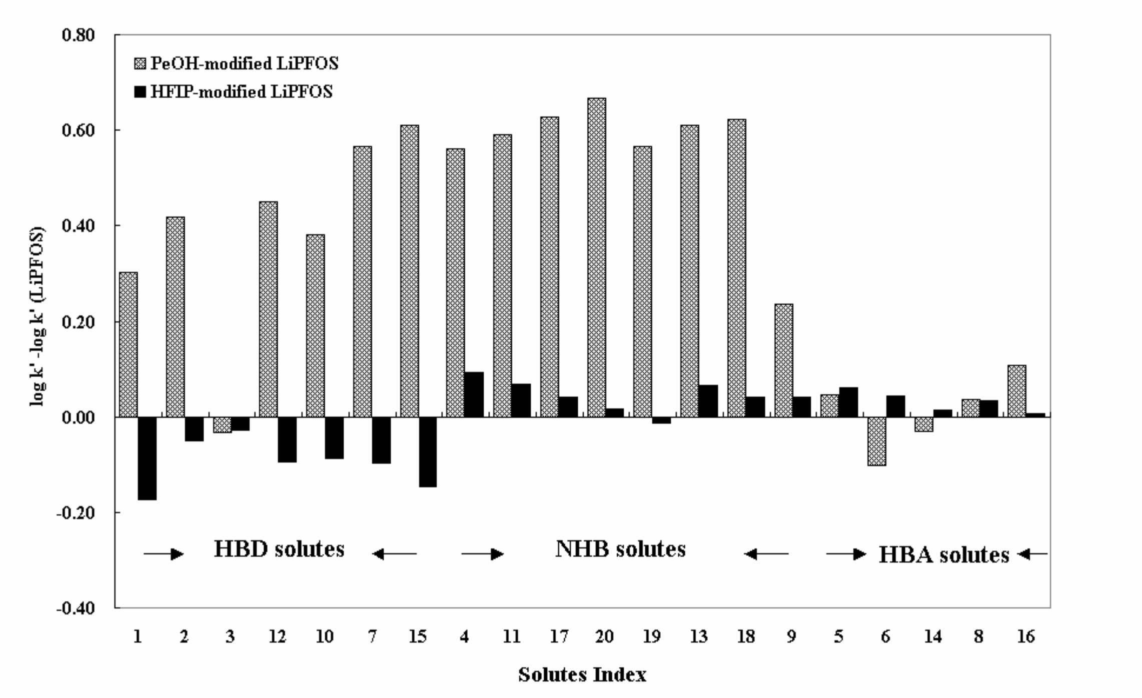

Figure 3-11. Comparisons of the solvent modification effects on LiPFOS

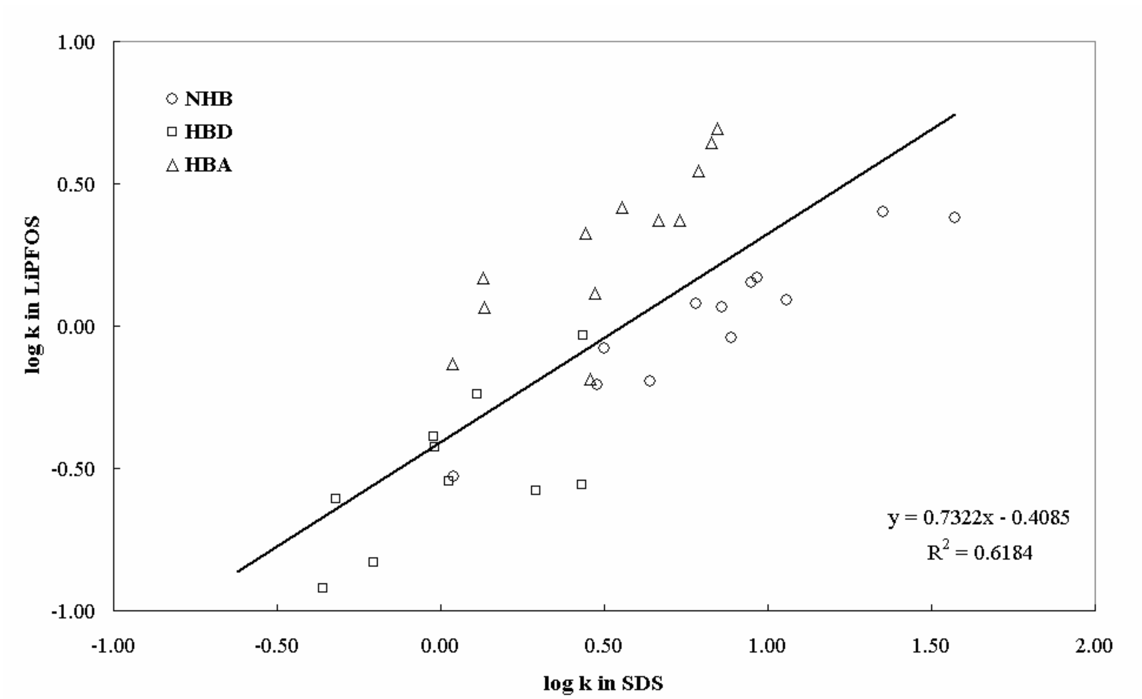

Figure 3-12 Correlation of the retention factors of test solutes between 40 mM SDS and 40 mM LiPFOS. (Open circle represents non hydrogen bond (NHB) solutes, Open square represents hydrogen bond donor (HBD) solutes, and open triangle represents hydrogen bond acceptor (HBA) solutes)

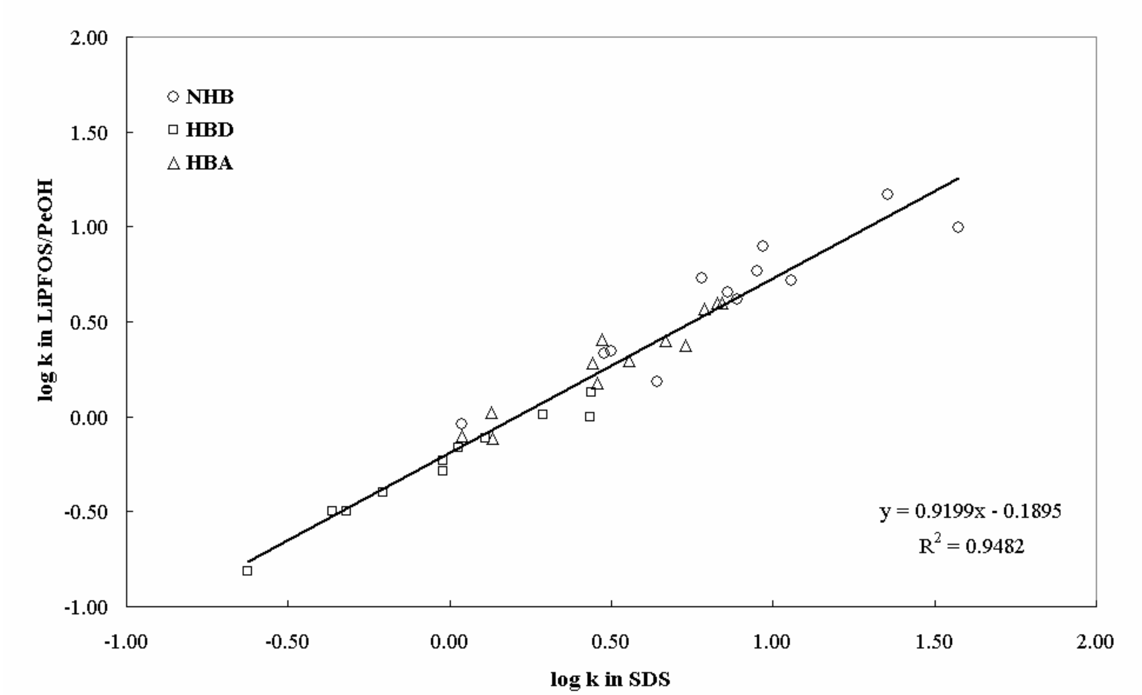

Figure 3-13. Correlation of the retention factors of test solutes between 40 mM SDS and pentanol modified LiPFOS. (Open circle represents non hydrogen bond (NHB) solutes, Open square represents hydrogen bond donor (HBD) solutes, and open triangle represents hydrogen bond acceptor (HBA) solutes)

CHAPTER 4

Characterization and Classification of Pseudo Stationary Phases in Micellar Electrokinetic Chromatography (MEKC) Using Chemometric Methods

ABSTRACT

Two types of chemometric methods, principal component analysis (PCA) and cluster analysis, are employed to characterize and classify 70 pseudo-stationary phases from micellar electrokinetic chromatography (MEKC). It is shown that PCA is able to remove redundant information in the micellar phase characterization, and retain key information about the phase classification. Hydrogen bond acidity and dipolarity of micelle phases are the primary factors determining the first principal component while hydrophobicity mainly influences the second principal component. A comparison between PCA and cluster analysis is also made. While PCA is useful in the characterization of micelle selectivities, it is ineffective in defining the grouping of micellar phases. Hierarchical clustering has the exact opposite trend in that it can yield complete and visually clear dendrogram of the cluster structure but can not provide sufficient cluster characterizations. The combination of these two chemometric methods leads to a comprehensive interpretation of the phase classification. Moreover, the k-means analysis is a powerful tool used to recognize subtle differences among those seemingly similar micellar phases. These chemometric methods result in similar classifications with the respect to the similarities and differences of the 70 micelle systems investigated. The 70 micelle systems are categorized into 3 clusters where fluorosurfactants represent the cluster, identified as strong hydrogen bond donor and dipolar but weak hydrogen bond acceptor micelle systems. Cluster III includes siloxane

based polymeric micelles, exhibiting weak hydrophobicity and medium hydrogen bond acidity and basicity. The last cluster consists of two sub clusters, cluster II and cluster IV. These micelle systems are characterized by strong hydrophobicity, medium hydrogen bond acidity and basicity but rather weak dipolarity. Cluster II differs from cluster IV only in terms of being more hydrophobic but weaker hydrogen bond donating capability. The classification by chemometric methods is in good agreement with the classification according to the Micellar Selectivity Triangle (MST).

1. INTRODUCTION

Micellar electrokinetic chromatography (MEKC) has received enormous attention since its introduction in the 1980s [1,2]. In spite of rapid development, the selection of optimum micellar phase in a systematic manner for a given separation, has been a challenge and is mostly accomplished by trial-and-error or analysts' experience and intuition. The imminent urgency for a systematic characterization of pseudo-stationary phases in MEKC has encouraged a large number of efforts [3-5]. Terabe and co-workers [3] reviewed the selectivity of a variety of micelle systems in MEKC and few conclusive recommendations on micelle system selection were given. In another report, Terabe [4] introduced a general guideline in the context of both theoretical and practical considerations. However, this simplified guideline did not accommodate surfactant type as a major variable for separation optimization. Poole et al. [5] summarized the linear solvation energy relationships (LSER) parameters of a large number of surfactant phases that had been applied to MEKC in the literature. General recommendations on micellar phase selection were suggested on the basis of significantly different interactive properties of the surfactant type. We shall also note that the LSER parameters for the micellar phases are partially correlated. This is especially true for the dipolarity parameter (s) and polarizability term (e). Therefore, the redundancy of information in the LSER database could complicate the classification and characterization of micelle systems. Unfortunately, these approaches only provided limited empirical recommendations for micelle system selection or redundant information on various micellar phases. In our previous study, a novel Micellar Selectivity Triangle (MST) scheme was successfully developed and was used for the characterization of the chemical selectivity of more than 70 pseudo-phases, including anionic, cationic, bile salts, fluorinated micelles, micro-emulsion, ionic polymers, polymeric micelles, solvent-modified and mixed micelles as well as vesicles and liposomes. The MST classification is based on the relative strength of the underlying chemical interactions that have been derived from the LSER. The elution patterns in EKC could be readily estimated on the basis of chemical selectivities of the pseudo-phases as characterized and classified by the MST as well as the interactive properties of the solutes. In addition, correlation analysis of retention patterns using different pseudo-phases provide additional support for the accuracy of the MST classification scheme as the extent of correlation between retention factors in different EKC systems is directly related to their location on the MST. As the distance between different systems on the MST increases, the correlation between the retention factors decreases. This is quite useful in identifying pseudo-phases in MEKC that provide the highest correlations between the retention factor in EKC and octanol-water partition coefficients. However, there are still questions that remain to be answered and can't be resolved solely by the triangle scheme, for example the minimum number of variables that are sufficient enough to represent the interactive properties of micelle phases, or the extent to which each variable can influence the partitioning process of the solute. In this chapter, two chemometric methods, namely principal component analysis (PCA) and cluster analysis are used as alternative and complementary approaches for characterization and classification of selected pseudo-phases in MEKC.

The principal component analysis (PCA) and cluster analysis methods are very powerful in processing large-quantities of multi-dimensional and inter-correlated data. The applications of these chemometric methods have been reported in a wide range of disciplines such as gene sequencing and expression analysis [6], pattern recognition [7,8], image compression [9], just to name a few. These multivariate analysis techniques have also been employed in understanding retention patterns and characterization of selectivity of stationary and mobile phases in various LC and GC techniques [10-16]. Abraham *et. al.* [17] reviewed the chemometric classifications of stationary phases in gas chromatography and identified the dipole–dipole interactive strength and the hydrogen bond basicity of the stationary phases as the main factors contributing to the first principal component in PCA. Cluster analysis also clearly visualized the classification structure on the basis of the hierarchical trees. Chemometric methods have also gained significant attention in liquid chromatography. This is due to the complex solute-stationary phase interactions in liquid chromatography dispersion, dipole-dipole, dipole-induced dipole, hydrogen bonding, ion–ion, ion-dipole, ion-induced dipole, and steric interactions. In addition, column perspectives such as ligand surface coverage, the size and uniformity of the silica particles, carbon content and trace metal activity in the silica support all have considerable effects on the chromatographic behaviors. Therefore, it is of great importance to employ chemometric methods for an accurate characterization of these LC stationary phases. Carr and coworkers [18] evaluated three types of bonded phases (alkyl, aromatic, and fluorinated phases) with a PCA method in comparison to the LSER model. It was shown that the PCA method had more accuracy in predicting solute retention than the LSER model, but the principal components could not provide a satisfactory explanation for the differences between these three stationary phases. Euerby et al. [12] characterized 135 commercially available reversed-phase in terms of their surface coverage, hydrogen bonding capacity, hydrophobicity and ion exchanging capability. The PCA analysis enabled the rationalization and identification of the columns with similar selectivity. Ivanyi and the colleagues [19] applied PCA method to determine the minimal number of chromatographic parameters necessary for the classification of 69 reversed phase columns. The PCA results indicated that only 4 measured parameters were needed to produce a fairly good classification. It shall be noted that the above investigations all involved the analysis with test compounds that were significantly different in structure and number in the test set. As a consequence, contradictory results sometimes have been reported when columns were characterized with different groups of test compounds. In our study, we apply the chemometric methods for the analysis of system parameters derived from the LSER models, which are known for being less dependent on the test solutes number and properties. To the best of our knowledge, this is the first report on the application of chemometric methods for characterization and classification of pseudo-stationary phases in MEKC.

Principal component analysis (PCA) is a dimension-reduction method, where interrelated variables are replaced by a new orthogonal set of variables (PC) that are a function of the original variables. The principal components (PCs) are linear combination of the original variates. Given an (n x p) data matrix **X**, where the n rows represent different types of pseudo-stationary phases (observations) and p represents the characteristics of the various micellar phases (variables). The standardization of data series $\mathbf{X_c}$ is carried out with mean-centering method, as a result the mean for the adjusted data series will be the origin, such that the covariance matrix **S** of the sample can be written as

$$S = \frac{1}{n-1} X_c{}^T X_c \qquad \text{Eq. 4-1}$$

where the superscript T denotes the transpose of the matrix. The $\mathbf{S_{jk}}$ element of the covariance matrix is expressed as

$$S_{jk} = \frac{1}{n-1}\sum_{i=1}^{n}\left(x_{ij} - \overline{x_j}\right)\left(x_{ij} - \overline{x_k}\right) \qquad \text{Eq. 4-2}$$

with

$$\overline{x_j} = \frac{1}{n}\sum_{i=1}^{n} x_{ij} \text{ and } \overline{x_k} = \frac{1}{n}\sum_{i=1}^{n} x_{ik} \qquad j, k = 1,..., p \qquad \text{Eq.4-3}$$

It can be seen that the covariance matrix **S** is a square matrix with a dimension of (p x p). The second stage is to determine the eigenvectors and eigenvalues of covariance matrix **S**. The singular value decomposition (SVD) is the algorithm of choice to calculate these variates for two reasons. First, it provides a straightforward and effective computationally method to calculate eigenvectors and eigenvalues, hence the principal components and its variance. Second, scores of each observation in the new PC subspace could be obtained simultaneously. SVD algorithm is written as

$$X_c = ULA^T \qquad \text{Eq. 4-4}$$

Where **U** is an (n x p) matrix containing the scores of PCs, **L** is a (p x p) diagonal matrix with the square root of the eigenvalues along the diagonal, the *i*th column of the matrix **A** represents the eigenvector for the *i*th principal component. It shall be noted that matrix **U** and **A** are orthonormal. The SVD results also closely relate to the chromatographic parameters in our test. For example, the contribution of each chemical interaction to the linear parameter is given in the eigenvector matrix **A** and the space coordinate of pseudo-stationary phase in the new subspace of the PCs is summarized in the matrix **U**. Finally, the principle components matrix **Y** could be calculated as

$$Y = X_c A^T \qquad \text{Eq. 4-5}$$

So the *j*th largest principal component could be expressed as linear combination of the original variables as

$$Y_j = a_{j1}X_1 + a_{j2}X_2 + a_{j3}X_3 + ... + a_{jp}X_p \qquad j = 1,..., p \qquad \text{Eq. 4-6}$$

The first principal component always aligns in the direction of the largest variances; the subsequent order of the PCs indicates smaller explanation of the variations. While the PCA method can extract valuable principle factors for pattern recognition and characterization, special care should be paid when applying the PCA for classification, because the projection of the original vectors to the principal subspaces sometimes might overlay part of the information crucial to system classification. Thus, it is necessary to justify the classification in PCA with other classification methodologies. A more in-depth explanation of the PCA method could be found in the following references. [5,20-23]

Cluster analysis is another chemometric approach to categorize the pseudo stationary phases in MEKC. The algorithm in cluster analysis evaluates the linkage and similarity of the objects with the inter-point distances. In other words, this technique operates on a matrix of the distances between the points rather than the individual measurements themselves. There are generally three types of distance definitions commonly used to describe the linkage within objects: single linkage, complete linkage and centroid linkage.

Single linkage might be the most frequently used method in agglomerative (merged) clustering. The characteristic distance between clusters is given by the smallest distance between two objects, the so-called “nearest neighbors”, that belong to two individual groups. The mathematical expression of the distance could be written as,

$$d_c(r,s) = \min\{d(x_{ri}, x_{sj})\} \qquad i=1,...,n_r;\ j=1,..., n_s \qquad \text{Eq. 4-7}$$

n_r and n_s are the number of elements in the cluster r and s respectively, $d(x_{ri},x_{sj})$ representing the distance between the two elements and could be obtained with classic Euclidean distance.

$$\delta_{ij} = \sqrt{\sum_k (x_{ik} - x_{jk})^2} \qquad \text{Eq. 4-8}$$

The single linkage method operates in a fashion that the nearest neighboring two objects are first grouped in a cluster, and then continues with the next closest pair until all the objects are taken into account. The next step will be the fusion of the closest cluster or the addition of points that results in smallest sum of distance.

Complete linkage is also known as the furthest neighbor method where the distance between clusters is measured by the largest distance of a pair of elements, one from each group. This operation could be expressed as,

$$d_c(r,s) = \max\{d(x_{ri}, x_{sj})\} \quad i=1,\ldots,n_r;\ j=1,\ldots,\ n_s \qquad \text{Eq. 4-9}$$

Centroid linkage uses the Euclidean distance between the centroids of the two clusters,

$$d_c(r,s) = d(\overline{x_r}, \overline{x_s})$$

where $\overline{x_r} = \frac{1}{n_r}\sum_1^{n_r} x_{ri}$ and $\overline{x_s}$ is the defined similarity.

After the definition of linkage, the next step will be the choice of clustering model. Here, for the classification of pseudostationary phases, we employ two models: one is hierarchical clustering and another is the k-means clustering method. Hierarchical clustering is a bottom-up model, where the closest related elements first merge together then link with secondary groups. The hierarchical tree or dendrogram best describes the relationship within the elements. Individual elements are connected by inverted U-shaped links, so-called the fusion of objects. The height of the U bar calibrates the similarity of the objects: the shorter the height of the U bar is, the more similarity among the linked objects. The fusion levels usually arrange in a monotonically increasing fashion, such that the ranking of the clusters could be visually clear.

The k-means clustering method is a top–down method where the centroids of clusters are randomly assigned and objects are then partitioned into the clusters according to the score of the distance to each centroid. Iterative element rearrangements are made to satisfy the criteria that the sum of the total distance reaches the minimum. Evaluation of the validity of the clustering is carried out by the applications of three different validation tests: cophenetic correlation, upper tail rule and silhouette plot.

2. EXPERIMENTAL

Chemometric modeling was performed on a Dell Inspiron 4100, the software platform is Matlab 6.5 release 13 (The Math Works, Inc., Natick, MA). A database composed of the LSER models for 70 MEKC micelle systems was collected from the literature and this lab.

3. RESULTS AND DISCUSSIONS

The distribution pattern of the mean-centered LSER system parameters is presented in figure 4-1. The distribution map reveals some intriguing information about the original data set before any chemometric analysis. First, most of the distributions among the system parameters show a center-focused pattern. This is especially true for the hydrophobic parameter *v*. Most of the distribution concentrates in a rather narrow range at the center. For system parameters *b, a* and *s,* we observe a much wider spreading of normal distribution, however, one still can not recognize any pattern for grouping. One exception is found for the distribution with system parameter *e*. A "tadpole" shape distribution is observed, and the obvious tailing is mostly because the fluorinated surfactants have a very weak interaction with the n and π electrons of solutes and obtain a negative system parameter *e*. Another piece of useful information is that the highly centered distribution indicates an overlapping and inter-correlated relationship between these system parameters which cannot be differentiated without further data management. Thus, it is essential to employ chemometric methods to recognize grouping information from the redundant data.

3.1 Principal Component Analysis

PCA is applied to the standardized LSER system parameters of the 70 MEKC pseudo-stationary phases. The eigenvectors and eigenvalues are listed in table 4-2 and 4-3. The first principle component accounts for the largest variance, 56.8%. The combination of the first and second principal components describes 78.8% of the total variance. With the incorporation of the third and fourth principal components, 96.5% of the total variances can be explained. The dependency of the cumulative variance on the number of principal components is shown in figure 4-2. Clearly, to obtain a satisfactory classification of the MEKC micelle systems, at least 4 parameters shall be taken into account. It is also informative to investigate the influence of each system parameter on the principle component, which is shown in the eigenvectors. As shown in table 4-2, hydrogen bond acidity (*b*) and dipolarity (*s*) are the two major factors that contribute to the first principal component. It is surprising that the hydrophobic interaction (*v*) does not have a significant effect on the first principal component. On the contrary, the second principal component gains contribution mainly from the hydrophobic interaction with minor input from the dipolarity (*s*). The third principal component features the dominant negative contribution from system parameters (*a* and *s*). Two system parameters (*b* and *e*) play significant roles in the fourth principal components while the fifth principal components obtain positive contribution from system parameter (*v*, *b*, *a*) and negative contribution from *s* and *e*. The initial PCA results confirm that the best representation of the micelle systems require all five variables. These explain the success of LSER methodology using five different molecular interactions to characterize pseudo-stationary phases in MEKC. However, since these five types of molecular interactions do not contribute evenly to the system characterization and contain correlated and redundant information, there is an opportunity to use reduced parameters to describe the selectivity of the micellar phases.

The plot of the first principal component against the second principal component in figure 4-3 reveals insightful information about the characteristics of the micelle systems. There are two clusters of micelle systems well separated in the plot, namely cluster I and cluster II. For two other clusters, III and IV, no clear boundary could be defined, meaning these two clusters have similar selectivities in some aspects. Cluster I is the fluorinated surfactant series. They are located at the upright hand corner and possess a large first principal component and intermediate second principal component. As discussed above, the first principal component is mainly determined by the strength of the hydrogen bond acidity and dipolarity. Thus, cluster I shall have a rather strong hydrogen bond acidity and dipolarity, which agrees well with the LSER characterization. Moreover, our micellar selectivity triangle scheme also distinguishes these fluorosurfactants as strongly hydrogen bond acidic micelles. Cluster II consists of two micelle genres: one is cationic surfactant (38 hexadecyltrimethyl ammonium bromide); another one is a group of alkyl methacrylate based polymeric micelles. The location of cluster II is on the top left corner of the plot, implying a small first principal component but a large second principal component. This unique observation is attributed to the rather weak hydrogen bond acidity and dipolarity but a strong hydrophobic type of surfactants. Again, these findings are in good agreement with the LSER results. It should be pointed out that our MST scheme did not differentiate these surfactants as a separate group. It could probably due to the fact that hydrophobic interaction is not included in the selectivity triangle. The division of cluster III and IV is not based on any clear boundary as the first two clusters. However, we still can make a tentative classification on the basis of the scales of the first and second principal components. Cluster III is a collection of those micelle systems located in the lower-left corner. The first two principal components for these pseudo-phases are both small. Consequently, these surfactants have the lowest hydrogen bond acidity, dipolarity, and weakest hydrophobic effects. The pseudo-phases 40 to 47 are siloxane-based polymers composed of allyl glycidyl ether *N*-methyl taurine sidechains. The pseudo-phase 33 is an anionic triblock copolymer, poly (methyl methacrylate-ethyl acrylate-methacrylic acid, Elvacite 2669). These surfactants share a common feature that all of them are rather weakly hydrophobic as indicated by a small second principal component. These types of surfactants are considered as strong hydrogen bond accepting agents in the MST method. However, the strength of the hydrogen bond basicity of the micellar phases cannot be evaluated in the plot of the first and second principal component because neither of the two PCs is influenced substantially by the hydrogen bond basicity of the pseudo-phases. Cluster IV is a collection of various types of pseudo-phases in the center region of the plot, indicating most of these systems have similar selectivity patterns and could be categorized as a group with intermediate strength in hydrogen bond acidity, dipolarity, as well as hydrophobicity. These surfactants are clustered in a similar pattern in the classification of the MST. It is worthwhile to note that the SDS micelle systems (1-6,8-14,66 and 70) from different labs and under various buffer solutions are located closely in the Cluster IV. This is an evidence of the robustness of the LSER characterization and the validity of the classification. One interesting finding is that micelle system 34 (mixed micelle of LiDS and LiPFOS) is located midway between the SDS micelles and the LiPFOS micelles indicating the opportunity for constructing continuous stationary phases selectivity with these mixed micelles. A similar result was observed in the MST method.

The plot of third and fourth principle component (figure 4-4) shows a widespread distribution of the micelle systems and no systematic clustering pattern is observed. This is not unexpected because these two variables only account for a minor part of variance as compared to the first two principal components. Similarly, the relationship between the fifth principle component and the 70 micelles systems (figure 4-5) only appears as a random fluctuation in a narrow range.

For a better view and representation of pseudo phase properties, we incorporate the third principal component together with the first two principal components to construct a 3-D score plot (figure 4-6) of the 70 micelle phases. It is clear that the addition of another dimension enhances the separation of the original condensed clustering. Thus, it enables one to further scrutinize the subtle differences between the micelle phases. It is worthwhile to mention that the new dimension does not alter the previous classification.

3.2 Cluster Analysis

The hierarchical clustering method has resulted in a dendrogram structure for the classification of the original MEKC micelle systems. We ran a cophenetic correlation test to assess the validity of the classification. Cophenetic correlation coefficient is often used to evaluate a hierarchical clustering model by comparing the fusion level of between sub-level elements and their distance. A cophenetic correlation coefficient close to unity indicates a good correlation between the fusion level and the object distance. In our test, we ran the cophenetic correlation test on the three different linkages: single linkage, average linkage and complete linkage. The ranking of the cophenetic correlation coefficients is as follow: average linkage (0.8807) > single linkage (0.8063) > complete linkage (0.7051). The relative high cophenetic correlation coefficient values of all three linkages indicate a satisfactory classification of micelle systems without distorting the intrinsic structure. The complete linkage has the lowest cophenetic correlation coefficient probably due to the fact that complete linkage tends to lead to a spherical shape clustering, which is not the best description of current data.

We also carried out the "upper tail rule" test as a way to determine reasonable number of clusters for best description of the data structure. The idea underlying the method is that at an optimum number of clusters, the fusion level shall be higher than the average level of previous clusters. The appearance of this transition point on the plot of the fusion level vs. the cluster number (figure 4-7) will be a plateau or shallower slope. It can be seen that the first transition occurs at 3 clusters and there is another transition at 5 clusters indicating some clusters could be further divided into sub-clusters.

The complete classification of the 70 micellar phases using hierarchical clustering method is shown in figure 4-8. Overall, it shows three big clusters of micellar phases and one of the clusters is actually formed by two sub clusters on the left-hand side of the hierarchical tree. We also compare the classification results of the PCA method and hierarchical clustering. For cluster I, these fluorosurfactants (in blue) again show significant dissimilarity from the others, they are the least similar to the other pseudo-phases in the hierarchical clustering. The next cluster on the hierarchical clustering map is the cluster III in the PCA method with only the addition of micelle system (15). The hierarchical clustering method merged cluster II together with some of the micelle phases in cluster IV. Close examination of these micellar phases that were re-classified reveals that these micelle phases are located on the left side of original cluster in PCA method which could be assigned to one individual sub cluster or merge with cluster II. Apparently, the algorithm of hierarchical clustering includes these pseudo-phases together with cluster II.

The advantage of hierarchical clustering is that it leads to a visually and structurally clear classification of micelle phases. However the pitfall is as obvious as the advantage. There is not a qualitative description of the chemical meaning of the classification in the hierarchical clustering. Consequently, one would not have knowledge about the characteristics of each cluster. On the contrary, the PCA method provides details on the properties of the micellar phases but can not have a visually clear boundary to separate the cluster. Now with the combination of these two complementary chemometric methods, the analyst can easily make the classification with confidence.

K-means clustering is another clustering method investigated in this study. As with other clustering methods, we have to define the number of clusters. Here, a silhouette plot (figure 4-9) is employed for this purpose. For a two-cluster division, the silhouette plot yields one huge cluster with most of the points having a silhouette value lower than 0.5, which is not desirable and indicates that a large population of the cluster tends to intercalate with another cluster. In a three clusters trial, one can see that two small clusters receive very large silhouette value and well separated. Meanwhile, we observed significant improvement of the silhouette values for the components in the big cluster. We also attempted a four-cluster classification, in which the first two clusters yield high silhouette values indicating complete separation. However clusters 3 and 4 result in a rather small silhouette values reflecting an overfitting of the classification. By using the silhouette plot, we found that the classification of these micellar phases with 3 clusters gives a better representation of the data. Meanwhile, one should keep in mind that even the 3-cluster division contains a big group of micelle phases which might consist of several closely relevant sub-clusters. Table 4-5 demonstrates a detailed simulation of the k-means clustering. In the first phase, data points are assigned randomly to the clusters with pre-defined centroids and the sum of distance to each centroid is calculated. Then a series of iterative rearrangements of the points in different cluster is carried out for the purpose of minimizing the sum of the intra-cluster distance. The iteration ends at a stage where no more adjustment of point is needed and the summed distance reaches a minimum.

The results of the classification by the k-means method are shown in figure 4-10. The division of three clusters is similar to the classification of the hierarchical clustering. The cluster in pink is the fluorosurfactant series. The location of these micelle systems indicates they are better hydrogen bond donating agents but weak hydrogen bone acceptors. By contrast, the cluster in red contains those micelle systems originally included in cluster III of the classification in the PCA. These micelle systems show opposing characteristics of the fluorosurfactants. They are more hydrogen bond basic but less hydrogen bond acidic. The remaining micelle systems are all classified into one cluster, located at the center of the 3-D plot. In other words, these micelle systems show moderate hydrogen bond acidity and basicity. One of the advantages of k-means clustering is that the detailed analysis of the influence of each chemical interaction on the clustering can be seen in one distribution plot (figure 4-11). In comparison to the distribution plot without any chemometric data processing (figure 4-1), k-means clustering methods could resolve those subtle differences of micelle phases which benefit the recognition of the pattern and characterization of the micelle phases. The three clusters are well resolved in the distribution map, especially in the case involving the hydrophobic interaction parameter (v). In the first column of the map, the three clusters exhibit significant dissimilarities in various plots. For instance, fluorosurfactants could be assigned as strong hydrogen bond donating (b) and dipolar (s) micelles, medium hydrophobicity (v) but very weak hydrogen bond basicity (a) and polarizability (e). The cluster in blue is represented by the siloxane-based polymeric micelles. These micelle systems also have unique selectivity characteristics, which are identified as better hydrogen bond acceptors and very polarizable, medium hydrogen bond donating ability and dipolarity but with significantly lower hydrophobicity (*v*). The last cluster represented by the SDS type of hydrocarbon surfactants, demonstrates a high level of hydrophobicity (v), but rather moderate characters for all other four types of molecular interactions. We also observe a sub-cluster appearing in the green group. These trends are obvious in the distribution plots with *v* and *b* but merged in plots involving *a*, *s*, *e*. Further examination of the plot reveals that these divided sub-cluster consisting of mainly the elements from cluster II of the PCA classification. These evidences cast new light on the characters of the clusters: cluster II has similar strength in *a, s, e* parameters with cluster IV but appears to be less relevant in term of the hydrophobicity and hydrogen bond donating ability.

4. CONCLUSIONS

We systematically investigated the applications of the chemometric methods for the classification of the 70 pseudo-phases in MEKC. The PCA is shown to be best at filtering redundant information and reducing the dimensionality of the data. Hydrogen bond basicity and dipolarity are two main factors contributing to the first principal component while the hydrophobicty is the leading factor influencing the magnitude of second principal component. It is also concluded that in order to obtain the best representation of the selective characteristics of the pseudo-phases, the five LSER parameters are required for an intact and accurate description of the micelle interactive properties. Meanwhile, we recognize that the first four principle components could account for over 96% of the total variances and represent a satisfactory classification of the pseudo-phases.

All chemometric analysis methods are assessed with the corresponding test methods to ensure the validity of the classifications. The classifications on the basis of the three chemometric methods result in good agreement. Slight differences between the PCA method and cluster analysis exist, mainly because the PCA method is not specialized for the classification and does not define the boundary for each cluster. In contrast, the dendrogram of hierarchical clustering presents a visually clear classification of the micelle systems but lacks the chemical characterization of the micelle systems. The combination of the PCA and hierarchical clustering yields a satisfactory classification of the 70 micelle phases into three clusters. Furthermore, the k-means clustering reveals more subtle differences than any of the previous two methods in the distribution map. With the k-means clustering, we can resolve the details of the contributions of each molecular interaction in the classification and characterize each cluster. For future classification of micelle systems, one should employ at least the PCA method and one clustering method in order to obtain a panoramic and accurate understanding of the classifications.

REFERENCES

1. Terabe S, Otsuka K, Ando T: **Electrokinetic chromatography with micellar solution and open-tubular capillary**. *Analytical Chemistry* 1985, **57**:834-841.

2. Terabe S, Otsuka K, Ichikawa K, Tsuchiya A, Ando T: **Electrokinetic separations with micellar solutions and open-tubular capillaries**. *Analytical Chemistry* 1984, **56**:111-113.

3. Muijselaar PG, Otsuka K, Terabe S: **Micelles as pseudo-stationary phases in micellar electrokinetic chromatography**. *Journal of Chromatography, A* 1997, **780**:41-61.

4. Terabe S: **Selectivity manipulation in micellar electrokinetic chromatography**. *Journal of Pharmaceutical and Biomedical Analysis* 1992, **10**:705-715.

5. Poole CF, Poole SK, Abraham MH: **Recommendations for the determination of selectivity in micellar electrokinetic chromatography**. *Journal of Chromatography, A* 1998, **798**:207-222.

6. Yeung KY, Ruzzo WL: **Principal component analysis for clustering gene expression data**. *Bioinformatics* 2001, **17**:763-774.

7. Rajkiran Gottumukkal VKA: **An improved face recognition technique based on modular PCA approach**. *Pattern Recognition Letters* 2004, **25**:429-436.

8. Waters NJ HE, Williams A, Waterfield CJ, Farrant RD, Nicholson JK.: **NMR and pattern recognition studies on the time-related metabolic effects of alpha-naphthylisothiocyanate on liver, urine, and plasma in the rat: an integrative metabonomic approach.** *Chem Res Toxicol* 2001, **14**:1401-1412.

9. Clausen CW, H: **Color image compression using PCA and backpropagation learning**. *Pattern Recognition Letters* 2000, **33**:1555-1560.

10. Huber JFK, Reich G: **Characterization and selection of stationary phases for gas-liquid chromatography by pattern recognition methods**. *Journal of Chromatography* 1984, **294**:15-29.

11. Heberger K, Milczewska K, Voelkel A: **Principal component analysis of polarity and interaction parameters in inverse gas chromatography**. *Journal of Chromatographic Science* 2001, **39**:375-384.

12. Euerby MR, Petersson P: **Chromatographic classification and comparison of commercially available reversed-phase liquid chromatographic columns using principal component analysis**. *Journal of Chromatography, A* 2003, **994**:13-36.

13. Liu Y, Guo Y-f, Wang H, Xing Y-j, Zuo Y-m: **Evaluation of octadecene-polybutadiene-coated zirconia stationary phase based on linear solvation energy relationships**. *Journal of Liquid Chromatography & Related Technologies* 2003, **26**:723-736.

14. Bermejo JMS, Gonzalez VM, de la Fe CG, Dominguez JAG: **Cluster analysis of McReynolds constants for 384 gas chromatographic stationary phases**. *ACH - Models in Chemistry* 1996, **133**:243-266.

15. Delaney MF, Papas AN, Walters MJ: **Chemometric classification of reversed-phase high-performance liquid chromatography columns**. *Journal of Chromatography* 1987, **410**:31-41.

16. Poole SK, Poole CF: **Chemometric classification of the solvent properties (selectivity) of commonly used gas chromatographic stationary phases**. *Journal of Chromatography, A* 1995, **697**:415-427.

17. Abraham MH, Poole CF, Poole SK: **Classification of stationary phases and other materials by gas chromatography**. *Journal of Chromatography, A* 1999, **842**:79-114.

18. Reta M, Carr PW, Sadek PC, Rutan SC: **Comparative study of hydrocarbon, fluorocarbon, and aromatic bonded RP-HPLC stationary phases by linear solvation energy relationships**. *Analytical Chemistry* 1999, **71**:3484-3496.

19. Ivanyi T, Vander Heyden Y, Visky D, Baten P, De Beer J, Lazar I, Massart DL, Roets E, Hoogmartens J: **Minimal number of chromatographic test parameters for the characterization of reversed-phase liquid chromatographic stationary phases**. *Journal of Chromatography, A* 2002, **954**:99-114.

20. Jolliffe IT: **Principal component analysis**. *New York : Springer-Verlag* 1986.

21. Malinowski ER: **Factor Analysis in Chemistry**. *Wiley New York* 1991.

22. Martinez AR, Martinez, W. L.: **Exploratory Data Analysis with Matlab**. *Chapman & Hall CRC PRESS* 2005.

23. Krzanowski WJ: **Principles of Multivariate Analysis**. *Oxford Statistical Science Series 3 Oxford Science Publications* 1988.

24. Poole SK, Poole CF: **Characterization of surfactant selectivity in micellar electrokinetic chromatography**. *Analyst (Cambridge, United Kingdom)* 1997, **122**:267-274.

25. Abraham MH: **Hydrogen bonding. 31. Construction of a scale of solute effective or summation hydrogen-bond basicity**. *Journal of Physical Organic Chemistry* 1993, **6**:660-684.

26. Herbert BJ, Dorsey JG: **n-Octanol-Water Partition Coefficient Estimation by Micellar Electrokinetic Capillary Chromatography**. *Analytical Chemistry* 1995, **67**:744-749.

27. Yang SY, Khaledi MG: **Chemical Selectivity in Micellar Electrokinetic Chromatography - Characterization of Solute Micelle Interactions for Classification of Surfactants**. *Analytical Chemistry* 1995, **67**:499-510.

28. Chen N, Zhang Y, Terabe S, Nakagawa T: **Effect of physico-chemical properties and molecular structure on the micelle-water partition coefficient in micellar electrokinetic chromatography**. *Journal of Chromatography, A* 1994, **678**:327-332.

29. Muijselaar PG, Claessens HA, Cramers CA: **Characterization of Pseudostationary Phases in Micellar Electrokinetic Chromatography by Applying Linear Solvation Energy Relationships and Retention Indexes**. *Analytical Chemistry* 1997, **69**:1184-1191.

30. Trone MD, Leonard MS, Khaledi MG: **Congeneric behavior in estimations of octanol-water partition coefficients by micellar electrokinetic chromatography**. *Analytical Chemistry* 2000, **72**:1228-1235.

31. Peterson DS, Palmer CP: **Novel alkyl-modified anionic siloxanes as pseudostationary phases for electrokinetic chromatography: II. Selectivity studied by linear solvation energy relationships**. *Electrophoresis* 2001, **22**:3562-3566.

32. Palmer CP: **Recent progress in the development, characterization and application of polymeric pseudophases for electrokinetic chromatography**. *Electrophoresis* 2002, **23**:3993-4004.

33. Trone MD, Khaledi MG: **Characterization of chemical selectivity in micellar electrokinetic chromatography. 4. Effect of surfactant headgroup**. *Analytical Chemistry* 1999, **71**:1270-1277.

34. Trone MD, Khaledi MG: **Influence of ester and amide-containing surfactant headgroups on selectivity in micellar electrokinetic chromatography**. *Electrophoresis* 2000, **21**:2390-2396.

35. Trone MD, Khaledi MG: **Characterization of chemical selectivity in micellar electrokinetic chromatography: V. The effect of the surfactant hydrophobic chain**. *Journal of Microcolumn Separations* 2000, **12**:433-441.

36. Vitha MF, Carr PW: **A linear solvation energy relationship study of the effects of surfactant chain length on the chemical interactions governing retention and selectivity in micellar electrokinetic capillary chromatography using sodium alkyl sulfate buffers**. *Separation Science and Technology* 1998, **33**:2075-2100.

Table 4-1LSER system parameters of MEKC pseudo-stationary phases

	Micelle systems	v	b	a	s	e
1	0.01 M SDS	2.95	-1.77	-0.12	-0.59	0.43
2	0.015 M SDS	3.11	-1.95	-0.05	-0.58	0.52
3	0.02 M SDS	2.95	-1.92	-0.08	-0.64	0.52
4	0.025 M SDS	2.89	-1.88	-0.11	-0.63	0.54
5	0.04 M SDS	3.01	-1.88	-0.20	-0.46	0.33
6	0.06 M SDS	2.95	-1.76	-0.17	-0.54	0.41
7	Micro emulsion [a]	3.05	-2.81	-0.06	-0.69	0.28
8	SDS [b]	2.99	-1.88	-0.30	-0.44	0.46
9	SDS [c]	2.62	-1.57	-0.31	-0.67	0.56
10	SDS [d]	2.91	-1.87	-0.44	-0.24	0.31
11	SDS [e]	2.83	-1.71	-0.15	-0.44	0.47
12	SDS [e]	2.81	-1.71	-0.16	-0.48	0.46
13	SDS [f]	2.51	-1.51	-0.14	-0.70	0.51
14	SDS [f]	2.56	-1.56	-0.33	-0.66	0.57
15	0.04 M SDS+0.4 M PeOH	2.85	-2.40	-0.03	-0.89	0.51
16	0.04 M SDS+0.4 M TFE	2.77	-1.63	-0.32	-0.47	0.38
17	0.04 M SDS+0.2 M TCE	2.56	-1.56	-0.60	-0.57	0.39
18	0.04 M SDS+0.4 M HFIP	2.72	-1.38	-0.63	-0.38	0.20
19	0.04 M SDS+0.1 M OCFP	2.69	-1.52	-0.64	-0.49	0.25
20	0.04 M SDS+0.4 M BuAN	2.77	-1.93	-0.15	-0.52	0.42
21	0.04 M SDS+1% Brij 35	2.84	-2.26	0.04	-0.60	0.62
22	0.04 M SDS+1% FC 4300	2.90	-2.31	0.04	-0.65	0.59
23	0.01 M TTAB	2.85	-2.23	0.80	-0.62	0.77
24	0.01 M TTAB + 0.3 M PTOH	2.79	-2.43	0.29	-0.93	0.69
25	0.08 M LiPFOS	2.46	-0.72	-0.60	0.32	-0.25
26	0.04 M LiPFOS[a]	2.35	-0.54	-0.71	0.31	-0.46
27	0.04 M LiPFOS + 0.4 M PeOH	2.55	-1.63	-0.29	-0.50	0.02
28	0.04 M LiPFOS + 0.4 M HFIP	2.14	-0.48	-0.92	0.35	-0.50
29	0.04 M LiPFOS[h]	2.36	-0.61	-0.80	0.46	-0.68
30	0.06 M SC [h]	2.75	-2.51	0.08	-0.65	0.55
31	0.04 M SDCV[h]	3.07	-2.53	0.14	-0.59	0.42
32	0.04 M LSA[h]	2.98	-2.49	0.15	-0.38	0.56
33	2% Elvacite 2669[h]	2.05	-1.88	0.07	-0.19	0.36
34	20/20mM LiDS/LiPFOS[h]	2.85	-1.32	-0.51	-0.05	-0.11
35	30/30mM SDS/SC[h]	2.67	-2.24	0.08	-0.51	0.45

36	30/30mM SDS/SDC [h]	2.65	-1.99	0.02	-0.59	0.49
37	0.04 M SDS + 0.4 M PeOH	3.07	-2.63	0.01	-0.68	0.33
38	HTAB [a]	3.40	-3.08	0.58	-0.55	0.61
39	PSUA [j]	2.11	-1.18	-0.27	-0.16	0.26
40	AGENT [i]	2.07	-1.93	0.45	-0.07	0.76
41	OAGENT 10% C8 [i]	1.71	-2.36	0.25	-0.22	0.54
42	OAGENT 15% C8 [i]	1.76	-1.90	0.20	-0.38	0.46
43	OAGENT 20% C8 [i]	2.21	-2.53	0.11	-0.90	0.49
44	OAGENT 25% C8 [i]	2.06	-2.29	0.11	-1.08	0.71
45	DAGENT 10% C 12 [i]	1.34	-1.96	0.51	-1.05	0.58
46	DAGENT 20% C 12 [i]	2.39	-2.38	0.21	-0.86	0.32
47	SAGENT 10% C 18 [i]	1.49	-2.00	-0.10	-0.57	0.16
48	POMAt-21 [j]	3.56	-3.75	-0.41	-0.60	0.47
49	pLMAt-15 [j]	3.65	-3.70	-0.27	-0.67	0.43
50	pSMAt-16 [j]	3.78	-3.83	-0.50	-0.85	0.65
51	pLAt-13 [j]	3.59	-3.52	-0.02	-0.40	0.39
52	pLMAm-19 [j]	2.88	-2.45	0.25	-0.32	0.37
53	pDHCHAT-33 [j]	3.40	-3.20	0.24	-0.46	0.65
54	ptOAm-49 [j]	3.36	-3.22	0.43	-0.44	0.33
55	SDSu [k]	2.84	-1.78	-0.02	-0.42	0.33
56	SDC [k]	2.96	-1.77	0.23	-0.39	0.15
57	SDP [k]	3.01	-2.00	0.15	-0.55	0.24
58	SDCV [k]	2.94	-2.38	0.11	-0.61	0.42
59	SLSA [k]	2.96	-2.39	0.1	-0.37	0.41
60	LMT [l]	2.88	-2.37	0.39	-0.35	0.51
61	ALE [l]	2.92	-2.41	0.49	-0.37	0.44
62	SLN [l]	2.92	-2.32	0.45	-0.39	0.44
63	SLN [m]	3.02	-2.34	0.47	-0.33	0.39
64	SMN [m]	2.99	-2.46	0.44	-0.42	0.48
65	SPN [m]	3.10	-2.58	0.48	-0.45	0.42
66	SDS [m]	2.86	-1.70	-0.15	-0.31	0.25
67	STS [m]	3.01	-1.82	-0.18	-0.34	0.26
68	SOS [n]	2.85	-1.88	-0.11	-0.31	0.46
69	SDecS [n]	2.69	-1.59	0.00	-0.24	0.32
70	SDS [n]	2.98	-1.91	-0.24	-0.42	0.36

a: Ref. [5], b: Ref. [24], c: Ref. [25], d: Ref. [26], e: Ref. [27], f: Ref. [28], g: Ref. [29], h Ref. [30], i: Ref. [31], j: Ref. [32], k: Ref.[33] , l: Ref. [34]m: Ref. [35], n: Ref. [36]

Table 4-2 Contributions of LSER system parameters to principal components**.**

	PC1	PC2	PC3	PC4	PC5
v	-0.254	0.829	-0.072	0.402	0.287
b	0.510	-0.304	0.121	0.694	0.389
a	-0.419	-0.357	-0.729	0.053	0.403
s	0.472	0.199	-0.654	0.154	-0.535
e	-0.526	-0.232	0.146	0.575	-0.564

Table 4-3 Eigenvalues for principal components

	PC1	PC2	PC3	PC4	PC5
Eigenvalue	2.84	1.10	0.62	0.26	0.18
Cumulated variance (%)	56.78	78.84	91.30	96.46	100.00

Table 4-4 Scores of micellar systems in the subspace of principal components.

Micelle systems	v	b	a	s	e
1	-0.08	0.14	0.51	0.52	0.33
2	-0.55	0.36	0.34	0.68	0.19
3	-0.50	0.05	0.56	0.54	0.19
4	-0.42	-0.05	0.63	0.57	0.08
5	0.31	0.55	0.30	0.30	0.18
6	0.11	0.24	0.49	0.50	0.23
7	-0.85	0.79	0.33	-0.83	0.36
8	0.21	0.52	0.53	0.56	-0.26
9	0.09	-0.52	1.24	0.65	-0.11
10	1.06	0.78	0.30	0.26	-0.51
11	0.23	0.00	0.28	0.64	-0.11
12	0.21	-0.05	0.39	0.58	-0.04
13	0.04	-0.89	0.96	0.52	0.21
14	0.15	-0.61	1.28	0.63	-0.20
15	-1.25	-0.12	0.95	-0.19	0.39
16	0.66	0.08	0.68	0.43	-0.05
17	0.97	-0.12	1.53	0.25	-0.29
18	1.75	0.41	1.06	0.26	-0.07
19	1.39	0.31	1.34	0.14	-0.08
20	0.07	-0.02	0.41	0.21	-0.02
21	-0.97	-0.17	0.24	0.35	-0.23
22	-1.06	-0.05	0.32	0.26	-0.06
23	-2.19	-1.08	-1.20	0.82	0.38
24	-2.05	-0.73	0.48	0.15	0.39
25	4.39	0.50	-0.67	0.11	-0.15
26	5.12	0.51	-0.49	-0.28	0.22
27	1.41	-0.05	0.52	-0.55	0.67
28	5.67	0.38	-0.12	-0.50	-0.10
29	5.85	0.94	-0.77	-0.75	0.28
30	-1.10	-0.23	0.20	-0.16	-0.14
31	-1.01	0.44	-0.19	-0.14	0.28
32	-0.87	0.27	-0.58	0.24	-0.43
33	0.90	-1.28	-0.70	-0.28	-0.67
34	2.73	0.99	-0.11	-0.05	0.23
35	-0.43	-0.31	-0.11	-0.09	-0.08

36	-0.37	-0.49	0.26	0.18	0.05
37	-0.90	0.63	0.22	-0.51	0.43
38	-2.44	0.70	-1.23	0.08	0.19
39	2.04	-1.03	-0.01	0.24	-0.46
40	-0.20	-1.87	-1.55	0.67	-1.33
41	0.10	-2.03	-0.94	-0.67	-1.28
42	0.38	-2.13	-0.45	-0.42	-0.57
43	-1.14	-1.34	0.75	-0.90	0.14
44	-1.61	-2.03	1.34	-0.40	0.05
45	-1.13	-3.74	0.55	-0.90	0.47
46	-0.84	-1.01	0.36	-0.93	0.74
47	1.09	-2.14	0.46	-1.55	-0.15
48	-1.66	2.37	0.70	-0.95	-0.83
49	-1.87	2.35	0.55	-0.92	-0.37
50	-2.50	2.56	1.50	-0.60	-0.77
51	-1.48	2.13	-0.56	-0.70	-0.44
52	-0.43	0.18	-1.01	-0.17	-0.06
53	-2.06	1.12	-0.73	0.04	-0.52
54	-1.60	1.16	-1.34	-0.67	0.31
55	0.33	0.05	-0.12	0.30	0.27
56	0.38	0.19	-0.82	0.08	0.96
57	-0.16	0.27	-0.29	-0.02	0.87
58	-0.82	0.16	-0.03	-0.11	0.29
59	-0.41	0.38	-0.56	0.00	-0.14
60	-0.86	-0.14	-1.14	0.22	-0.09
61	-0.93	-0.10	-1.35	0.07	0.21
62	-0.85	-0.11	-1.20	0.14	0.25
63	-0.74	0.14	-1.43	0.13	0.32
64	-1.11	0.03	-1.13	0.13	0.17
65	-1.23	0.27	-1.22	-0.04	0.40
66	0.87	0.33	-0.13	0.27	0.14
67	0.67	0.65	-0.04	0.27	0.17
68	0.28	0.17	-0.13	0.53	-0.37
69	0.85	-0.19	-0.52	0.44	-0.01
70	0.36	0.55	0.30	0.32	-0.04

Table 4-5 Iteration of point rearrangement for k-means clustering

Iteration	Phase	Number	Sum
1	1	70	247.611
2	1	10	219.799
3	1	7	209.291
4	1	3	207.362
5	1	5	203.362
6	1	5	195.797
7	1	5	188.222
8	1	3	182.034
9	1	1	180.027
10	1	2	175.872
11	1	1	173.776
12	1	1	170.426
13	2	0	170.426

Figure Captions.

Figure 4-1 Scatter plot of LSER system parameter distribution for MEKC micelle systems.

Figure 4-2 PCA analysis of LSER models in EKC: eigenvalues explained by each principal component.

Figure 4-3 PCA analysis of LSER models in EKC: plot of the first principal component vs. the second principal component.

Figure 4-4 PCA analysis of LSER models in EKC: plot of the third principal component vs. the fourth principal component.

Figure 4-5 PCA analysis of LSER models in EKC: plot of the fifth principal component vs. micelle systems

Figure 4-6 PCA analysis of LSER models in EKC: 3D plot of the distribution of micelle systems in three principal components space.

Figure 4-7 Upper-tail rule for the determining the number of clusters

Figure 4-8 Hierarchical clustering for classification of MEKC micelle systems.

Figure 4-9 Silhouette plot to determine the number of clusters for k-means clustering

Figure 4-10 K-means clustering for classification of MEKC micelle systems

Figure 4-11 Scatter plot of the distribution of MEKC micelle systems parameter after k-means clustering

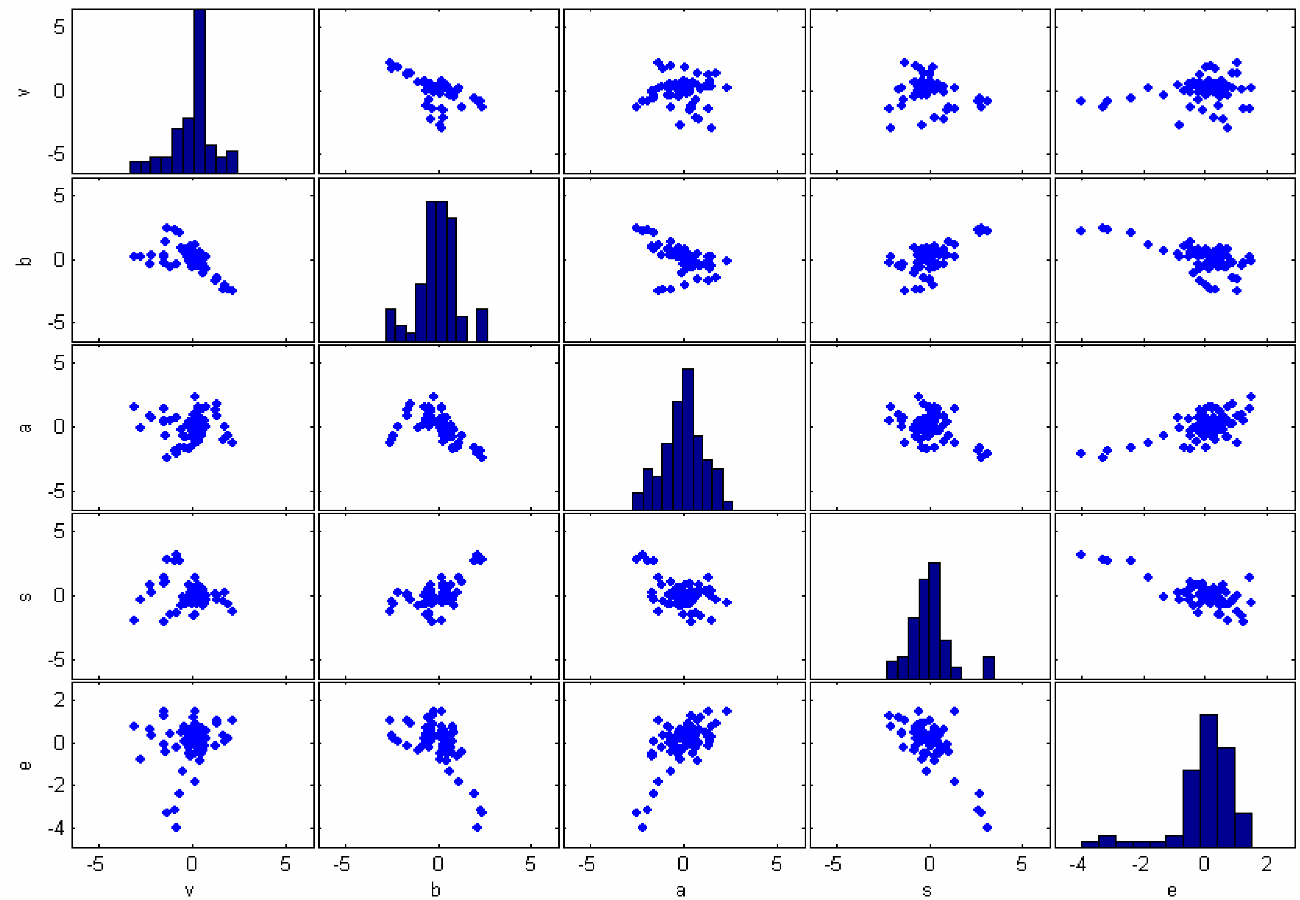

Figure 4-1 Scatter plot of system parameter distribution for MEKC micelle systems.

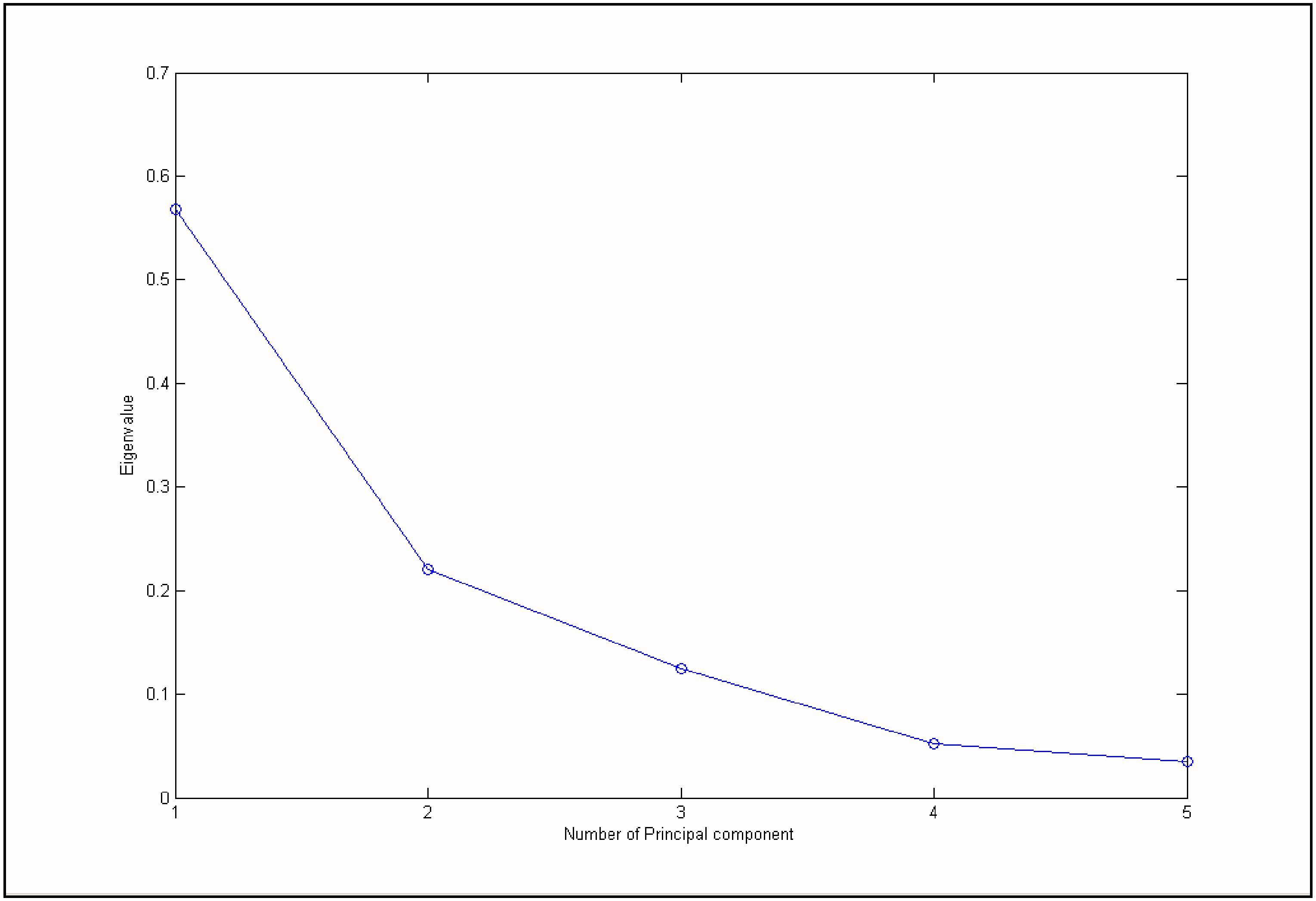

Figure 4-2 PCA analysis of LSER models in EKC. eigenvalues explained by each principal component.

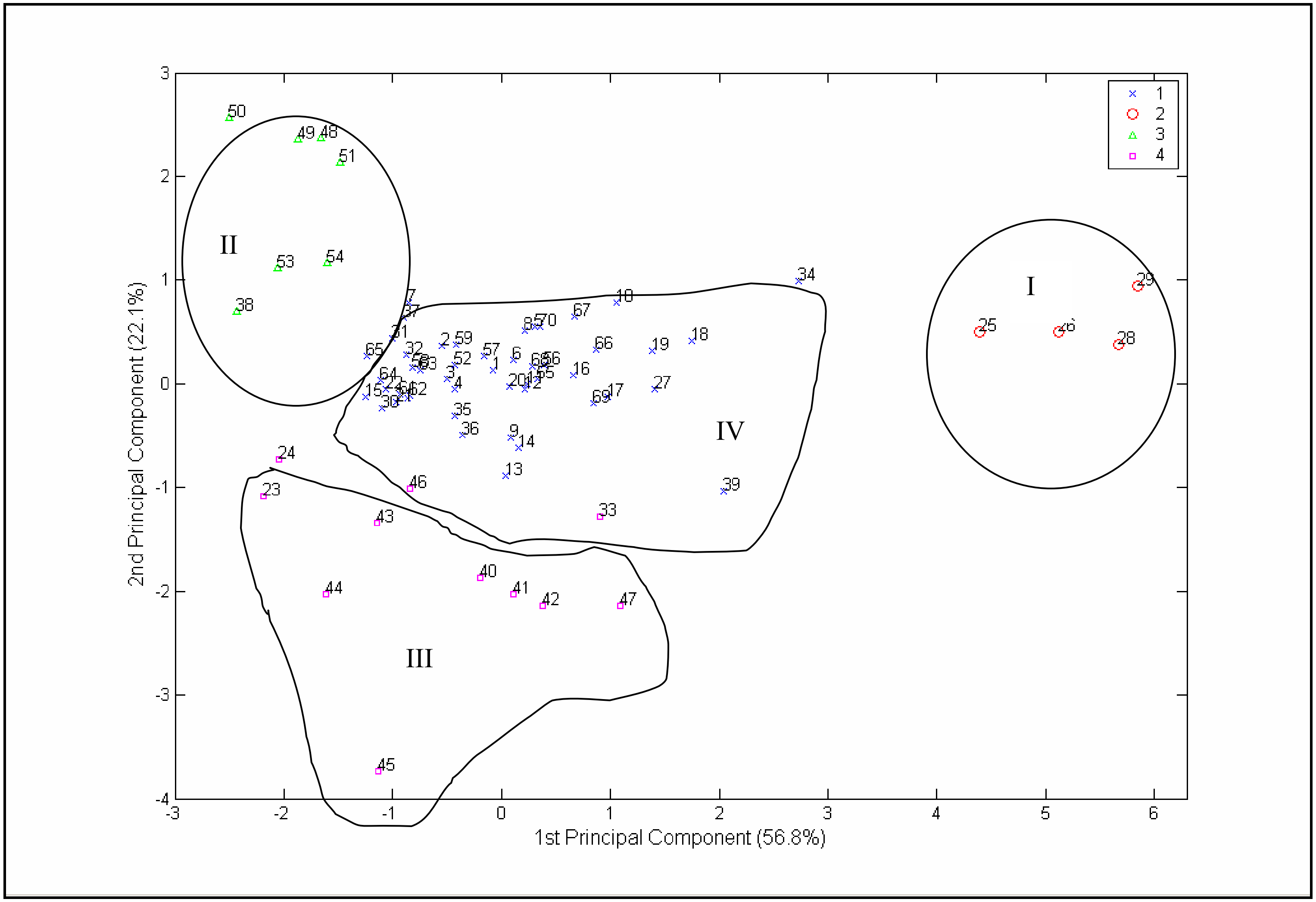

Figure 4-3 PCA analysis of LSER models in EKC: plot of the first principal component vs. the second principal component.

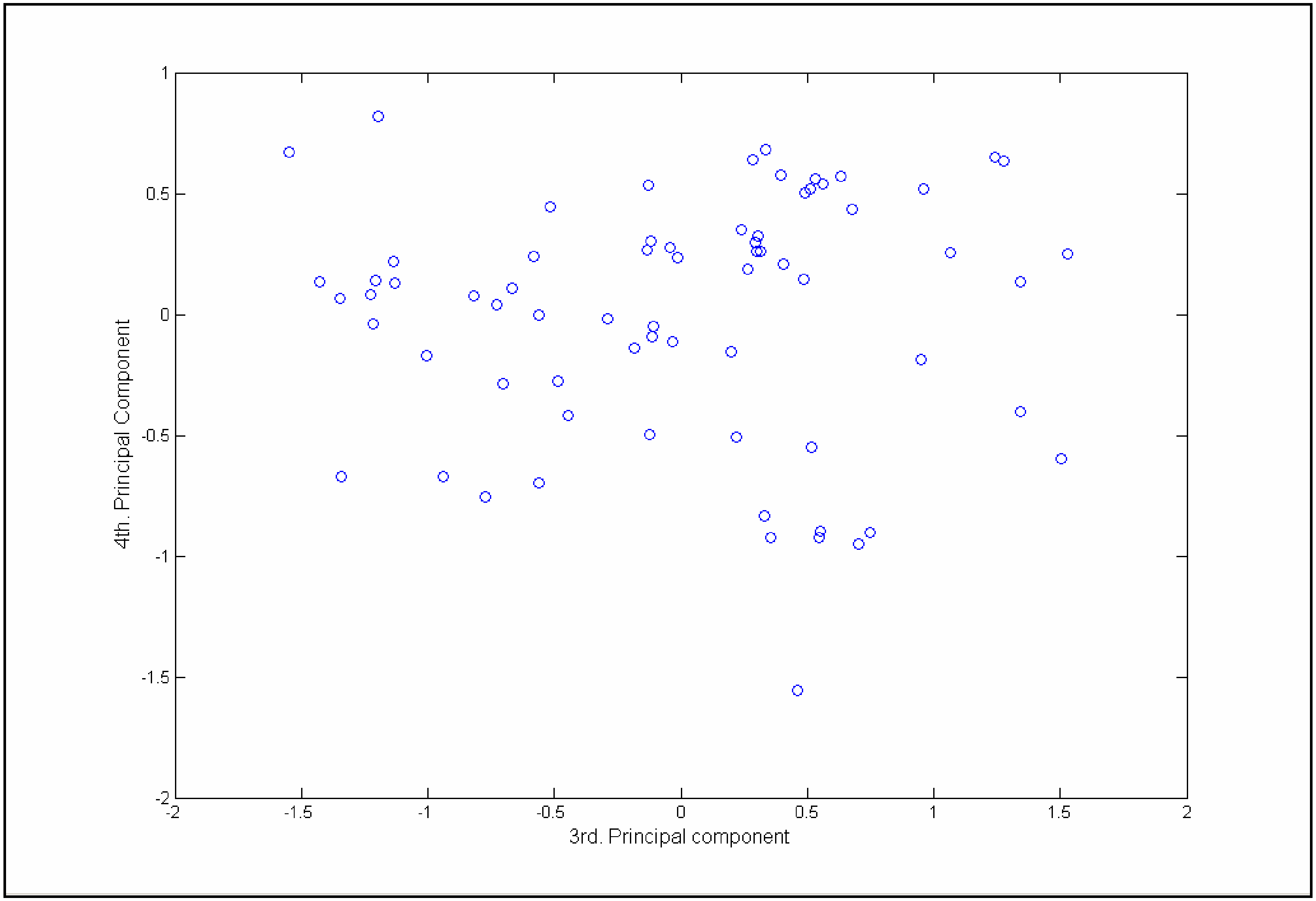

Figure 4-4 PCA analysis of LSER models in EKC: plot of the third principal component vs. the fourth principal component.

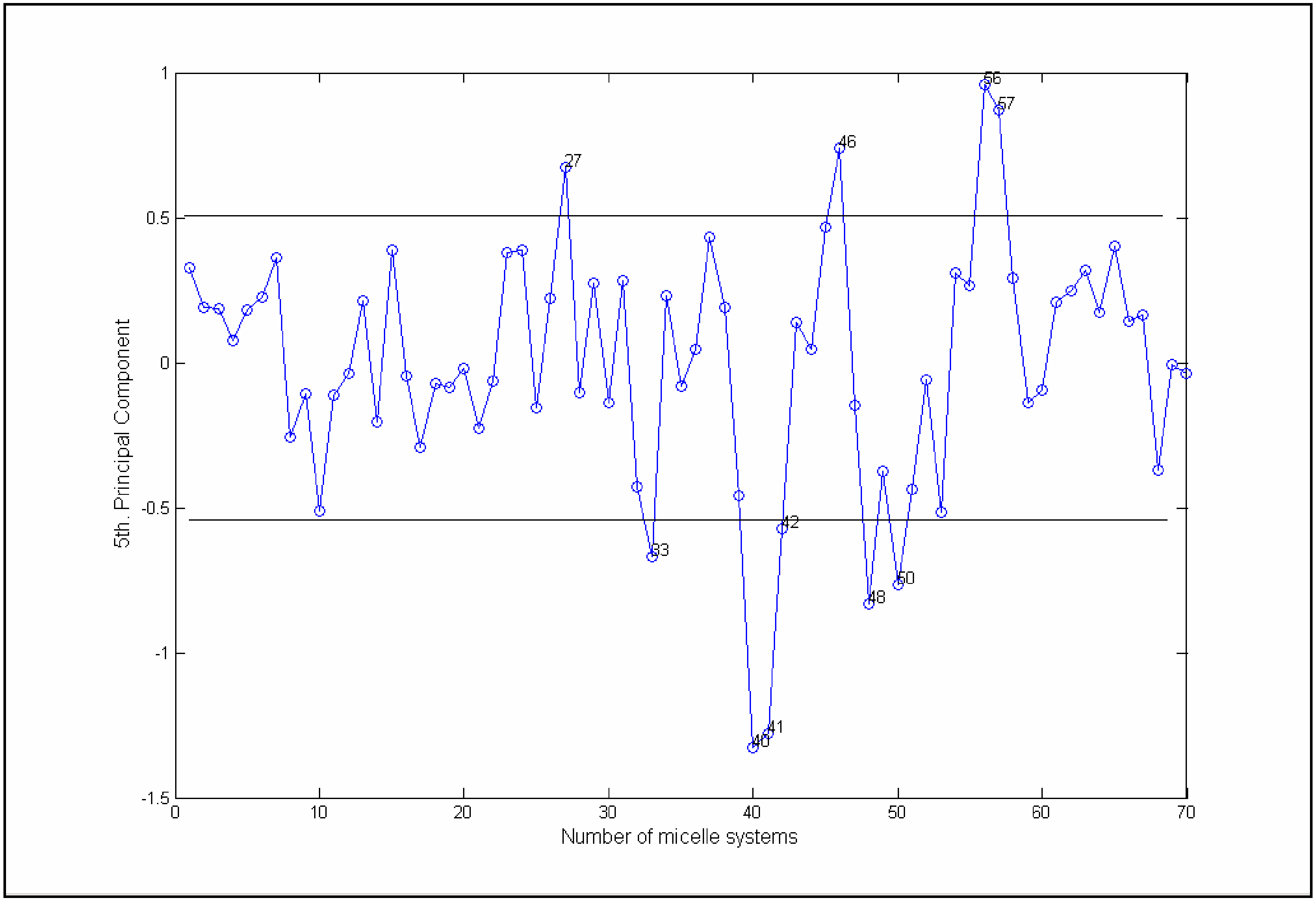

Figure 4-5 PCA analysis of LSER models in EKC: plot of the fifth principal component vs. micelle systems.

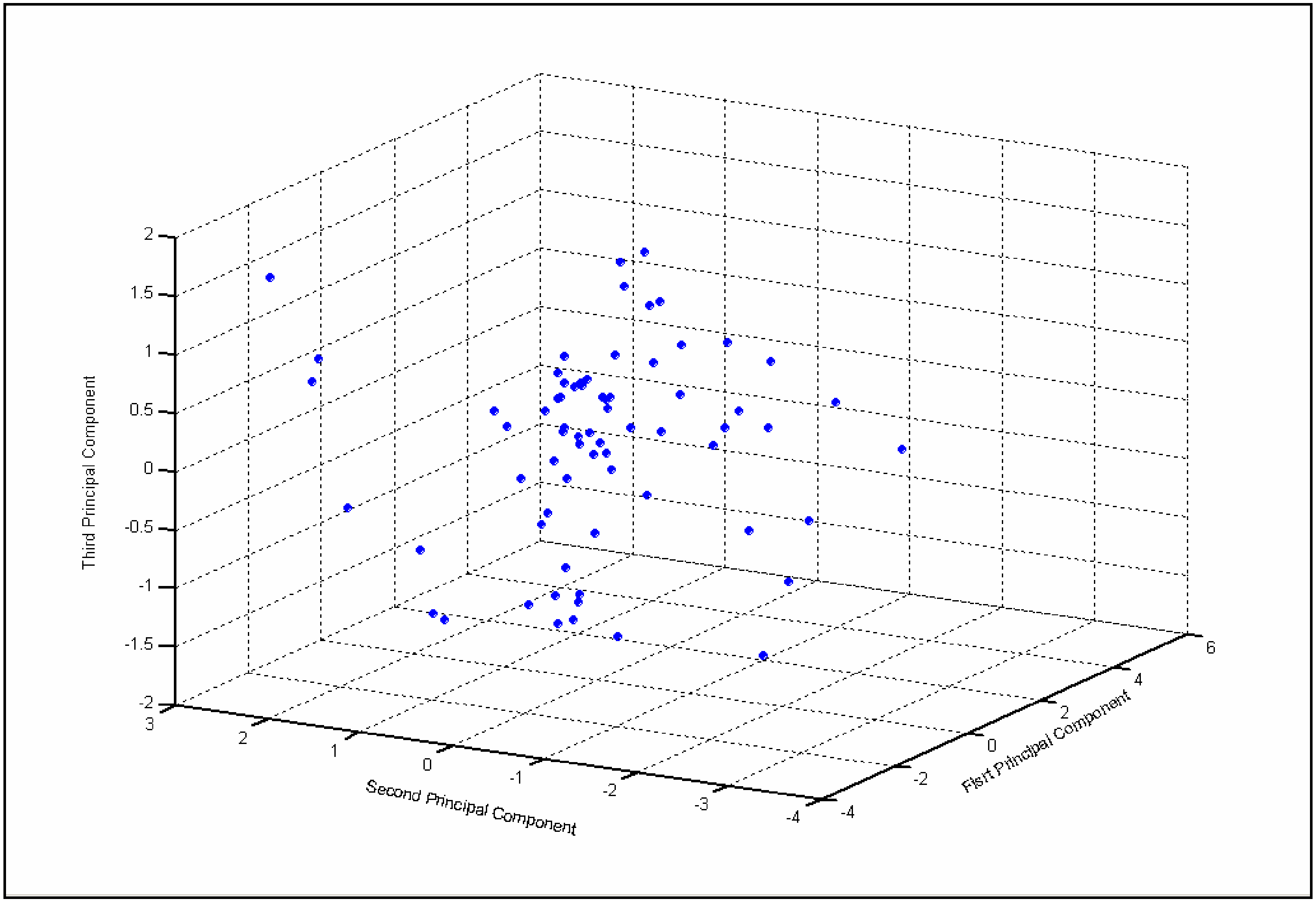

Figure 4-6 PCA analysis of LSER models in EKC: 3D Plot of the distribution of micelle systems in three principal components space.

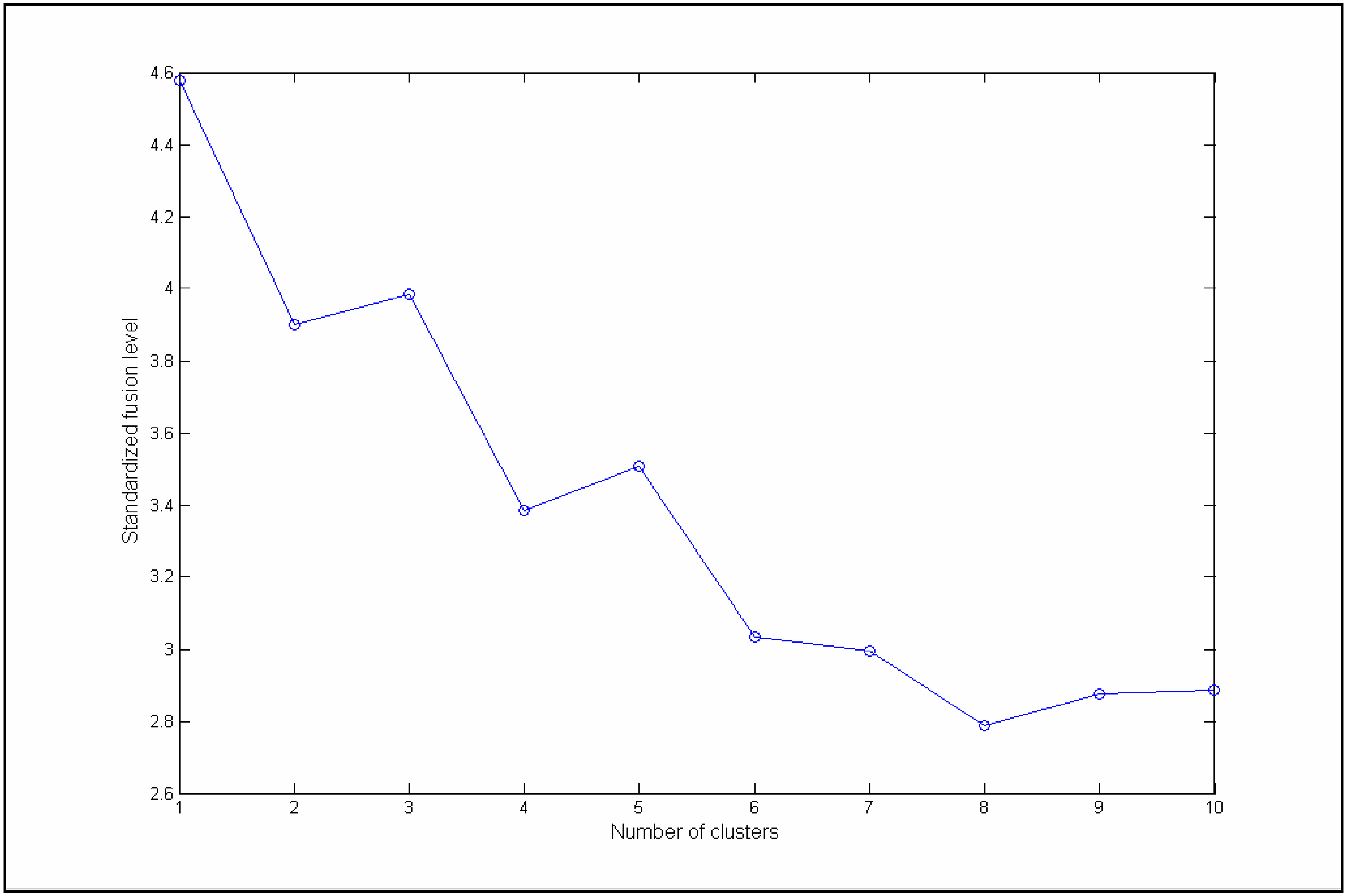

Figure 4-7 Upper-tail rule for determining the number of clusters.

(The steepness of the slope indicate the degree of the clusters separation)

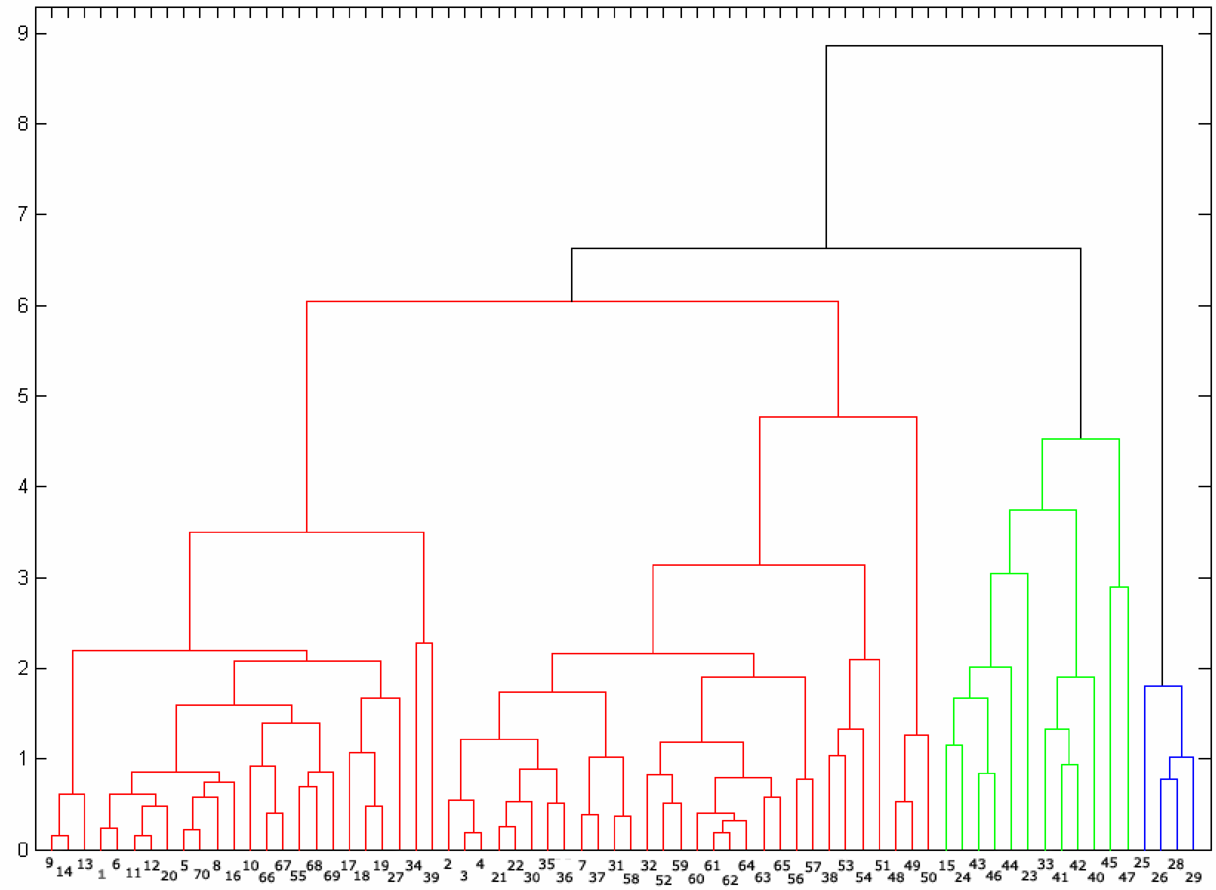

Figure 4-8 Hierarchical clustering for classification of MEKC micelle systems.
Note: The leaf node numbers are the same as the micelle system identities in table 4-1

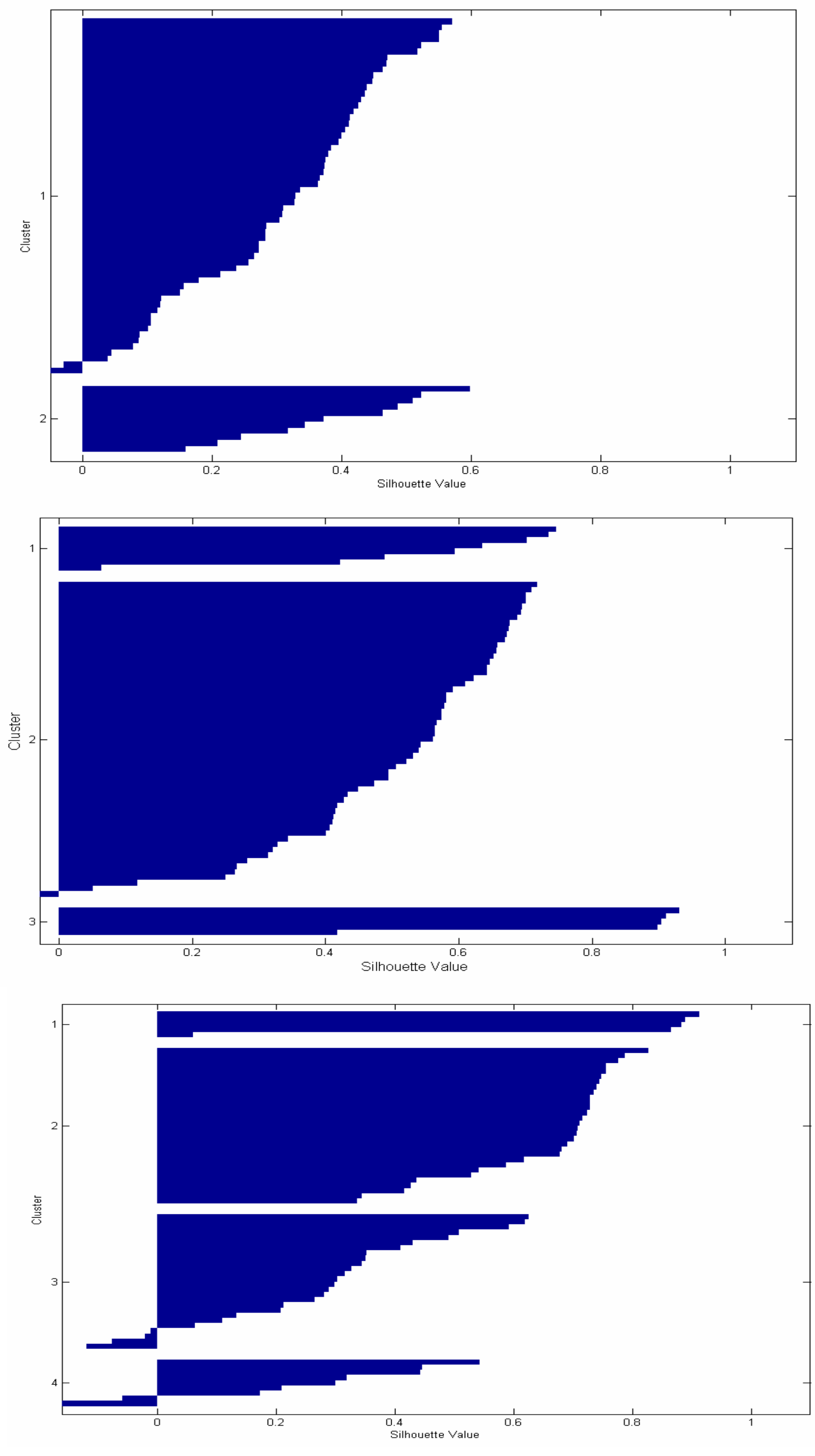

Figure 4-9 Silhouette plot to determine the number of clusters for k-means clustering.

From top to bottom are silhouette plots for 2, 3 and 4 clusters respectively.

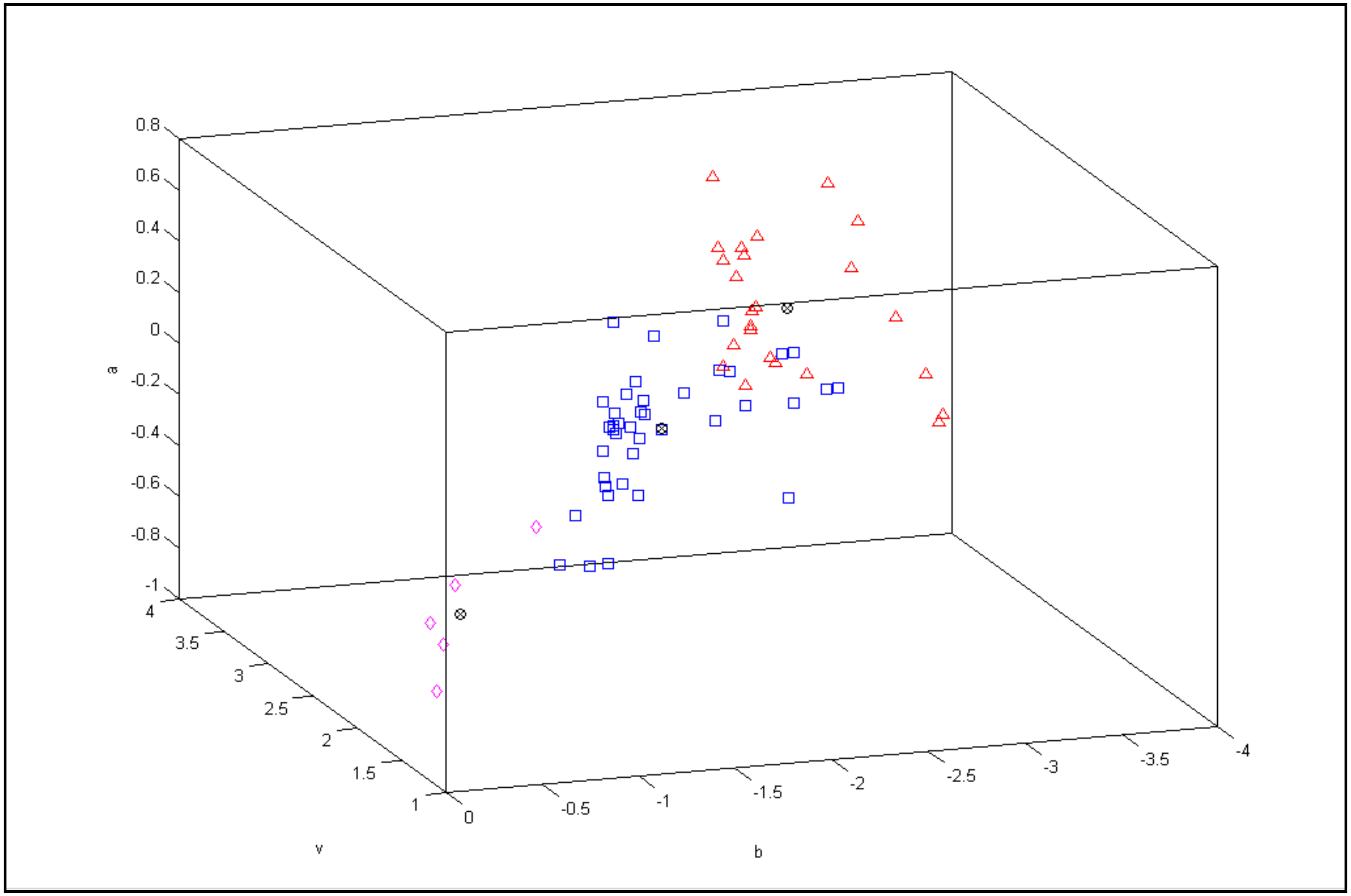

Figure 4-10 K-means clustering for classification of MEKC micelle systems

Note: the circles with a cross inside indicate the centroids of the clusters.

The axes are the LSER system parameters after k-means clustering.

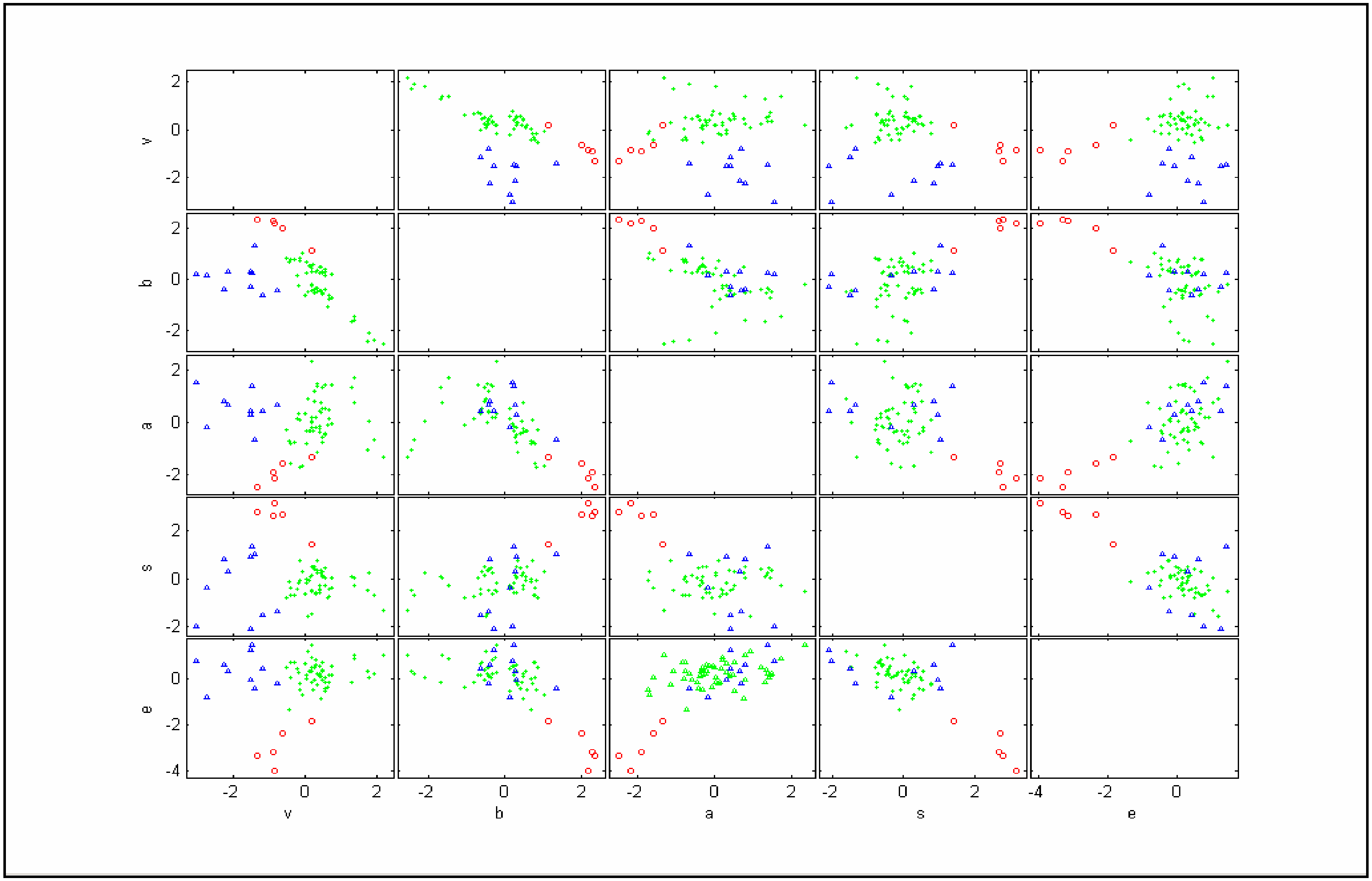

Figure 4-11 Scatter plot of the distribution of LSER coefficients after k-means clustering

CHAPTER 5

Multivariate Optimization of PTH (Phenylthiohydantoin) Amino Acids Separation in Micellar Electrokinetic Chromatography (MEKC)

ABSTRACT

Optimization of PTH amino acids separation in MEKC is carried out with a multivariate approach including surfactant types, surfactant concentrations, solvent additives and temperature adjustments. The Micellar Selectivity Triangle (MST) is used as a guideline for the optimization. The quality of separation is evaluated with a chromatographic exponential response (CER) function of resolution. Optimum separation for pentanol modified SDS micelle systems is found at 40 ~ 50 mM SDS and 200 mM pentanol concentrations. Hydrogen bond donor solvent hexafluoro isopropanol (HFIP) exerts different selectivity patterns to moderately hydrophobic solutes. A combination of the modification effects of HFIP and pentanol results in a complete resolution of 20 PTH amino acids. The application of a parallel separation scheme with semi-orthogonal micelle systems also obtains satisfactory resolution of the 20 PTH amino acids.

The solvation energies and substituent constants of amino acid residues that measured in EKC methods are compared to the values obtained from other methods including Octanol/water, POPC and amino acid transfer free energy from the unfolding of globular proteins. The free energy of transfer of the methylene group is used to evaluate the hydrophobicity of all condensed phases. Finally principal component analysis (PCA) is used to classify the condensed phases and amino acid residues according to their different binding affinity.

1. INTRODUCTION

In the early 1950s, Edman [1,2] introduced a method of cyclic degradation of the N terminus of peptides or protein fragments. This method was later developed as a standard procedure for protein and peptide sequencing. The Edman degradation was carried out initially with phenylisothiocyanate (PITC) under basic condition, which reacts with the free amino group of the N terminus of peptide to form a phenylthiocarbamyl cyclic derivative. In the second stage, a mildly acidic condition was used to promote the cyclic cleavage and the formation of PTH (Phenylthiohydantoin) amino acid derivatives. The advantage of edman degradation is that it removes only one amino acid unit in each cleavage ensuring the validity of the sequencing. In contrast, highly sensitive mass spectral techniques for peptide or protein sequencing often encounter ambiguity in the sequencing because of the poor differentiation between isomeric amino acids such as I and L, or isobaric amino acids such as Q and K. Edman sequencing is usually limited to a length of 30 to 40 amino acid units mostly due to the fact that the efficiency of the degradation reaction is less than 100% yield. However this problem could be circumvented by enzymically or chemically cleaving large proteins or peptides into smaller segments, before proceeding to edman sequencing. The identification of the amino acid residues is normally performed with chromatographic techniques. Initially, thin layer chromatography (TLC) [3] and gas liquid chromatography (GLC) [4,5] were used to separate these PTH derivatives. But poor sensitivity and poor volatility of some derivatives restricted further development of these techniques in edman sequencing. High performance liquid chromatography (HPLC) has succeeded in replacing them and attracted much attention since the early 1970s. Using isocratic elution, all of 20 PTH amino acids could be resolved by reversed phase liquid chromatography (RPLC) [6-8], however, the analysis time is rather long. Several gradient programs [8,9] also were capable of complete resolution of these PTH amino acids in a short period of time. However, potential column equilibrium problems and complex gradient programs are not desirable for an automated sequencing machine. The automatic protein sequencer requires compatible characteristics of both the degradation chemistry and chromatography process in terms of time span, sensitivity and sample size. Rapid development of RPLC column technique enabled the production of first automated proteins sequencer.[10-12]

Minor problems still remain since the presence of impurities from the degradation reaction often interfere with the identification of the cleaved amino acid units. It is necessary to employ a fast screen of eluents with orthogonal or partly orthogonal separation systems in which amino acids have markedly different retention patterns. Micellar electrokinetic chromatography (MEKC) is suitable for this purpose with multiplexed capillary systems and flexible manipulation of selectivity by simply switching to a new micelle. Terabe [13] first employed MEKC to separate the complete series of PTH amino acids. They observed dramatically different separation selectivity in SDS and DTAB, however complete separation of all PTH amino acids derivatives was not obtained in these surfactant systems. Waldron and his colleagues [14,15] enhanced the detection limit of these PTH amino acids in MEKC separation to a sub-femtomole level with the thermooptical detection. However, three critical pairs of solutes were only partially resolved which led to uncertainty in the residue amino acid identification. Many other authors [7,9,16,17] found that the separation of these amino acid derivatives was very sensitive to ionic strength, pH, temperature, ion pairing reagent and organic additives. This is not unexpected, because PTH amino acids contain hydrophilic and hydrophobic solutes as well as a wide variety of polarity, ionizable species which also add to the complexity. Previously we developed a micellar selectivity triangle (MST) to characterize the selective characteristics of various pseudo-phases in MEKC. One of our aims is to utilize the micellar selectivity triangle as a guideline to optimize the separation of these PTH amino acids. In the final part of the study, free energies of transfer of amino acid sidechains from micellar phases to aqueous phase were determined and compared to the values obtained from other partitioning models and biological systems.

2. EXPERIMENTAL

All MEKC experiments were performed on a laboratory-built CE system equipped with a 0-30 kV high-voltage power supply (Spellmann, Plainview, NY) and a SSI 500 variable UV-Visible detector (SSI, State College, PA). Data were acquired and processed with PC/chrom+ version 4.0.9 (H&A Scientific, Greenville, NC). A 50-µm-i.d. × 375-µm-o.d. fused-silica capillary (Polymicro Technologies, Phoenix, AZ) was used. The total length of the capillary was 70 cm, with an effective length of 50 cm to detector. Newly installed capillary was conditioned with a rinsing procedure using Mili-Q water for 10 min, 0.1 mM NaOH (0.1 M LiOH was used when LiPFOS was the pseudostationary phase) for 20 minutes to ionize free silanol groups, methanol for 20 minutes to clean organic impurity, 5 minutes Mili–Q water rinses were carried out between all washing steps. Finally, the capillary was rinsed with the buffer solution for 20 minutes and equilibrated for at least 3 hours to ensure constant micelle elution time. The capillary was thermostated at a designated temperature with a circulating oil bath

(Lauda K-2/R, Brinkmann Instruments, Westbury, NY), and two 250-mL jacketed beakers were used to thermostat the buffer reservoirs. A positive 20 kV was applied throughout the experiment.

All PTH amino acids standards and SDS (Sodium Dodecyl Sulfate) were obtained from Sigma (St. Louis, MO). LiPFOS (Lithium Perfluorooctane Sulfonate) was a gift from 3M. SDS solutions were prepared in 20 mM potassium phosphate buffer (pH 7.0) and LiPFOS solution was made in 20 mM lithium phosphate buffer (pH 7.0). The required amounts of organic modifiers were then added to the surfactant solutions. All surfactant solutions were filtered with a 0.45-μm polypropylene filter and sonicated for ~5 minutes.

3. RESULT AND DISCUSSIONS

3.1 Separation in mono–surfactant micelle systems. Figure 5-1 is the chromatogram of 20 PTH amino acid separations with 40 mM SDS solution at pH 7.0. Out of 20 solutes, 14 are baseline resolved and 3 pairs of compounds are coeluted under the separation conditions. The three unresolved solute pairs are (PTH–S and PTH–T), (PTH–C and PTH–D), and (PTH–I and PTH–L). It is surprising to see PTH–S and PTH-T having identical retention, because T has one additional methylene increment than S in structure. One possible explanation could be that the branching structure in T sidechain compromises the hydrophobic contribution of methylene group; in addition, proximity effects from the nearby polar peptide bond will tend to reduce hydrophobic-type interactions. The elution order is in good agreement with the results reported by Terabe and Waldron groups. The only common deviation among the three reports is the migration behavior of PTH–H. This could be attributed to the fact that the pKa (6.43) of the side chain residue of PTH–H approaches closely to the buffering pH (7.0). Partially positively charged PTH–H is very sensitive to the pH and ionic strength of eluent buffer. As a consequence, significant differences of SDS concentration and buffer type in all three reports lead to the differences in the retention behavior of PTH–H in different systems. Table 5-2 summarizes the common physio–chemical properties of these PTH amino acids. PTH-S, -T, -N, -G, and -Q can be assigned to a group as hydrophilic compounds. These observations are consistent with their small octanol–water partition coefficients (log Pow < 0.9). A second group of solutes including PTH–A, -C, -E, -D, -Y, -V, -P, -M could be classified as solutes with moderate hydrophobicity and the octanol–water partition coefficients range from 1.09 to 2.35. One might notice that acidic PTH amino acids PTH–N and E are assigned to this group because the deprotonated forms of these acidic amino acid residues carry negative charges and have a negative eletrophoretic mobility migrating against electrokinetic flow (EOF). By contrast, the octanol–water partitioning scales for these acidic PTH amino acids are very negative indicating that polar water molecules are more capable of solubilizing these charged molecules than non–polar solvent octanol. The third group of solutes consists of some hydrophobic amino acids PTH–F, -W, -I, -L and basic amino acids PTH–H, -R, -K. These hydrophobic amino acids all contain a long hydrocarbon chain and have octanol–water partition coefficients larger than 2.8. The basic amino acids, PTH–H, -R, -K, are partially or fully positively charged under the buffering pH. There are mainly three factors contributing to the strong retention of these basic amino acids in MEKC. First, these positively charged amino acids derivatives have favorable interaction with negatively charged SDS micelles; secondly, free SDS monomers act as ion pairing agents to couple with PTH cations. Together the hydrophobicity of the ion pair complex leads to a stronger interaction with the micelles. The third factor originates from the interaction of these positively charged amino acids with deprotonated silanol group on capillary wall, which also contributes to a longer retention.

The effect of surfactant concentrations on the separation of PTH amino acids was also investigated. Figure 5-2 shows the separation of these 20 PTH amino acids in 80 mM SDS with other conditions remaining the same as that in figure 5-1. A pronounced widened elution window is observed at the higher SDS concentration. As a result, several coeluted solutes in lower SDS concentration separation previously could be partially or completely resolved. Theoretical understanding of this observation is necessary for further optimization.

Resolution in MEKC is a non-linear function of multiple variables, including efficiency N, selectivity a, retention factor k' and elution window (t_{mc}/t_{eo}), as in equation 5-1.

$$R_s = \frac{\sqrt{N}}{4}\left(\frac{a-1}{a}\right)\left(\frac{k'}{1+k'}\right)\left[\frac{1-t_{eo}/t_{mc}}{1+(t_{eo}/t_{mc}).k'}\right] \qquad \text{Eq. 5-1}$$

As revealed by the resolution function, resolution increases with efficiency and selectivity a. Foley et. al. [7] also concluded from this equation that an optimum value of k' around $\sqrt{t_{mc}/t_{eo}}$ could result in a maximum resolution. A wider elution ranges (smaller t_{eo}/t_{mc}) generally leads to higher resolution of the separation. It is worthwhile to note that most practical electrokinetic chromatograms have an elution window between 2.5 and 5, which translates to a range of 0.17 ~ 0.4 for t_{eo}/t_{mc} scale. Improved resolutions are seen for all the PTH amino acids which is mainly due to the increase of elution window (almost double). More importantly, the widened elution window greatly improves the separation of PTH amino acids with medium retention factor. Critical pairs (PTH–C and PTH-N), (PTH–L and PTH-I) could be partially or completely separated. The polar solute pair PTH-S and PTH-T, however, remains unresolved even with higher SDS concentration.

Perfluorinated surfactant LiPFOS was also employed for the separation of the complete series of PTH amino acids. LiPFOS micelles are stronger hydrogen bond donors as compared to SDS micelles in the micellar selectivity triangle (MST) classification scheme. Additionally, the fluorinated backbone of LiPFOS promotes a fluorocarbon–rich environment that is significantly different from the hydrocarbon surfactant. Thus, we expect distinguished elution patterns from these two surfactant systems. Figure 5-3 presents the separation of these 20 PTH amino acids in 40 mM LiPFOS. One of the remarkable trends is that most solutes become less retentive in LiPFOS micelle with the exception of two fully positively charged PTH amino acids R and K, which strongly interact with the LiPFOS micelles. This observation is not totally unexpected. According to our previous study, those bulky hydrocarbon solutes tend to have weaker interactions with the fluorinated surfactants mostly due to the unfavorable fluorocarbon–hydrocarbon phobicity. In our case here, PTH–I, L, F, W, V with bulky hydrophobic residues inevitably interact weakly with the fluorosurfactant LiPFOS. The strong bindings of positively charged PTH amino acids–H, K, R with LiPFOS are most likely driven by electrostatic interaction. Low retentions for a majority of solutes in the LiPFOS micelles are not desirable for the optimization because a large number of solutes are densely packed in a narrow range. The two pairs of polar amino acids coelute together as (PTH S and T), (PTH N and G), also (PTH A and D), (PTH Y and V) are only partially resolved. Another remarkable feature of the separation of PTH amino acids in LiPFOS is the unique elution pattern for moderate hydrophobic solutes including PTH P, C, M, V, Y, D, and E as compared to the separation in SDS. This is beneficial for fine-tuning the separations of these solutes with mixed micelles, given other types of solutes are less impacted. The effect of LiPFOS concentration on PTH amino acids separation is also studied. As shown in figure 5-4, again the increase in surfactant concentration results in a wider elution window (larger t_{mc}/t_{eo}) which is consistent with the observation in SDS. We also observe that the elution time of positive charged PTH amino acids H, K and R shift to less retention compared to lower LiPFOS concentrations. This is explained by the fact that after a threshold value the increase of LiPFOS concentration dramatically increases the concentration of free cation counterion (Li^+) in the solution, eventually suppressing the interaction of those positively charged PTH amino acids with LiPFOS micelles. These observations confirm the electrostatic–type interactive mechanism for these cationic PTH derivatives. Marginally better resolution can be seen in separation with higher LiPFOS concentrations. This is primarily because of a widening elution window as interpreted in the previous section. It is noteworthy that most solutes have retention factors lower than 1, much smaller than the optimum k value ($\sqrt{t_{mc}/t_{eo}}$ ~2.4) for optimization of resolution. This explains that there is only marginal improvement of resolution by increasing the concentration of LiPFOS.

3.2 Solvent–aided modification of PTH amino acids separation. Previously, we showed the solvent modification effects on the solute–micelle interaction with neutral solutes. The two kinds of organic solvents that exhibit the most remarkable modification effects are the hydrogen bond acidic solvent HFIP and hydrogen bond basic solvent pentanol. We further investigated the modification effects of PeOH and HFIP on the separations of PTH amino acids that also involve ionizable compounds.

Figure 5-5 presents the PTH amino acids separation using 20 mM SDS and 50 mM pentanol (0.54% v/v). A higher efficiency of separation could be seen, attributing to the alleviation of resistance to mass transfer induced by the incorporation pentanol to the SDS micelle. Higher theoretical plate numbers are favorable for enhancing resolution of the PTH mixture as indicated by the resolution function in equation 5-1. We notice that most of the elution orders remain unchanged as compared to the separation with unmodified SDS micelles, except for a number of moderately hydrophobic solutes PTH G, P, M, and V. Meanwhile, solute pairs PTH S-T, E-C and L-I are overlapping. To obtain a better understanding of this solvent–assisted manipulation effect, we investigated the PTH amino acids separation at four different SDS surfactant concentrations together with various pentanol content.

Figure 5-6 shows the separation of PTH amino acids in 20 mM SDS with increasing pentanol concentration from A (50 mM 0.54% v/v) to E (300 mM 3.24% v/v). A significant reduction of the retention of positive PTH amino acids H, K and R is observed with the increase of pentanol content. This is explained by a decrease of surface charged density of the SDS micelle with the incorporation of pentanol, which observed in our previous work. As a consequence, weakened electrostatic attraction with reduced charged micelles lead to a consistently decreased retention for positively charged PTH amino acids. Another consequence of reducing charge density on micelle is the shorter micelle elution time. We also find that the incorporation of pentanol into SDS micelle systems improves the resolution of poorly resolved solute pairs PTH S-T, and I-L. The trend is more obvious with pentanol concentration above 150 mM, however when the pentanol concentration approaches 300 mM, a large population of solutes jam into the low retention range which is not favorable for optimizing the separation. Thus, an optimum pentanol concentration shall be in the range of 150 to 200. The trend is more easily visualized in figure 5-7, which plots the retention factors of PTH amino acids as a function of pentanol concentration. It can be seen that PTH amino acids (i.e. PTH H, K, R,) with positive charge have a decreasing retention factor with the addition of pentanol. The polar solute pair PTH S-T is better resolved at very high concentration of pentanol. However, very high concentration of pentanol (e. g. 300 mM) leads to the coelution of PTH G-P and compresses the elution of moderate hydrophobic PTH amino acids into narrow and crowded region.

The separation at a higher SDS concentration of 30 mM with the addition of various pentanol concentrations is shown in figure 5-8. First of all, the elution range is wider because of the higher surfactant concentrations. Secondly, a similar effect on the elution window with the addition of pentanol is observed: the more pentanol that is present in the system, the narrower the elution window obtains. We also observe that the overall resolution improved dramatically with the addition of 150 mM pentanol in 30 mM SDS, especially for the eight peaks with moderate elution strength identified as PTH G, N, P, Y, M, V, E, C (E and C overlapping). These eight peaks with similar retention strength are evenly spread out and baseline-resolved. Nevertheless, the critical pairs solutes, PTH S-T and PTH L-I are still partially coeluted. Again, we plot the log k' of PTH amino acids as a function of pentanol concentration in figure 5-9. The reduction of retention factors for positively charged PTH amino acids H, K, and R with increasing pentanol concentration is consistent with the previous observation at 20 mM SDS. One can also observe that the critical polar solute pair, PTH S and T, is better resolved at higher SDS concentrations. Moreover, another critical pair, PTH L and I, could be partially resolved with the highest pentanol concentration applied (300 mM) at the expense of reduced separation between PTH M and C. The plot also suggests that an optimum level is at intermediate concentration between 200 mM and 300 mM pentanol to resolve this mixture leaving only PTH L and I partially resolved. We also apply similar optimization strategy at higher SDS concentration of 40 mM and 50 mM. The separations under optimal conditions for the twenty PTH amino acids mixture are shown in Figure 5-10 and 5-11. These optimized separations show improved resolution for the poorly resolved solute pairs PTH S-T and PTH L-I as compared to that at lower SDS concentrations. However, addition of pentanol also influences the extent of the retention of some moderately hydrophobic solutes and new overlapping peaks are observed in both chromatograms.

In order to elucidate the relationship between the separation quality and surfactant/pentanol concentration, it is advisable to construct an optimization criterion to evaluate the overall chromatogram performance. Jones et. al. [18] suggested to use minimum resolution between pairs of neighboring peaks in a chromatogram. Schoenmakers [19] and his colleagues proposed an overall resolution function, where the quantity r_p was defined as the product of resolutions between pairs of peaks in the chromatogram.

$$r_p = \prod_{1}^{n-1} R_i \qquad \text{Eq. 5-1}$$

The design was favored because of several advantages: first, poorly resolved peaks would have strongest effect on the magnitude of r_p (approaching zero for overlapping peaks); second, large r_p corresponds even-spreading of peaks in the separation ranges. A normalized version of overall resolution was also developed by other authors [20,21] and successfully optimized the separation of metal complexes and small organic compounds in MEKC. In the normalized overall resolution scheme, the resolution of the adjacent peaks was first normalized by the mean resolution before multiplication. In this way, criterion r is in the range of 0 and 1 and could be expressed as,

$$r_n = \prod_{1}^{n-1} \frac{R_i}{\frac{1}{n-1}\sum_{1}^{n-1} R_i} \qquad \text{Eq. 5-2}$$

Liu et. al. [22] criticized this scheme for failing to take into consideration the range of separation in MEKC separation. Therefore, they incorporated the retention time of last peak (t_l) and resolution between the first peak and last peak (R_{fl}) as a compensation of the existence of an elution window. Their overall resolution function could be written as:

$$r_e = \frac{R_{fl}}{t_l} \prod_{1}^{n-1} \frac{R_i}{\frac{1}{n-1}\sum_{1}^{n-1} R_i} \qquad \text{Eq. 5-3}$$

Although the overall resolution function has become a satisfactory optimization criterion in some cases, it shall be noted that all these applications only investigated in a simple mixture of few compounds without serious peaks clustering. In other words, peak spacing was adequate in the elution range owing to the small number of peaks and drastically different retention strength of the solutes. Another drawback of the overall resolution approach is that one overlapping peak pair will result in a minimum response of the function. This is disadvantageous for developing optimization strategy, because occasionally one peak pair is poorly resolved while other peaks could reach optimum resolution. The overall resolution scheme can not distinguish this kind of information, which otherwise would be useful for the optimization of the separation. For example in our more complex PTH amino acids mixture, solute grouping is found for polar solutes, moderately hydrophobic solutes and highly hydrophobic solutes. It is unrealistic to optimize these peaks into an even-spreading chromatogram. An alternative approach using a mathematically transformed resolution response function was proposed by Morris [23] et. al. This novel response function evaluates the separation quality in term of resolution and duration of separation and could be written as:

$$r_s = \left[\left(\sum_{i=1}^{n-1} 1 - e^{a(R_{opt} - R_i)} \right)^2 + 1 \right] . (1 + \frac{t_f}{t_{\max}}) \qquad \text{Eq. 5-4}$$

R_{opt} is the optimum resolution, which we set at 1.5. Parameter a relates to the weight between resolution and elution time, which we assign the value as 3. t_f and t_{max} are the retention time of the final sample peak and the ideal maximum elution time (we set at 30 minutes) respectively. The exponential response function is used to evaluate the separation quality of pentanol modified SDS micelles systems and the optimal condition will return a minimum value of response. The values of the response function for pentanol-modified SDS micelle systems are summarized in table 5-3. The acquisition of resolution response enables us to visualize the relationship between these responses with our chromatographic conditions, i.e. concentrations of SDS and pentanol. As shown in figure 5-12, the resolution response attains its minimum value at SDS concentration of 40 ~ 50 mM together with a pentanol concentration around 200 mM which is consistent with our above chromatographic quality discussion. The high plateau of the response surface appears at low concentration s of both SDS and pentanol. This is not surprising, because a low SDS concentration might not provide adequate space capacity to accommodate the peaks, and a low concentration of pentanol could not effectively modify solute-SDS micelle interactive strength.

As stated above, the mole ratio of surfactant to organic additives plays an important role in not only influencing the elution window and efficiency, but also in improving the resolution between some poorly resolved solutes with minimum effect on the elution order of other solutes. We successfully refined the resolution of critical solute pairs by varying the SDS and pentanol concentrations, but complete resolution of all solutes in one chromatogram was not achieved. In light of the solvent modification effects that have been reported in our previous work, we adopted HFIP as a solvent with different selectivity pattern to optimize the separation of PTH amino acids. As shown in Figure 5-13, the separation of 20 PTH amino acids is carried out in 40 mM SDS and 400 mM HFIP. It is worth to note that most PTH amino acids are successfully resolved, except for three PTH amino acid pairs that are partially resolved as PTH S-T, PTH C-A, and PTH I-L. We can also see that the elution of very polar solutes or hydrophobic solutes maintains the patterns as with pentanol modified SDS micelle systems. Significantly different elution orders for moderately hydrophobic solutes are observed. The comparison of elution order alterations in both solvents modified SDS micelle systems are highlighted in figure 5-14. The elution order for the moderately hydrophobic solutes is as follow: PTH G < Q < A < V < Y ~ P < M < E < N in pentanol modified SDS micelle. The elution sequence changes dramatically in HFIP-modified SDS micelle as PTH Q < G < P < A ~ E < N < V < Y < M. The different elution patterns suggest that the moderately hydrophobic solutes are sensitive to the micelle environment, especially hydrogen bonding ability of micelle because these two organic additives have a major impact on the hydrogen bonding properties of the SDS micelles. This is advantageous for the complete separation of the moderately hydrophobic solutes with similar elution strength because we can simply combine both solvents as modifiers to adjust the resolution of moderately hydrophobic solutes, with minor impact on the retention of very polar solutes and hydrophobic solutes. The use of these two solvents collectively to modify the SDS micelles result in a satisfactory resolution of the 20 PTH amino acids as shown in figure 5-15. Resolutions between PTH S-T, PTH Y-C, and PTH L-H are 1.65, 1.19 and 0.97 respectively. All other peaks are evenly spaced in the separation window, which is beneficial for the peak identification of amino acid derivatives from Edman sequencing.

To achieve a more precise and complete resolution of these 20 PTH amino acids, we employ a 2D parallel separation scheme. In this 2D parallel separation strategy, two micelle systems are selected according to their markedly different retention selectivity for PTH amino acids. In our case, SDS/Pentanol and LiPFOS/Pentanol micelle systems are considered as appropriate candidates owing to their similar elution window and evenly spaced peak patterns, but more importantly, for the supplemental resolving ability for critical solute pairs that otherwise will be partially or fully overlapping in the other micelle system. Figure 5-16 illustrates the successful 2D parallel separation mapping of these 20 PTH amino acids. One can see that with the combination of the resolving ability of two selectively different micelle systems, we can obtain superior identification of each PTH amino acid derivatives. Several critical solute pairs such as PTH S-T, PTH I-L and

PTH C-N could be easily separated from each other. The complete set of PTH amino acids could be resolved simultaneously in a parallel separation which consequently ensures the accuracy of PTH amino acid peak identification. In addition, the 2D scheme also enhances the peak capacity of MEKC system dramatically, which tackles one of the limitations of MEKC that separation scope is harnessed by the elution window between elution time of EOF and micelle. Another example of a semi–2D separation is presented in figure 5-17, in which all 20 PTH amino acids can also be satisfactorily resolved. Note that SDS micelles are used in both dimension: one is unmodified SDS micelles at higher surfactant concentration, the other one is a HFIP-modified SDS micelles, it is not surprising to observe a large correlation between the elution patterns. Nevertheless, the solvent modification effect is sufficient to resolve the critical solute pairs in a single SDS system. Additionally, the solvent additive provides different elution strength for the moderately hydrophobic solutes leading to improved resolution for solutes in the crowded region under SDS condition. With the recent implementation of a multiplexed capillary electrophoresis system, one can conveniently apply multiple micelle systems simultaneously to obtain drastically different selectivity patterns of the analytes. Hence, the analysis time for each identification cycle could be greatly shortened to a ~15 minute run time and provide unparalleled accuracy for peak identification.

3.3 Temperature effect on separations in solvent modified micelle systems. Temperature is a very important variable to optimize separation quality in terms of speed and resolution, mainly because it greatly impacts the viscosity of eluent, solubility of solute, ionization of solute, and resistance of mass transfer of solute from mobile phase to micellar phases. However, temperature has not received much attention for separation optimization in MEKC so far, mostly because of the consideration of the loss of mobile phase due to evaporation at elevated temperature and complex effects on micellization (e. g. shape and size transition of micelles, CMC), hence producing less reliable experimental results. It is of our interest to examine the stability of separation with the variation of temperature and to locate the optimum operational temperature for a reproducible and robust separation of PTH amino acids.

Figure 5-18 and 5-20 illustrate the separations of these PTH amino acids in the solvent-modified SDS micelles under the influence of different temperatures. The applied temperatures are confined to the range between 20 and 40 ^{o}C. The reason for not using a higher temperature is that temperatures higher than 50 ^{o}C would accelerate the dissolution of silica and form a temperature gradient across the capillary center to capillary wall. Furthermore very high temperature would lead to possible sample degradation. Three marked behaviors could be seen in the chromatograms. First, better resolution and efficiency could be obtained with higher temperatures partly due to faster diffusivity of solute. Second, elution times of the EOF marker and micelle reduce as the temperature increases. This behavior could be accounted for by the reduction of viscosity of the eluent, which relieves the resistance to the migration flow. The third behavior is the universal increase in retention factors of the PTH amino acids with the increase in temperature. This behavior is better represented in figure 5-19. There are three groups of solutes that distinguish themselves from the mixture: polar solutes including PTH S, T, N, Q, A; moderately hydrophobic solutes including PTH C, E, G, N, Y, P, M, V and hydrophobic solutes including PTH I, L, W, H, F, K and R. It is clear that all these solutes uniformly gain more retention as the temperature increases, with the exception of

PTH P and E. This observation suggests that temperature does not selectively impact the retention patterns of most PTH amino acids. This is not surprising, as temperature influence the micelle-water partition coefficients of solutes unanimously with negligible selective effects. It should be noted that the temperature effect on the phase ratio of the separation system is negligible for two reasons. First, as we reported previously, the critical micelle concentration (CMC) of a SDS–Pentanol system does not show significant temperature dependence within the investigated temperature range. Second, the relatively high SDS concentration (40 mM) ensures a constant micelle concentration in spite of the minor variations of CMC. It is noteworthy that changes in temperature do not induce the alteration of the relative spacing of the PTH amino acids.

3.4 Substituent constants of amino acids side chain residues. The 20 natural amino acids are fundamental building blocks that encode intriguing structural and functional information into polypeptides, oligopetides and proteins. These amino acid-based biopolymers play significant roles in a variety of biological activities such as protein stability, protein folding and unfolding, protein–ligand binding affinity, membrane insertion and transportation etc. To unveil the individual function of an amino acid unit, it is necessary to understand the characteristics of each amino acid, given the variety of size, charge state and hydrophobicity. Hydrophobic scales of these amino acids, as determined mainly the chemical composition of the side chain residue, have been of great interest to researchers. Various scales for hydrophobicity of amino acids have been developed, mainly based on the free energy of transfer of amino acids from various condensed phases including Octanol, HPLC non-polar stationary phase, liposome and micelles into water. Many of these models resulted in substantially different rankings of the hydrophobicity of the amino acid residues. The origin of the discrepancy is likely due to the diverse nature of these condensed phases and model compounds in use. For example, deprotonated silanol groups on a RPLC column induce strong electrostatic interaction with positively charged amino acid residue. This greatly alters the ranking of the hydrophobicity of amino acid residues. In the case of model compounds, there are generally two types of model compounds that are frequently used. One is amino acid derivative (i. e. PTH amino acids, Dansyl amino acids) and another is short peptide. When comparing these two sets of model compounds, deviation of the hydrophobicity scales was occasionally discovered. This was attributed to the interference of neighboring amino acid in the sequence, the so-called "near neighbor effect". Bui *et. al*. [24] recently used an electrokinetic chromatography (EKC) method to measure fragment constants of amino acid residues in liposome and micelles. The experimental values of EKC approach were consistent with the reference values from other methods. The EKC method is also beneficial for its fast analysis time, small sample requirement and capability for high throughput screening. In order to obtain insightful information on the amino-acid-residue–micelle interaction, we expand micelle systems with solvent modification and monitor the response of the individual amino acid residues. We also compared the free energies of transfer of amino acid residues that were acquired by partitioning methods with the biological models for transferring amino acid moieties from protein interior to the surface.

The hydrophobic parameter κ in MEKC is defined by the difference of partition coefficients between an amino acid of interest and a reference amino acid Glycine as

$$\kappa = \log \mathrm{Kmw}\,(\mathrm{PTH} - \mathrm{AA}) - \log \mathrm{Kmw}\,(\mathrm{PTH} - \mathrm{Glycine}) \qquad \text{Eq. 5-5}$$

Note that proline and cysteine do not fit in this model due to their special residue structures. Alternative calculation approaches are taken for these two amino acid residues. In the case of Proline, it is reasonable to consider the cyclic side chain as a fragment of three methylene groups ($-CH_2CH_2CH_2-$) with a missing hydrogen atom on the amine group due to its cyclic structure. The substituent constant for proline residue then could be expressed as

$$\kappa = \log \text{Kmw (PTH–Proline)} - \log \text{Kmw (PTH–Glycine)} + f\text{(H)} \qquad \text{Eq. 5-6}$$

The fragmental constant for a hydrogen atom in SDS micelle had been determined to have a value of 0.117. [25] In order to prevent Cysteine from degradation during edman sequencing, a methyl carbonyl group is often used to protect the end group of the cysteine side chain. It is interesting to note that the methyl carbonyl group is the side chain residue of Asparatic acid, thus we can obtain the substituent constant for cysteine indirectly with the difference between these two PTH AAs, together with the correction of one hydrogen atom fragment. The relevant equation for the calculation of fragment κ for cysteine could be written as:

$$\kappa = \log \text{Kmw (PTH–Cysteine)} - \log \text{Kmw (PTH–Asparatic Acid)} + f\text{(H)} \qquad \text{Eq. 5-7}$$

The substituent constants and micelle–water partition coefficients of amino acids in various micelle systems are summarized in table 5-4. It can be seen that S, T, and N fragments have negative substituent constants in all cases implying a very hydrophilic nature of these residues. It is interesting to find T with a methylene group increment has a very similar substituent constant with S. The reduced substituent constant for methylene group was also found in other partitioning models [26-29] and attributed to the proximity effect of polar peptide bonds. Positively charged moieties of R, K, and H have large substituent constants in negatively charged micelle systems, mainly due to strong electrostatic interaction with negatively charged micelle. Wimley *et. al.*[28] also found an unexpected increase of hydrophobicity of R and K in the octanol/water partition coefficients. They suggested that the formation of ionic salt bridge between the basic side chain and acidic carboxyl terminus of the pentapeptide enhanced the solvation dramatically. However, other partitioning models classify these three amino acids as very hydrophilic residues, probably due to the absence of a favorable electrostatic interaction for solvation. The substituent constants for isomeric residues I and L are almost identical in these micelle systems. It is evident that these micelle systems are not capable to recognize shape difference. When comparing the two aromatic amino acids residues, F appears to be more hydrophobic than W in micelle systems, but reversed trends are observed for liposome and octanol/water systems. To solve this puzzle, it is necessary to evaluate the hydrophobicty of these two amino acids residues in several important systems. Wolfenden [30] used cyclohexane/water partition coefficients as a measure of the amino acid side chain polarity. In the cyclohexane/water scale, the contribution to solvation is merely from dispersion because of the absence of a hydrogen-bonding agent in wet cyclohexane (only one water molecule in 20000 cyclohexane molecules). κ(F) is 0.65 logarithm units larger than κ(W) in the cyclohexane/water system. On the other hand, in the octanol/water system, octanol and dissolved water molecules could act as hydrogen bond donors, which couple strongly with the lone pair electrons of the nitrogen atom from the indole ring of W. This specific interaction could explain the reversal of the hydrophobicity between W and F in an octanol/water system. However, it could not give a satisfactory explanation for the larger hydrophobicity of F in micelle systems. A closer view of the structures of these two amino acid residues reveals that, W has a more rigid and bulky ring system than F. The solvent accessible areas are 219 and 176 (A^2) [26] for W and F respectively. Since steric effects are more pronounced in a smaller-size micelle than liposome or bulky solvents (i. e. octanol), W is less favorable for solvation in micelle systems when compared to F. As in the above discussion, the discrepancies of the relative hydrophobicity scales of F and W are due to two competing factors: hydrogen bonding favors the interaction of W with condensed phases, on the other hand, steric hindrance disfavors W solvation in condensed phases in comparison with F.

The free energy of transfer of a methylene fragment from a non-polar phase to an aqueous phase, also known as methylene selectivity, is useful to evaluate the hydrophobicity scale because of the exclusion of interferences from other types of interaction. As illustrated by figure 5-21, free energy of transferring alkyl side chains (G, A, V and L) linearly correlates with the carbon number of side chain in our EKC methods. The slope of the linear plot relates to the free energy of transfer of one methylene group from condensed phase to aqueous phase. Table 5-7 presents the results of the linear relationships in all the condensed phases of interest. It can be seen that excellent linear regressions could be obtained in EKC models including all the micelle and liposome systems. The free energy of transferring a methylene group of an amino acid side chain is lower than its analogous alkyl benzenes for all the micelle systems. This is again due to the proximity effect of the nearby polar peptide bond. It is interesting to note that the free energy of transfer of a methylene group is much lower in solvent-modified micelle systems than the unmodified micellar phases. This behavior suggests that the introduction of more polar interactions into a micelle system suppresses hydrophobic type interaction, when one takes into consideration the adjacent polar functional groups in the PTH amino acids. One would also notice that for two octanol/water partition models, the one using hydrophobic parameter π from Fauchere and Pliska's work [31] exhibits better linearity than the correlation from Wimley's experimental values [27]. The difference can be accounted for by the different probe molecules in these two methods. Fauchere and Pliska used N–acetyl–X–amide as the model compound, while Wimley employed pentapeptides Ac-WL–X–LL, where X represents the 20 amino acids. It is obvious that the presence of highly non-polar W and L in the latter probe molecules could occlude the X side chain from the exterior environment. This is especially true for non-polar amino acid residues, as Wimley stated that A, V, L, I, F, and W all show smaller values compared to the results from Fauchere and Pliska. In addition, the presence of these hydrophobic neighbors impacts greatly on the dihedral angle of the target's peptide bond and increases the uncertainty of experimental results, and therefore the conformation of the probe molecules [32]. Similarly, the deviation from linearity for POPC system is due to the same reasons because the same pentapeptide probes were used. In comparison, those N–acetyl–X–amides are free from these kinds of interferences, and reflect in better correlation between the methylene solvation energy and the carbon number. The last two models that describe the easiness of transporting amino acid residues from the non–polar core of globular proteins to surface departing significantly from linearity. The observation suggests that the free energy for extracting a methylene group from the protein interior to its surface is not additive. The anomaly is probably due to several facts.

First the definitions of the buried and exposed areas of molecules are ambiguous and subjective in Chothia and Janin's schemes, especially for the bulky amino residues that could span across the boundary. The second factor is that these methods do not compensate for the entropy effect for conformation rearrangement with the departure of amino acid residues from protein interior. Both of these effects are not additive, consequently leading to a poor correlation of the free energy of transfer of methylene group with carbon number.

Cross correlation among the solvation energies of amino acid residues for various condensed phase is presented in table 5-8. The correlations of the solvation energies are generally good within the same type of methods. For example our EKC method demonstrates linkage between the pseudo phases used. It is worth noting that reasonable correlation is found between the Octanol/Water partition parameters from Wimley's measurement and the solvation models of the EKC method. The correlated behaviors are mainly due to the similar responses to charged amino acid side chains, namely K, R, H, N, and E. Nevertheless, in Fauchere and Pliska's hydrophobic parameter treatment, these charged residues are classified together as very hydrophilic solutes because of the poor charge stabilizing ability of the octanol solvent. The classification is arbitrary and misleading because these cationic and anionic residues would behave differently in various biological events, for instance, membrane binding, protein–ligand interaction, even enzyme activity. Poor correlation is found between the free energy of transfer of amino acid side chains from the protein interior to the surface and our solvation models. It indicates that neither of these condensed phases could simulate the anisotropic environment that the amino acid residues experience in the protein interior. Other factors also contribute to the dissimilarity. For example, C ranks as a very hydrophobic residue in protein unfolding method, because of the formation of disulfide bonds in protein interior. Another common contradiction is that basic amino acids are more favorable to stay on the polar surface than in the non-polar interior of the globular proteins, however electrostatic effects in EKC method shows more interaction of these positive charged residues with micelles. The principle component analysis (figure 5-22) reveals that all the condensed phases in EKC method as well as octanol/water model of Wimley's method cluster together implying similar solvation behaviors. The two models for free energy of transfer of amino acid residues during protein unfolding closely related to each other. The model from Fauchere and Pliska's hydrophobic parameter is greatly distinguished from other models. According to their diverse response of solvation energy within various condensed media, we can use principal component analysis as a tool for classification of amino acids residues. As shown in figure 5-23, W, F, I, L and C could be included into one cluster because of their highly hydrophobic nature. V, P, M, Y, and H (only partially charged in our case) represent a group of solutes with both a non-polar and a polar moiety. A, S, T, G, N, and Q, along with negatively charged E and N are considered very polar solutes. Positively charged residue R and K are located at a good distance from the other solutes indicating very unique solvated behavior within our condensed phase in comparison to other amino acids residues. It should be noted that for a more accurate and comprehensive classification of amino acid properties, a larger database of residue solvation energy measurements by more distinct methods is preferred.

CONCLUSIONS

The optimization of the 20 PTH amino acids separation in MEKC is extensively studied with the assistance of the Micellar Selectivity Triangle (MST). Surfactant concentration greatly impacts the elution window for improved resolution at the cost of longer analysis time. SDS and LiPFOS demonstrate significantly different selectivity patterns for the PTH amino acids, but the hydrophobic interaction is still the driving force for the partition process. The main exception is found for positively charged R and K, the strong retention in both micelle systems are predominantly because of their strong electrostatic interactions with the micelles. The quality of the separation is evaluated with an exponential response function of resolution. Optimal conditions for pentanol-modified SDS micelle are located at 40 ~ 50 mM SDS and 200 mM pentanol concentrations. The modification effects of organic additives mainly alter the elution pattern of moderately hydrophobic residues. Pentanol and HFIP exhibit a different tendency to alter the selectivity of these moderate hydrophobic solutes. A combination of these two solvent modifications with SDS results in a satisfactory resolution of the 20 PTH amino acids. The retention of most of the PTH solutes increases with an increase in temperature to the same extent, consequently temperature has minor effect on the selectivity pattern. Also solvent modified separations of PTH amino acids are thermo-stable with the variation of temperature.

The free energies of transfer of amino acid residues that were measured by the EKC method, are poorly correlated with transfer free energies obtained from globular proteins unfolding experiments. This indicates the unlikeness between the condensed phases and protein interior surrounding. The implementation of the principal component analysis to classify condensed phases and amino acid residues is informative. According to PCA, micelle systems and liposomes in the EKC method have great similarity in terms of the binding affinity with the amino acid residues. Conversely, the models for globular unfolding are distinct from all other condensed phases. The classification of amino acid residues in PCA reveals that four groups are distinguished from each other as: very hydrophobic amino acids including, F, I, L and C; moderately hydrophobic residues including V, P, M, Y, and H. A, S, T, G, N, and Q, along with negatively charged E and N are very polar solutes. Positively charged residues R and K behave remarkably different from other groups and are classified as a unique amino acid group.

REFERENCES

1. Edman P: **Preparation of phenylthiohydantoins from some natural amino acids**. *Acta Chemica Scandinavica* 1950, **4**:277-282.

2. Edman P, Begg G: **A protein sequenator**. *European journal of biochemistry / FEBS* 1967, **1**:80-91.

3. Kulbe KD, Konschewski H: **Micropolyamide thin-layer chromatography of phenylthiohydantoin amino acids (PTH) at subnanomolar level. Rapid microtechnique for simultaneous multisample identification after automated Edman degradations**. *Analytical Biochemistry* 1974, **59**:564-573.

4. Bober H: **Gas chromatographic detection of PTH [phenylthiohydantoin] amino acids in the picomolar region**. *Beckman Report* 1973:10-13.

5. Tripier D: **Fused silica capillary gas chromatography. A novel procedure for the identification of PTH in the analysis of protein**. *Methods Protein Sequence Anal., [Proc. Int. Conf.], 4th* 1982:519-527.

6. Zimmerman CL, Appella E, Pisano JJ: **Rapid analysis of amino acid phenylthiohydantoins by high-performance liquid chromatography**. *Analytical Biochemistry* 1977, **77**:569-573.

7. Foley JP: **Optimization of micellar electrokinetic chromatography**. *Analytical Chemistry* 1990, **62**:1302-1308.

8. Abrahamsson M, Groningsson K, Castensson S: **Separation of PTH-amino acids by isocratic high-performance liquid chromatography**. *Journal of Chromatography* 1978, **154**:313-317.

9. Fohlman J, Rask L, Peterson PA: **High-pressure liquid chromatographic identification of phenylthiohydantoin derivatives of all twenty common amino acids**. *Analytical Biochemistry* 1980, **106**:22-26.

10. Laursen RA: **Solid-phase Edman degradation. An automatic peptide sequencer**. *European Journal of Biochemistry* 1971, **20**:89-102.

11. Tempst P, Geromanos S, Elicone C, Erdjument-Bromage H: **Improvements in microsequencer performance for low picomole sequence analysis**. *Methods (San Diego)* 1994, **6**:248-261.

12. Hewick RM, Hunkapiller MW, Hood LE, Dreyer WJ: **A gas-liquid solid phase peptide and protein sequenator**. *Journal of Biological Chemistry* 1981, **256**:7990-7997.

13. Otsuka K, Terabe S, Ando T: **Electrokinetic chromatography with micellar solutions. Separation of phenylthiohydantoin-amino acids**. *Journal of Chromatography* 1985, **332**:219-226.

14. Chen M, Waldron KC, Zhao Y, Dovichi NJ: **Micellar capillary electrophoresis separation and thermo-optical absorbance detection of products from manual peptide sequencing**. *Electrophoresis* 1994, **15**:1290-1294.

15. Waldron KC, Dovichi NJ: **Sub-femtomole determination of phenylthiohydantoin-amino acids: capillary electrophoresis and thermooptical detection**. *Analytical Chemistry* 1992, **64**:1396-1399.

16. Little EL, Foley JP: **Optimization of the resolution of PTH-amino acids through control of surfactant concentration in micellar electrokinetic capillary chromatography: SDS vs. Brij 35/SDS micellar systems**. *Journal of Microcolumn Separations* 1992, **4**:145-154.

17. Castagnola M, Rossetti DV, Cassiano L, Rabino R, Nocca G, Giardina B: **Optimization of phenylthiohydantoinamino acid separation by micellar electrokinetic capillary chromatography**. *Journal of Chromatography* 1993, **638**:327-334.

18. Peter Jones CAW: **Optimisation in chromatography : Theory and application to the separation of aromatic acids in reversed-phase liquid chromatography**. *Journal of Chromatography A* 1981, **213**:357-361.

19. Schoenmakers PJ, Drouen ACJH, Billiet HAH, De Galan L: **A simple procedure for the rapid optimization of reversed-phase separations with ternary mobile phase mixtures**. *Chromatographia* 1982, **15**:688-696.

20. Havel J, Breadmore M, Macka M, Haddad PR: **Artificial neural networks for computer-aided modeling and optimization in micellar electrokinetic chromatography**. *Journal of Chromatography, A* 1999, **850**:345-353.

21. Li Q, Zhou Y, Wang H, Zhang H, Liu S, Chen X, Hu Z: **Application of artificial neural networks in multifactor optimization of selectivity in capillary electrophoresis**. *Analytical Letters* 2000, **33**:2333-2347.

22. Liu B-F, Zhang J-F, Lu Y-T: **Predicting and evaluating separation quality of micellar electrokinetic capillary chromatography by artificial neural networks**. *Electrophoresis* 2002, **23**:1279-1284.

23. Morris VM, Hargreaves C, Overall K, Marriott PJ, Hughes JG: **Optimization of the capillary electrophoresis separation of ranitidine and related compounds**. *Journal of Chromatography, A* 1997, **766**:245-254.

24. Bui HH: **Thermodynamic study and prediction of solute partitioning into micelles and liposomes using electrokinetic chromatography**. *Thesis (Ph.D.)--North Carolina State University* 2003.

25. Burns ST: **Characterization and prediction of partition coefficients of uncharged solutes into micelles and liposomes using electrokinetic chromatography**. *Dissertation North Carolina State University.* 2002.

26. Chothia C: **The nature of the accessible and buried surfaces in proteins**. *Journal of Molecular Biology* 1976, **105**:1-12.

27. Wimley WC, White SH: **Experimentally determined hydrophobicity scale for proteins at membrane interfaces**. *Nature Structural Biology* 1996, **3**:842-848.

28. Wimley WC, Creamer TP, White SH: **Solvation Energies of Amino Acid Side Chains and Backbone in a Family of Host-Guest Pentapeptides**. *Biochemistry* 1996, **35**:5109-5124.

29. Janin J: **Surface and inside volumes in globular proteins**. *Nature (London, United Kingdom)* 1979, **277**:491-492.

30. Radzicka A, Wolfenden R: **Comparing the polarities of the amino acids: side-chain distribution coefficients between the vapor phase, cyclohexane, 1-octanol, and neutral aqueous solution**. *Biochemistry* 1988, **27**:1664-1670.

31. Fauchere JL, Pliska V: **Hydrophobic parameters p of amino acid side chains from the partitioning of N-acetyl-amino acid amides**. *European Journal of Medicinal Chemistry* 1983, **18**:369-375.

32. Roseman MA: **Hydrophobicity of the peptide C=O...H-N hydrogen-bonded group**. *Journal of molecular biology* 1988, **201**:621-623.

Table 5-1 Structure of PTH amino acids.

Phenylthiohydantoin (PTH) Amino acids	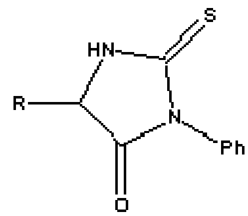
PTH-Alanine	R= $-CH_3$
PTH-Arginine	R= 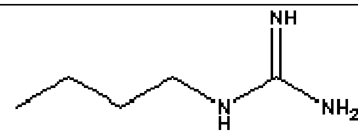
PTH-Asparagine	R= 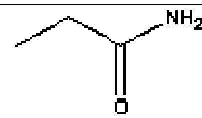
PTH-Aspartic acid	R= 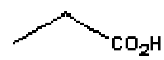
PTH-Carboxymethyl-L-cysteine	R= 
PTH-Glutamine	R= 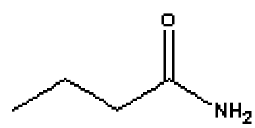
PTH-Glutamic acid	R= 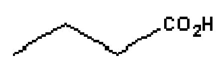
PTH-Glycine	R= -H
PTH-Histidine	R= 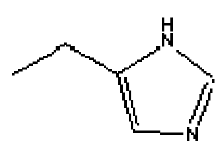
PTH-Isoleucine	R= 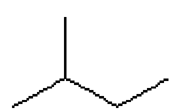
PTH-Leucine	R= 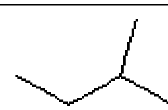
PTH-Lysine	R= 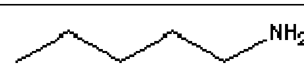

PTH-Methionine	R= 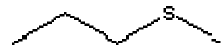
PTH-Phenylalanine	R= 
PTH-Proline	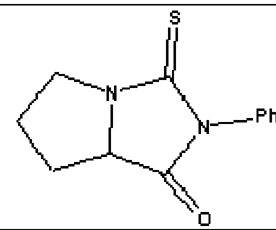
PTH-Serine	R= CH_2OH
PTH-Threonine	R= CH (OH) CH_3
PTH-Tryptophan	R= 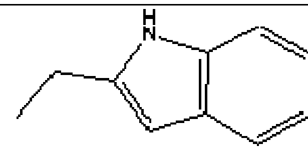
PTH-Tyrosine	R= 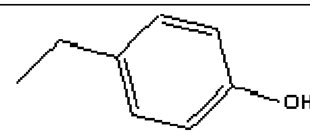
PTH-Valine	R= 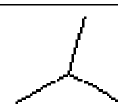

Table 5-2 Physio–chemical properties of PTH amino acid residues.

		Abr.	MW	Occurrence %	Log Pow^a	PKa^b
1	PTH - Alanine	A, Ala	206.27	7.49	1.39	10.17
2	PTH - Arginine	R, Arg	291.37	5.22	-3.07	10.05
3	PTH - Asparagine	N, Asn	249.29	4.53	-0.18	9.75
4	PTH - Aspartic acid	D, Asp	250.27	5.22	-2.3	3.89
5	PTH - Carboxymethyl- Cysteine	C, Cys	296.37	1.82	-1.62	3.69
6	PTH - Glutamine	Q, Gln	263.32	4.11	0	9.85
7	PTH - Glutamic acid	E, Glu	264.30	6.26	-1.62	4.42
8	PTH - Glycine	G, Gly	192.24	7.1	0.9	10.11
9	PTH - Histidine	H, His	272.33	2.23	0.6	6.43
10	PTH - Isoleucine	I, Ile	248.35	5.45	2.8	10.17
11	PTH - Leucine	L, Leu	248.35	9.06	2.8	10.17
12	PTH - Lysine	K, Lys	263.36	5.82	-1.88	10.09
13	PTH - Methionine	M, Met	266.38	2.27	2.04	9.84
14	PTH - Phenylalanine	F, Phe	282.36	3.91	3.08	10.11
15	PTH - Proline	P, Pro	232.30	5.12	1.09	
16	PTH - Serine	S, Ser	222.26	7.34	0.33	9.44
17	PTH - Threonine	T, Thr	236.29	5.96	0.68	9.87
18	PTH - Tryptophan	W, Trp	321.40	1.32	3.01	10.1
19	PTH - Tyrosine	Y, Tyr	298.36	3.25	2.35	9.93
20	PTH - Valine	V, Val	234.32	6.48	2.27	10.05

a: For charged residue at pH 7, Pow measured the distribution coefficient.
b: pKa value for side chain residue.

Table 5-3 Resolution response of PTH amino acids separations.

SDS concentration (mM)	Pentanol Concentration (mM)	Peaks Resolved	Log(r)
20	50	17	4.38
20	100	18	4.20
20	150	17	4.20
20	200	16	3.90
20	300	17	4.20
30	50	17	4.38
30	100	17	4.20
30	150	17	4.38
30	200	18	3.90
30	300	17	4.20
40	50	17	4.38
40	100	17	4.38
40	200	18	3.90
40	300	19	1.20
40	400	17	4.20
50	50	16	4.38
50	100	17	4.20
50	150	18	3.90
50	200	19	1.20
50	300	18	3.90

Table 5-4 Micelle–water partition coefficients and substituent constants for 20 PTH amino acids in various micellar systems

Amino acid	SDS		SDS/PeOH		SDS/HFIP		LiPFOS		LiPFOS/PeOH		LiPFOS/HFIP	
	log K_{mw}	**κ**	**log K_{mw}**	**κ**	**log K_{mw}**	**κ**	**log K_{mw}**	**κ**	**log K_{mw}**	**κ**	**log K_{mw}**	**κ**
A	1.93	0.27	1.50	0.21	1.51	0.27	1.35	0.24	1.34	0.24	1.36	0.21
C	2.00	0.34	1.82	0.53	1.54	0.30	1.96	0.85	1.79	0.70	1.88	0.72
D	2.00	0.34	1.85	0.57	1.65	0.42	1.39	0.28	1.68	0.58	1.88	0.73
E	1.95	0.30	1.74	0.45	1.49	0.26	1.57	0.46	1.72	0.63	1.83	0.68
F	2.94	1.28	2.34	1.05	2.31	1.07	2.22	1.11	1.89	0.80	1.78	0.62
G	1.66	0.00	1.29	0.00	1.23	0.00	1.11	0.00	1.09	0.00	1.15	0.00
H	2.73	1.07	2.28	1.00	2.10	0.87	2.32	1.21	1.34	0.24	1.74	0.59
I	2.80	1.14	2.20	0.92	2.20	0.96	2.11	1.00	1.89	0.80	1.90	0.75
K	3.33	1.67	2.39	1.10	2.58	1.34	3.41	2.30	1.93	0.84	2.04	0.89
L	2.80	1.14	2.21	0.92	2.20	0.97	2.15	1.04	1.86	0.76	1.90	0.75
M	2.45	0.79	1.88	0.59	2.08	0.85	1.64	0.53	1.48	0.38	1.67	0.52
N	1.46	-0.20	1.36	0.07	0.93	-0.30	1.11	0.00	0.93	-0.16	1.01	-0.14
P	2.43	0.78	1.78	0.49	1.36	0.13	1.94	0.83	1.54	0.44	1.68	0.53
Q	1.79	0.13	1.73	0.44	1.10	-0.13	1.27	0.16	1.22	0.13	1.15	0.00
R	4.25	2.59	2.69	1.41	3.34	2.11	3.98	2.87	2.22	1.13	2.64	1.49
S	1.37	-0.29	1.09	-0.20	0.86	-0.37	1.09	-0.02	0.91	-0.18	0.92	-0.23
T	1.37	-0.29	1.14	-0.15	0.86	-0.37	1.09	-0.02	1.02	-0.08	1.01	-0.14
V	2.40	0.74	1.90	0.62	1.81	0.58	1.90	0.79	1.62	0.53	1.68	0.53
W	2.86	1.20	2.14	0.86	2.14	0.90	1.99	0.88	1.83	0.74	1.47	0.32
Y	2.24	0.58	1.84	0.55	1.86	0.63	1.90	0.79	1.33	0.23	1.24	0.09

Table 5-5 Free energy of transfer (kcal/mol) of 20 PTH amino side chains from micellar phases to aqueous phase

	(1) SDS	**(2) SDS PeOH**	**(3) SDS HFIP**	**(4) LiPFOS**	**(5) LiPFOS PeOH**	**(6) LiPFOS HFIP**
Amino acid	**ΔΔG (kcal/mol)**	**ΔΔG (kcal/mol)**	**ΔΔG (kcal/mol)**	**ΔΔG (kcal/mol)**	**ΔΔG (kcal/mol)**	**ΔΔG (kcal/mol)**
A	0.36	0.29	0.37	0.33	0.33	0.29
C	0.47	0.73	0.41	1.16	0.95	0.99
D	0.47	0.77	0.57	0.38	0.79	0.99
E	0.40	0.62	0.35	0.63	0.86	0.92
F	1.74	1.44	1.46	1.52	1.09	0.85
G	0.00	0.00	0.00	0.00	0.00	0.00
H	1.46	1.36	1.18	1.65	0.33	0.80
I	1.55	1.25	1.31	1.37	1.09	1.02
K	2.27	1.50	1.83	3.14	1.14	1.21
L	1.55	1.26	1.32	1.42	1.04	1.02
M	1.08	0.81	1.15	0.72	0.52	0.71
N	-0.27	0.10	-0.41	0.00	-0.22	-0.19
P	1.06	0.67	0.17	1.14	0.61	0.72
Q	0.18	0.60	-0.18	0.22	0.18	0.00
R	3.53	1.92	2.87	3.91	1.53	2.03
S	-0.40	-0.27	-0.51	-0.03	-0.25	-0.31
T	-0.40	-0.20	-0.51	-0.03	-0.11	-0.19
V	1.01	0.84	0.79	1.08	0.72	0.72
W	1.63	1.17	1.23	1.20	1.01	0.44
Y	0.79	0.75	0.86	1.08	0.32	0.12

Table 5-6 Free energy of transfer (kcal/mol) of 20 PTH amino acid side chains from various condensed phases to aqueous phase.

Amino acid	**(7) SDS[a]** ΔΔG (kcal/mol)	**(8) SDS HexOH[a]** ΔΔG (kcal/mol)	**(9) Liposome[a]** ΔΔG (kcal/mol)	**(10) Octanol FP[b]** ΔΔG (kcal/mol)	**(11) POPC[c]** ΔΔG (kcal/mol)	**(12) Octanol W[d]** ΔΔG (kcal/mol)	**(13) Chothia[e]** ΔΔG (kcal/mol)	**(14) Janin[f]** ΔΔG (kcal/mol)
A	0.61	0.51	0.27	0.42	-0.17	-0.14	0.05	0
C	2.42	2.02	1.92	2.09	0.24	0.22	0.34	0.6
D	0.72	0.83	-0.23	-1.05	-1.23	-0.26	-0.68	-0.9
E	0.65	0.81	-0.04	-0.87	-2.02	-0.02	-0.56	-1
F	1.95	1.71	1.82	2.44	1.13	1.67	0.34	0.2
G	0	0	0	0	0	0	0	0
H	1.48	0.83	0.58	0.18	-0.17	-0.09	-0.6	-0.4
I	1.77	1.55	1.48	2.46	0.31	1.15	0.58	0.4
K	2.47	1.82	2.34	-1.35	-0.47	1.48	-1.71	-2.1
L	1.77	1.54	1.51	2.32	0.56	1.28	0.22	0.2
M	1.3	1.06	1.09	1.68	0.23	0.7	0.1	0.1
N	-0.03	-0.04	-0.27	-0.82	-0.42	-0.71	-0.84	-0.8
P	1.23	0.99	0.76	0.98	-0.45	-0.11	-0.56	-0.6
Q	0.42	0.31	-0.23	-0.3	-0.58	-0.71	-1.19	-1
R	3.63	2.43	2.19	-1.37	-0.33	1.98	-2.37	-1.7
S	0.07	0.06	0.08	-0.05	-0.13	-0.16	-0.41	-0.4
T	0.3	0.21	0.23	0.35	-0.14	-0.06	-0.37	-0.5
V	1.27	1.1	0.99	1.66	-0.07	0.6	0.43	0.3
W	1.85	1.64	2.42	3.07	1.85	1.95	-0.25	0
Y	1	0.86	1.3	1.31	0.94	0.66	-0.68	-0.7
A	0.61	0.51	0.27	0.42	-0.17	-0.14	0.05	0

Note: a: Ref [24], b: Ref. [31], c: Ref. [27], d: Ref. [28] e: Ref [26], f: Ref. [29]; e and f measure the free energy of transfer amino acids residues from the interior to the surface of proteins.

Table 5-7 Solvation energy of methylene group in amino acid side chains from condensed phases to aqueous phases and comparison with those obtained from alkyl benzene homologous series.

	(1) SDS	**(2) SDS / PeOH**	**(3) SDS / HFIP**	**(4) LiPFOS**	**(5) LiPFOS / PeOH**	**(6) LiPFOS / HFIP**
Slope	0.375	0.307	0.305	0.359	0.246	0.248
R^2	0.991	0.993	0.967	0.999	0.988	0.996
$\Delta\Delta G$ ($-CH_2-$) (kcal/mol) [a]	0.573	0.561	0.542	0.478	0.497	0.416

a: Obtained with alkyl benzenes as probe molecules.

Table 5-7 Continued.

	(9) Liposome	**(10) Octanol FP**	**(11) POPC**	**(12) Octanol W**	**(13) Chothia**	**(14) Janin**
Slope	0.374	0.588	0.122	0.330	0.082	0.07
R^2	0.987	0.995	0.463	0.864	0.594	0.726

Table 5-8 Correlation matrix of free energy of transfer of amino acid residues among various condensed phases.

Condensed Phases	**1**	**2**	**3**	**4**	**5**	**6**	**7**	**8**	**9**	**10**	**11**	**12**	**13**	**14**
1	1.00													
2	0.94	1.00												
3	0.97	0.94	1.00											
4	0.95	0.88	0.91	1.00										
5	0.85	0.87	0.85	0.79	1.00									
6	0.85	0.86	0.85	0.84	0.92	1.00								
7	0.91	0.88	0.89	0.92	0.88	0.87	1.00							
8	0.86	0.87	0.86	0.84	0.94	0.87	0.97	1.00						
9	0.79	0.75	0.79	0.78	0.76	0.61	0.89	0.90	1.00					
10	0.11	0.18	0.13	-0.07	0.23	-0.02	0.21	0.33	0.48	1.00				
11	0.26	0.23	0.28	0.13	0.13	-0.11	0.29	0.32	0.61	0.78	1.00			
12	0.84	0.76	0.85	0.75	0.78	0.62	0.80	0.82	0.91	0.41	0.58	1.00		
13	-0.36	-0.25	-0.30	-0.51	-0.16	-0.31	-0.25	-0.13	-0.04	0.78	0.45	-0.08	1.00	
14	-0.25	-0.18	-0.19	-0.41	-0.07	-0.20	-0.12	-0.01	0.06	0.83	0.51	0.01	0.94	1.00

FIGURE CAPTIONS

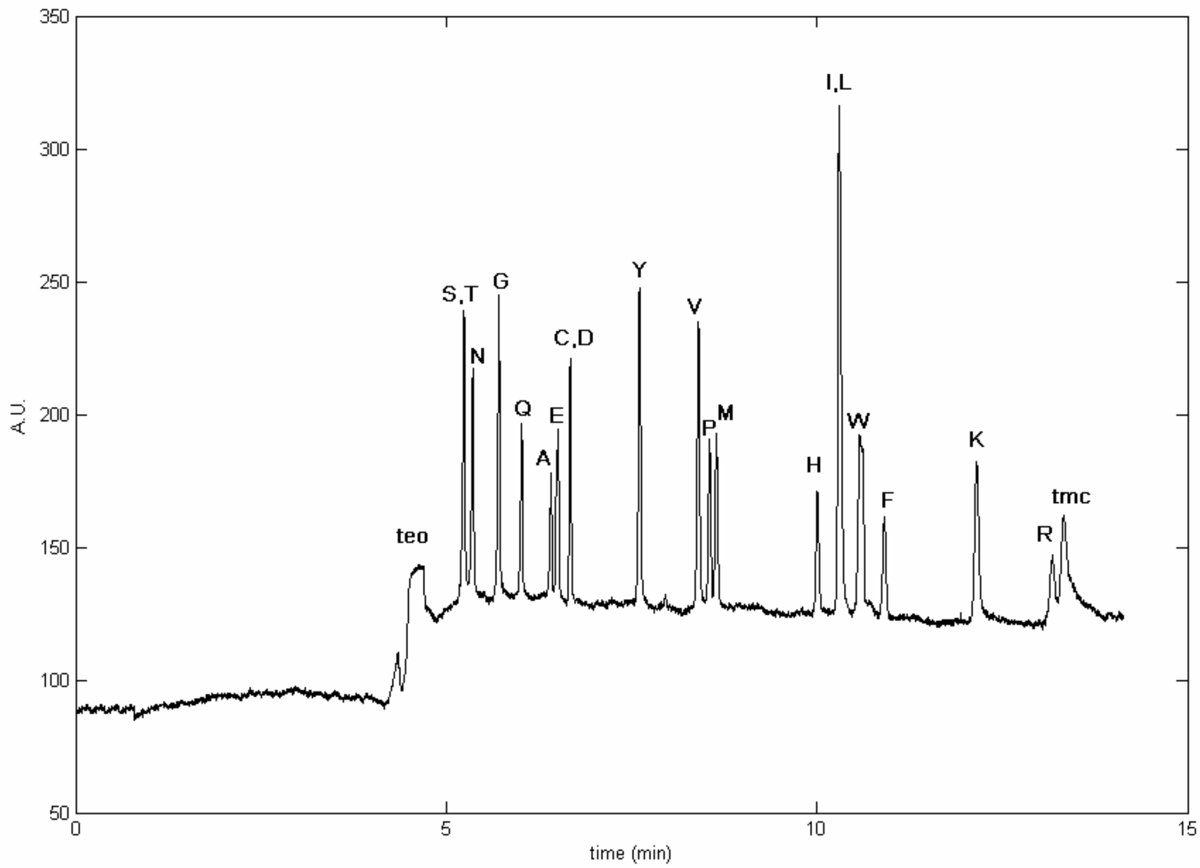

Figure 5-1 Chromatogram of 20 PTH Amino Acid in 40 mM SDS. Running buffer: 20 mM Phosphate at pH 7.0, applied voltage with 20 kv and detector wavelength at 254 nm. The peaks are identified with one letter abbreviation for amino acids.

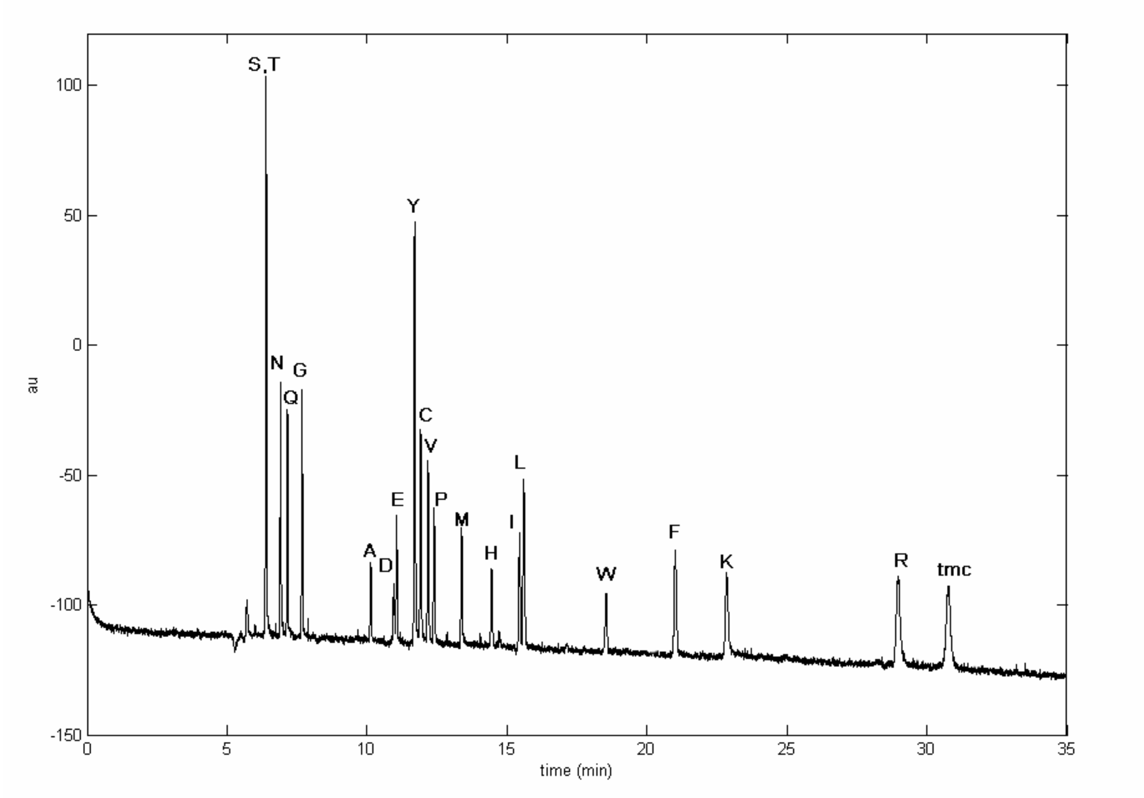

Figure 5-2 Chromatogram of 20 PTH amino acids separation in 80 mM SDS. (Other chromatographic conditions are the same as those in Figure 5-1)

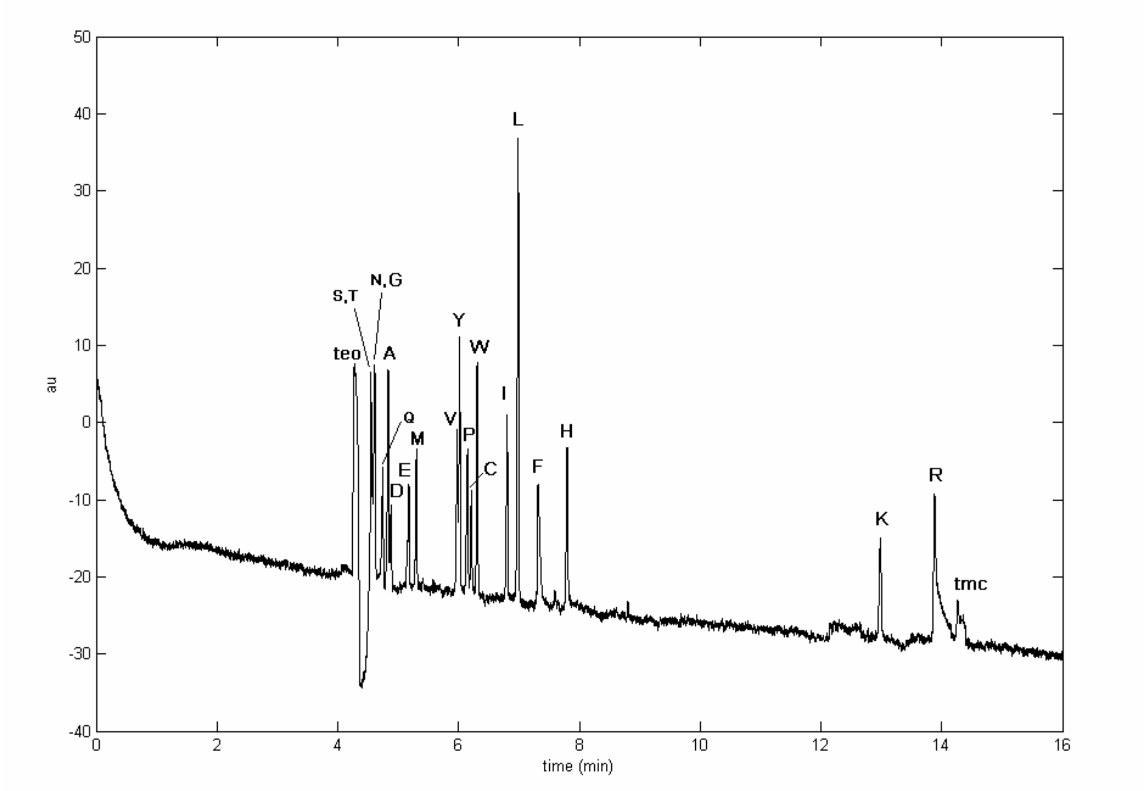

Figure 5-3 Chromatogram of 20 PTH amino acids separation in 40 mM LiPFOS.

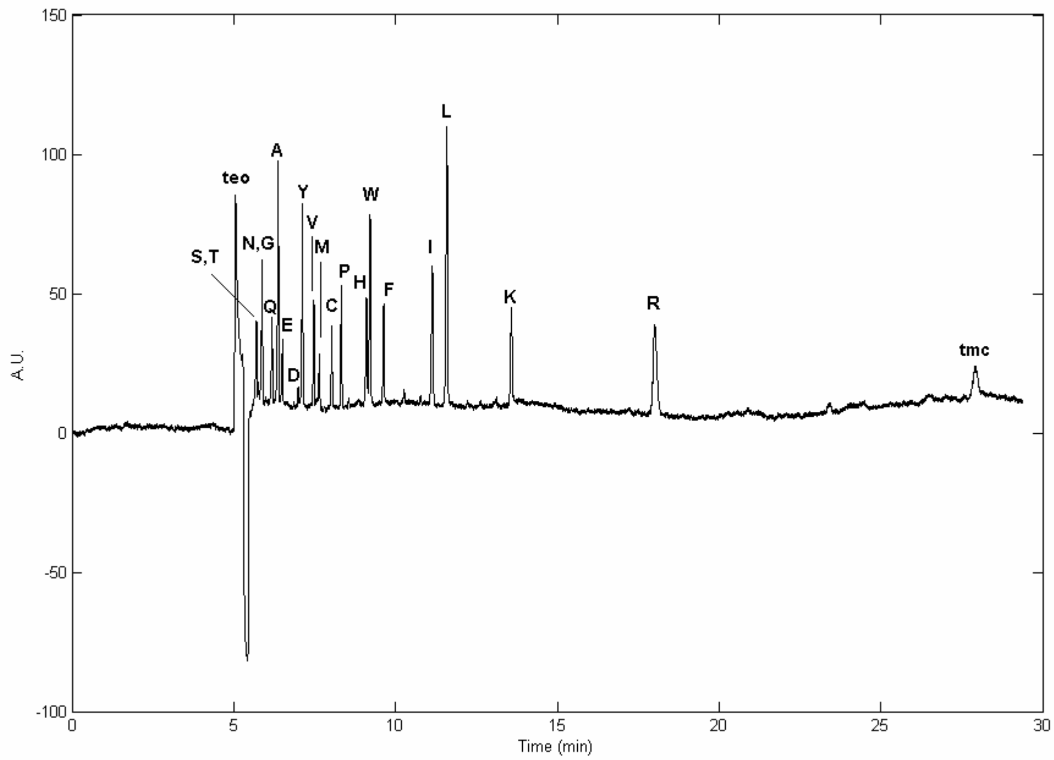

Figure 5-4 Chromatogram of 20 PTH amino acids separation in 60 mM LiPFOS.

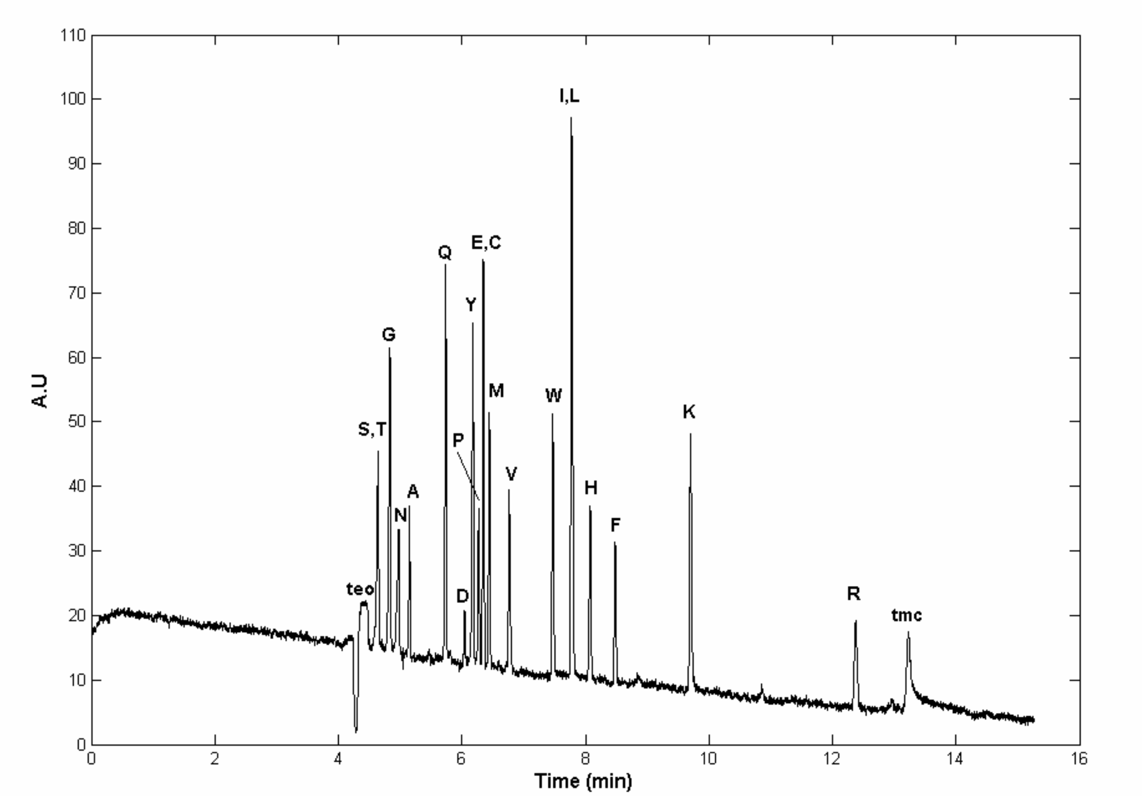

Figure 5-5 Chromatogram of 20 PTH amino acids separation in 20 mM SDS and 50 mM pentanol.

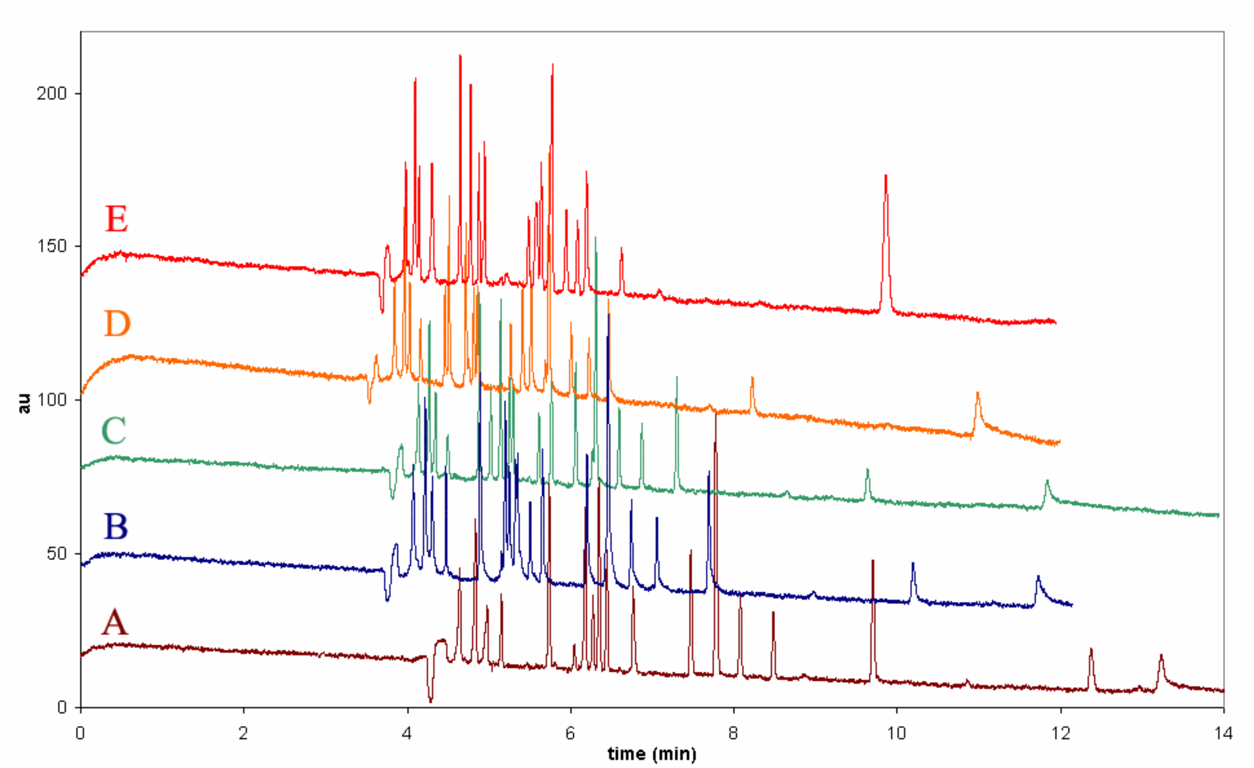

Figure 5-6 Modification effects of pentanol on the separation of PTH amino acids in 20 mM SDS. A) 50 mM Pentanol, B) 100 mM Pentanol, C) 150 mM Pentanol, D) 200 mM Pentanol, E) 300 mM Pentanol.

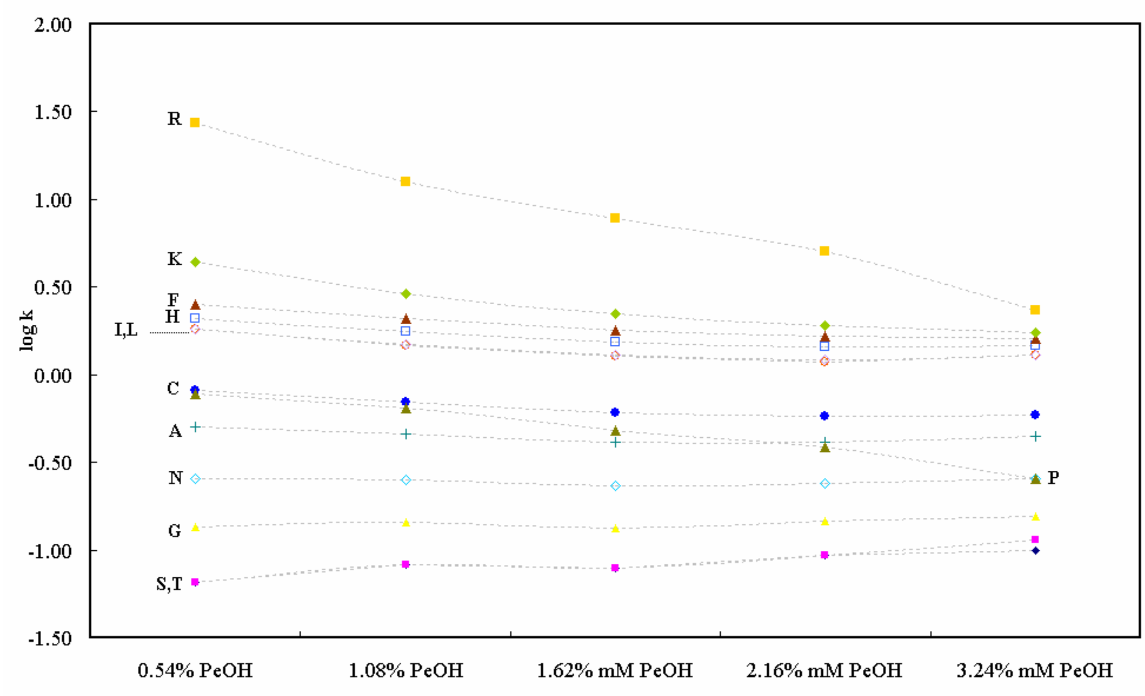

Figure 5-7 Effect of pentanol concentration on the retention factor of PTH amino acids with 20 mM SDS (For clarity reason, only portion of 20 PTH amino acids show in the graph)

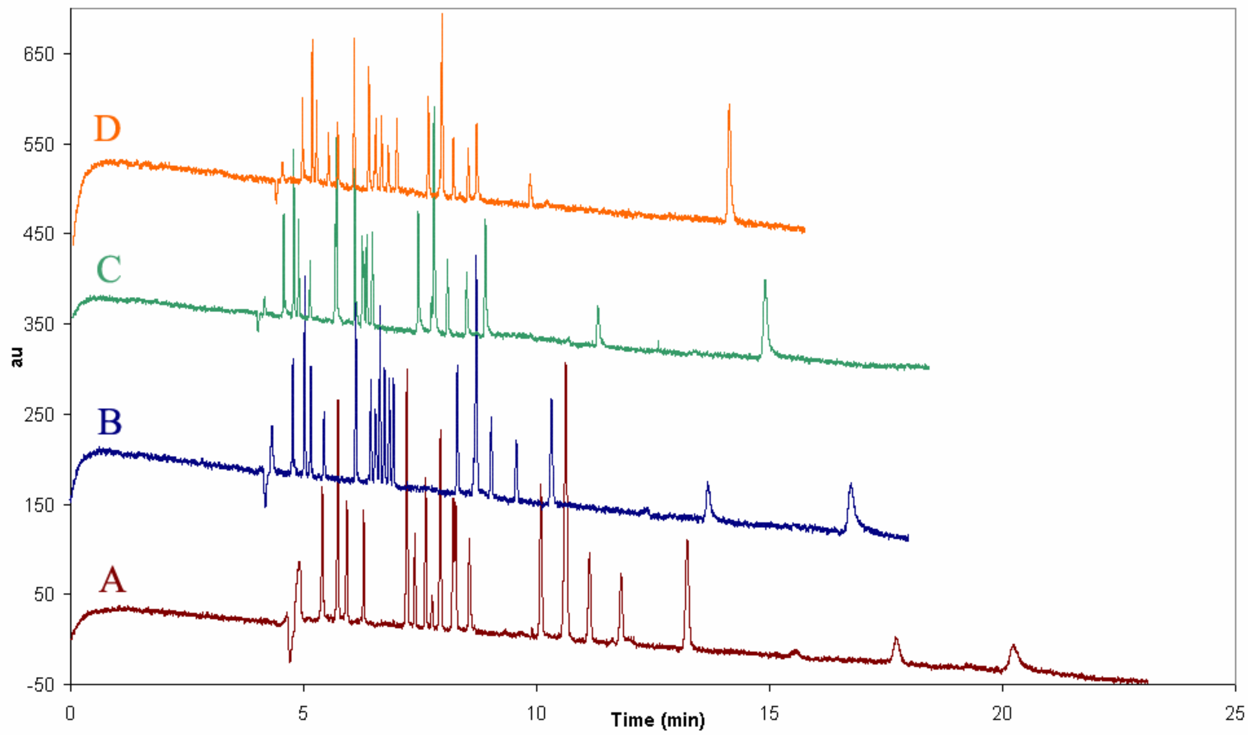

Figure 5-8 Modification effects of pentanol on the separation of PTH amino acids in 30 mm SDS. A) 100 mM Pentanol, B) 150 mM Pentanol, C) 200 mM Pentanol, D) 300 mM Pentanol.

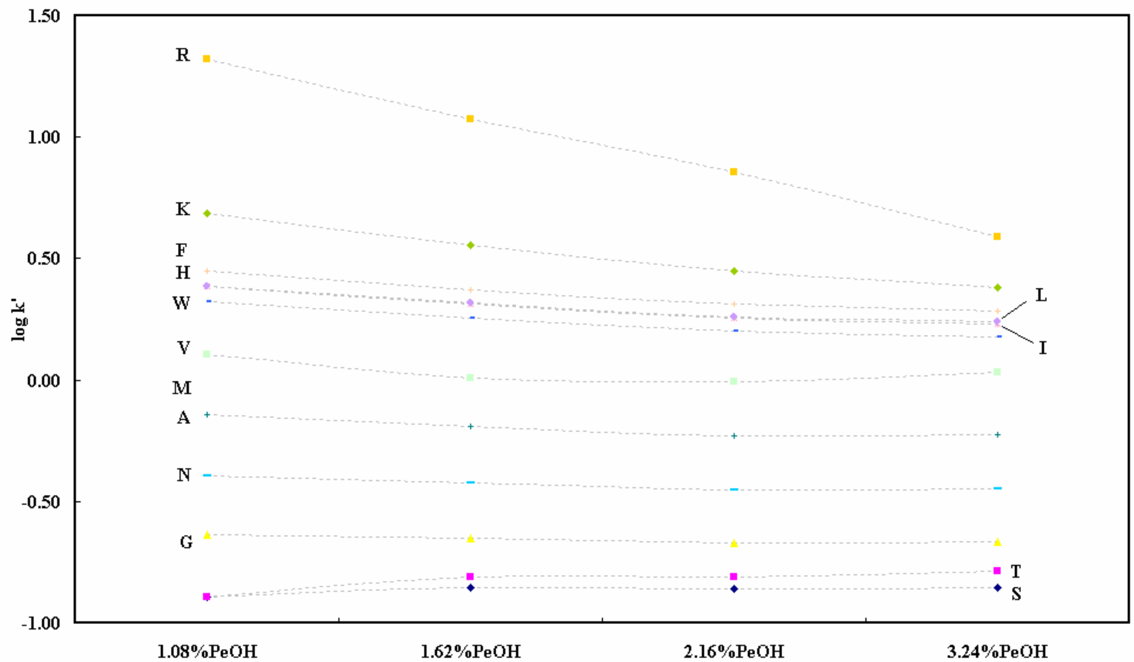

Figure 5-9 Effects of pentanol concentration on the retention factor of PTH amino acids with 30 mM SDS. (For clarity reason, only portion of 20 PTH amino acids show in the graph)

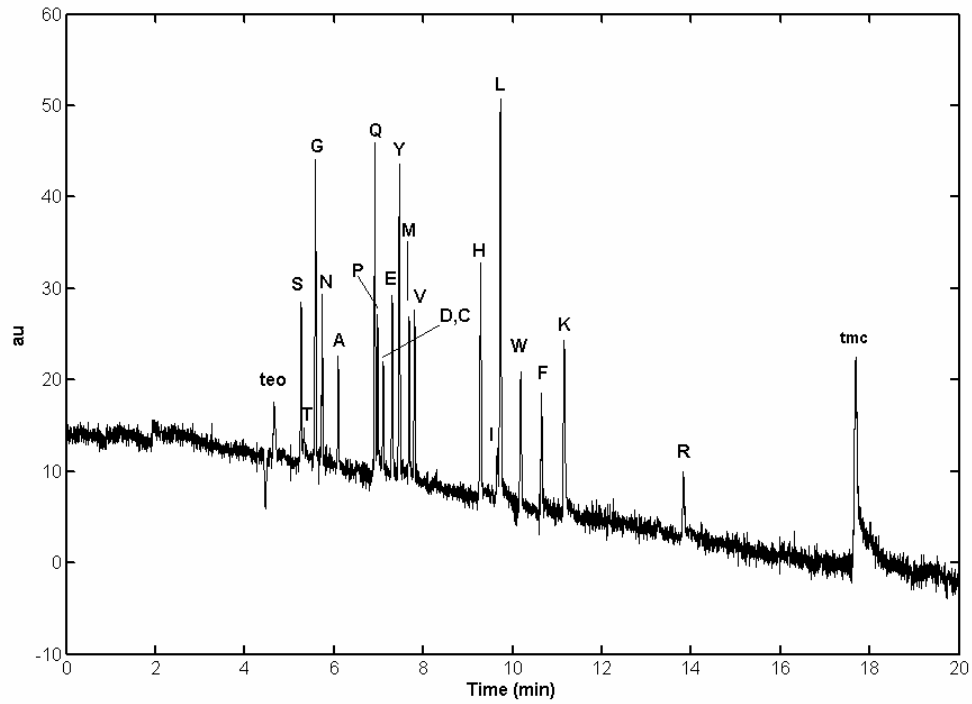

Figure 5-10 Chromatogram of 20 PTH amino acids separation in 40 mM SDS and 200 mM pentanol

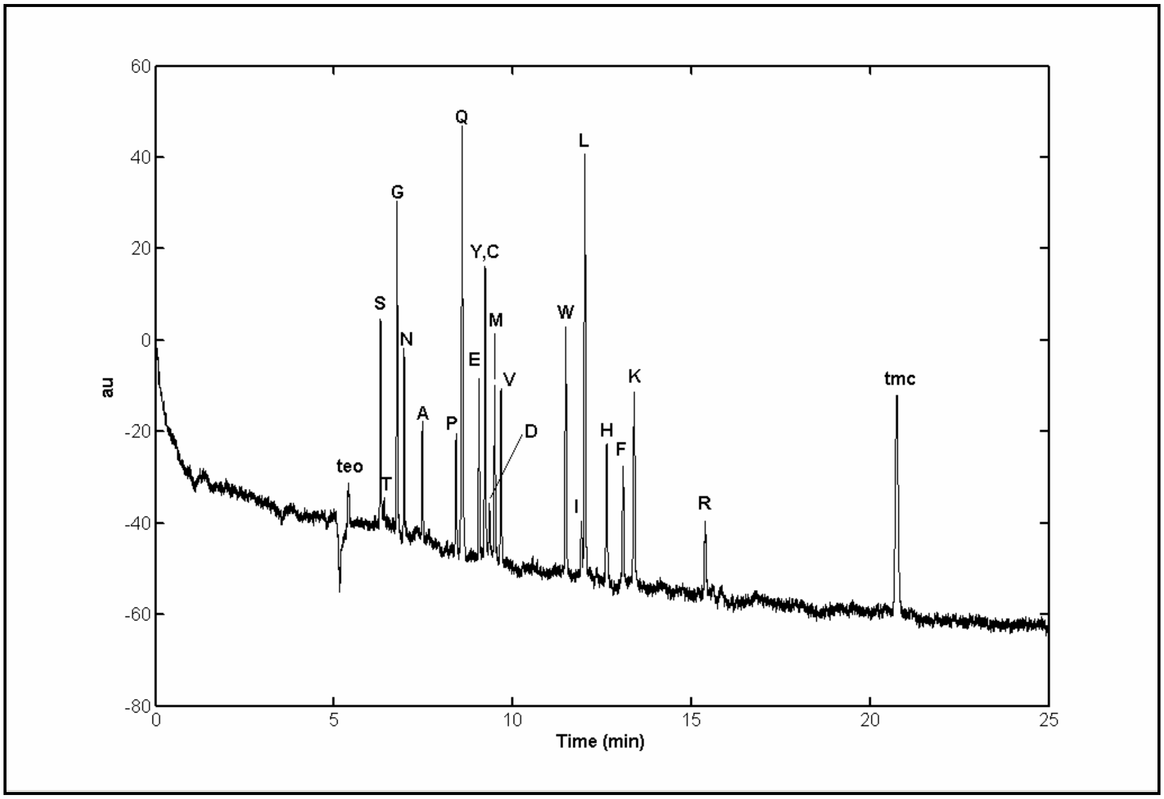

Figure 5-11 Chromatogram of 20 PTH amino acids separation in 50 mM SDS and 300 mM pentanol

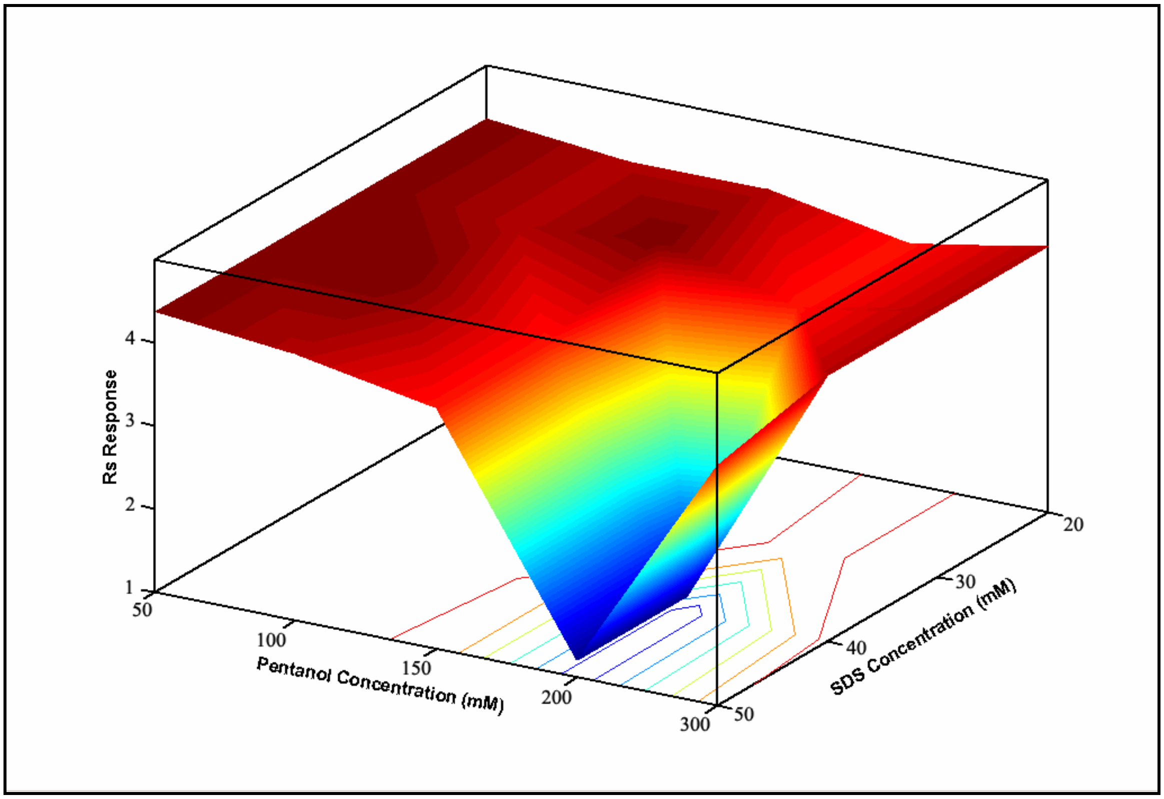

Figure 5-12 Optimization of resolution response of 20 PTH amino acids as a function of concentration of SDS and pentanol.

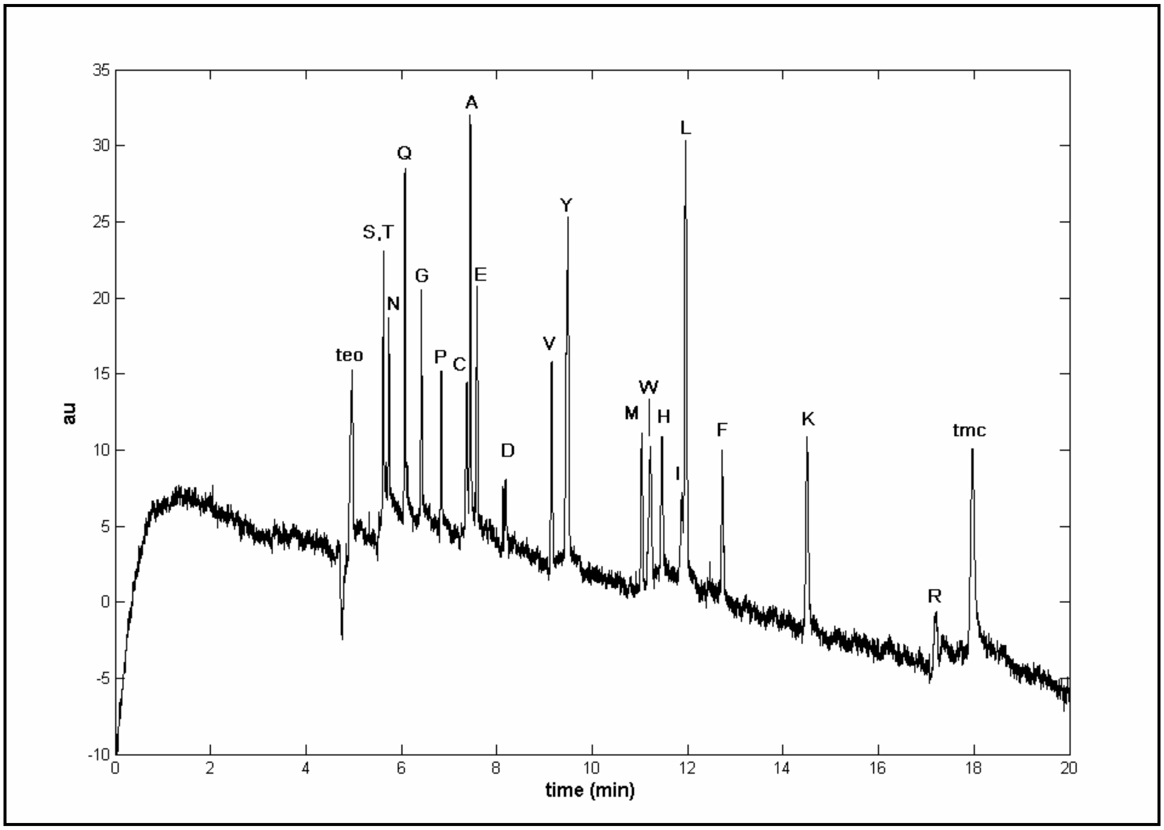

Figure 5-13 Chromatogram of 20 PTH amino acids separation in 40 mM SDS and 400 mM HFIP

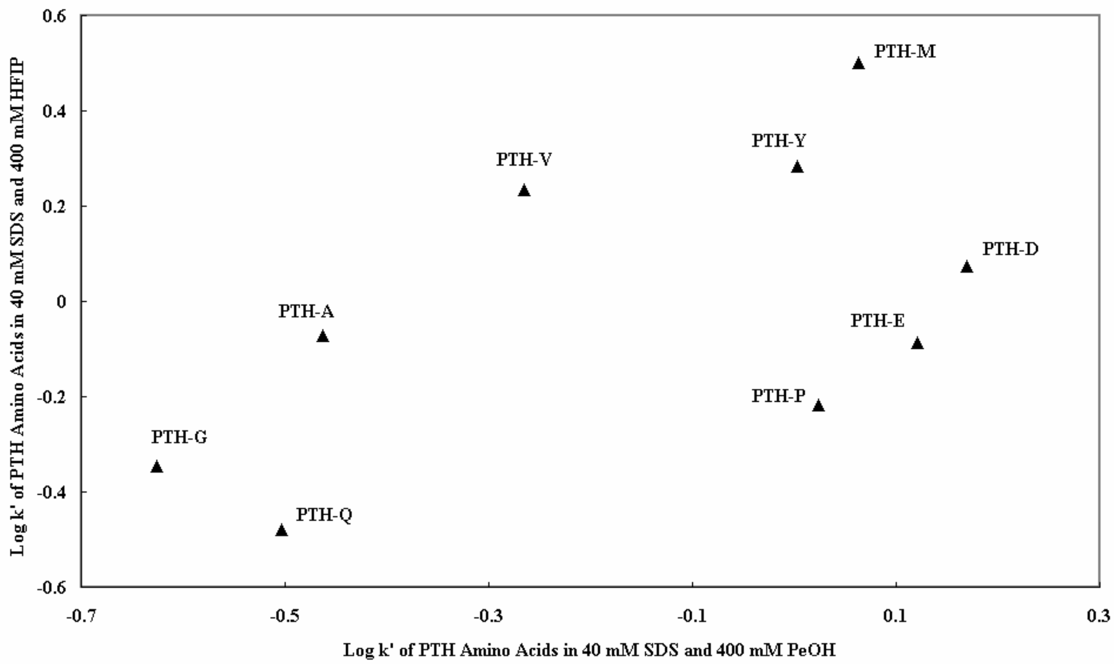

Figure 5-14 Elution order alterations of moderate hydrophobic PTH amino acids in PeOH and HFIP modified SDS micelles.

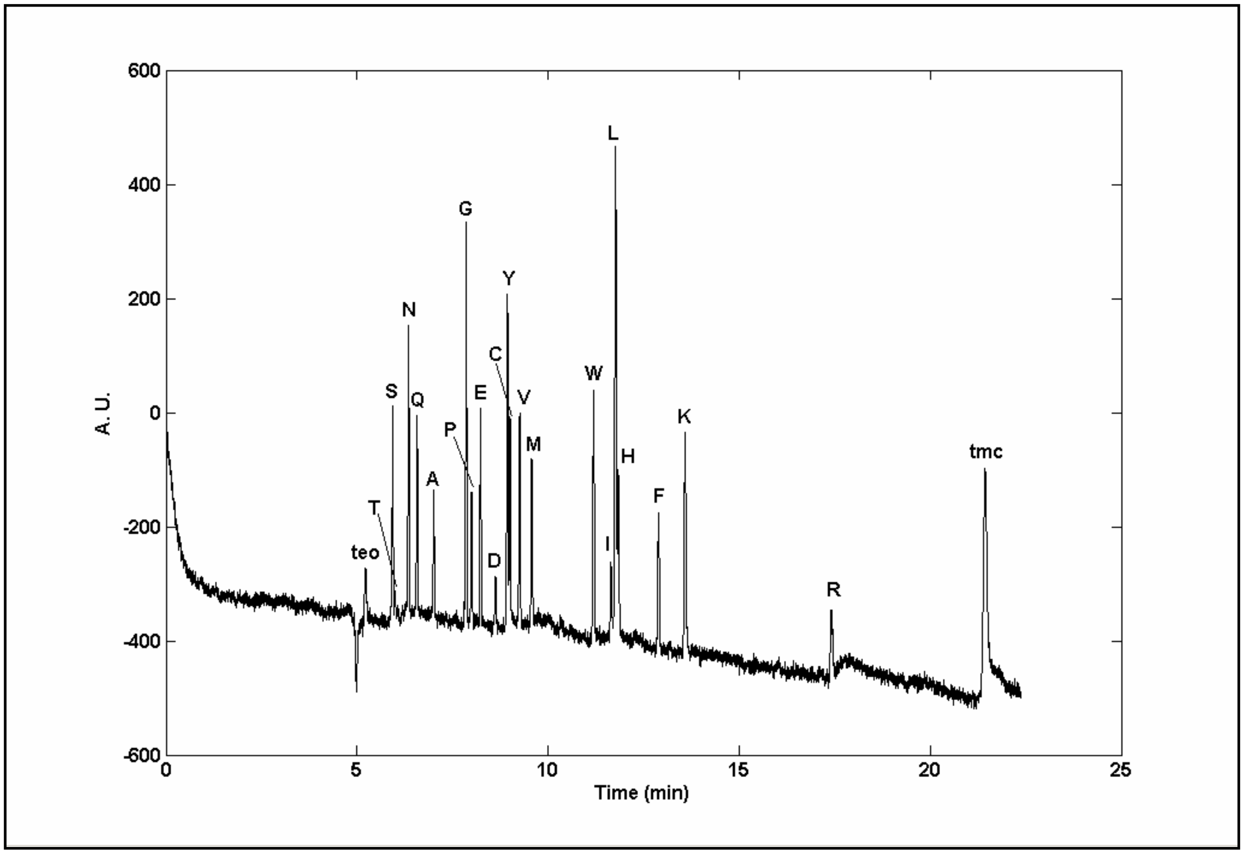

Figure 5-15 Chromatogram of 20 PTH amino acids separation in 40 mM SDS with the modification of both 200 mM PeOH and 200 mM HFIP

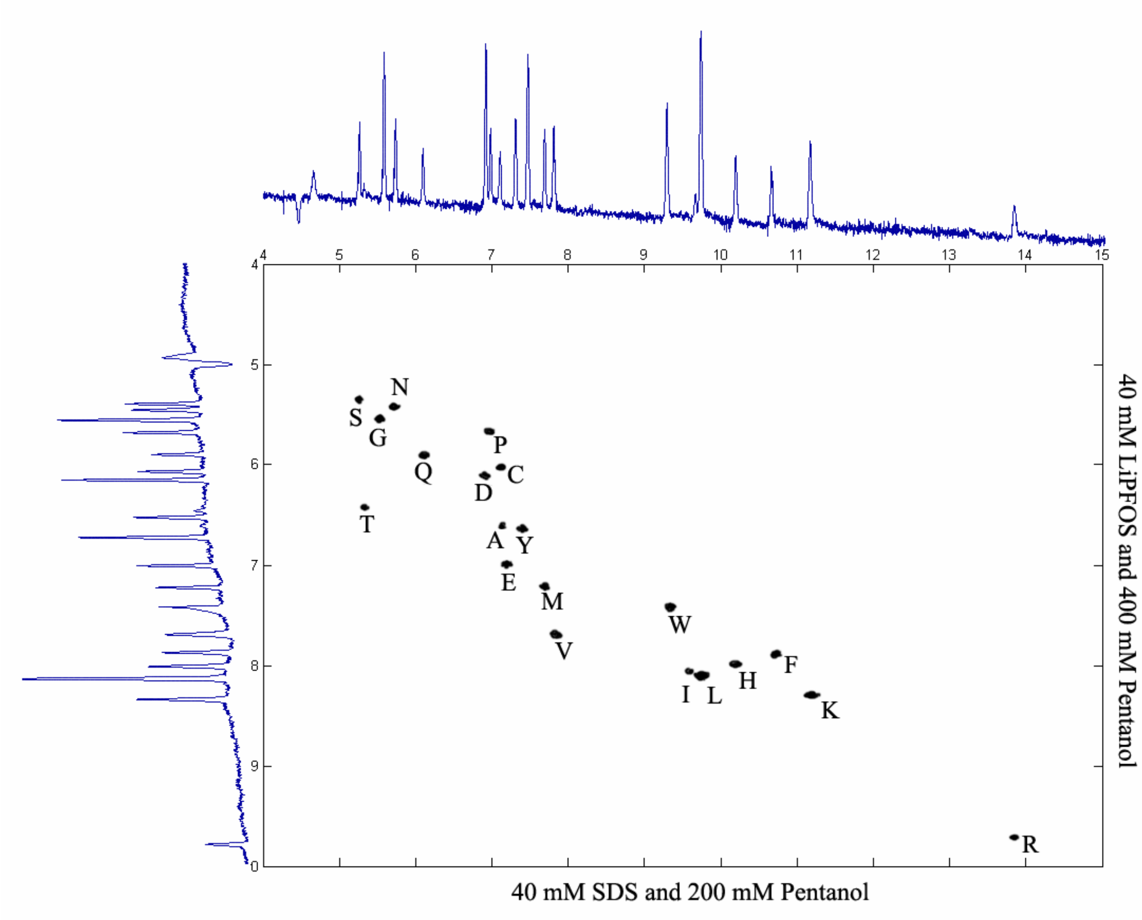

Figure 5-16 Complete resolution of 20 PTH amino acids in a semi–2D separation using micelle systems: 40 mM SDS with 200 mM pentanol Vs. 40 mM LiPFOS with 400 mM pentanol

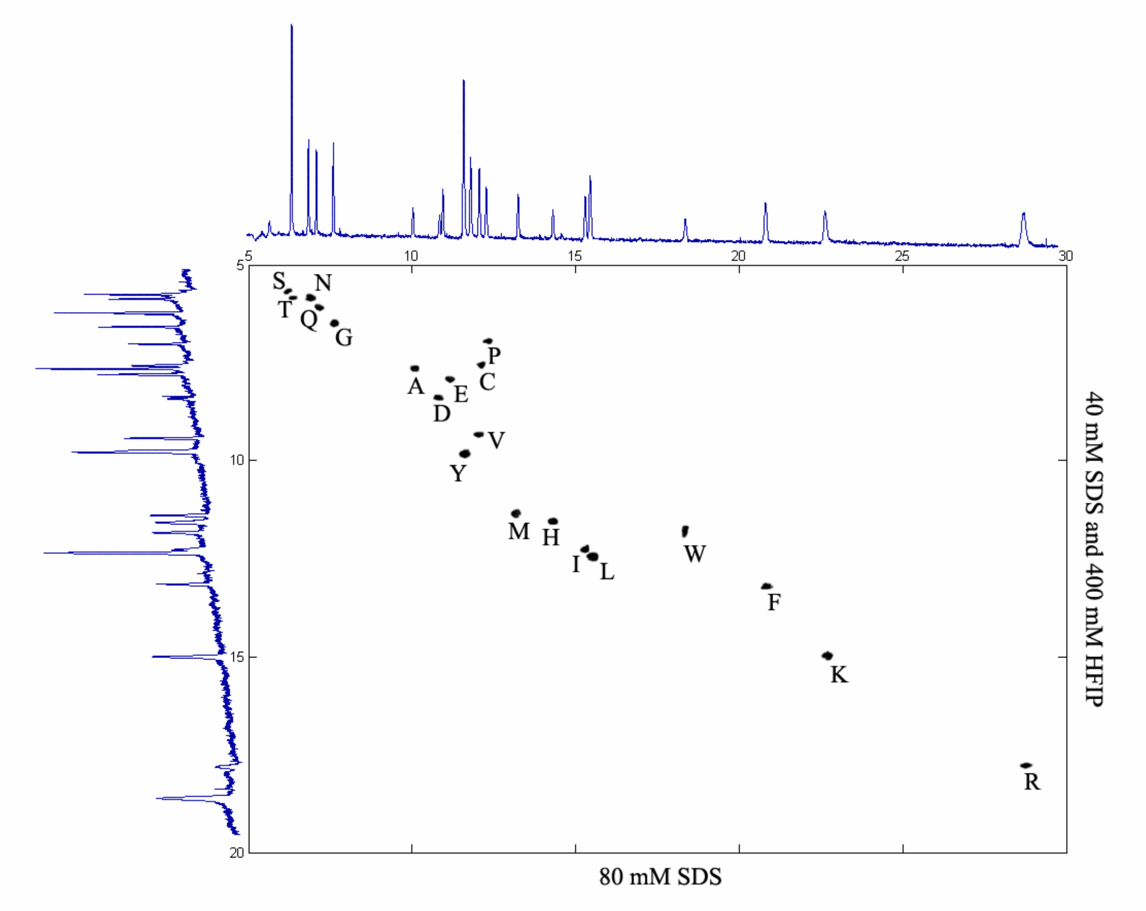

Figure 5-17 Complete resolution of 20 PTH amino acids in a semi–2D separation using micelle systems: 80 mM SDS Vs. 40 mM SDS with 400 mM HFIP

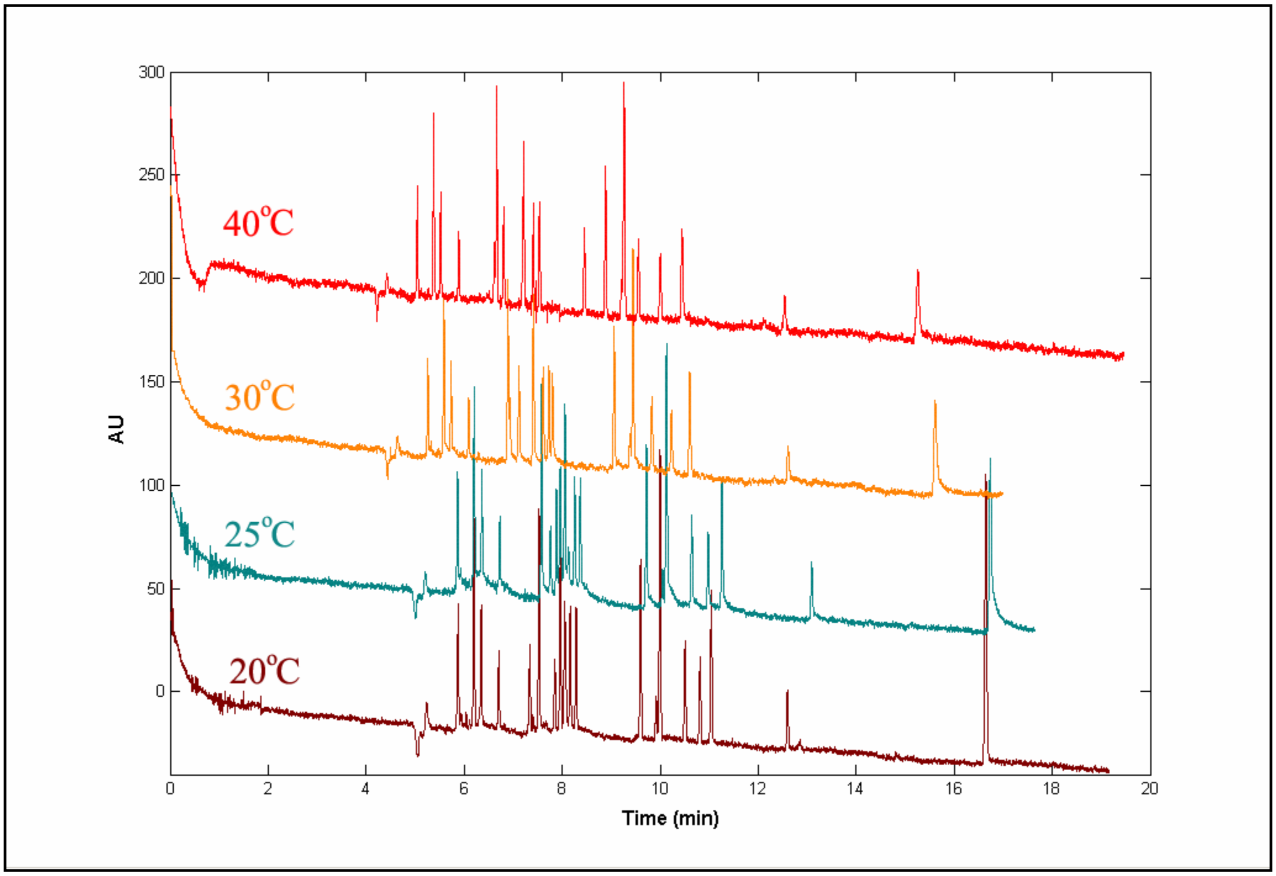

Figure 5-18 Temperature effects on the PTH amino acids separation in pentanol-modified SDS micelles.

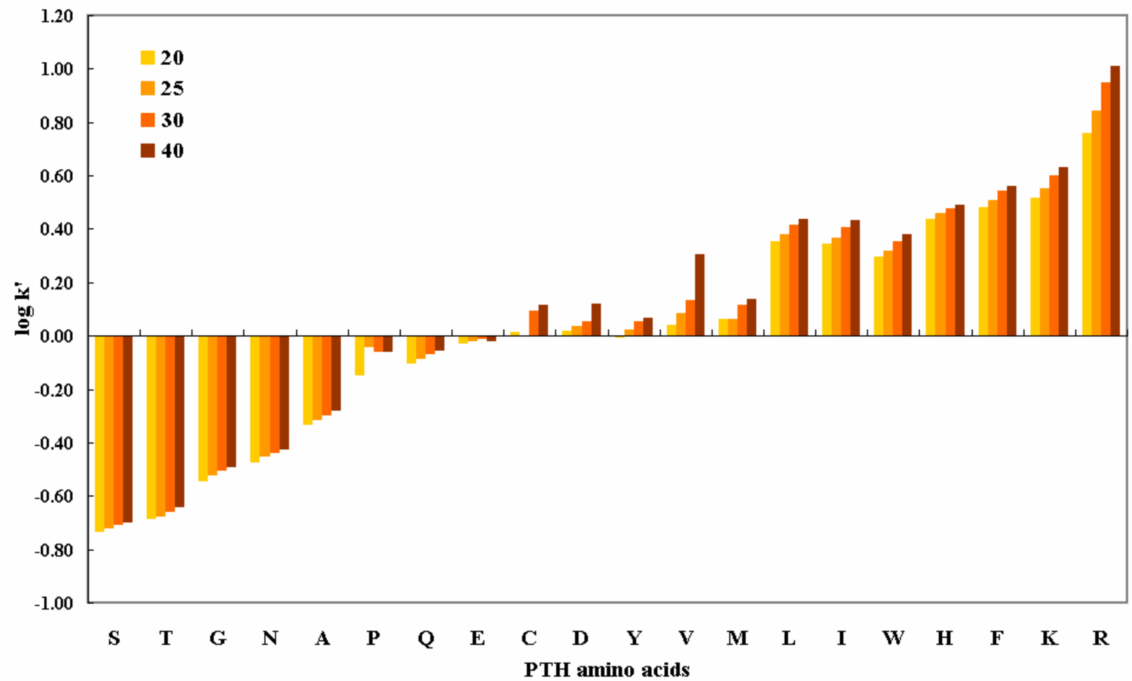

Figure 5-19 Temperature effects on the retention factors of PTH amino acids in pentanol-modified SDS Micelles.

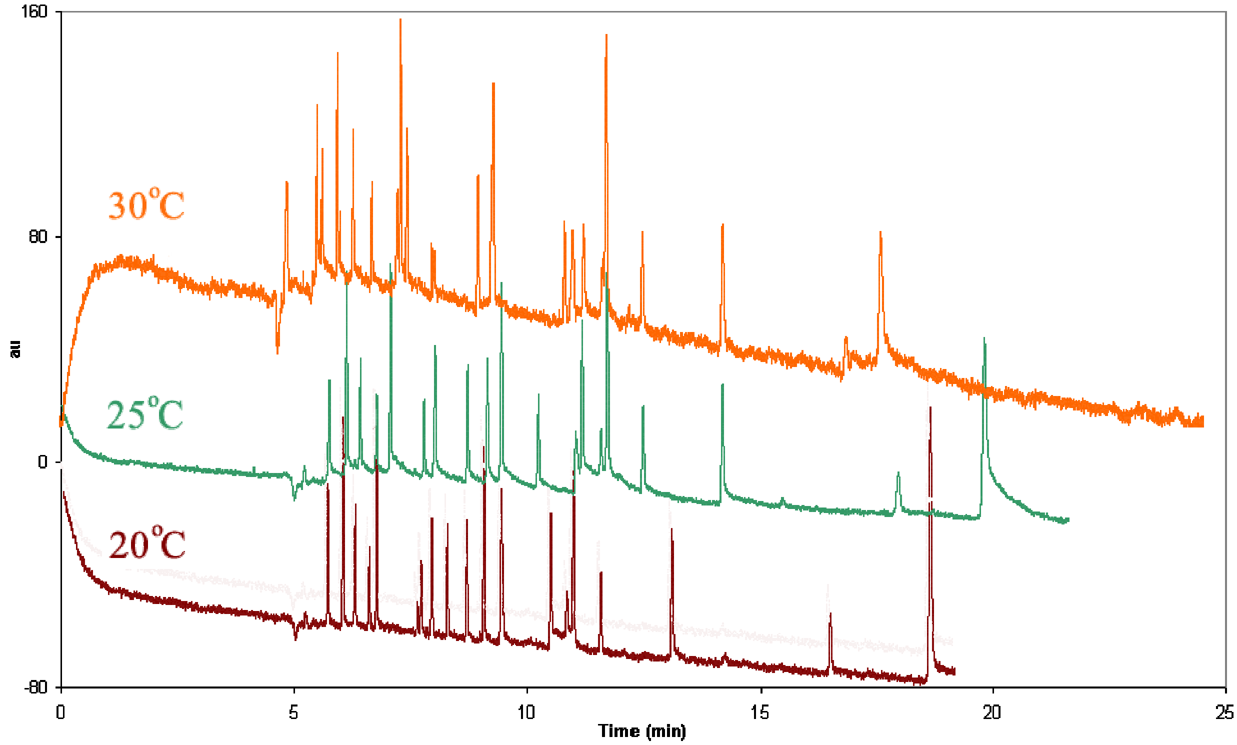

Figure 5-20 Temperature effects on the PTH amino acids separation in HFIP-modified SDS Micelles.

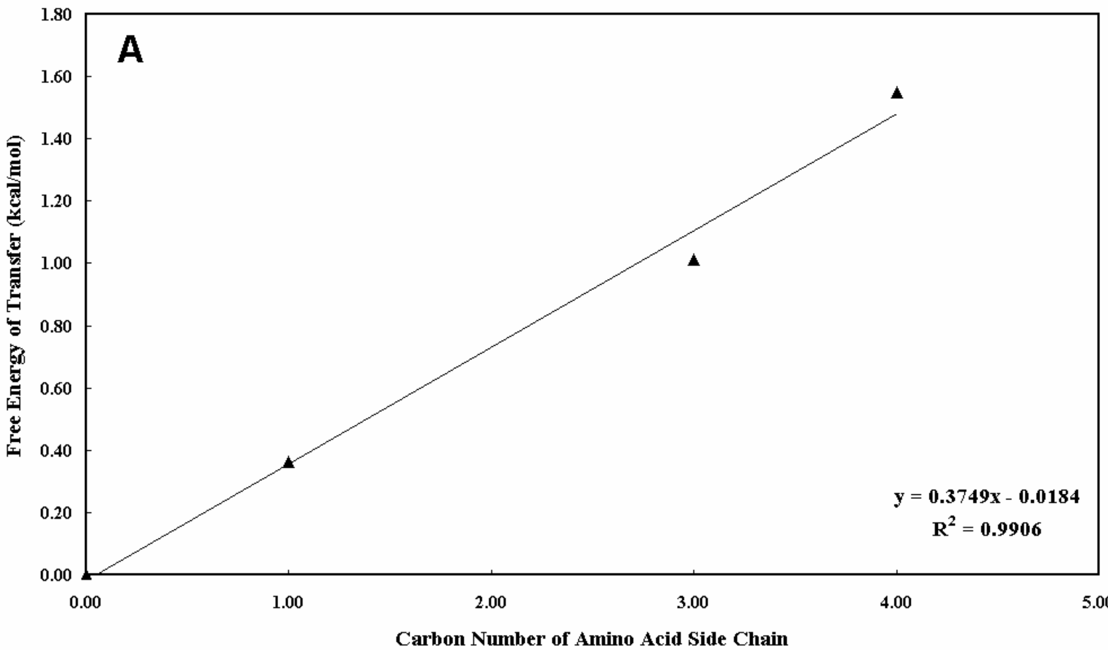
A
Free Energy of Transfer (kcal/mol)
Carbon Number of Amino Acid Side Chain
y = 0.3749x - 0.0184
R2 = 0.9906

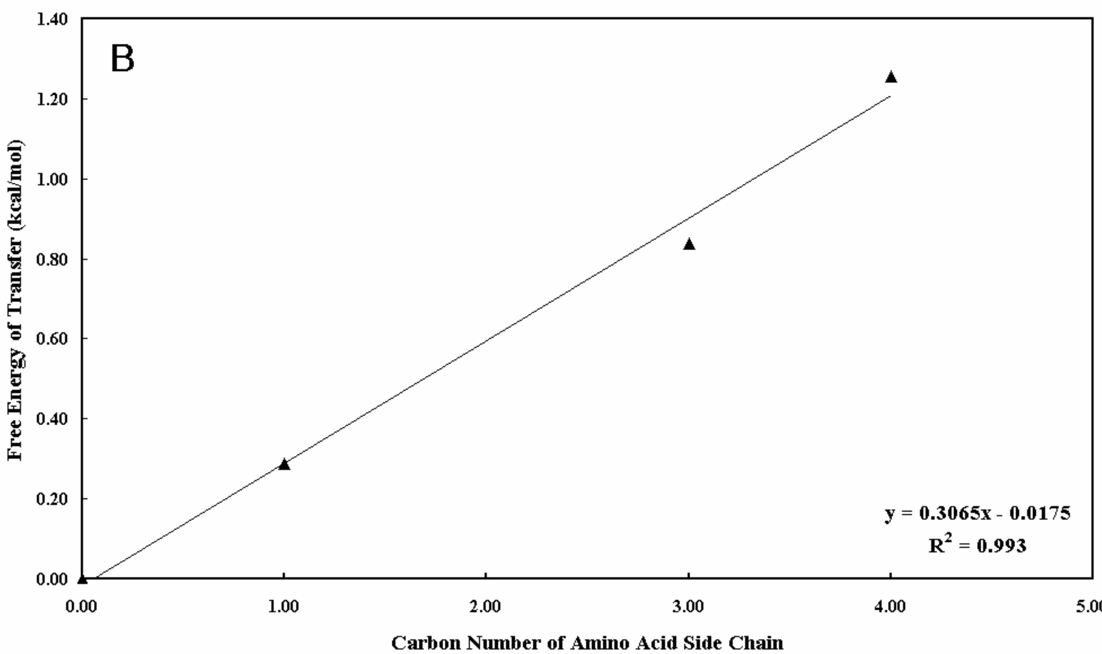
B
Free Energy of Transfer (kcal/mol)
Carbon Number of Amino Acid Side Chain
y = 0.3065x - 0.0175
R2 = 0.993

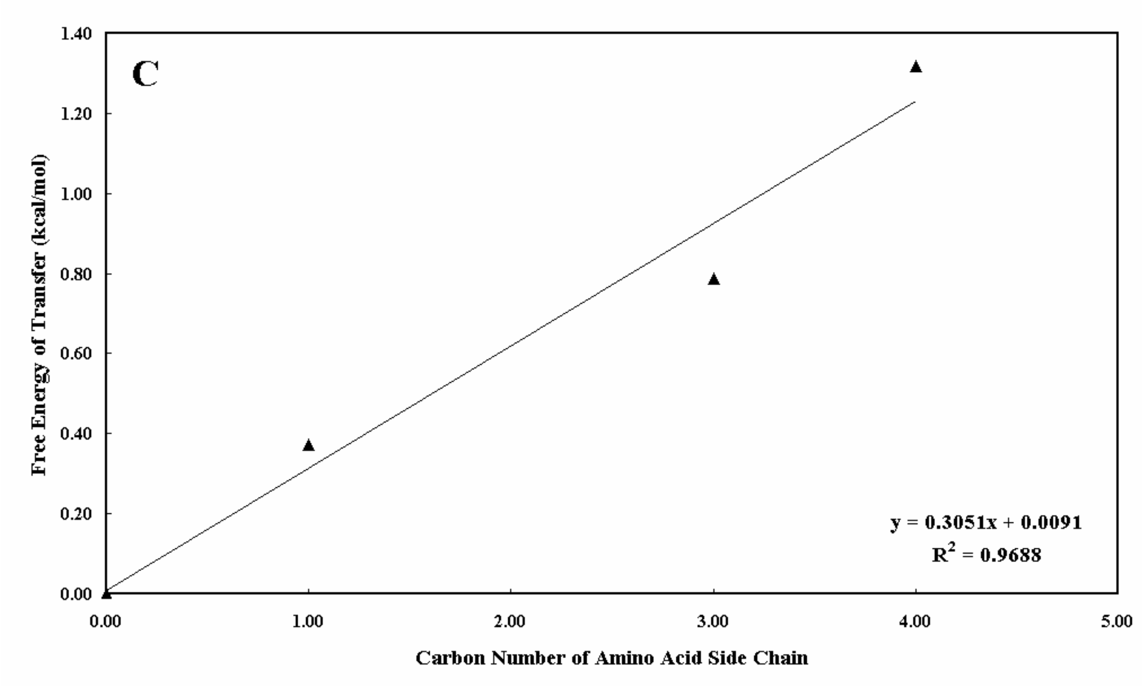
C
Free Energy of Transfer (kcal/mol)
Carbon Number of Amino Acid Side Chain
y = 0.3051x + 0.0091
R2 = 0.9688
1.40
1.20
1.00
0.80
0.60
0.40
0.20
0.00
0.00
1.00
2.00
3.00
4.00
5.00

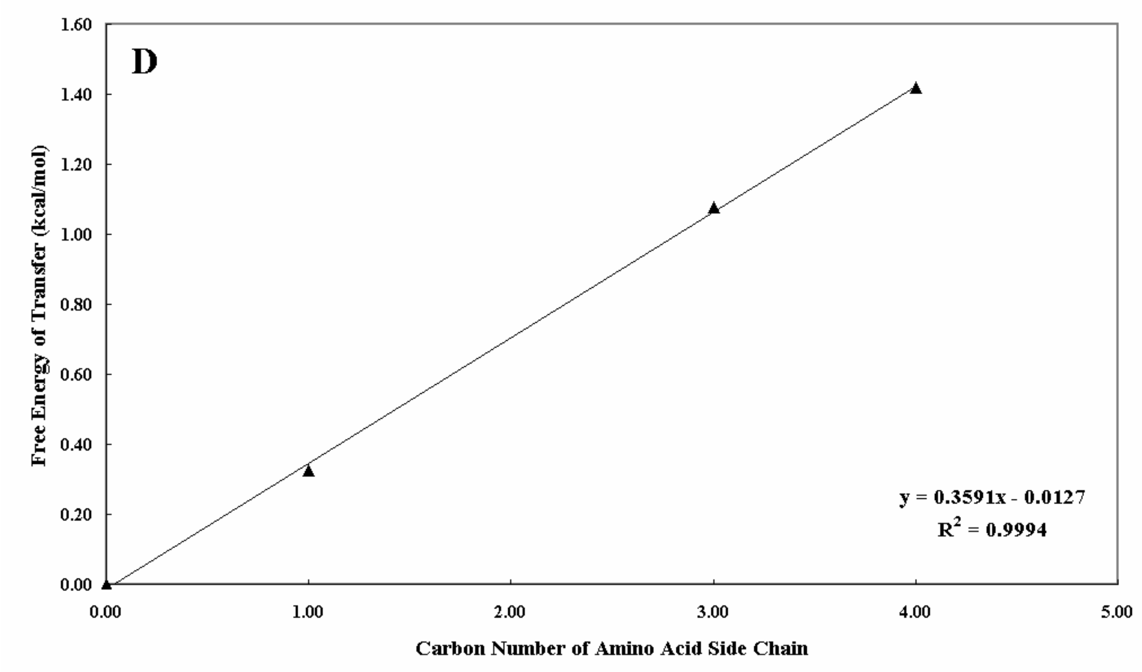
D
Free Energy of Transfer (kcal/mol)
Carbon Number of Amino Acid Side Chain
y = 0.3591x - 0.0127
R2 = 0.9994
1.60
1.40
1.20
1.00
0.80
0.60
0.40
0.20
0.00
0.00
1.00
2.00
3.00
4.00
5.00

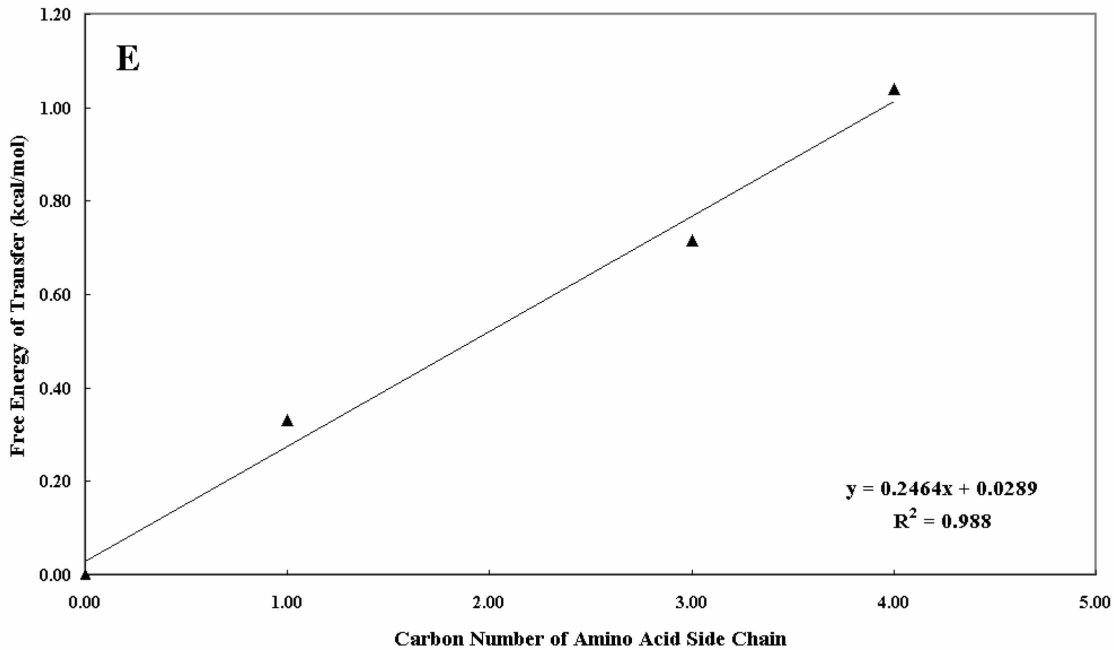
E
Free Energy of Transfer (kcal/mol)
Carbon Number of Amino Acid Side Chain
y = 0.2464x + 0.0289
R2 = 0.988
1.20
1.00
0.80
0.60
0.40
0.20
0.00
0.00
1.00
2.00
3.00
4.00
5.00

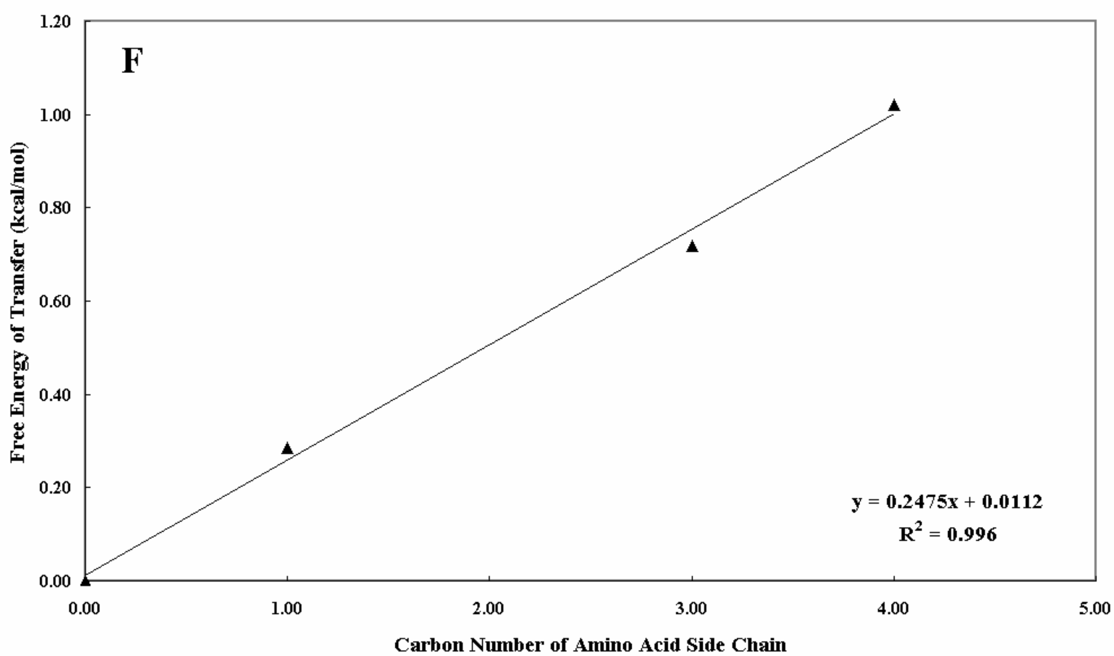
F
Free Energy of Transfer (kcal/mol)
Carbon Number of Amino Acid Side Chain
y = 0.2475x + 0.0112
R2 = 0.996
1.20
1.00
0.80
0.60
0.40
0.20
0.00
0.00
1.00
2.00
3.00
4.00
5.00

Figure 5-21 Free energy of transfer of alkyl side chains from micellar phases to aqueous phases as a function of carbon number of amino acid side chains. A) SDS, B) SDS / PeOH, C) SDS / HFIP, C) LiPFOS, D) LiPFOS / PeOH, E) LiPFOS / HFIP.

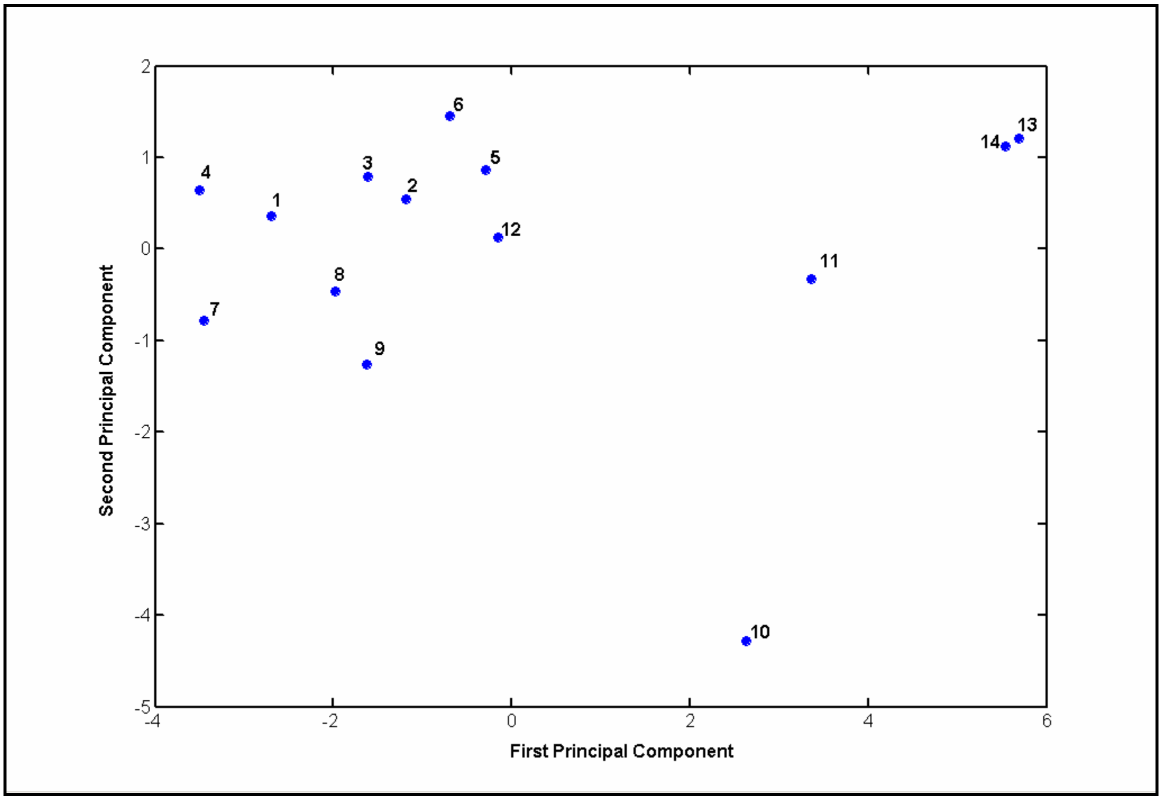

Figure 5-22 Principal component analysis of different solvation models for free energy of transfer of amino acid side chains from condensed phases to aqueous phases.

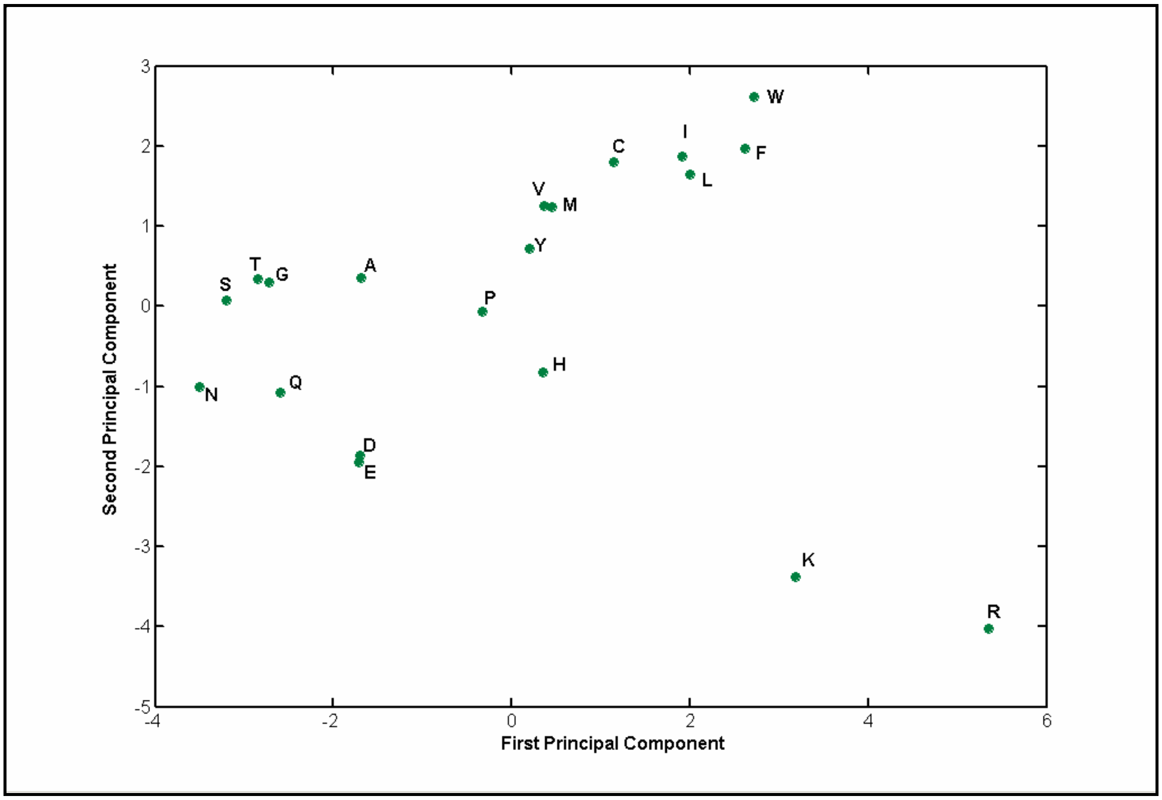

Figure 5-23 Principal component analysis for the classification of amino acid residues according to their solvation energies with various condensed mediums.

CHAPTER 6

Comparative study of Chemical Selectivity of Micellar Electrokinetic Chromatography (MEKC) and Reversed Phase Liquid Chromatography (RPLC)

ABSTRACT

The chemical selectivities of 518 reversed-phase systems and 83 EKC pseudo-phases are evaluated with the unified selectivity triangle (UST) and chemometric methods. The UST scheme focuses on the comparison of the differences in the polar selectivities (hydrogen bonding and dipolarity) between the phases of these two chromatographic techniques. The type and volume fraction of organic co-solvents are found to greatly impact the reversed-phase column selectivity. The solvent modification effects on the selectivities, in terms of dipolarity, hydrogen bonding basicity and acidity, correlate well with the solvatochromic properties of the organic solvents. The effects of column types are also discussed in the context of the UST.

The classification of chemical selectivity was accomplished using three different methods: the UST, principal component analysis (PCA) and hierarchical clustering. A selectivity ranking system based on the Euclidean distance of these phases is constructed and used for the prediction of the similarities and differentiations in phase selectivity.

1. INTRODUCTION

Since it was first introduced by Terabe [1,2] in the early 1980s, the applications of Micellar electrokinetic chromatography (MEKC) has undergone a continuous upsurge for the analysis of a wide variety of neutral, cationic and anionic compounds. The scope of MEKC applications is similar to that of reversed phase liquid chromatography (RPLC), which is the most popular and versatile separation techniques so far. MEKC is an electro-driven method while RPLC is a pressure-driven method. Both chromatographic methods are based on the differential partitioning of the solutes in a two-phases partitioning equilibria. In MEKC, solutes are distributed from the polar aqueous phase to a non-polar micellar phase, while in RPLC, solutes partition between the polar aqueous phase and a chemically bonded non-polar stationary phase. These two techniques also have their own unique advantages. As compared to RPLC, MEKC provides generally higher efficiency, shorter analysis time, faster and more convenient method development due to the feasibility of replacing micellar pseudo-phase, and the possibility of a priori prediction of retention factor from solute structure. The shortcomings of MEKC are the existence of an elution window and the difficulty in interfacing with MS detection. RPLC provides a broad range of elution strength and selectivity, relative easiness of interfacing with MS detection, reproducibility, a wide range of reported applications and capability of preparative scale of separations.

Column architectures and designs have long been at the heart of the developments in liquid chromatography for over a century. Silica particle is the classic packing support for the LC columns for its mechanical stability under high pressures, uniformity of size and shape, feasibility of surface modification with a wide variety of chemical functionalities, and solute-accessible porous structure. However, the chemically bonded silica stationary phases are limited in terms of practical pH range. By contrast, the polymer-based substrates are stable in nearly the entire 1-14 pH range. However, these polymer-based phases have smaller mechanical stability toward high pressure. Another drawback of the polymer-based phases is due to its hindrance of mass transfer into the stationary phases, leading to the loss of efficiency. Furthermore, these polymer-based supports suffer from serious swelling and shrinking problems with the alterations of solvent composition resulting in poor reproducibility. Other stationary phase supports including graphitized carbon materials, and inorganic oxides (alumina, titania and zirconia etc.), have been investigated. In addition to solid support particles, there are rapid developments of monolithic column materials producing a continuous bed with better column stability.

Chromatographic retention and selectivity depend primarily on the properties of the mobile phase and bonded stationary phases. For RPLC, alkyl, phenyl, alkyl phenyl, cycloalkyl, cyano, amino, diol, fluorophases, alkyl-bonded phases with embedded polar groups as well as polymers such as polyethylene glycol (PEG) are widely used to derivatize the solid support. Among them octadecyl (C18) and octyl (C8) phases are most widely used in RPLC, while other bonded phases provide unique selectivity. The number of commercially available RPLC columns keeps soaring as both chromatographers and manufacturers are in pursuit of the ideal packing columns with high efficiency, low cost, extraordinary stability and diverse selectivity. This has facilitated the optimization of various difficult separation problems via stationary phase selection. However, selecting a right column for a specific problem from a large number of RPLC columns is not an easy task. This situation is further complicated by the fact that column manufacturers apply different test protocols and evaluation parameters for their columns.

Many methods for characterization the stationary phases in RPLC could be found in the literature. One popular class of these methods [3-6] uses selected test compounds to determine a variety of the chemical and chromatographic properties of the RP columns such as column efficiency, asymmetric factor, silanol affinity, steric selectivity, shape selectivity, hydrophobic selectivity, hydrogen bonding capacity, ion exchange capacity and metal activity etc. There are heated debates on the criterion of the test compounds selection and the representative properties for the characterizations of the column selectivities. As pointed out by many authors [7-9], the precisions of column characterizations are greatly influenced by the column descriptors and test compounds selected. Furthermore, the effectiveness of these test methods requires the mandatory use of virtually the same mobile phase composition. Therefore, these kinds of methods are often considered as “in-house” methods and could hardly be used as universal standard tests for column characterizations.

Chemometric and statistical methods are useful tools to peel the redundant information from the column descriptors from numerous tests; and extract only the primary and important variables for the column classification and pattern recognition. Principal Component Analysis (PCA) and cluster analysis are suitable for these purposes because both methods could be carried out without prior knowledge of the objects. Olsen and Sullivan used PCA and cluster analysis to characterize 17 Octadecylsilyl (ODS) columns. They found that the first four principal components readily accounted for over 95% of the variances. Euerby and Petersson [10] examined 85 columns with the PCA method. They found that three of the original seven column properties were highly correlated. Therefore, they suggested the use of five column parameters for a successful classification of these columns. In their subsequent work [11], they characterized 135 commercially available columns with the same PCA scheme. Ivanyi and co-workers [12] continued to explore the possibility of characterizing column properties with a minimal number of test parameters. They reexamined the column properties in Euerby's work and stated that 3 or 4 chromatographic parameters could be sufficient for a reasonable rationalization of column performance without much loss of accuracy. These chemometric techniques are useful for the identification of equivalent columns and classification of columns with similarity and differences. However these pure mathematical approaches tend to interweave the responses of column properties which complicates the recovery of the chemical meaning of the classifications.

Empirical models have also been developed to describe column properties. One of these models based on linear solvation energy relationships (LSER), has been used to characterize a wide variety of RPLC columns [13-22]. The general form of LSER interprets the chromatographic retention into several free-energy-related intermolecules interactions that could be written as:

$$\log k = vV + bB + aA + sS + eE + c \qquad \text{Eq. 6-1}$$

The *v*V is a hydrophobic term that is related to the relative cavity formation ability between the stationary phase and the aqueous phase. The *b*B and *a*A represent two types of the hydrogen bond interactions. The *s*S term measures the capability of stationary phase for the dipolar-type interactions. The *e*E term accounts for the excess molar refraction describing the propensity of stationary phase to interact with n or π lone pair electrons. In general, a suitable set of test solutes with known solute descriptors is used in multiple linear regression (MLR) to train the solvation model. Thus, the useful physio-chemical information for the characterizations of columns is preserved in the regression parameters. The LSER methods have been used for the prediction of solute retention and selectivity for the RPLC with a reasonable precision, especially for neutral solutes. Wilson and coworkers [23-30] published a series of papers to promote a novel empirical model for characterizing the chromatographic behaviors of RPLC columns. Their intermolecular interactions include the hydrophobic-type interaction, ion interaction (dipolar interaction), hydrogen bondings, and steric hindrance. The newly established models are considered by the authors to be more suitable for describing chromatographic parameters in RPLC and have greater accuracy for the prediction of retention and selectivity than the original LSER model developed by Abraham and coworkers [31]. However, the new solvation model mainly improves the interpretation of the chromatographic behaviors of the charged or bulky solutes. The main purpose of this study is to compare the phase selectivity between the MEKC and the RPLC. Indeed the underlying driving forces for retentions and selectivity in RPLC and MEKC are in most parts very similar; that is, hydrophobic interaction is the predominant force behind retention, while hydrogen bonding and dipolar interactions determine selectivity of phases. In MEKC, charged compound could electrostatically interact with the charged pseudo-phase. Since in RPLC the stationary phase is neutrally charged. We limited our initial studies to neutral solutes and used LSER solute descriptors that were independent of retention behavior in the given chromatographic systems.

There are frequent comparisons between RPLC and MEKC in the literature for different purposes. Poole et al. [32] reviewed the published LSER models for characterization of column selectivity in RPLC and MEKC, but made no systematic comparison between them. Slonecker and co-workers [33] used informational entropy of chromatographic retention to evaluate the orthogonality of different chromatographic techniques. Ferguson and Goodall [34] observed that equal partition coefficients were obtained for a series of benzene and phenol derivatives between RPLC and MEKC. Detroyer and his colleagues [35] compared the retention characteristics of 21 basic pharmaceutical substances among MEKC, immobilized artificial membrane columns (IAM) and RPLC columns with PCA methods. They found that the first principal component was linearly correlated with the octanol-water partition coefficient of these basic drugs indicating the main retention principles for these chromatographic techniques were identical as hydrophobicity-driven. The differences within these separation methods were mainly derived from the secondary interactions (polar interactions). In the same paper, the authors reported the correlation coefficients of the retention factors of these drug substances varying from 0.75 to 0.95 between the micellar phase and seven RPLC columns. In many cases [18,36-49], MEKC and RPLC have been used to estimate the octanol-water partition coefficient which is a measure of hydrophobicity of solutes. From the literature survey, we can see many of the interests, more than coincidently, arise from the comparisons of the intrinsic similarities and differences of these two powerful chromatographic techniques. Unfortunately, there is no systematic study to address the linkage between the two chromatographic techniques.

Previously, we have developed a micellar selectivity triangle (MST) with the phase descriptors derived from the LSER regression coefficients. This novel MST in conjunction with the PCA and cluster analysis was successful used to rationalize and classify the pseudo-phases in MEKC. Here, we will attempt to apply a similar strategy to characterize the selectivity patterns of over 470 RPLC columns together with the micellar phases in prior works.

Our method is by no means comprehensive, since it limited to small and neutrally charged solutes. Thus, the method does not consider electrostatic or steric effects (ion-exchange/silanol interaction and shape selectivity etc.). As the matter of fact, these secondary interactions are often suppressed in the practice by the manipulation of pH, ionic strength or addition of silanol masking agent (e. g. triethyl amine) and ion pairing agent (trifluoroacetic acid).

2. EXPERIMENTAL

Chemometric modeling was performed on a Dell Inspiron 4100, the software platform was Matlab 6.5 release 13 (The Math Works, Inc. Natick, MA). A database composed of 83 MEKC micelle systems and 518 reversed-phase systems was collected from the literatures and this lab. The UST is constructed with JMP release 5. 1. 1 (SAS Institute Inc., Cary NC).

3. RESULTS AND DISCUSSIONS

3.1 LSER system parameters for 601 separation systems.

We collected 83 pseudo-phases of MEKC and 518 stationary-phase systems of RPLC from this lab and the literatures. The database contains an extensive coverage of commercially available RPLC columns from various manufactures that differ in the type of bonded ligands (alkyl, phenyl, fluorinated phases, cyano, diol, polymeric and polar embedded alkyl phases etc.), supported particles (silica, aluminia, titania, zirconia, polymer and graphite-like carbon bases), mobile phase compositions etc. The pseudo-phases examined in this work, include cationic and anionic surfactants, bile salts, polymeric micelles, fluorinated surfactants, mixed micelles, solvent-modified micelles, liposomes, vesicles, bicelles etc. The 601 separation systems (different mobile and stationary phases compositions) were collected in a database. The reported LSER coefficients covered a wide range of values; for example, the hydrophobic parameter (v) varied from 0.41 (ID. 94: a Unisil C18 column with 90/10 ACN/H_2O mobile phase) to 6.04 (Phase ID. 478: fluorooctyl column with a DMF gradient). The small v parameter for the Unisil phase indicates similar cohesiveness for stationary phase and mobile phase. By contrast, the fluorooctyl phase is much less cohesive than the mobile phase. Hydrogen bond acidity parameter (b) has the highest value (-0.14) in a cyano-bonded silica column (ID. 501) with 10% methanol and the lowest b (-5.64) is obtained with a polymer-based column (ID.484 PLRP S-100 with ACN gradient). We can see that all the phases in the database have negative hydrogen bond acidity parameters, implying that the aqueous mobile phase is better hydrogen bond donor than these 'stationary' phases. Polar cyano-bonded silica columns appear to be better hydrogen bond donor than the other phases in the database, but still a weaker hydrogen bond donor than the mobile phase. Hydrogen bond basicity (a) of the stationary phase also spans a wide range from –3.1 in Inersil ODS with a TFE gradient (ID. 466) to 0.9 in the cationic micellar phase TTAB (ID. 601). When comparing to the prior three LSER system parameters, the dipolarity (s) and polarizability (e) of the RPLC systems obtain narrower ranges from –1.96 (Inersil ODS with a TFE gradient ID. 466) to 0.46 (LiPFOS micelles in MEKC, ID. 535) and from –1.21 (ID. 478: fluorooctyl column with a DMF gradient) to 1.26 (Shodex RP18-413 with 75% TFE ID.379) respectively. The collection of the very large hybrid database characterizes the selectivities of a great number of the commercially available RPLC columns, self-packed RPLC columns, and MEKC pseudo-phases. The integration of these varying phases into one database is advantageous for systematically comparing the similarities and differences of phases selectivities in these two chromatographic techniques. The availability of a strikingly wide variety of RPLC columns and EKC pseudo-phases with different selectivities could be quite beneficial in the selection of the proper system for separations of complex mixtures. In addition, the large-size of the database will reveal valuable information on the chemical origin of the selectivity differences between the RPLC and EKC systems, which could easily be overlooked in smaller databases.

The compilation of the extensively large database enables us to study the relationships between these LSER parameters. As pointed out by Abraham and coworkers [19], the LSER parameters were somewhat linearly correlated and the relationships were independent on the mobile phase composition for 17 different C18 columns. We investigated the potential intrinsic correlation within the five system parameters in a larger scope of RPLC columns. Figure 6-1 shows the relationship between the five parameters for 601 phases. For subplot A, a strong linear correlation between the hydrophobic parameter v and the hydrogen bond acidity b could be seen for the majority of the phases with only minor number of phases departs from the linear relationships. Similar trend is observed for the correlation between the dipolarity (s) and the polarizability (*e*) in the subplot B, where large number of phases are linearly correlated and only a small fraction of these phases randomly scatter from linearity. The relationship between the hydrogen bond acidity (*b*) and the hydrogen bond basicity (*a*) in the subplot C is not as well correlated as the previous two pairs of system parameters and a significant number of the phases deviate from the linear relationship. Subplot D shows the correlation between the hydrogen bond acidity (*b*) and the dipolarity (*s*) of the systems. As can be seen, the relationship between these two parameters exhibits a scattering pattern. The correlation plots of LSER system parameters r in our database reveal some useful information. First, the intrinsic correlations between (*v* and *b)*, (*s* and *e*) enable the use of reduced parameters to represent the chemical selectivity of the phases. Second, the system parameters with scattering or poorly correlated patterns are useful to for identifying systems with different selectivities. Third, it is worthy to note that C18 columns, which highlight in the circle area, still show strong linearity in all the system parameter pairs studied and are in agreement with Abraham's conclusion [19]. However, the more important scattering patterns of the selectivity characteristics of 'stationary' phases will be invisible in their limited dataset.

3.2 Analysis and comparison of phase selectivity in UST

As mentioned above, three LSER parameters, *b*, *a* and *s,* are less correlated and are more important for the selectivity characterization, the hydrophobic parameter *v* and polarizability *e* are linearly correlated with b and s respectively. Therefore, *b*, *a* and *s* are the three parameters selected to characterize phase selectivity in the triangle scheme without much loss of the information. The Unified Selectivity Triangle (UST) is constructed with a similar normalization scheme to that of previous work and will only be discussed briefly here. First the three parameters are normalized by the hydrophobic parameter *v*. Then, a scaling procedure is applied to standardize the normalized parameters (*b/v, a/v, s/v*) into the range between 0 and 1 (the preset value of each parameter are listed in table 6-1). In the final step, each scaled parameter is averaged by the sum of the three parameters and processed by the graphical software.

Figure 6-2 illustrates the characterizations of the phase selectivity of the RPLC columns and the EKC pseudo-phases in the selectivity triangle. We observe that the RPLC columns (red open square) have more diverse selectivity patterns than the EKC pseudo-phases. There are several reasons for the phenomenon. First, RPLC has long been the mainstream of chromatographic techniques for nearly forty years. Development of novel columns with different selectivities has been a main focus of research in both academia and industry. Second, a great number of the RPLC systems in the UST with distinct selectivity characteristics utilize high concentration of organic solvents such as methanol (MeOH), acetonitrile (ACN) and tetrahydrofuran (THF). Similar solvent compositions are not compatible with conventional micelles due to their instability at high concentration of organic solvents. Nevertheless, Polymeric micelles are reasonably stable in the presence of high levels of organic modifiers. In addition, the selectivity characteristics of the polymeric micelles could be easily modulated by varying the sidechain compositions of the polymers. For instance, the selectivities of the AGENT-type polymeric micelles in figure 6-2 exhibit significant changes with the variations of the percentage of the octyl side chains in the polymer composition. The unique merits such as the stability with organic solvent, the convenience of selectivity control via sidechain modifications, as well as the compatibility with mass spectrometry, make the polymeric micelles promising pseudo-phases for the EKC separation. The LiPFOS micelle systems, as identified in figure 6-2, are of great interest. Because they are the strongest hydrogen bond donating pseudo-phases in EKC. As compared to the RPLC systems, the LiPFOS systems are right below group B which contains the very strong HBD solvent of TFE at considerably high concentration. These LiPFOS micelles also show very distinguished selectivity patterns from other EKC pseudo-phases and RPLC columns with only one RPLC system (ID. 500: Perfluorinated Fluorophase with ACN gradient) that is located in the vicinity of the LiPFOS micelles. (More details about the comparison between this Perfluorinated Fluorophase column and LiPFOS micelle will be discussed in a later session.)

In the UST, the RPLC columns can be clustered into 6 groups with different selective characteristics. The representative columns and descriptions of the selectivities are summarized in table 6-2. Although the classifications are somewhat subjective, the columns in the same cluster certainly contain similar chemical selectivities. Special care shall be paid to those columns near the boundaries that generating most ambiguities of the classifications. Cluster A is mainly comprised of C18 columns with mild content of organic solvents possess intermediate strength for the three polar selectivities (Hydrogen bond acidity, hydrogen bond basicity and dipolarity). Interestingly, Sodium dodecyl sulfate (SDS) micelle and its analogues are also located in the same group with similar selectivity strength. While group A contains the largest entries of our columns database, the other five groups demonstrate the wide range of chemical selectivities. Cluster B is located in the upper vertex of the triangle, indicating a strong hydrogen bond acidity but relatively weak hydrogen bond basicity and dipolarity. Most of the phases in the cluster B utilize Trifluoro ethanol (TFE) at a relatively high level of 50% as the organic co-solvent together with water in the mobile phase. As can be seen from the solvatochromic solvent parameters of these common solvents in table 6-3, TFE is even a stronger hydrogen bond donor solvent than water, but weaker hydrogen bond basic and dipolar solvent. Like other organic modifiers in RPLC, the TFE is preferentially extracted into the alkyl bonded stationary phase. Consequently, the selectivity patterns of these columns are likely to reflect the solvent properties of TFE as a strong hydrogen bond donating phase and poor hydrogen bond accepting and dipolar abilities. The columns in the C Cluster have similar hydrogen bond acidity and dipolarity with those in cluster B, but are better hydrogen bond acceptors. Methanol is the common solvent for the phases in the C cluster, which partially explains the improvement of the hydrogen basicity of the separation system, because methanol (β = 0.62) is a better hydrogen bond acceptor than water (β = 0.47) as shown in the solvatochromic parameters tables. Meanwhile, the HB acidity of the ODS columns originates from the silanol groups on the silica support. Dramatically lower hydrogen bond acidity is observed for the systems in cluster D, as the hydrogen bond basicity is enhanced and the systems retain very weak dipolarity. Additionally, a few RPLC systems with ACN-water mobile phases are also located in this cluster. ACN is an aprotic solvent with weak hydrogen bonding properties, but relatively strong dipolarity among the RPLC organic modifiers. Therefore, it is an anomaly that these systems are classified as strong HBA and weak dipolarity. Cluster E mainly consists of ODS columns with Tetrahydra furan (THF) as co-solvent, diol-bonded columns (J. T. Baker Diol 50% ACN, Lichrosorb Diol 25% MeOH), and polymer coated zirconia and silica columns. According to the solvatochromic properties of THF, it is a non-hydrogen bond donor solvent (α = 0.00), intermediate hydrogen bond acceptor and dipolarity strength. This explains the very weak hydrogen bond acidity and intermediate HBA and dipolarity for the RPLC systems in cluster E. Cluster F consist of columns with very high dipolarity, but weak in hydrogen bonding. We notice that these columns are mostly polystyrene–divinylbenzene coated polymer columns. One of the unique properties of these polymer columns is the elimination of silanol groups which are considered as the sources for the strong hydrogen bonding in traditional silica-based columns. Thus it is not surprising to observe a weak hydrogen bonding interactions in these polymer columns, and their polar selectivities are dominated by the dipolarity contribution.

3.3 Column selectivity comparison under constant solvent composition.

The reversed-phase type stationary phase is a complicated, heterogeneous media, whose chemical properties vary greatly with the mobile phase composition. In the above section, we have shown the effective modulations of column selectivity with different types of co-solvents (MeOH, THF, ACN etc.) leading to the various column groups with unique selectivity. Due to the difficulties in separating mobile and stationary phases effects, we compared column selectivities at constant mobile phase compositions. The first group contains 37 columns in a 50/50 methanol/water (volume fraction) binary solvent system, while the second group consists of 216 columns in a 50/50 acetonitrile/water binary solvent.

Figure 6-3 shows the characterization of the column selectivities for the 37 columns in 50:50 MeOH/Water. The filled squares represented the alkyl-bonded phases including methyl, octyl, octadecyl and hybrid C18-C3 etc. In addition, these columns vary greatly in manufactures, porosity, size and shape of the particle, bonding chemistry, surface ligand coverage, carbon loading and contain both end-capped and non end-capped columns. Nevertheless, they cluster very closely to each other in the UST and can be categorized into one group with similar chemical selectivity. The open square symbols in Fig. 6-3 show the cyano, phenyl and polymer bonded phases that are more dipolar than the alkyl counterparts. This is not surprising because all of these polar functionalities are more favorable for dipolar-type interactions than alkanes.

As illustrated in figure 6-4, column selectivities exhibit a more diverse pattern in the acetonitrile / water binary solvent. However a large portion of the phases still clusters in the center of the UST, again mainly consisting of the alkyl-bonded phases. For these alkyl-bonded silicas, it is well known that the alkyl groups only involve weakly in the polar interactions. Since identical solvent system is used in the case, these alkyl-bonded phases have similar polar selectivities pattern, mostly due to their analogous chemical nature of bonded-ligand and its weak tendency to be "wetted" by the polar solvents. We notice that all the bonded phases are located in the lower part of the UST and far away from the vertex of hydrogen bond acidity in the acetonitrile / water solvent, indicating a weak propensity of hydrogen bond donating ability of these columns systems. This is in accordance with the solvatochromic properties of ACN, which has a very weak hydrogen bond donating ability ($\alpha = 0.19$). By contrast, the dipolarity of these columns has a wider range from very weak dipolar column (267 Platinum EPS C8) to the polymer-based column (383. PRP-1, a styrene-divinylbenzene based column), where the chemical nature of these bonded-ligand plays an important role. For example the PRP-1 phase with a styrene-divinylbenzene support replacing the conventional silica support, greatly suppresses the hydrogen bond interaction by the removal of silanol groups. A similar trend could be seen for the polystyrene-coated zirconia phase (ID 384), which used extensive polymer coverage to shield the hydrogen bonding sites on the zirconia surface resulting in a very weak hydrogen bond donating and intermediate hydrogen bond accepting phase.

We also investigated the modification effects of different organic solvents on a given column by the UST (figure 6-5). The first example is a Zorbax C8 column with the modifications of MeOH, ACN, THF and TFE at 50:50 volume fractions respectively. It is clear that the HB acidic solvent TFE successfully improved the HB donating ability of the Zorbax column and the weak HB acidic solvent THF rendered the column with weak HB acidity as expected. The ACN-modified column systems exhibit stronger dipolarity but weaker HB acidity and similar HB basicity as compared to the MeOH-modified Zorbax C8 columns. Similar results were observed on the solvent modification effect on another RPLC columns Spherisorb ODS-2. These solvent-modified column systems greatly expand the range of selectivities of the RPLC and can be readily predicted with the UST. Among them, THF, TFE and MeOH (or ACN) provide complementary selectivities that are useful for the development of optimization strategy. These observations are consistent with the characterizations of these solvent selectivities in the SST.

In summary, one of the most interesting findings of this study is that the type of solvent greatly impact on the polar selectivities of RPLC columns. And these solvent effects are readily predicted from the UST and in accordance with the solvatochromic characters of the solvents. On the other hand, the non-polar phases (alkyl, phenyl etc.)

tend to have similar polar selectivities, while polymer or other polar functionalities render significant different columns selectivities from silica-based alkyl-bonded phases.

3.4 Column selectivity ranking in the UST.

The degree of similarities and differences of the RPLC columns and EKC pseudo-phases are measured by the distance between their locations in the UST. In order to describe the column selectivity ranking in a quantitative manner, we utilized the Euclidean distance between two objects to define the likeness of the phases and to create a column selectivity ranking according to their interpoint distances in a three dimensional space. For a n-dimensional space, the Euclidean distance *d* is defined as

$$d = \left|X - Y\right| = \sqrt{\sum_{i,j=1}^{n} \left|x_i - x_j\right|^2} \qquad \text{Eq. 6-2}$$

Where x_i and x_j are the corresponding space coordinates of the object X and Y respectively. With the equation, we computed the Euclidean distances between a specific phase and the remaining 600 phases. After that, we rank the distances from the lowest to the highest. The closer the distance between the two phases is, the more similar they are in terms of their chemical selectivities. This approach is obviously attractive for two purposes: one is to find a replacement system with similar selectivities and the other is to assess the degree of 'orthogonality' between different systems. Figure 6-5 depicts the interpoint distances for all the system pairs in our database. For the demonstration of the ranking systems, we choose several interesting phases including SDS, LiPFOS and Octanol-water systems and study the selectivity rankings of them with remaining phases. To confirm the validity of the ranking, a κ– κ plot of 43 aromatic compounds (table 6-4) with diverse sizes and polarities is used to evaluate the similarity level of phase selectivity. Where κ is defined as

$$\kappa = \log k' - \log k'(\text{benzene}) \qquad \text{Eq. 6-3}$$

In essence, κ is the differential retention strength between the test solute and a reference compound (benzene in this case). The treatment will remove the effect of different phase ratios in various separation systems. The correlation coefficient of the κ- κ plots is an effective criterion for the evaluation of the phase similarity. We have summarized the selectivity rankings for the three selected systems (SDS, LiPFOS and Octanol-water), together with the interpoint distances and κ- κ plot correlation constants in table 6-5. For the first thirteen phases with the highest ranks in our SDS selectivity ranking system, they have the shortest distance toward SDS micelle indicating the great similarity of these phases in term of phase selectivity. This is also evident by the high correlation coefficients ($R^2 > 0.97$). For the LiPFOS micelles, the first four systems with highest ranking are all fluorinated phases, several ODS and polymeric phases could also simulate a similar selectivity pattern of the LiPFOS micelles. The κ- κ plot coefficients for these top-rank systems range from 0.85 to 0.99. These κ- κ plot coefficients are not as good as those with the SDS micelles. This is not unexpected, given the interpoint distances for the LiPFOS-like systems are larger than those in the SDS systems. Interestingly as shown in figure 6-6, the non hydrogen bond solutes (NHB) show stronger binding for the RPLC column than for the LiPFOS micelles and deviate cogenerically from the main correlation tendency. This is indicative that the LiPFOS micelles are more cohesive than these RPLC columns. After the exclusion of the NHB solutes, an improved correlation is obtained. Seeking the alternative systems for the estimation of the octanol-water partition coefficients has long been the focus of numerous efforts. In our selectivity ranking system, we can easily identify the proper phases with similar selectivity to the octanol-water system. In the last column of table 6-5, DHP, microemulsion, sodium Cholate (SC) and RPLC system YMCPack ODS (30% ACN) obtain both short interpoint distances and high κ- κ plot coefficients. These four phases have the most similar selectivities to the octanol-water system, and shall be the system of choice for estimating the octanol-water partition coefficients with great accuracy. The phases with the lowest ranks in the SDS, LiPFOS and octanol-water selectivity rankings are mainly comprised of these four RPLC systems: 378 (Jordi RP–C18 75% MeOH), 380 (PRP-1 80% ACN), 381 (PRP-1 70% ACN), and 379 (Shodex RP18-413 75% TFE). This is consistent with the UST, where the first three systems (ID 378, 380, 381) are the strongest dipolar as well as the weakest hydrogen bond acidic and basic phases. Phase 379 (Shodex RP18-413 75% TFE) represents another extreme extent, with the strongest hydrogen bond basicity, the weakest dipolarity and minor strength for hydrogen bond donating ability. It is worthwhile to note that the use of the Euclidean distance to evaluate the likeness of the phases does not necessarily carry the exact chemical selectivity characteristics of the phase. In other words, a certain phase with a Euclidean distance (*d*) to one reference phase can be viewed as any point on a circle that defined by the reference point as the center and Euclidean distance (d) as the radius. The combination of the selectivity ranking method with the unified selectivity triangle (UST) would provide complementary methods to analyze the similarities and differences in chemical selectivities between different systems.

3.5 PCA method for phase characterizations and classifications

Principal component analysis (PCA) is a useful chemometric tool for interpreting complicated data. The main algorithm of PCA is carried out by decomposing multidimensional data into fewer orthogonal spaces, while the space vectors, the so-called principal components (PCs) are linear combinations of the original data descriptions. Usually, the first principal component will describe most of the variances from the original data and the second and other principal components will explain the remaining variances that are not accounted for by the first principal component. In our previous work, the PCA method was successfully used to elucidate the pseudo-phase classifications in EKC. Here, we expand the PCA method to a larger and more complex database of LSER parameters of 518 RPLC systems and 83 EKC pseudo-phases.

Table 6-6 lists the eigenvectors of the principal components. The coefficients in each column indicate the weights of the LSER parameters in the linear transformation to a specific principal component. Figure 6-7 illustrates the contributions of these five LSER parameters toward the first three principal components. For the first principal component, hydrophobicity and hydrogen bond acidity parameters of the systems are the major contributors. The hydrogen bond basicity of the system plays an important role to determine the second principal component. Meanwhile, the third principal component is more likely to be the collective contribution from all five parameters. Interestingly, the contributions of v and b to the first three principal components have similar absolute values but opposite in signs, implying a certain degree of correlation between these two parameters. It agrees well with the prior observation of the linear relationships between v and b for the 601 systems. It shall be noted that the contributions of v and b to the fourth PC and fifth PC do not follow the relationships, the variations to these secondary PCs could be the possible reasons that a small portion of the systems departing from the linear correlations between *v* and *b*. The eigenvalues and the percentage of variances explained by the individual PCs are presented in table 6-7 and figure 6-8. It is clearly that the first PC accounts for 51% of the variances and the second PC describes an additional 23% of the total variance. With the incorporation of the third PC, the first three PCs combine to account for a 90% of the variances and could afford a fair description of the columns selectivity characteristics. In such a manner, the utilization of the first four PCs could describe over 97% variances and shall give a satisfactory representation of the system selectivities.

Figure 6-9 shows the plot of scores for these 601 phases between the first PC and the second PC. It is clear the RPLC columns behave quite differently from the EKC pseudo-phases. The majority of RPLC columns congregates tightly in the center of the plot as cluster 1. This is explained by the fact that most of the RPLC column systems are eluted with high content of organic solvents (>30% volume percentage) which reduces the column hydrophobicity greatly. As stated earlier, the first dimension (the first PC) is primarily determined by the positive contribution from hydrophobicity together with the negative contribution from hydrogen bond acidity of the system. By contrast, most of the EKC pseudo-phases are located in the upright corner of the plot, indicating higher scores for both PCs. Cluster 2 is mainly comprised of SDS analogues and bile salts. They are identified as moderately hydrophobic and hydrogen bond basic, but weak in hydrogen bond donating ability. Inferring from the high score of cluster 3 and 4 on the second dimension (i. e. the second PC), the components in these two clusters possess strong hydrogen bond accepting ability. The phases in cluster 4 tend to be more hydrophobic and/or less hydrogen bond acidic than those in cluster 3. As it turns out, cluster 3 contains cationic surfactant TTAB, and the siloxane based polymeric micelles (allyl glycidyl ether-N-methyl taurine AGENTs) which have been categorized as strong hydrogen bond acceptor but weak hydrogen bond donor micelles in the UST. Liposomes, vesicles, bicelles and Alkyl methacrylate based polymeric micelles (pLMAt-type polymeric micelle) are the main components for the cluster 4. In general, these phases are more hydrophobic and stronger hydrogen bond acceptors; on the other hand, they are weakest hydrogen bond donor in the series. Cluster 5 contains those fluorinated micelles (LiPFOS). The localizations of these phases show their weak hydrogen bond accepting ability, weak hydrophobicity and/or strong hydrogen bond acidity. One unusual cluster for RPLC columns could be seen in the plot as cluster 6. Unlike other columns eluting with isocratic solvent systems, the column systems in cluster 6 are the only phases running with gradient conditions. But the reasons for the origination of anomalously high hydrophobicity and weak hydrogen bond acidity of these phases are still unclear. In figure 6-10, the inclusion of the third dimension (the third PC), improves the resolution and precision for the classification of phase selectivity by accounting more than 90% of the total variances.

3.6 Cluster analysis for classification of phase selectivity.

Cluster analysis is a classification method based on the assumption that the closer the distance between two objects is, the more similar these two objects are. The ideal clustering will be a cluster with minimal distance for the intra-cluster objects while a maximum distance for the inter-cluster objects. In our study, a hierarchical type clustering method is used. In the hierarchical clustering for n objects, the two objects with the shortest linkage are merged into the same cluster in the first step, which will return n-1 objects. The linkages between these n-1 objects will be calculated and ranked. Again the closest two will be merged to one cluster. This process continues until no more object is left. In such an approach, the successors (leaves) on the same node shall have more similarity than the antecedents at the higher level of the hierarchical tree. Figure 6-11 presents the dendrogram of the hierarchical clustering of our 601 phases. For the purpose of clarity, only 40 end nodes are shown in the plot (the clustering with complete database could be seen in figure 6-13). Therefore each end node might represent multiple phases. The identifications of the phases in each node are listed in table 6-8. In order to determine the optimum number of clusters for the best representations of the phase clustering, we apply the upper-tail rule method, in which we plot the normalized fusion levels against the number of clusters in figure 6-12. The break point of the plot will be the number of clusters with satisfactory classifications and further division of cluster does not have a significant effect on the magnitude of normalized fusion level. It is clear that the break point occurs with four clusters in our case. Among these four clusters, the RPLC columns with gradient elution are significantly different from other phases and classified into a unique cluster. Also RPLC columns with isocratic mode are well separated from the EKC pseudo-phases, with only a few phases diffusing within these two groups. The classifications of four clusters are also supported by the distance matrix plot of these 601 phases. As shown in figure 6-13, four horizontal bands are readily visible indicating the data tend to agglomerate into four groups with minimum interpoint distances within individual group. Also from the clusters, most of the alkyl and phenyl bonded phases cluster into the neighboring nodes of 1, 2, 13 and 7. Fluorinated micelles (LiPFOS series) have closer distance with the alkyl-bonded phases and are grouped together with these non-polar reversed phases. The cyano-bonded phases and the congeners are merged into the same node 6. Polymer based phases join the cluster and distribution into node 8, 35, 9 and 10. So these alkyl, phenyl, cyano and polymer based phases together with fluorinated micelles are the main components of the group separated from the other three. The pseudo-phases of the EKC method form another big group. SDS and its analogues are focused in the node 5, microemulsion and pentanol-modified SDS are joined in node 4, while liposome, vesicles, bicelles form a parallel sub-cluster with nodes 39, 19, 38, 36 and 40. It shall note that the AGENT-type polymeric micelles and the TTAB micelles are not grouped together in the hierarchical clustering, although the UST and PCA method tend to have them into the same category. The AGENT-type polymeric micelles are found in nodes 15 and 18, while the TTAB micelles are merged with the cluster of the liposomes.

We will also use the Euclidean distance to evaluate the similarity of the phase selectivities in hierarchical clustering. In this case, the Euclidean space is a 5 dimensional space with *v, b, a, s* and *e* LSER parameters to describe each vector. Previously, the Euclidean distance in the UST scales was used to rank the top 13 phases that are analogous to the SDS, LiPFOS and Octanol-water system, separately. Interestingly, most of those phases are still located in the nodes within 1.5 fusion levels of the targets. However, we also discover several phases which are not in the top 13 list of SDS, clustered together with SDS micelles in the same node 5. For example, 79 (Hypersil ODS 10% MeOH) and 441 (PBS 15% MeOH) are two phases that are not included in the top 13 list of the UST scale for SDS, but are considered as phases with similar selectivity to the SDS micelles. These correlations are further supported by the κ-κ plots where a slope of 1.12 and regression coefficient (R^2 = 0.987) for the linear relationship between phase 79 and SDS micelle, a slope of 1.16 and regression coefficient (R^2 = 0.983) for phase 441 and SDS are observed. The observations indicate that hierarchical clustering is indeed, specialized for the identifications of phase similarity with the Euclidean distance approach, since the evolution of the hierarchical structure is essentially based on interpoint distances. Several reversed-phase column pairs: Hypurity C18 (phase 343) and Discovery C18 (511), Discovery C8 (phase 332) and Ace5 C8 (phase 302) are considered as exchangeable columns with similar selectivity in the literatures.[11,26] While these equivalent columns were identified by the test-compound methods in the literatures, we intentionally reexamined the degree of equivalency of these column pairs with our hierarchical clustering. First of all, Hypurity C18 and Discovery C18 are assigned to the end node 13, while Discovery C8 and Ace5 C8 locate in the end node 1. The Euclidean distances between these two column pairs are 0.074 and 0.0062 respectively. The κ-κ plots between these columns obtain the slopes approaching 1 and excellent correlation coefficients (0.999). Therefore, our hierarchical clustering obtains consistent identifications of the column equivalencies with the literatures. As a matter of fact, we shall have more confidence on the hierarchical clustering method, because it is less dependent on the test compounds and could be integrated with the column selectivity ranking (Euclidean distance) and the κ-κ plots methods.

With the comparisons of the three classification methods, we can see that the UST scheme reveals good details on the polar selectivities of the phases and further classify the RPLC columns into 6 clusters according to their selectivity differences in terms of the dipolarity, hydrogen bond acidity and basicity. The PCA and hierarchical clustering do not reveal as much details as the UST on the polar selectivities of the RPLC column systems. Instead, the PCA and hierarchical clustering provide more comprehensive and accurate descriptions of the phase selectivity due to the inclusion of all five LSER parameters, especially the hydrophobicity term. As shown in the PCA and hierarchical clustering methods, the hydrophobicity term plays a significant role in the classifications of the phase selectivities. This is mainly because the large scales of changes in the phase hydrophobicity induced by the organic co-solvents tend to shield the differences in the polar selectivities. It is well documented that increasing the volume fraction of organic solvent in the mobile phase dramatically lowers the cohesiness of the mobile phase and facilitates the cavity formation for solute accommodation in solvent. For instance, Vonk et al. [50] have reported that the hydrophobic terms for a series of reversed-phase ODS columns decreased significantly from 2.80 to 0.82 with the increase of the methanol volume fraction from 40% to 90%. The PCA is the method of choice to elucidate the principal variables that governs the selectivity classifications but it does not clearly define the boundary of the clusters. By contrast, hierarchical clustering provides a visually clear dendrogram on the clustering structure, which enables the comparison of the similarity and differences of phase selectivities simply by measuring the linkage between the objects. The drawback of hierarchical clustering is the lack of the descriptions of the chemical meaning of each cluster. Despite the differences discussed above, all three methods show a common trend that the selectivities of RPLC columns and EKC pseudo-phases are not overlapping in the most part.

4. CONCLUSIONS

The study lays the groundwork for the characterization of the RPLC mobile-stationary phases selectivities in a large scale and constructs the linkage to another promising chromatographic technique EKC. For the three classification methods, the UST method could reveal the 'hidden' clustering information on the polar selectivities. It is shown in the UST that organic co-solvents could effectively modulate the column polar selectivities according to the solvatochromic properties of the solvents. The PCA method identifies that the hydrophobicity term and hydrogen bond acidity of the phases are the primary factors to govern the first principal component. It is also concluded in the PCA that three PCs could give a reasonable classification of the phase selectivities, especially when some of the LSER system parameters such as v and b, s and e are correlated. It is shown by the three methods that most of the RPLC columns and MEKC pseudo-phases do not possess identical selectivity patterns and often exhibit complementary selective properties. The hierarchical clustering presents a visually clear classification of the phases. The degree of similarity and differences between the phases could be measured by the length of the linkage between them. The advantages and shortcomings of the three methods indicate that a combination of these three methods would give a complete and successful interpretations of the selectivity classifications of the total 601 phases.

We also set up a selectivity ranking system using the Euclidean distance as a measure of the selectivity similarities and differences. The selectivity ranking system is proved to be effective in identifying phases with similar selectivities in our database. Our results of the phases with similar selectivities are consistent with the correlation analysis of retention behavior in different systems.

REFERENCES

1. Terabe S, Otsuka K, Ichikawa K, Tsuchiya A, Ando T: **Electrokinetic separations with micellar solutions and open-tubular capillaries**. *Analytical Chemistry* 1984, **56**:111-113.

2. Terabe S, Otsuka K, Ando T: **Electrokinetic chromatography with micellar solution and open-tubular capillary**. *Analytical Chemistry* 1985, **57**:834-841.

3. Sander LC, Wise SA: **Shape selectivity in reversed-phase liquid chromatography for the separation of planar and non-planar solutes**. *Journal of Chromatography* 1993, **656**:335-351.

4. Engelhardt H, Jungheim M: **Comparison and characterization of reversed phases**. *Chromatographia* 1990, **29**:59-68.

5. Neue UD, Serowik E, Iraneta P, Alden BA, Walter TH: **Universal procedure for the assessment of the reproducibility and the classification of silica-based reversed-phase packings I. Assessment of the reproducibility of reversed-phase packings**. *Journal of Chromatography, A* 1999, **849**:87-100.

6. Neue UD, Alden BA, Walter TH: **Universal procedure for the assessment of the reproducibility and the classification of silica-based reversed-phase packings II. Classification of reversed-phase packings**. *Journal of Chromatography, A* 1999, **849**:101-116.

7. Claessens HA: **Trends and progress in the characterization of stationary phases for reversed-phase liquid chromatography**. *TrAC, Trends in Analytical Chemistry* 2001, **20**:563-583.

8. Cruz E, Euerby MR, Johnson CM, Hackett CA: **Chromatographic classification of commercially available reverse-phase HPLC columns**. *Chromatographia* 1997, **44**:151-161.

9. Visky D, Heyden Yvan V, Ivanyi T, Baten P, De Beer J, Kovacs Z, Noszal B, Roets E, Massart Desire L, Hoogmartens J: **Characterization of reversed-phase liquid chromatographic columns by chromatographic tests. Evaluation of 36 test parameters: repeatability, reproducibility and correlation**. *Journal of chromatography. A* 2002, **977**:39-58.

10. Euerby MR, Petersson P: *LC-GC Europe* 2000, **13,**:665.

11. Euerby MR, Petersson P: **Chromatographic classification and comparison of commercially available reversed-phase liquid chromatographic columns using principal component analysis**. *Journal of Chromatography, A* 2003, **994**:13-36.

12. Ivanyi T, Vander Heyden Y, Visky D, Baten P, De Beer J, Lazar I, Massart DL, Roets E, Hoogmartens J: **Minimal number of chromatographic test parameters for the characterization of reversed-phase liquid chromatographic stationary phases**. *Journal of Chromatography, A* 2002, **954**:99-114.

13. Li J, Cai B: **Evaluation of the retention dependence on the physicochemical properties of solutes in reversed-phase liquid chromatographic linear gradient elution based on linear solvation energy relationships**. *Journal of chromatography. A* 2001, **905**:35-46.

14. Tan LC, Carr PW, Abraham MH: **Study of retention in reversed-phase liquid chromatography using linear solvation energy relationships. I. The stationary phase**. *Journal of Chromatography, A* 1996, **752**:1-18.

15. Zhao J, Carr PW: **Comparison of the retention characteristics of aromatic and aliphatic reversed phases for HPLC using linear solvation energy relationships**. *Analytical Chemistry* 1998, **70**:3619-3628.

16. Tan LC, Carr PW: **Study of retention in reversed-phase liquid chromatography using linear solvation energy relationships. II. The mobile phase**. *Journal of Chromatography, A* 1998, **799**:1-19.

17. Reta M, Carr PW, Sadek PC, Rutan SC: **Comparative study of hydrocarbon, fluorocarbon, and aromatic bonded RP-HPLC stationary phases by linear solvation energy relationships**. *Analytical Chemistry* 1999, **71**:3484-3496.

18. Abraham MH, Roses M: **Hydrogen bonding. 38. Effect of solute structure and mobile phase composition on reversed-phase high-performance liquid chromatographic capacity factors**. *Journal of Physical Organic Chemistry* 1994, **7**:672-684.

19. Abraham MH, Roses M, Poole CF, Poole SK: **Hydrogen bonding. 42. characterization of reversed-phase high-performance liquid chromatographic C18 stationary phases**. *Journal of Physical Organic Chemistry* 1997, **10**:358-368.

20. Kim IW, Lee HS, Lee YK, Jang MD, Park JH: **Selectivity of amino-, cyano- and diol-bonded silica in reversed-phase liquid chromatography**. *Journal of Chromatography, A* 2001, **915**:35-42.

21. Szepesy L: **Evaluation of column characteristics in RPLC using linear solvation energy relationships (LSERs)**. *Journal of Separation Science* 2003, **26**:201-214.

22. Liu Y, Guo Y-f, Wang H, Xing Y-j, Zuo Y-m: **Evaluation of octadecene-polybutadiene-coated zirconia stationary phase based on linear solvation energy relationships**. *Journal of Liquid Chromatography & Related Technologies* 2003, **26**:723-736.

23. Wilson NS, Nelson MD, Dolan JW, Snyder LR, Wolcott RG, Carr PW: **Column selectivity in reversed-phase liquid chromatography. I. A general quantitative relationship**. *Journal of Chromatography, A* 2002, **961**:171-193.

24. Wilson NS, Nelson MD, Dolan JW, Snyder LR, Carr PW: **Column selectivity in reversed-phase liquid chromatography. II. Effect of a change in conditions**. *Journal of Chromatography, A* 2002, **961**:195-215.

25. Wilson NS, Dolan JW, Snyder LR, Carr PW, Sander LC: **Column selectivity in reversed-phase liquid chromatography. III. The physico-chemical basis of selectivity**. *Journal of Chromatography, A* 2002, **961**:217-236.

26. Gilroy JJ, Dolan JW, Snyder LR: **Column selectivity in reversed-phase liquid chromatography IV. Type-B alkyl-silica columns**. *Journal of Chromatography, A* 2003, **1000**:757-778.

27. Gilroy JJ, Dolan JW, Carr PW, Snyder LR: **Column selectivity in reversed-phase liquid chromatography V. Higher metal content (type-A) alkyl-silica columns**. *Journal of Chromatography, A* 2004, **1026**:77-89.

28. Wilson NS, Gilroy J, Dolan JW, Snyder LR: **Column selectivity in reversed-phase liquid chromatography VI. Columns with embedded or end-capping polar groups**. *Journal of Chromatography, A* 2004, **1026**:91-100.

29. Marchand DH, Croes K, Dolan JW, Snyder LR: **Column selectivity in reversed-phase liquid chromatography. VII. Cyanopropyl columns**. *Journal of chromatography. A* 2005, **1062**:57-64.

30. Marchand DH, Croes K, Dolan JW, Snyder LR, Henry RA, Kallury KMR, Waite S, Carr PW: **Column selectivity in reversed-phase liquid chromatography. VIII. Phenylalkyl and fluoro-substituted columns**. *Journal of Chromatography, A* 2005, **1062**:65-78.

31. Abraham MH: **Scales of solute hydrogen bonding: their construction and application to physicochemical and biochemical processes**. *Atual. Fis.-Quim. Org., [Conf. Latinoam. Fis.-Quim. Org.], 1st* 1991:89-109.

32. Poole CF, Poole SK: **Column selectivity from the perspective of the solvation parameter model**. *Journal of Chromatography, A* 2002, **965**:263-299.

33. Slonecker PJ, Li X, Ridgway TH, Dorsey JG: **Informational Orthogonality of Two-Dimensional Chromatographic Separations**. *Analytical Chemistry* 1996, **68**:682-689.

34. Ferguson PD, Goodall DM, Loran JS: **Systematic approach to links between separations in MEKC and reversed-phase HPLC**. *Analytical Chemistry* 1998, **70**:4054-4062.

35. Detroyer A, Vander Heyden Y, Cambre I, Massart DL: **Chemometric comparison of recent chromatographic and electrophoretic methods in a quantitative structure-retention and retention-activity relationship context**. *Journal of Chromatography, A* 2003, **986**:227-238.

36. Du CM, Valko K, Bevan C, Reynolds D, Abraham MH: **Rapid Gradient RP-HPLC Method for Lipophilicity Determination: A Solvation Equation Based Comparison with Isocratic Methods**. *Analytical Chemistry* 1998, **70**:4228-4234.

37. Abraham MH: **Application of solvation equations to chemical and biochemical processes**. *Pure and Applied Chemistry* 1993, **65**:2503-2512.

38. Dorsey JG, Khaledi MG: **Hydrophobicity Estimations by Reversed-Phase Liquid-Chromatography - Implications for Biological Partitioning Processes**. *Journal of Chromatography A* 1993, **656**:485-499.

39. Ishihama Y, Oda Y, Uchikawa K, Asakawa N: **Correlation of octanol-water partition coefficients with capacity factors measured by micellar electrokinetic chromatography**. *Chemical & Pharmaceutical Bulletin* 1994, **42**:1525-1527.

40. Herbert BJ, Dorsey JG: **n-Octanol-Water Partition Coefficient Estimation by Micellar Electrokinetic Capillary Chromatography**. *Analytical Chemistry* 1995, **67**:744-749.

41. Dinelli G, Mallegni R, Vicari A: **Micellar electrokinetic capillary chromatography as a method for the determination of n-octanol/water partition coefficients of pesticides**. *Electrophoresis* 1997, **18**:214-219.

42. Agbodjan AA, Bui H, Khaledi MG: **Study of solute partitioning in biomembrane-mimetic pseudophases by electrokinetic chromatography: Dihexadecyl phosphate small unilamellar vesicles**. *Langmuir* 2001, **17**:2893-2899.

43. Bailey DJ, Dorsey JG: **Linear solvation energy relationships of mixed micelles of sodium dodecyl sulfate and decanol: towards a better model of octanol/water partitioning**. *Journal of Chromatography, A* 2001, **919**:181-194.

44. Poole SK, Poole CF: **Separation methods for estimating octanol-water partition coefficients**. *Journal of Chromatography, B: Analytical Technologies in the Biomedical and Life Sciences* 2003, **797**:3-19.

45. Torres-Lapasio JR, Garcia-Alvarez-Coque MC, Roses M, Bosch E, Zissimos AM, Abraham MH: **Analysis of a solute polarity parameter in reversed-phase liquid chromatography on a linear solvation relationship basis**. *Analytica Chimica Acta* 2004, **515**:209-227.

46. Valko K: **Application of high-performance liquid chromatography based measurements of lipophilicity to model biological distribution**. *Journal of Chromatography, A* 2004, **1037**:299-310.

47. Hong M, Weekley B, Grieb SJ, Foley JP: **Electrokinetic chromatography using thermodynamically stable vesicles and mixed micelles formed from oppositely charged surfactants**. *Analytical Chemistry* 1998, **70**:1394-1403.

48. Jenke DR: **Liquid chromatographic estimation of octanol/water partition coefficients with a high efficiency, nonporous, ultrasmall particle size reverse phase stationary phase**. *Journal of Liquid Chromatography & Related Technologies* 1996, **19**:2227-2245.

49. Minick DJ, Brent DA, Frenz J: **Modeling octanol-water partition coefficients by reversed-phase liquid chromatography**. *Journal of Chromatography* 1989, **461**:177-191.

50. Vonk EC, Lewandowska K, Claessens HA, Kaliszan R, Cramers CA: **Quantitative structure-retention relationships in reversed-phase liquid chromatography using several stationary and mobile phases**. *Journal of Separation Science* 2003, **26**:777-792.

51. Marcus Y: **The Properties of Organic Liquids that are Relevant to their Use as Solvating Solvents**. *Chemical Society Reviews* 1993, **22**:409 - 416.

Table 6-1. Preset range for the LSER system parameter normalization in the UST

	b/v	a/v	s/v
I_{low}	-1.50	-0.80	-0.70
I_{high}	0.00	0.70	0.80

Table 6-2. Classifications of RPLC columns selectivity according to unified selectivity triangle.

Group ID.	Representative RPLC Columns	***b***	***a***	***s***
B	**361**[a]: 0.2% TEA Zobax C8 (50% MeOH)[b], **370**: Zobax C8 (50% TFE), **371**: 0.2% TFA Zobax C8 (50% TFE), **372**: 0.2% TEA Zobax C8 (50% TFE), **373**: 0.2% TEA 0.2% TFA Zobax C8 (50% TFE), **466**: Inersil ODS (TFE gradient), **493**: Luna C18 (TFE gradient), **494**: Mixed polymer/silica Xterra C18 (TFE gradient), **501**: Cyano-bonded silica (10% MeOH)	High	Low	Low
C	**49, 50, 78, 105, 144**: Spherisorb ODS 2 (MeOH or ACN), **100, 101** RSIL C18 LL and HL, **102, 103,104**: Partisil ODS 1, 2, 3 (30% MeOH), **106, 112**: μBondapak C18 (30% MeOH), **107**: Hypersil C18 (30% MeOH), **108**: Spherosil XOA, C18 (30% MeOH), **109**: Nucleosil C18 (30% MeOH), **110**: Nova Pac C18 (30% MeOH), **111**: Resolve C18 (30% MeOH), **113**: Zobax ODS (30% MeOH), **479, 480**: Novapak CN (MeOH/ACN gradient)	High	Medium	Low

D	**114,115,116,117,118,119**: Self-packed ODS columns (ACN), **240**: Nucleosil C8 (50% ACN), **260**: Spherisorb ODS-1 (50% ACN), **267**: Platinum EPS C8 (50 % ACN), **268**: Platinum EPS C18 (50% ACN), **279**: Shodex RP 18-413 (75% TFE)	Medium	High	Low
E	**41**: J. T. Baker Diol (50% ACN), **168,169,170**: Spherisorb ODS-2 (THF), **201**: Inertsil CN (50% CN), **366,367,368, 369**: Zorbax C8 (50% THF), **374**: Lichrosorb Diol (25% MeOH), **384**: PS-ZrO2 (50% ACN), **385**: PS-ZrO2 (40% ACN), **390**: PBD-ZrO2 (50% ACN), **442,443**: PBSO (MeOH), **468**: Inersil ODS (THF gradient)	Low	Medium	Medium
F	**378**: Jordi RP-C18 (75% MeOH), **380,381,382,383**: PRP-1 (ACN), **447, 448, 484**: PLRP-S 100 (i-propanol, ACN)	Low	Low	High
A	All the remaining RPLC columns	Medium	Medium	Medium

a: The numbers are corresponding to the columns IDs in the Appendix I.

b: The solvents in the parenthesis and water comprise of the binary solvent systems

c: TEA = Triethyl amine, TFA = Trifluoroacetic acid, MeOH = Methanol, ACN = Acetonitrile, THF = Tetrahydro Furan,

Table 6-3 Solvatochromic parameters of the solvents in the study [51].

Solvent	α	β	π
Water	1.17	0.47	1.09
Methanol (MeOH)	0.93	0.62	0.60
i-propanol (i PrOH)	0.76	0.84	0.48
Pentanol (PeOH)	0.84	0.86	0.40
Acetonitrile (ACN)	0.19	0.31	0.75
Tetrahydra Furan (THF)	0.00	0.55	0.58
Trifluoro Ethanol (TFE)	1.61	0.00	0.73
Hexafluoro Isopropanol (HFIP)	1.96	0.00	0.65

Table 6-4 Test solutes for evaluation of the likeness of phase selectivity.

	Solute	E	S	A	V	B
1	Benzene	0.61	0.52	0.00	0.72	0.14
2	Toluene	0.60	0.52	0.00	0.86	0.14
3	Ethylbenzene	0.61	0.51	0.00	1.00	0.15
4	Propylbenzene	0.60	0.50	0.00	1.14	0.15
5	Butylbenzene	0.60	0.51	0.00	1.28	0.15
6	o-xylene	0.66	0.56	0.00	1.00	0.16
7	Naphthalene	1.34	0.92	0.00	1.09	0.20
8	Iodobenzene	1.19	0.82	0.00	0.98	0.12
9	Chlorobenzene	0.72	0.65	0.00	0.84	0.07
10	Bromobenzene	0.88	0.73	0.00	0.89	0.09
11	1-methylnaphthalene	1.34	0.90	0.00	1.23	0.20
12	4-chlorotoluene	0.71	0.67	0.00	0.98	0.07
13	4-bromotoluene	0.88	0.74	0.00	1.03	0.09
14	Acetophenone	0.82	1.01	0.00	1.01	0.48
15	Propyrophenone	0.80	0.95	0.00	1.15	0.51
16	Butyrophenone	0.80	0.95	0.00	1.30	0.51
17	Valerophenone	0.80	0.95	0.00	1.44	0.50
18	Hexarophenone	0.72	0.95	0.00	1.58	0.50
19	Nitrobenzene	0.87	1.11	0.00	0.89	0.28
20	3-chloro acetophenone	0.92	1.07	0.00	1.14	0.40
21	Methyl-2methylbenzoate	0.77	0.87	0.00	1.21	0.43
22	4-chloroacetophenone	0.96	1.09	0.00	1.14	0.44
23	Ethyl benzoate	0.69	0.85	0.00	1.21	0.46
24	Methylbenzoate	0.73	0.85	0.00	1.07	0.46
25	Propyl benzoate	0.68	0.80	0.00	1.35	0.46
26	1-chloro-4-nitrobenzene	0.98	1.17	0.00	1.01	0.25
27	Phenyl acetate	0.66	1.13	0.00	1.07	0.54
28	Benzonitrile	0.74	1.11	0.00	0.87	0.33
29	Benzyl chloride	0.82	0.82	0.00	0.98	0.33
30	Phenol	0.81	0.89	0.60	0.78	0.30
31	3-chlorophenol	0.91	1.06	0.69	0.90	0.15
32	Resorcinol	0.98	1.00	1.10	0.83	0.58
33	3-methyl phenol	0.82	0.88	0.57	0.92	0.34
34	Benzyl alcohol	0.80	0.87	0.33	0.92	0.56
35	4-ethyl phenol	0.80	0.90	0.55	1.06	0.36
36	4-iodophenol	1.38	1.22	0.68	1.03	0.20
37	4-fluorophenol	0.67	0.97	0.63	0.79	0.23
38	Benzaldehyde	0.82	1.00	0.00	0.87	0.39
39	3-nitrophenol	1.05	1.57	0.79	0.95	0.23
40	Phenethyl alcohol	0.78	0.83	0.30	1.06	0.66
41	3,5-dimethyl phenol	0.82	0.84	0.57	1.06	0.36
42	4-methyl benzyl alcohol	0.81	0.88	0.33	1.06	0.60
43	3-bromo phenol	1.06	1.15	0.70	0.95	0.16

Table 6-5 Selectivity rankings for SDS, LiPFOS and Octanol-water.

Ranking	SDS			LiPFOS			Octanol-water		
	Phase	*d* [a]	R^2	Phase	*d*	R^2	Phase	*d*	R^2
1	**533**: LiPFOS/PeOH	0.014	0.97	**532**: LiPFOS (2)	0.033	0.99	**588**: DHP	0.011	0.97
2	**51**: Hypersil ODS (20% MeOH)	0.018	0.98	**500**: Fluorophase (ACN gradient)	0.042	0.93[b]	**570**: SPN	0.014	0.93
3	**70**: Bakerbond C18 (70% MeOH)	0.019	0.97	**477**: Fluoro Octyl (ACN gradient)	0.043	0.94[b]	**566**: ALE	0.015	0.91
4	**52**: Hypersil ODS (30% MeOH)	0.020	0.97	**535**: LiPFOS (3)	0.047	0.97	**544**: C16TAB	0.019	0.92
5	**121:** Hypersil ODS (75% MeOH)	0.021	0.94	**86**: ERC-1000 ODS (90% ACN)	0.052	0.92[b]	**536**: SC	0.019	0.99
6	**560**: SDSu	0.021	0.99	**159**: ERC-1000 ODS (90% ACN)	0.055	0.92[b]	**569**: SMN	0.020	0.92
7	**571**: STS	0.022	0.99	**540**: LiDS / LiPFOS	0.062	0.95	**145**: YMCPack ODS (30% ACN)	0.020	0.98
8	**12**: J. T. Baker ODS (50% MeOH)	0.022	0.97	**437**: PoEt Polymeric Phase (15% MeOH)	0.075	0.98	**565**: LMT	0.027	0.92
9	**10**: Capcell Pak C18 (50% MeOH)	0.023	0.93	**524**: LiPFOS / HFIP	0.078	0.89	**567**: SLN	0.029	0.91

10	**71**: Bakerbond C18 (100% MeOH)	0.024	0.97	**534**: LiPFOS / HFIP (2)	0.085	0.97	**520**: Micro Emulsion	0.030	0.99
11	**573**: SDecs	0.024	0.98	**416**: 2(C6H5) (45% ACN)	0.088	0.94	**589**: DHP / Cholesterol	0.034	0.98
12	**165**: Unisil C18 (70% ACN)	0.024	0.98	**414**: 2(C6H5) (55% ACN)	0.088	0.94	**558**: pDHCHAT-33	0.035	0.96
13	**91**: Unisil C18 (60% ACN)	0.025	0.98	**525**: LiPFOS / FPeOH	0.090	0.85	**568**: SLN (2)	0.037	0.90
...									
598	**378**: Jordi RP–C18 (75% MeOH)	0.63	0.78	**378**: Jordi RP–C18 (75% MeOH)	0.582	0.52	**379**: Shodex RP18-413 (75% TFE)	0.607	0.81
599	**381**: PRP-1 (70% ACN)	0.66	0.76	**379**: Shodex RP18-413 (75% TFE)	0.659	0.37	**381**: PRP-1 (80% ACN)	0.684	0.76
600	**380**: PRP-1 (80% ACN)	1.00	0.74	**380**: PRP-1 (80% ACN)	0.879	0.51	**380**: PRP-1 (70% ACN)	1.057	0.74

Table 6-6 Contributions of system parameters to principal components (eigenvectors).

	PC1	PC2	PC3	PC4	PC5
v	0.55	-0.21	0.36	0.03	0.72
b	-0.54	0.22	-0.41	-0.15	0.69
a	0.02	0.81	0.49	-0.32	-0.01
s	-0.49	-0.02	0.52	0.69	0.08
e	0.40	0.50	-0.44	0.63	0.03

Table 6-7 Eigenvalues and variances explained by principal components (PC)

	PC1	PC2	PC3	PC4	PC5
Eigenvalues	2.55	1.18	0.77	0.36	0.13
Cumulated variance (%)	51.02	74.66	90.16	97.44	100.00

Table 6-8 Identifications of various phases in the end node of hierarchical clustering.

End node [a]	Phase ID [b]
1	1, 28, 34, 36, 37, 48, 57, 58, 59, 66, 67, 74, 75, 83, 84, 85, 89, 90, 97, 98, 99, 101, 103, 105, 108, 110, 113, 114, 115, 116, 117, 118, 119, 121, 125, 126, 127, 134, 135, 136, 143, 148, 151, 152, 156, 157, 158, 162, 163, 170, 181, 182, 184, 185, 186, 187, 190, 191, 192, 193, 194, 195, 208, 209, 210, 211, 212, 213, 215, 216, 217, 220, 221, 222, 224, 228, 229, 230, 231, 232, 233, 234, 235, 236, 237, 238, 239, 241, 242, 243, 244, 245, 246, 248, 254, 255, 256, 257, 259, 261, 263, 266, 270, 271, 274, 277, 278, 281, 282, 285, 286, 287, 288, 295, 298, 300, 302, 304, 306, 307, 308, 311, 325, 327, 328, 332, 334, 335, 336, 337, 339, 342, 348, 350, 353, 354, 356, 357, 366, 367, 368, 369, 376, 389, 398, 399, 405, 409, 410, 415, 416, 421, 428, 429, 459, 460, 461, 462, 495, 496, 498, 499, 500, 518.
2	2, 4, 5, 7, 19, 403, 404, 406, 407, 408, 414, 418, 419, 420, 422, 423, 424, 425, 426, 427, 437, 438, 439, 497
3	3, 8, 9, 10, 14, 45, 46, 52, 53, 64, 65, 69, 87, 120, 123, 124, 129, 130, 140, 141, 160, 359, 360, 362, 430, 431, 432, 512, 513, 514, 515, 541, 542
4	4, 51, 63, 68, 80, 122, 128, 396, 489, 490, 491, 492, 520, 543
5	5, 79, 441, 519, 522, 526, 560, 561, 562, 571, 572, 573
6	6,20,39,40,41,49,50,60,61,62,71,76,77,78,86,91,92,93,94,100,102,104,106,107,109,111,112,137,138,139,144,153,154, 159,164,165,166,167,183,188,189,196,197,198,199,200,201,202,203,204,205,206,207,214,225,240,260,267,268,269,2 73, 276,274,275,388,400,401,411,412,413,417,434,435,436,463
7	169, 384, 385, 390, 442, 443, 552
8	361, 370, 371, 372, 372, 493,494
9	377, 378, 380, 381, 382, 383, 448

10	379
11	11, 21, 22, 23, 24, 26, 31, 35, 43, 44, 72, 81, 146, 149, 68, 264, 386, 387, 391, 395, 449, 450, 451, 452, 454, 455
12	12, 70, 88, 161,402, 440, 516, 517, 523, 524, 525, 533, 540, 545
13	13, 25, 27, 29, 30, 32, 33, 38, 47, 54, 55, 56, 73, 82, 95, 96, 131, 132, 133, 142, 147, 150, 155, 171, 172, 173, 174, 175, 176, 177, 178, 179, 180, 218, 219, 223, 226, 227, 247, 249, 250,251, 252, 253, 258, 262, 265, 272, 275, 279, 280, 283, 284, 289, 290, 291, 292, 293, 294, 296, 297, 299, 301, 303, 305, 309, 310, 312, 313, 314, 315, 316, 317, 318, 319, 320, 321, 322, 323, 324, 326, 329, 330, 331, 333, 338, 340, 341, 343, 344, 345, 346, 347, 349, 351, 352, 355, 358, 363, 364, 365, 392, 393, 394, 397, 453, 456, 457, 458, 502, 503, 504, 505, 506, 507, 508, 509, 510, 511
14	433
15	15, 18, 145, 549, 550, 551
16	16
17	17, 42, 446, 447
18	444, 539 546, 547, 548,
19	445, 521, 527, 528, 530, 536, 537, 538, 557, 563, 564, 565, 566, 567, 568, 569, 570, 591
20	464, 482
21	465, 474, 483
22	466
23	467,470
24	468
25	469

26	471, 472
27	473, 476, 485
28	475, 481
29	477
30	478
31	479, 480
32	484
33	486
34	487, 488
35	501
36	529, 600, 601
37	531, 532, 534, 535
38	544, 558, 559, 574, 575, 576, 583, 584, 585, 586, 587, 588, 589, 590, 592, 593, 594, 596, 597
39	553, 554, 555, 556, 581, 582, 595
40	577, 578, 579, 580, 598, 599

Note: The node numbers are identical with figure 6-11

b: Phase IDs are the same with Appendix I.

Figure Captions.

Figure 6-1 Correlations of LSER system parameters for 601 separation systems.

Figure 6-2 Classifications of RPLC columns in the unified selectivity triangle (UST).

Figure 6-3 Characterization of RPLC column selectivity in the UST with constant methanol/water (50/50) solvent systems.

Figure 6-4 Characterization of RPLC column selectivity in the UST with constant acetonitrile/water solvent systems.

Figure 6-5 Characterization of various organic solvent modification effects on selected RPLC columns in the UST.

Figure 6-6 κ-κ plot between LiPFOS micelle and a Fluorophase RPLC column.

Figure 6-7 Interpoint distances for 601 phases in the Euclidean space.

Figure 6-8 Contributions of LSER parameters to the principal components

Figure 6-9 Percent of variances explained by the principal components

Figure 6-10 Characterization of phase selectivity with first two principal components.

Figure 6-11 Characterization of phase selectivity with first three principal components

Figure 6-12 Classifications of phase selectivity with hierarchical Clustering.

Figure 6-13 Upper tail rule to determine the number of clusters.

Figure 6-14 Distance matrix for determination of number of clusters.

Figure 6-15 κ-κ plots for the comparison of phase similarity.

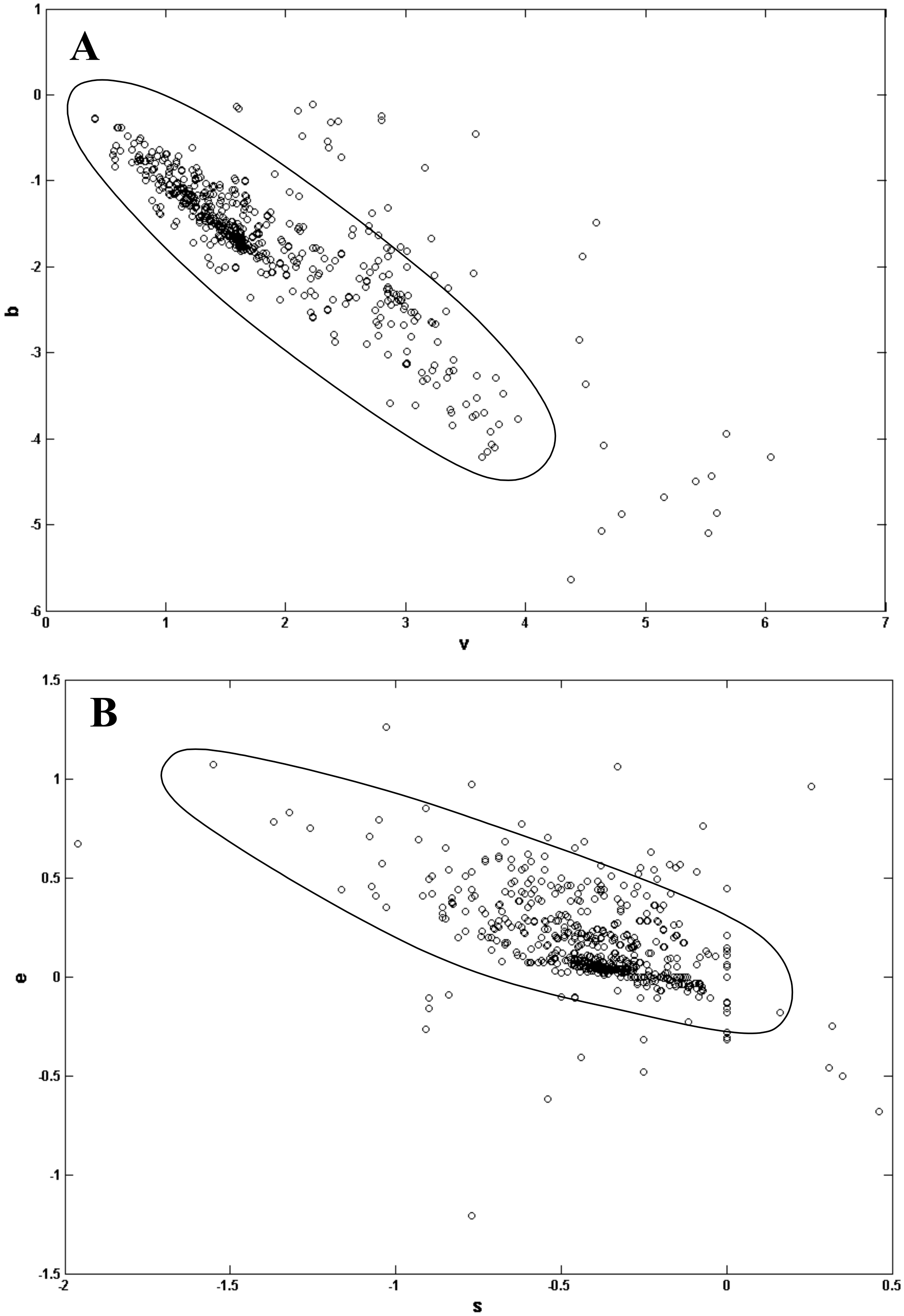
A
b
v
1
0
-1
-2
-3
-4
-5
-6
0
1
2
3
4
5
6
7
B
e
s
1.5
1
0.5
0
-0.5
-1
-1.5
-2
-1.5
-1
-0.5
0
0.5

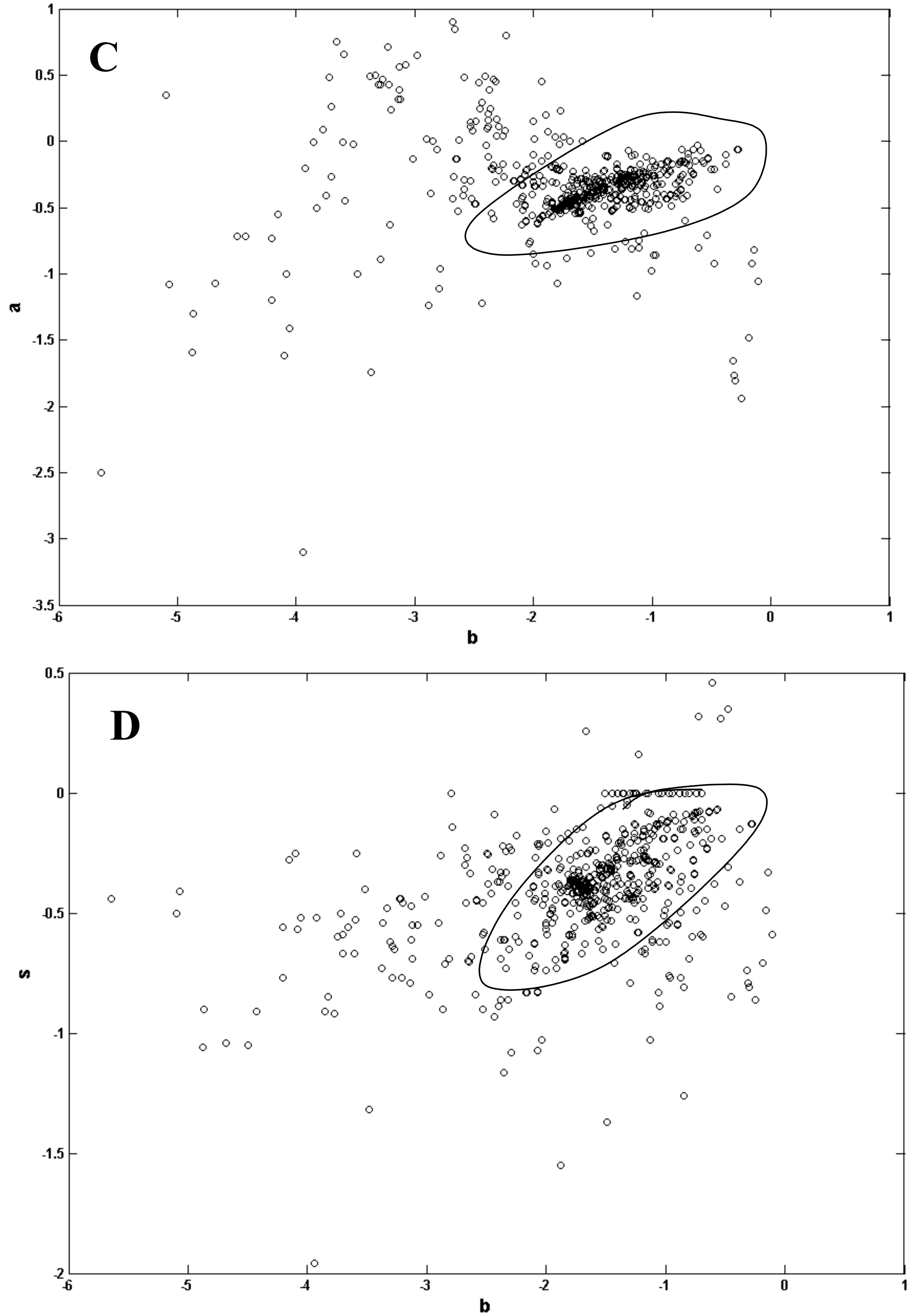

Figure 6-1 Correlations of LSER system parameters for 601 separation systems. A) *v* versus *b*, B) *s* versus *e*, C) *b* versus *a*, D) *b* versus *e*.

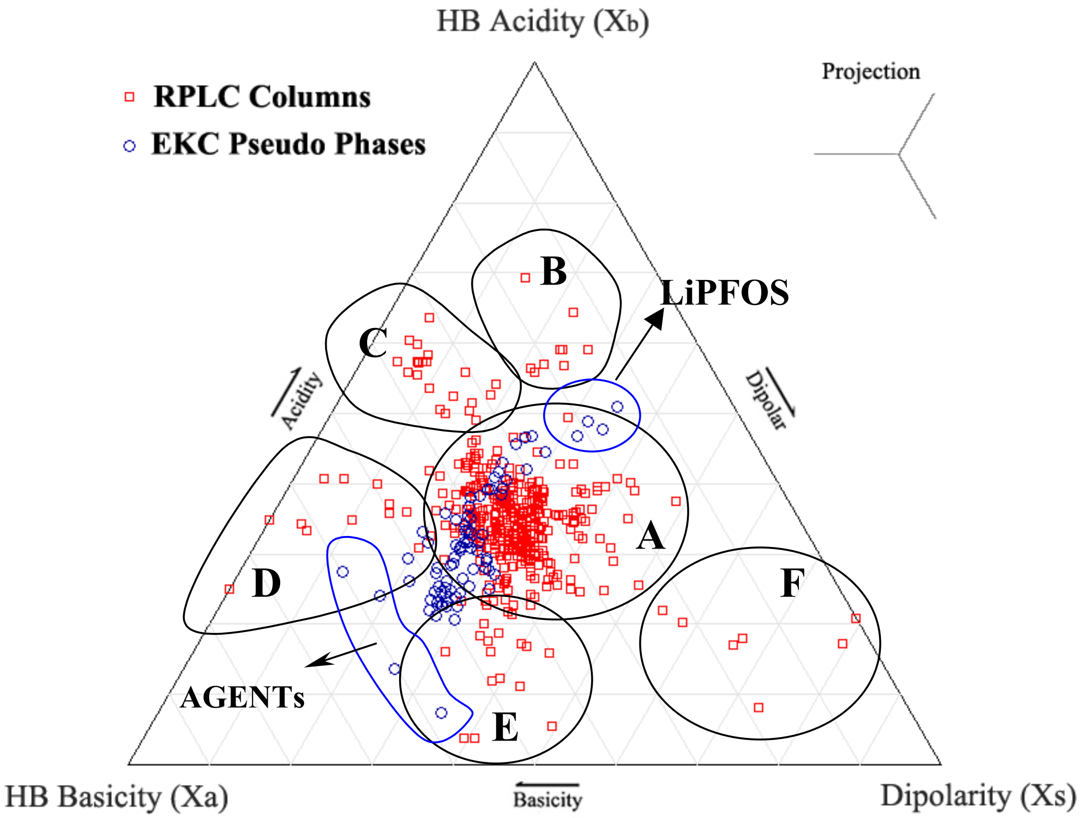

Figure 6-2 Classifications of RPLC columns in the unified selectivity triangle (UST).

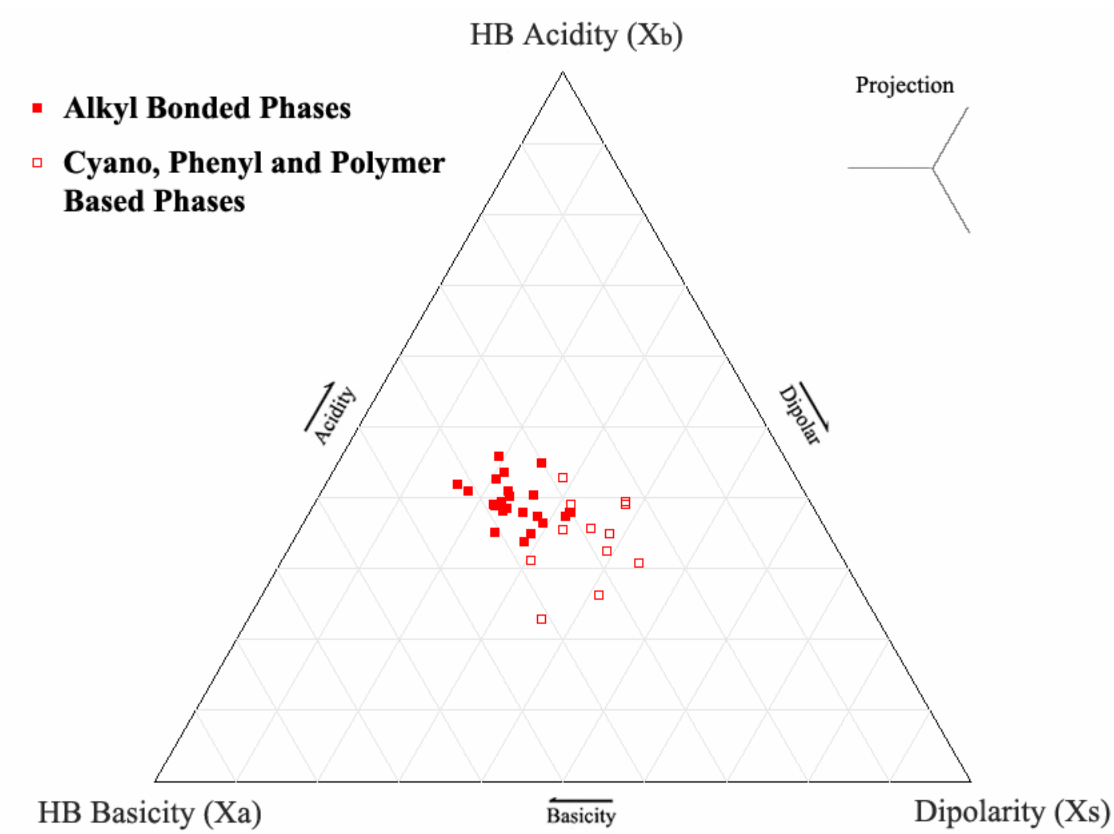

Figure 6-3 Characterization of RPLC column selectivity in the UST with constant methanol/water (50/50) solvent systems.

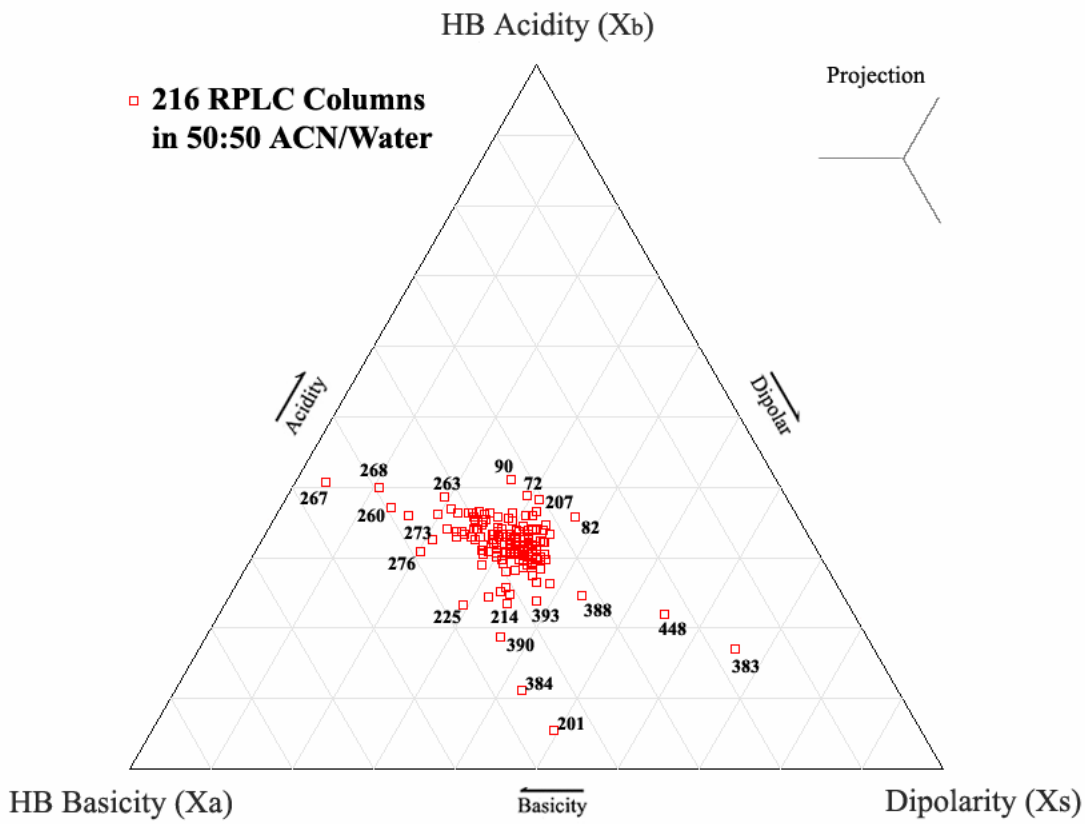

Figure 6-4 Characterization of RPLC column selectivity in the UST with constant acetonitrile/water solvent systems.

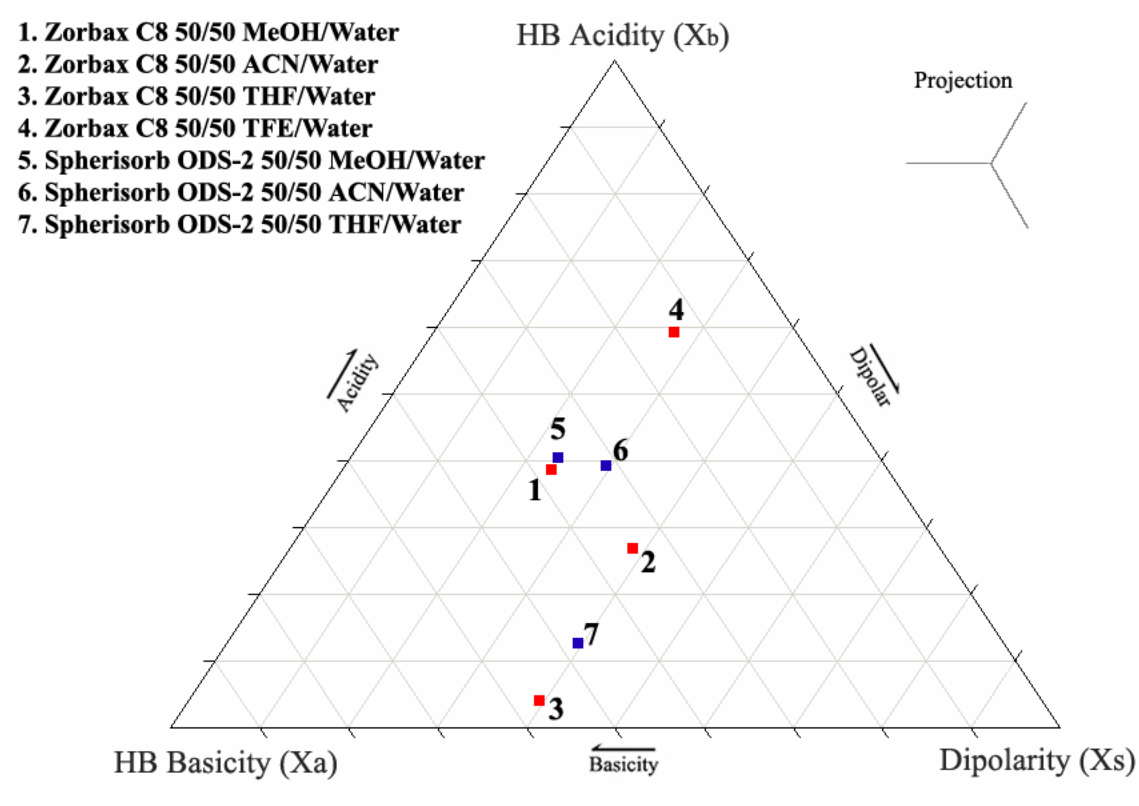

Figure 6-5 Characterization of various organic solvent modification effects on selected RPLC columns in the UST.

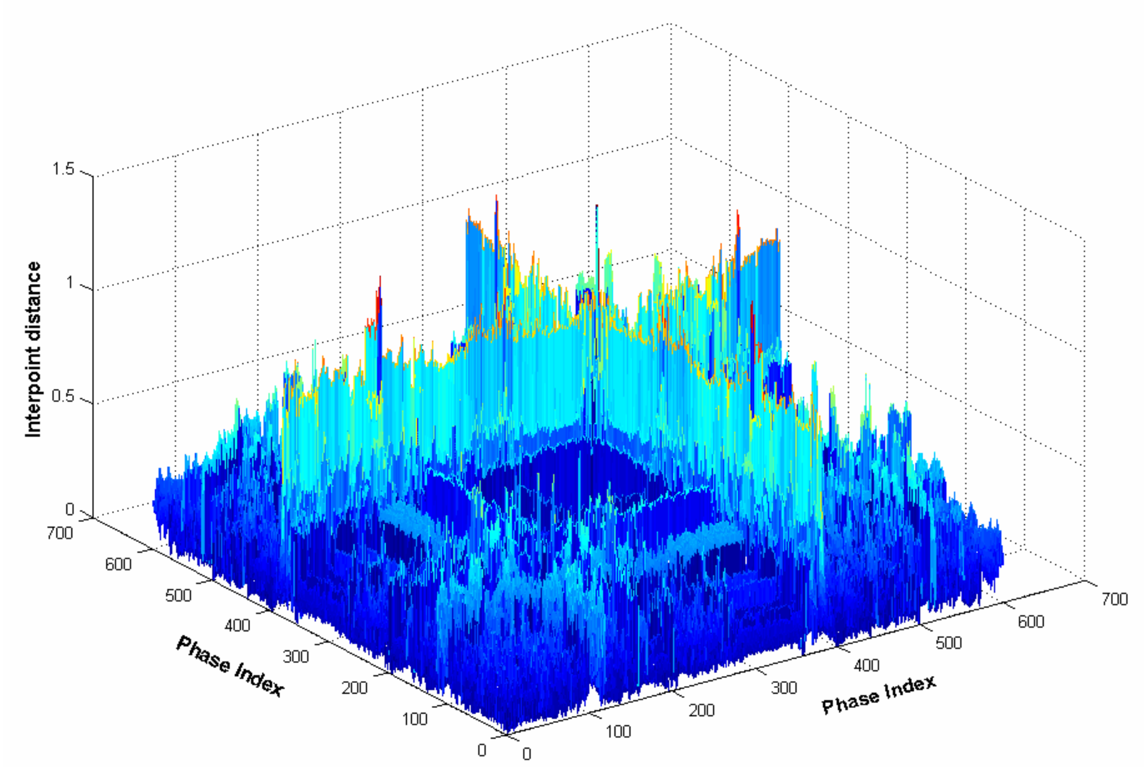

Figure 6-6 Interpoint distances for 601 RPLC column systems and EKC pseudo-phases in the Euclidean space.

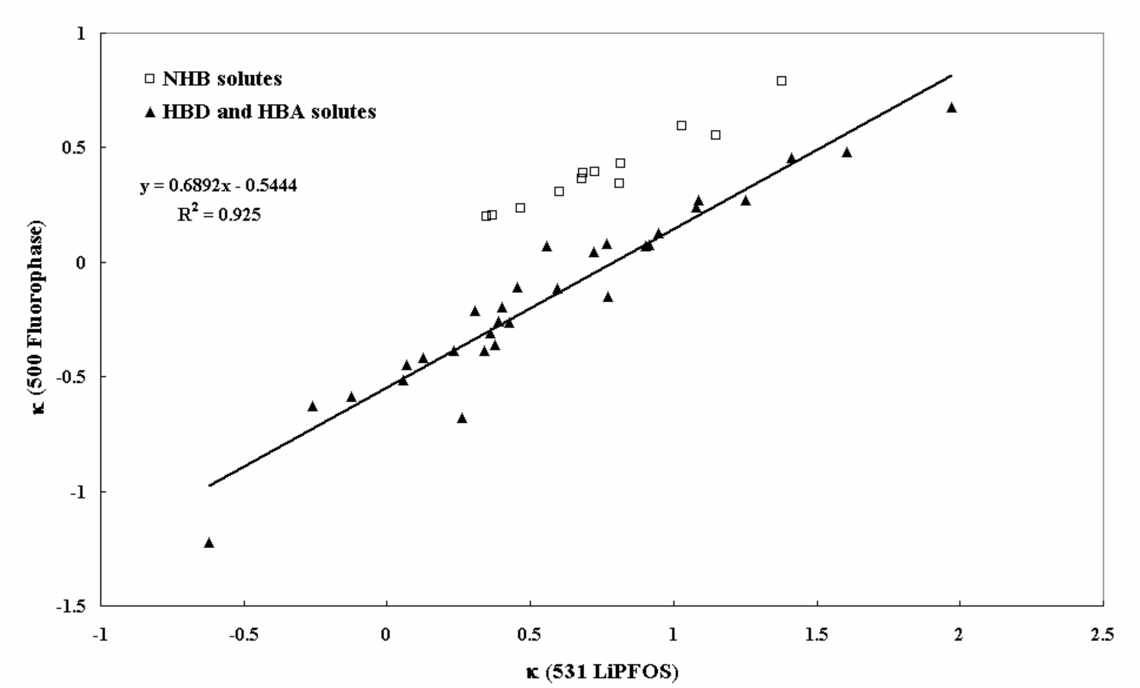

Figure 6-7 κ–κ plot of between LiPFOS micelle and a Fluorophase RPLC column, NHB solutes exhibit stronger retention with fluorophase column than with the LiPFOS micelles.

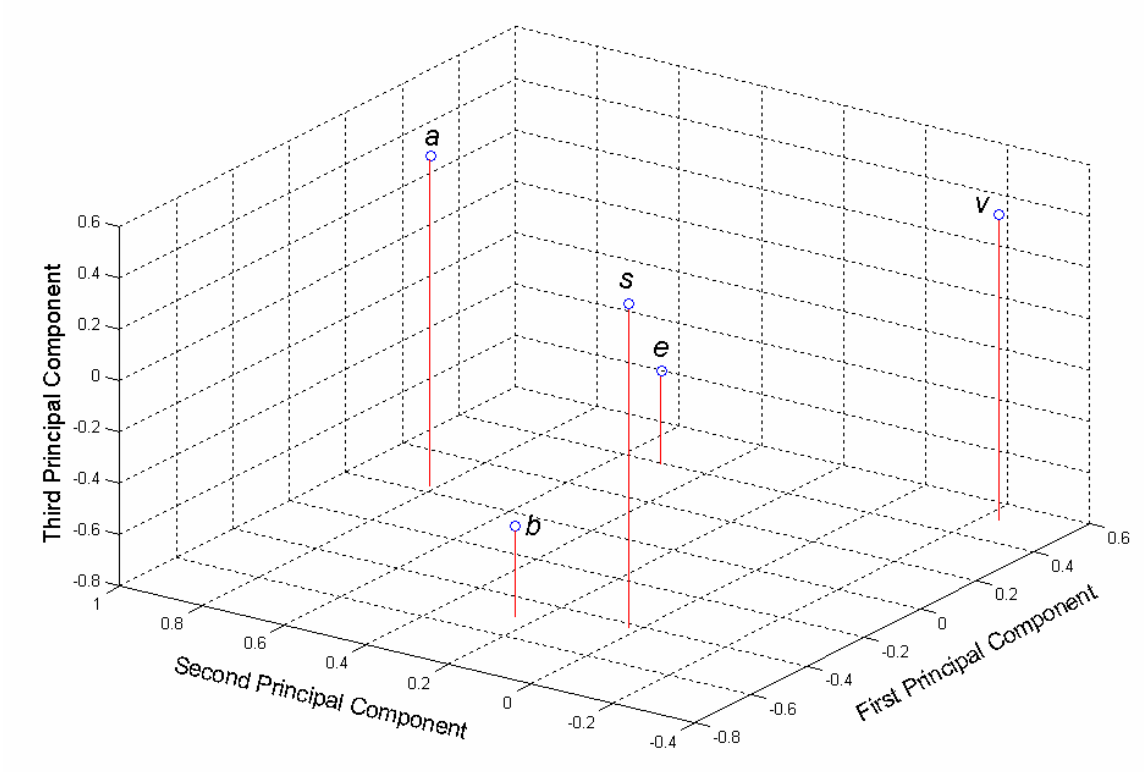

Figure 6-8 Contributions of the LSER parameters to the first three principal components.

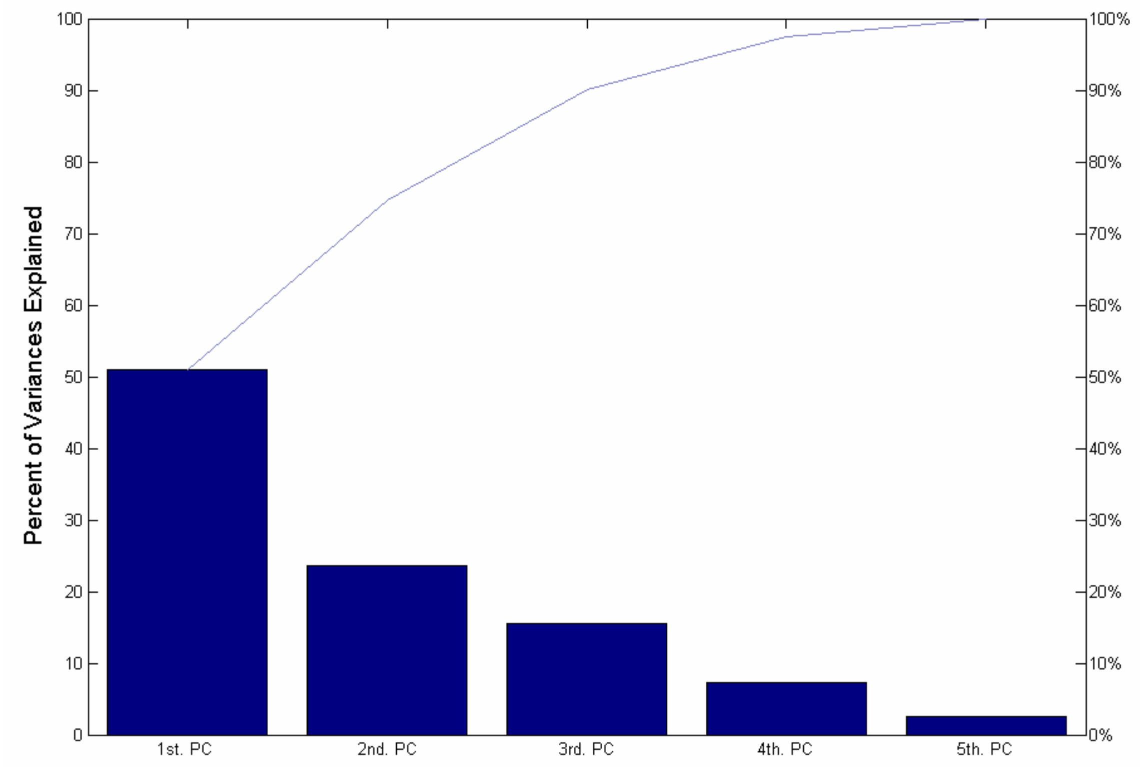

Figure 6-9 Percent of total variances explained by the principal components.

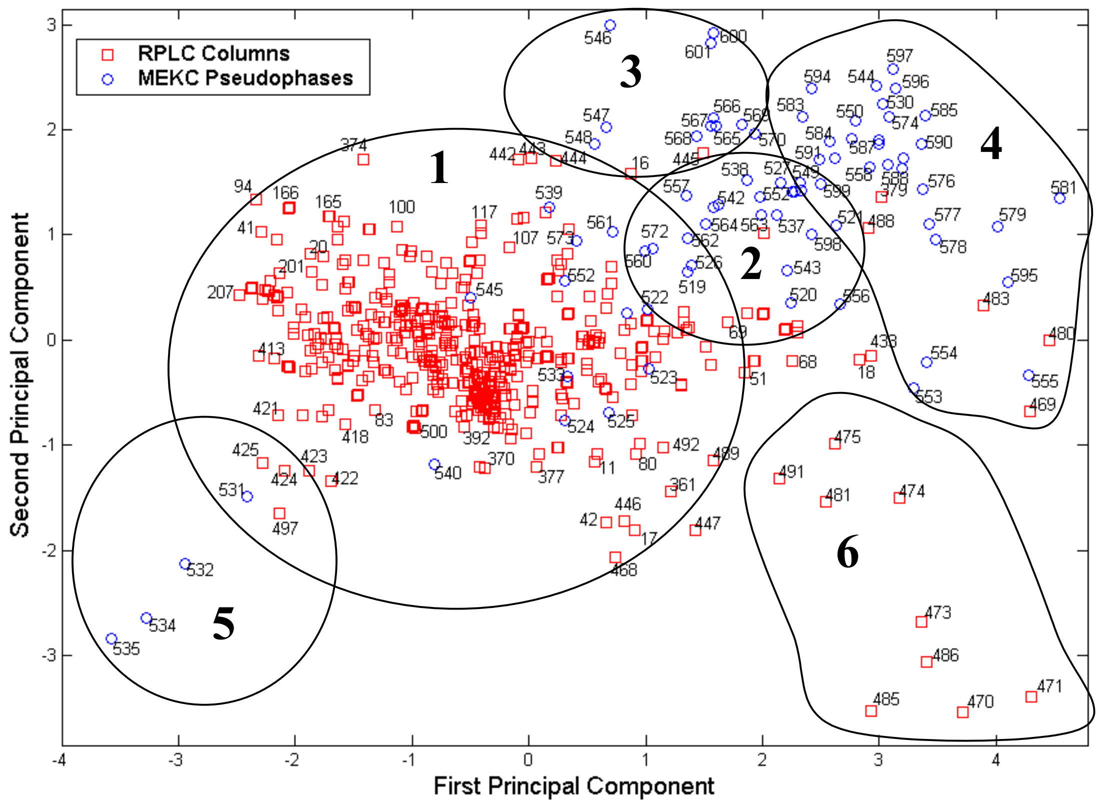

Figure 6-10 Characterization of the selectivities of 601 RPLC column systems and EKC pseudo-phases with the first two principal components.

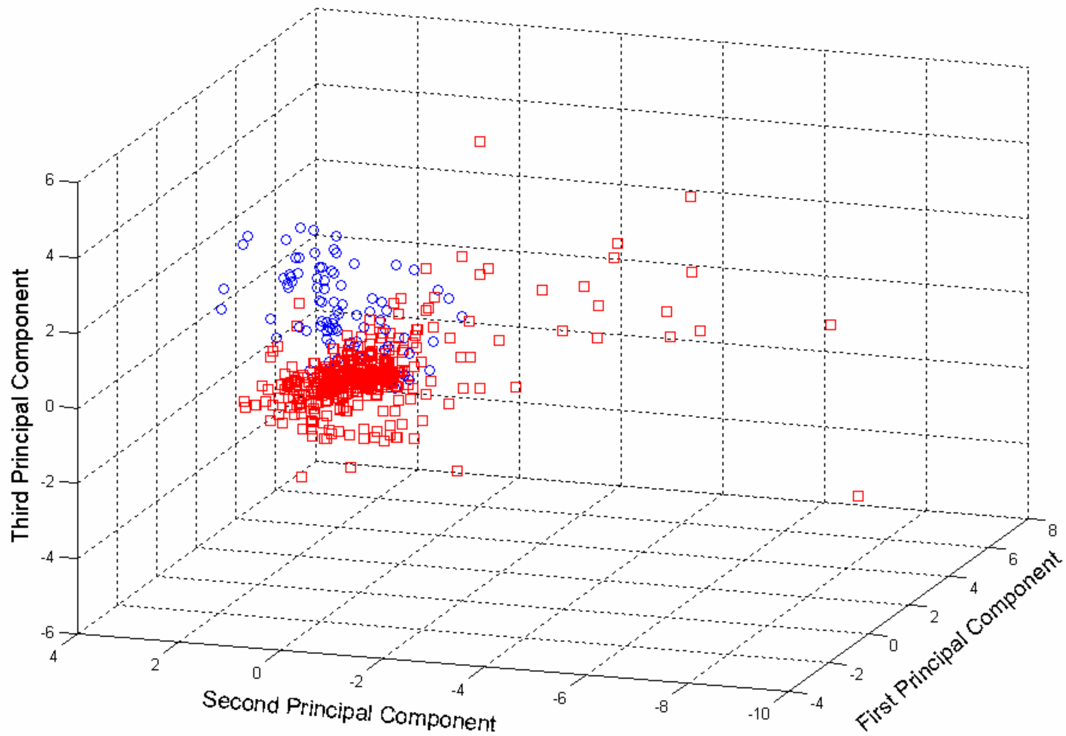

Figure 6-11 Characterization of the selectivities of 601 RPLC column systems and EKC pseudo-phases with the first three principal components.

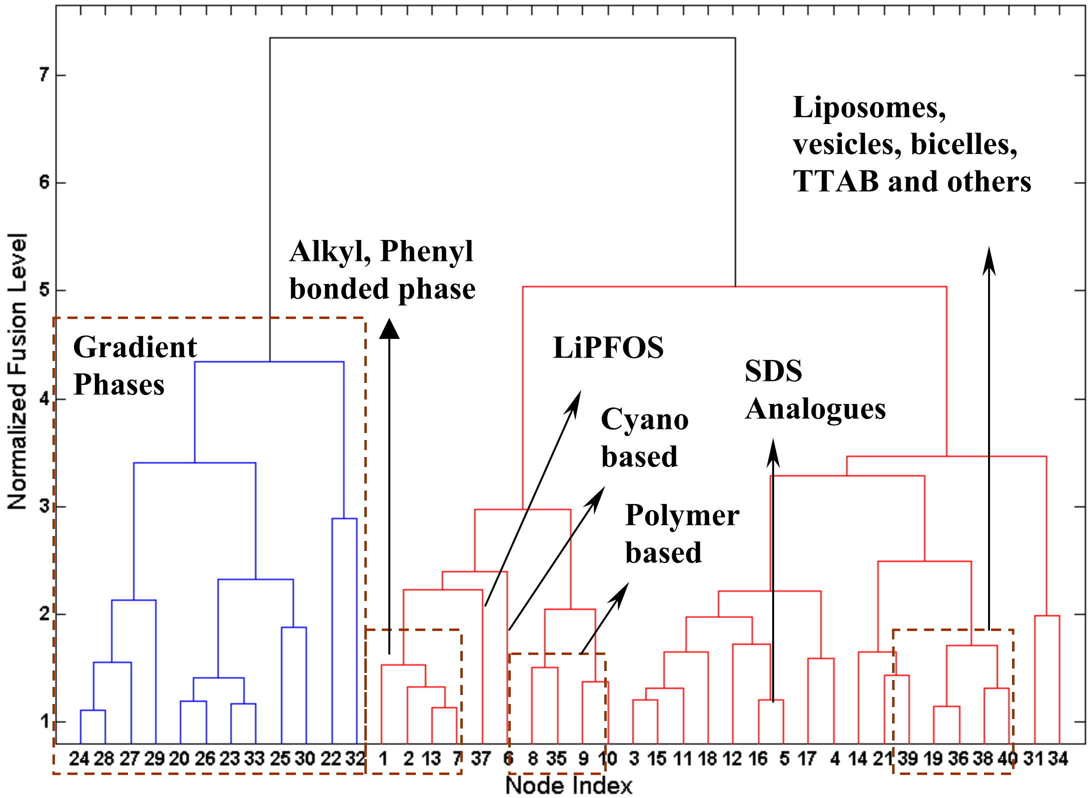

Figure 6-12 Classifications of the selectivities of 601 RPLC column systems and EKC pseudo-phases with hierarchical clustering.

(Note: The end node might represent multiple phases)

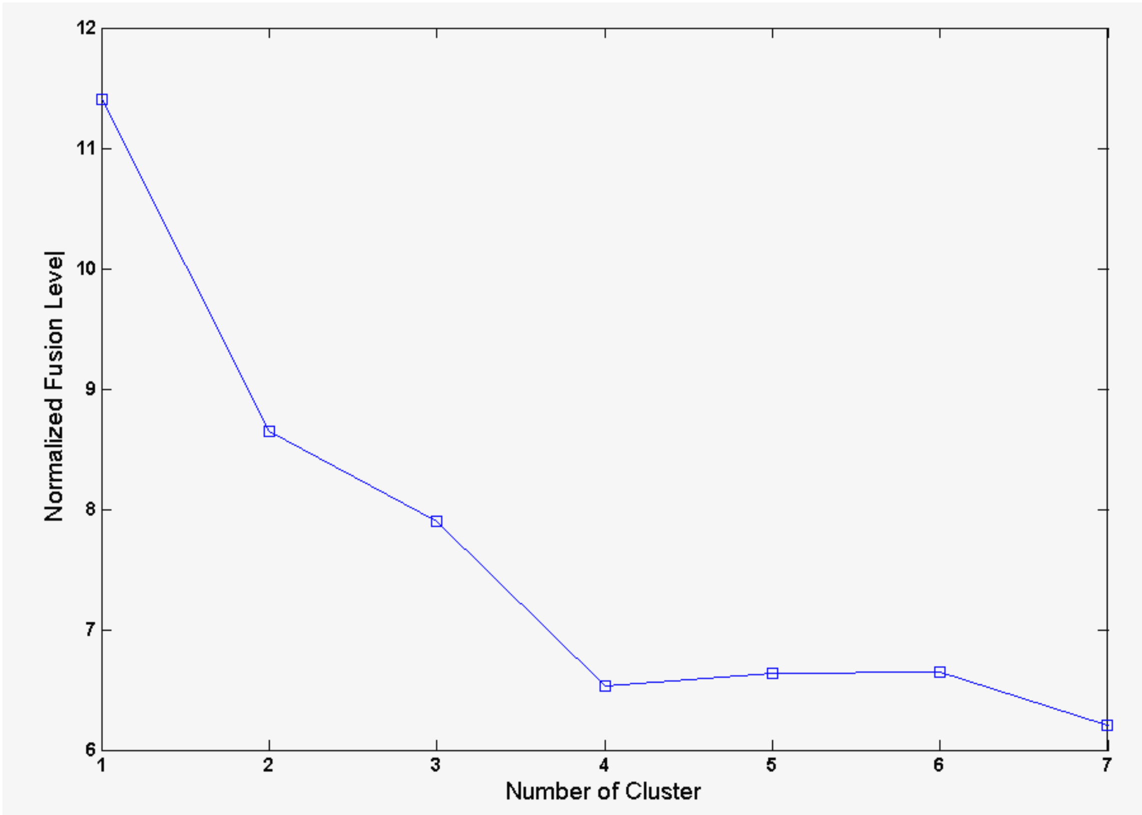

Figure 6-13 Upper-tail rule to determine the number of clusters in hierarchical clustering.

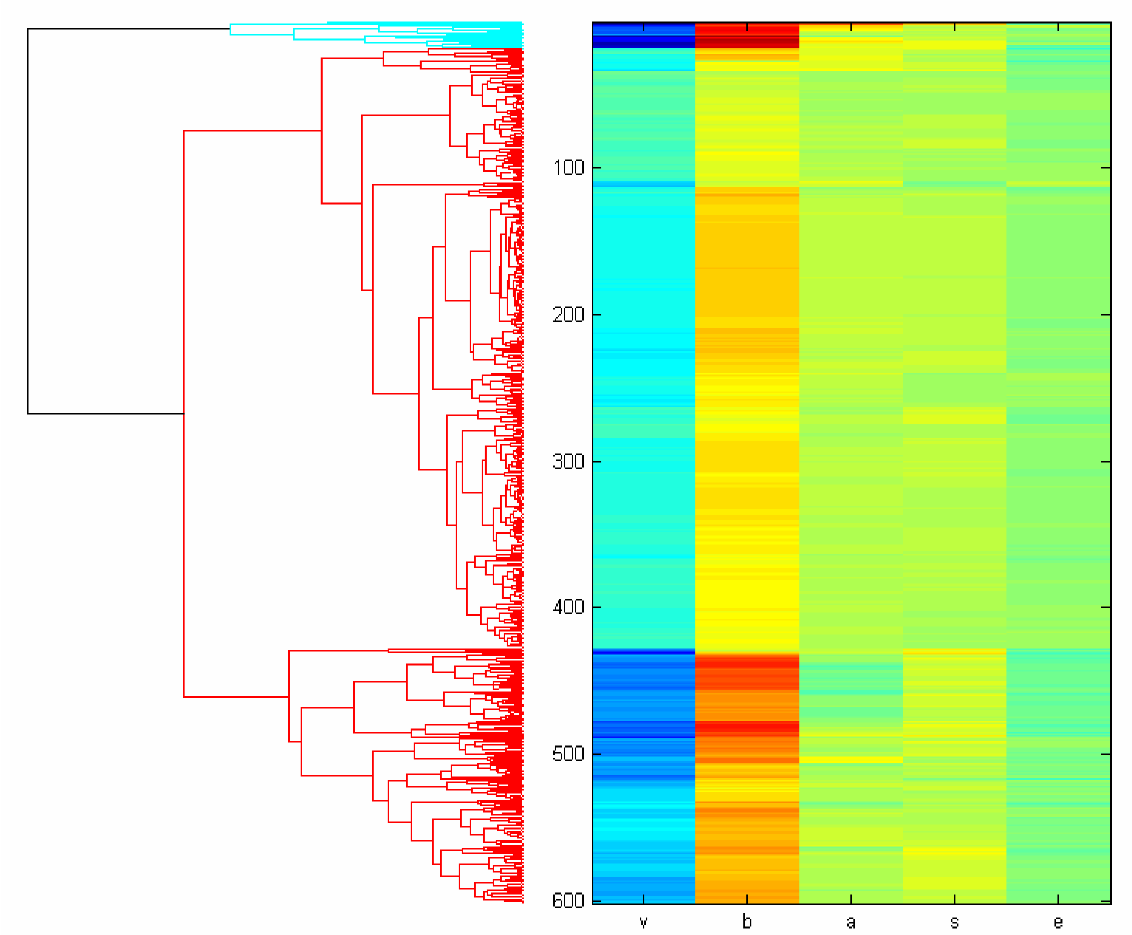

Figure 6-14 Distance matrix for determination of number of clusters in hierarchical clustering. (Similar color band in the distance matrix indicates that these objects belong to the same cluster, totally four color bands are distinguished in the plot)

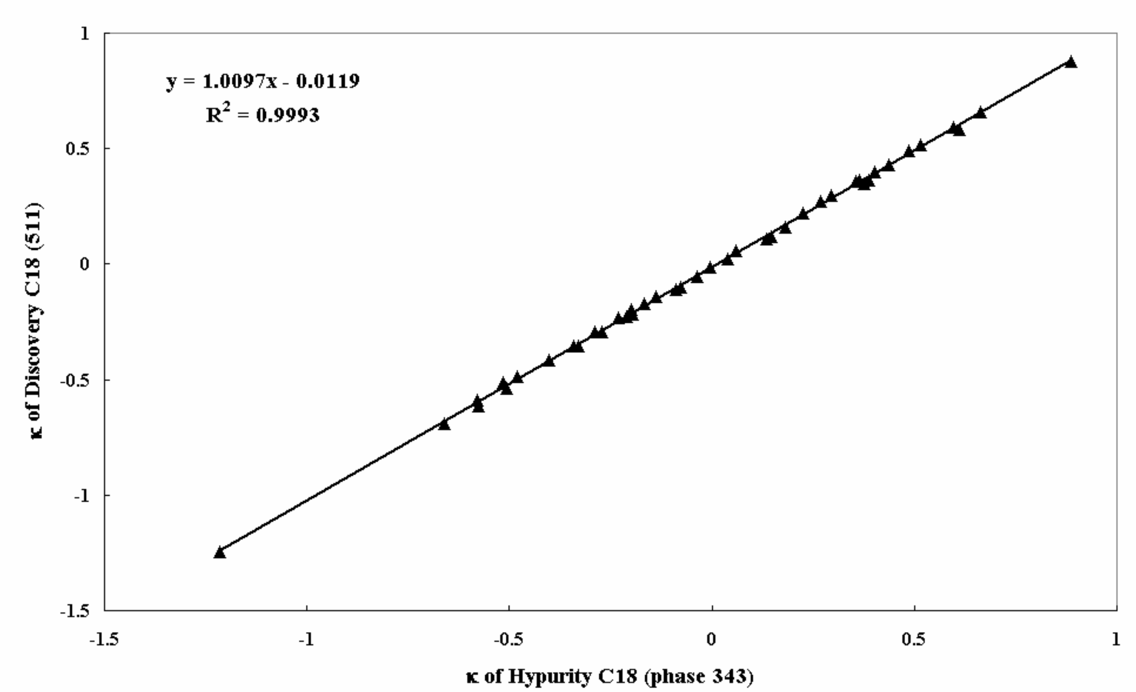

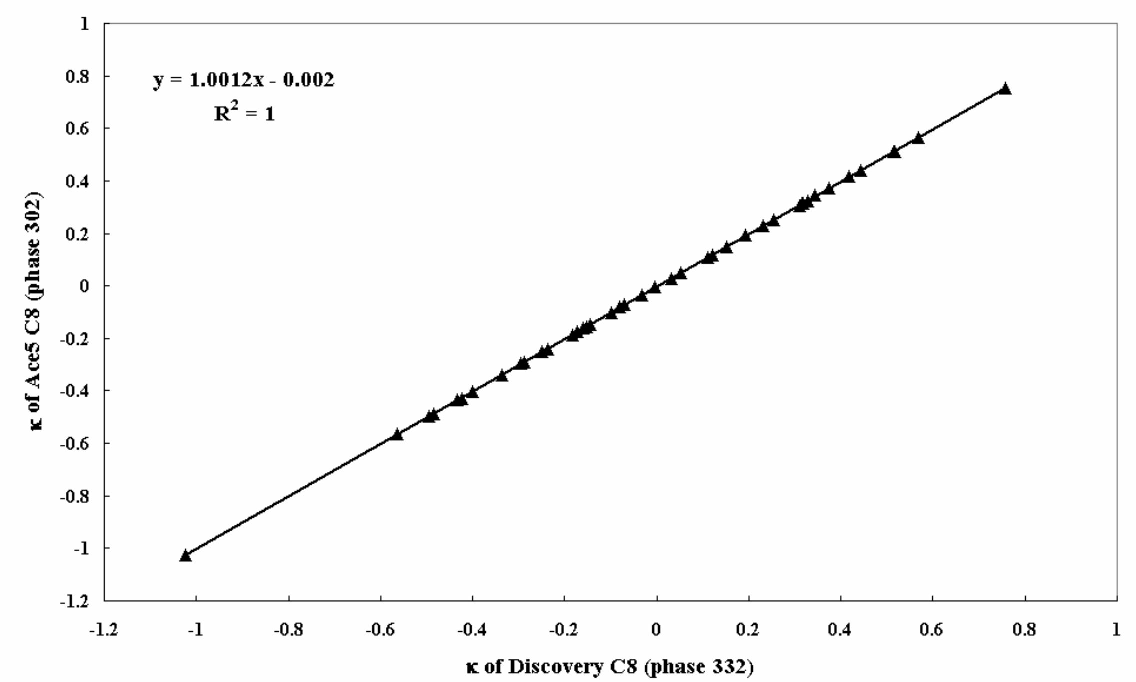

Figure 6-15 κ-κ plots for the comparison of phase similarity. Top plot: Hypurity C18 vs. Discovery C18. Bottom plot: Discovery C8 vs. Ace5 C8.

CHAPTER 7

FUTURE TRENDS

In our work, we have focused on the developments of novel schemes to characterize and classify phase selectivity for a wide variety of ‘stationary phases’ for MEKC and RPLC.

In chapter 2, we have found that organic solvents with hydrophobic moieties and functional polar headgroups could effectively manipulate the selective properties of micellar phases. Among those solvents, hexafluoro isopropanol (HFIP) and pentanol could selectively enhance the hydrogen bond acidity and hydrogen bond basicity respectively. However, those solvents, for example butyronitrile, hexanone and others, which were designed to manipulate the dipolarity of the micellar phases, did not work out as expected. This is probably due to the highly dipolar characteristics of water molecules as indicating by the solvatochromic parameter for water (π = 1.09).[1] Other than the dipolar solvents that we have investigated, there are several potential candidates that could possibly enhance the dipolarity of the micellar phase, such as 2-cyanopyridine (π = 1.20), tetramethyl-urea (π = 0.83) tetramethyl-guanidine (π = 0.76), tetramethyl sulfoxide (π = 1.06), su1folane (π = 0.98) and chlorinated acetonitrile (π = 1.01).

The combination of micellar selectivity triangle (MST) and chemometric methods has successfully characterized and classified the micellar selectivity in (MEKC). Polymeric micelles [2,3] demonstrate flexible controls of the phase selectivity by varying the side chain compositions. Moreover the reasonable stability with high content of organic solvent and compatibility with mass spectrometry are unmatched advantages compare to conventional micelles. The synthesis of novel polymeric micelles of high purity and diverse sidechain functionalities shall be a focus of the future developments of micellar phases.

The characterization and classification of phase selectivity are of great practical meaning. Our classification schemes could serve several different purposes such as the identification of phases with identical or similar selectivity for replacement, finding 'orthogonal' phases to enhance the capacity and resolution for the separation of vastly different compounds and provide guidelines for the optimization and refinement of a specific separation.

Chromatographic techniques, especially liquid-liquid partition chromatography, have been used for simulation of the partition process in various biological systems, mainly because of the short analysis time, high throughput ability, and tolerance of sample impurity. Previously in this lab, solutes partition coefficients measured from different pseudo-phases with EKC method have been used to correlate with the Octanol/water partition coefficients [4-6]. There are certainly more complicated biopartition processes such as drugs intestinal absorption [7], blood-brain distribution [8] etc that could be simulated with the partition model in EKC. The selectivity triangle in conjunction with hierarchical clustering and selectivity ranking system (Euclidean distance) offer useful tools for identifying 'liquid' phases with similar selectivity to these complex biological systems. There are also growing interests searching for 'orthogonal' phases to construct multiple dimension separations. With the implementation of the multiplexed capillary electrophoresis system, there are urgent needs for the developments of pseudo phases with 'orthogonal' selectivity to fully explore the strength of the multiplexed CE system. The combination of the selectivity triangle, hierarchical clustering and selectivity ranking system will great facilitate the selection process. Our selectivity triangle schemes also provide stepwise optimization strategy for the method development. For instance, three representative micellar phases, SDS, TTAB, and LiPFOS with significant different selectivities could be used to run trial separations for the initial stage. Depending on the quality of the trial separations, organic solvents (pentanol and HFIP) could be used to refine the separation.

Finally, we have laid the groundwork for the linkages between two powerful chromatographic techniques, RPLC and MEKC. We shall note that those linkages were established with mainly neutral solutes with limited range of size, in order to gain more in depth knowledge on the similarities and differences of the two techniques. One shall expand the sample size and diversity of the test compounds. There are other issues concerning the robustness of LSER parameters for RPLC columns. First, the physio-chemical properties of the reversed-phase columns, for example the purity of the solid support (trace metal impurity), the packing chemistries, the ligand surface coverage etc., all contributes to the differences of those nominally 'identical' columns. Second, columns degrade with the usage, as the early separations on a new column are often different from the successive separations after hundreds of injections. Third, different labs often work with different buffering systems, instrument setups, column rinse and maintaining procedures etc. Therefore, to ensure the quality of the selectivity classification, it is preferable to acquire the LSER characterization of RP columns in an independent lab with a standard measuring procedure. However, this will be a massive load of work. Considering to run 600 columns in three organic solvent systems (MeOH/water, THF/water, ACN/water) for three volume fractions (25%, 50% and 75%) at three pH buffering (4.0, 7.0 and 9.0) with 30 test solutes in triplicate measurements, one would work with $600 \times 3 \times 3 \times 3 \times 3 \times 30 = 1,458,000$ experiments. If the average run time for one separation is 20 minutes, one has to use more than 55 sleepless years to complete the database. Thus, the database of great importance shall be constructed in a collective effort from various sources such as academic, industrial and end-users with the application of a standard procedure.

REFERENCES

1. Marcus Y: **The Properties of Organic Liquids that are Relevant to their Use as Solvating Solvents**. *Chemical Society Reviews* 1993, **22**:409 - 416.

2. Palmer CP, Tanaka N: **Selectivity of polymeric and polymer-supported pseudo-stationary phases in micellar electrokinetic chromatography**. *Journal of Chromatography, A* 1997, **792**:105-124.

3. Palmer CP: **Recent progress in the development, characterization and application of polymeric pseudophases for electrokinetic chromatography**. *Electrophoresis* 2002, **23**:3993-4004.

4. Burns ST, Khaledi MG: **Rapid determination of liposome-water partition coefficients (K-lw) using liposome electrokinetic chromatography (LEKC)**. *Journal of Pharmaceutical Sciences* 2002, **91**:1601-1612.

5. Agbodjan AA, Bui H, Khaledi MG: **Study of solute partitioning in biomembrane-mimetic pseudophases by electrokinetic chromatography: Dihexadecyl phosphate small unilamellar vesicles**. *Langmuir* 2001, **17**:2893-2899.

6. Trone MD, Leonard MS, Khaledi MG: **Congeneric behavior in estimations of octanol-water partition coefficients by micellar electrokinetic chromatography**. *Analytical Chemistry* 2000, **72**:1228-1235.

7. Zhao YH, Le J, Abraham MH, Hersey A, Eddershaw PJ, Luscombe CN, Boutina D, Beck G, Sherborne B, Cooper I, et al.: **Evaluation of human intestinal absorption data and subsequent derivation of a quantitative structure-activity relationship (QSAR) with the Abraham descriptors**. *Journal of Pharmaceutical Sciences* 2001, **90**:749-784.

8. Platts JA, Abraham MH, Zhao YH, Hersey A, Ijaz L, Butina D: **Correlation and prediction of a large blood-brain distribution data set-an LFER study**. *European Journal of Medicinal Chemistry* 2001, **36**:719-730.